Oxygen balanced mixotrophy in microalgae

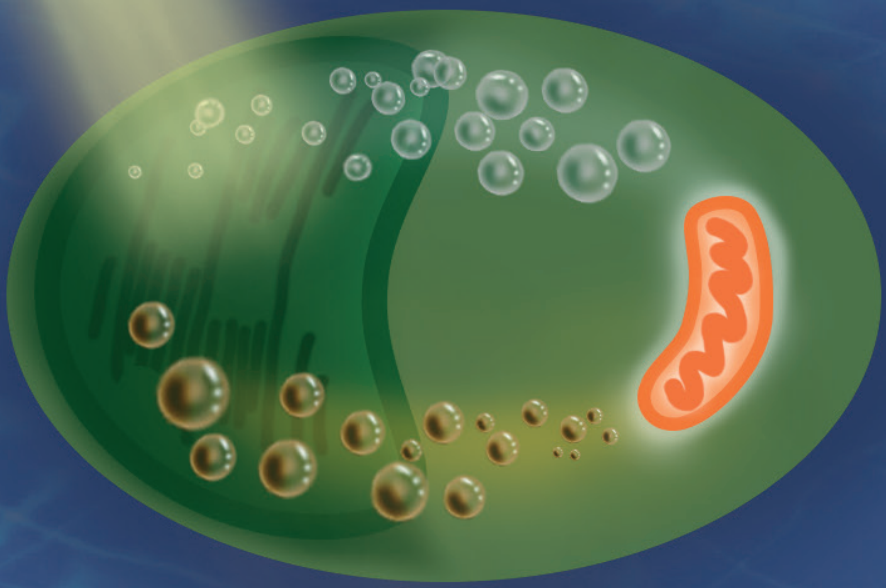

Fabian Abiusi

Propositions

1. A photobioreactor can be operated without gas exchange.
   (this thesis)
2. Oxygen balanced mixotrophy doubles biomass productivity.
   (this thesis)
3. Scientists and artists need the same amount of creativity.
4. In the last century famines were caused by political decisions.
5. Autarchy would increase circular economy and sustainable practices.
6. Cheap food is produced at high cost.

Propositions belonging to the thesis, entitled

Oxygen balanced mixotrophy in microalgae

Fabian Abiusi
Wageningen, 29 March 2021

Oxygen balanced mixotrophy in microalgae

Fabian Abiusi

Thesis committee

Promotor

Prof. Dr R.H. Wijffels

Professor of Bioprocess Engineering

Wageningen University and Research

Co-promotor

Dr M.G.J. Janssen

Assistant professor, Bioprocess Engineering Group

Wageningen University and Research

Other members

Prof. Dr V. Fogliano, Wageningen University and Research

Prof. Dr M.J.E.C. van der Maarel, University of Groningen

Dr N.T. Eriksen, Aalborg University Denmark

Dr J. Arfsten, Nestle, Switzerland

This research was conducted under the auspices of the Graduate School VLAG

(Advanced studies in Food Technology, Agrobiotechnology, Nutrition and Health sciences).

Oxygen balanced mixotrophy in microalgae

Fabian Abiusi

Thesis

submitted in fulfilment of the requirements for the degree of doctor

at Wageningen University

by the authority of the Rector Magnificus,

Prof. Dr A.P.J. Mol,

in the presence of the

Thesis Committee appointed by the Academic Board

to be defended in public

on Monday 29th March 2021

at 4 p.m. in the Aula.

Fabian Abiusi

Oxygen balanced mixotrophy in microalgae, 214 pages.

PhD thesis, Wageningen University, Wageningen, the Netherlands (2021)

With references and summary in English

ISBN: 978-94-6395-718-2

DOI: https://doi.org/10.18174/542064

Contents

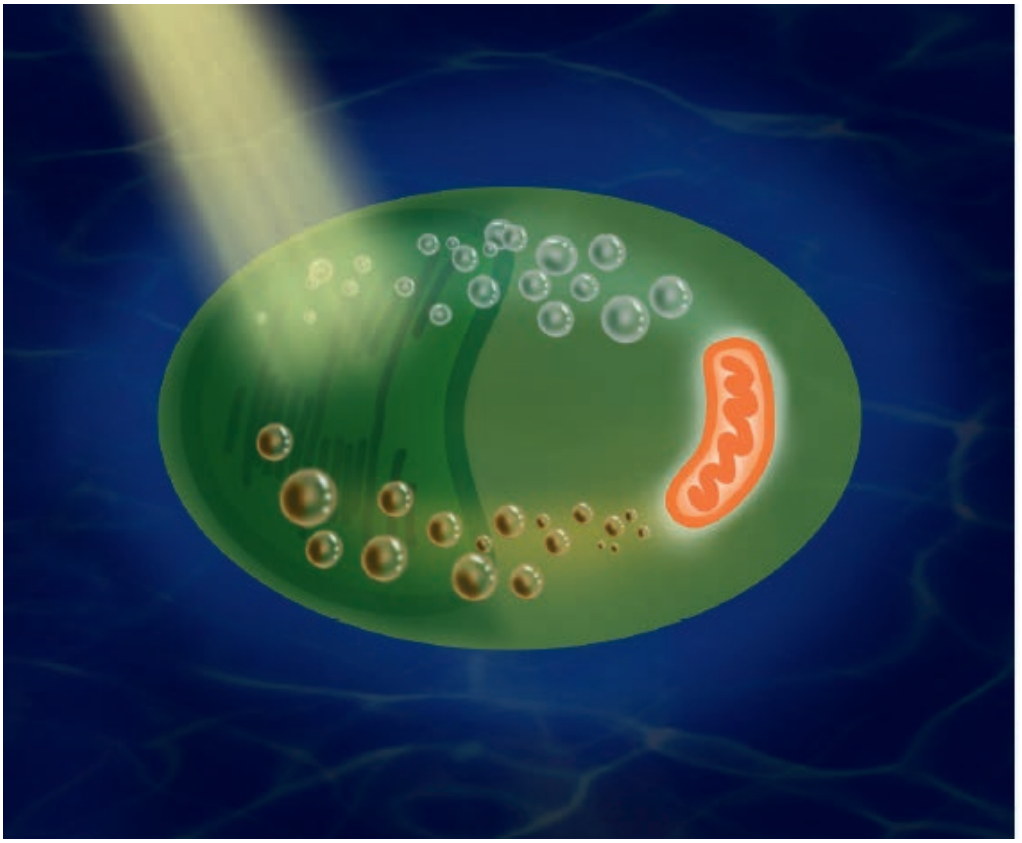

Chapter 1

Introduction and thesis outline

INTRODUCTION

Microalgae a sustainable source of food and feed commodities

The continuous growth of the human population is placing increasing pressure on our limited natural resources. Renewable and sustainable alternatives for fossil-derived products are required because of depleting fossil resources and concerns over climate change. Currently, these alternatives are mainly derived from agricultural crops. Plants can be used directly as food, converted into commodities abiotically (e.g. production of biodiesel from vegetable oil), or converted by microbial fermentation to other commodities (e.g. production of poly-3-hydroxybutyrate -based bioplastic from fermentation of sugars). Despite the constant increase in production, agroindustry is facing more and more challenges to meet the growing demand; there is competition for arable land, fresh water, and energy while, simultaneously, there is an urgent need to reduce the negative impact of agriculture on the environment. This has resulted in an ongoing search for renewable resources and more environmentally friendly production processes (Godfray et al., 2010).

Microalgae-derived products are considered as a promising source of food and crop-derived commodities (García et al., 2017; Wijffels et al., 2013). Microalgae can provide a significant number of essential nutrients, such as vitamins, minerals, pigments, and essential fatty acids and amino acids, to support human health (García et al., 2017; Lupatini et al., 2017). Their high protein content (up to 72%) (Lupatini et al., 2017) and well balanced amino acid profile (Muys et al., 2019) make microalgae a promising novel source of proteins. Under conditions of stress, some microalgae species can accumulate up to 60% of their dry weight as triacylglycerol (Rodolfi et al., 2009), the oil used for biodiesel production, but also suitable to replace palm oil (Draaisma et al., 2013). Microalgae can reach higher areal productivity than terrestrial plants, do not require arable land or fresh water, (Wijffels & Barbosa, 2010) and can use fertilizers with almost 100% efficiency (Tredici, 2010).

Despite of these advantages over conventional crop production, the current application of microalgae lies in specialties, or high value products, such as pigments (e.g. astaxanthin, phycocyanins) or ω-3 fatty acids (e.g. EPA, DHA) (Spolaore et al., 2006). One of the main reasons for these limitations is the relatively high production cost. In 2016 the cost of microalgae production and harvesting have been estimated between 6.2 and 28.4 €·Kg^{-1} for a facility of 1 hectare (Ruiz et al., 2016; Tredici et al., 2016). According to these studies, (Ruiz et al., 2016; Tredici et al., 2016) the production costs can be decreased to 3.2 €·Kg^{-1} by increasing the scale of the facility to 100 hectare.

Ruiz et al (Ruiz et al., 2016) performed a sensitivity analysis pinpointing the improvements needed to further drop microalgae production costs. The authors changed individual parameters in the production process to values expected in the future. The most influential improvements required to reduce production costs are the following:

1. Increasing the photosynthetic efficiency, which will lead to higher biomass productivity
2. Reducing photobioreactor light path, which will allow for reactor operation at a higher biomass concentration, thus reducing the downstream process cost
3. Decreasing the aeration needed for mixing and gassing, thus reducing the energy consumption

Mixotrophic cultivation of microalgae

Microalgae are commonly grown exploiting their photoautotrophic capacity (henceforth referred to as autotrophic) (Lin & Wu, 2015), in which cells harvest light energy, use carbon dioxide (CO_2) as a carbon source, and release oxygen (O_2) as a byproduct (Figure 1). Despite the advantage of CO_2 mitigation and use of free solar energy, autotrophic cultures have limitations. In autotrophic cultures, light availability is the main growth limiting factor. Cellular self-shading hinders light availability and therefore limits biomass production. To limit self-shading, generally low biomass concentrations are maintained in autotrophic cultures leading to a dilute harvest flow and a large volume of liquid to be handled. Another limitation of autotrophic culture is the need for gassing which demands a substantial amount of energy. Gas−liquid transfer is necessary to avoid O_2 accumulation in the liquid culture and to provide the CO_2 required for photosynthesis.

Alternatives to autotrophic cultures are chemo-organotrophic (henceforth referred to as heterotrophic) cultures in which organic carbon, such as sugars and organic acids, are used as carbon sources in the absence of light (Figure 1). In contrast to autotrophic cultures, heterotrophic cultures can be grown in conventional fermenters, providing the O_2 required by intensive aeration, reaching higher concentration and higher volumetric productivity. However, darkness can lead to reduced pigmentation, limiting the potential of heterotrophic cultivation for the large-scale production of these phytochemicals (Lee, 2001).

Autotrophic and heterotrophic cultivation of microalgae can be combined in mixotrophic cultivation (Figure 1). In this trophic mode, light and organic carbon are simultaneously provided and both heterotrophic and autotrophic metabolism operate concurrently within a single microalgal monoculture. Mixotrophic cultivation offers several advantages that can overcome limitations of both autotrophic and heterotrophic cultivation. In mixotrophic cultivation, the simultaneous presence of two energy sources (light and reduced organic carbon)

***Figure 1**. Schematic representation of the autotrophic, heterotrophic and mixotrophic microalgal cultivation. The generic molecular formula CH_2O is used to indicate sugars.*

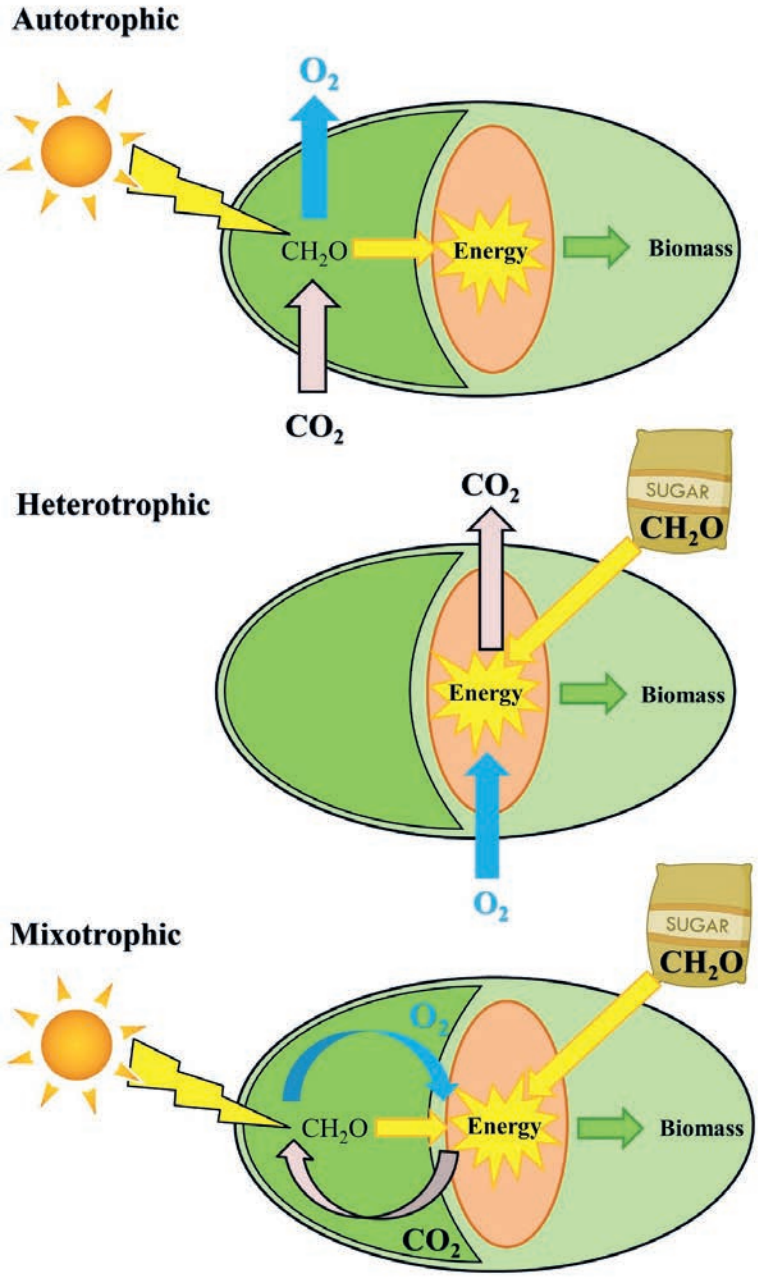

can significantly increase biomass productivity (Turon et al., 2015c; Wang et al., 2014). Moreover, a higher biomass concentration can be reached at a given light intensity, reducing downstream processing cost (Chandra et al., 2014; Deschênes et al., 2015). Mixotrophic cultivation has the potential to drastically reduce the need for gas−liquid exchange since the O_2 required by aerobic heterotrophic growth can be covered by oxygenic photosynthesis. Vice versa, the CO_2 needed to carry on photosynthesis can be provided by the heterotrophic metabolism. This internal CO_2 recirculation will maximize the biomass yield on substrate (Turon et al., 2015c), making the process close to carbon neutrality. Moreover, preventing the need for any gas−liquid exchange of oxygen and carbon dioxide greatly reduces the power required for the mixotrophic production process, as compared to either an autotrophic or a heterotrophic production process.

In order to minimize gas exchange, the heterotrophic and autotrophic contributions to the overall mixotrophic growth need to be equilibrated. Such balanced mixotrophic growth can only be obtained if the supply rate of organic carbon is controlled. Unfortunately, batch experiments are dominant in the literature on mixotrophic cultivation of microalgae. In such dynamic batch processes, the dominance of the autotrophic and heterotrophic metabolism changes over time (Smith et al., 2015), making balanced mixotrophic cultivation impossible. These batch dynamics might be a reason for contradictory conclusions in previous studies.

Although there are many indications that autotrophic and heterotrophic metabolism can take place non-competitively, and that overall growth is the sum of the two metabolisms (Martínez & Orús, 1991; Ogawa & Aiba, 1981; Turon et al., 2015c), interactions can occur and affect algal growth. Previous studies on mixotrophy indicated the presence of negative side-effects, such as decreased pigment content (Grama et al., 2016; Wilken et al., 2014; Yang et al., 2000) and reduced photosynthetic activity in the presence of organic carbon. (Martínez & Orús, 1991; Mozaffari et al., 2019; Ogawa & Aiba, 1981). Others reported that light inhibits glucose uptake

(Kamiya & Kowallik, 1987a; Kamiya & Kowallik, 1987b). Also, positive interactions have been reported. For example, photorespiration and carbon concentrating mechanisms seem to be suppressed due to an increase of intracellular CO_2 (Grama et al., 2016; Villarejo et al., 1995), increasing the energy available for growth. Designing a process strategy which balances contributions of the autotrophic and heterotrophic metabolisms within the overall mixotrophic growth is thus needed. A balanced mixotrophic strategy could finally clarify whether the overall growth in mixotrophy is the sum of the autotrophic and heterotrophic metabolisms or not.

On one hand, *Chlorella sorokiniana* has similar maximum growth rate under autotrophic and heterotrophic conditions (Cuaresma et al., 2009; Turon et al., 2015c) and is the most studied mixotrophic algal species (León-Vaz et al., 2019; Van Wagenen et al., 2015). On the other hand, organic substrate addition makes the culture more prone to contamination by heterotrophic microorganisms. A possible solution for this challenge is to use a microalgal strain able to grow under extreme conditions, such as low pH, where most of the common contaminants cannot grow. Unfortunately, acidophilic microalgae are less studied compared to the ones living in neutral or alkaline environments.

The most studied acidophilic microalgae is the species *Galdieria sulphuraria* (Sydney et al., 2019). *G. sulphuraria* has potential commercial application in the production of the blue pigment phycocyanin and given its high nutritional value *G. sulphuraria* may be a suitable component in foods (Abdelmoteleb et al., 2021; Graziani et al., 2013). Nevertheless, *G. sulphuraria* has been considered extremely photosensitive (Brock, 1978; Sloth et al., 2006). For this reason, before testing a balanced mixotrophic process on extremophile microalgae, their growth conditions need to be optimized.

AIM AND THESIS OUTLINE

The overarching aim of the research presented in this thesis is to decrease microalgae production costs by designing a balanced mixotrophic strategy where autotrophic and heterotrophic metabolic contributions to the overall mixotrophic growth are equilibrated. In order to reach this aim, the mixotrophic cultivation process was explored in a sequence of separate studies.

In a first step described in **Chapter 2**, *Chlorella sorokiniana* was used as model organism in the design of a new mixotrophic cultivation method denominated "oxygen balanced" mixotrophy. In "oxygen balanced" mixotrophy the dissolved oxygen concentration is controlled by adjusting the substrate supply rate to the light-limited rate of photosynthesis. Using this approach under continuous illumination, a closed photobioreactor was operated without any gas exchange. Steady state "oxygen balanced" mixotrophy was used to validate the hypothesis that mixotrophic stoichiometry is the sum of heterotrophic and autotrophic metabolisms.

When sunlight is used, microalgae are exposed to day−night cycles and seasonal variations of the irradiance on a microalgal cultivation system. For this reason, in **Chapter 3** "oxygen balanced" mixotrophy in *C. sorokiniana* was explored under day−night cycles. The reactor was operated at a fixed dilution rate (i.e. chemostat), only diluted during daytime and not during the night (cyclostat). During daytime the reactor was operated in "oxygen balanced" mixotrophy. During nighttime, no substrate was fed to the mixotrophic culture. In both the mixotrophic and autotrophic cultures the oxygen consumption related to night respiration was measured to elucidate the impact of day-time mixotrophy on night-time biomass loss.

Contamination by bacteria and fungi is a notable challenge when microalgae are cultivated in a medium that contains a source of organic carbon. In **Chapter 4** cultivation of the acidophilic microalgae *Galdieria sulphuraria* is proposed as a solution to prevent undesired contamination by heterotrophic microorganisms. In order to successfully cultivate light sensitive *G.*

sulphuraria the specific light supply rate needs to be optimized. This was done using a series of repeated batch experiments where the specific light supply rate continuously decreased during the batch phase because of the increasing biomass concentration. Under optimal light regime, autotrophic and "oxygen balanced" mixotrophic biomass production were compared.

A study aiming to stabilize biomass productivity of *G. sulphuraria* in a continuous process is described in **Chapter 5**. The optimal specific light supply rate found in chapter 4 was used for continuous biomass production in chemostat. Mixotrophic and autotrophic productivity, amino acid profile, C-phycocyanin and protein content were compared. Our results reveal that *G. sulphuraria* amino acid content and profile is superior to any other known food, especially regarding sulfureted amino acid. Moreover C-phycocyanins extracted from *G. sulphuraria* were more thermo- and acid-stable than C-phycocyanins extracted from *Spirulina* (*Arthrospira platensis*)

In **Chapter 6**, the insights of this thesis are combined in a techno-economic model for an objective evaluation of the cost-impact of the oxygen balanced mixotrophic process. Projections are presented on the biomass production costs for a 100-hectare facility located in southern Spain. Vertically stacked horizontal tubular photobioreactors are employed in the projections. The techno-economic model is used to compare the biomass production cost of autotrophic and "oxygen balanced" mixotrophic cultures of *Chlorella sorokiniana* and *Galdieria sulphuraria*. The techno economic analysis is then used to identify targets for a further improvement of the process. In addition, water and land use of large-scale mixotrophic cultivation of algal protein is compared to traditional soy protein.

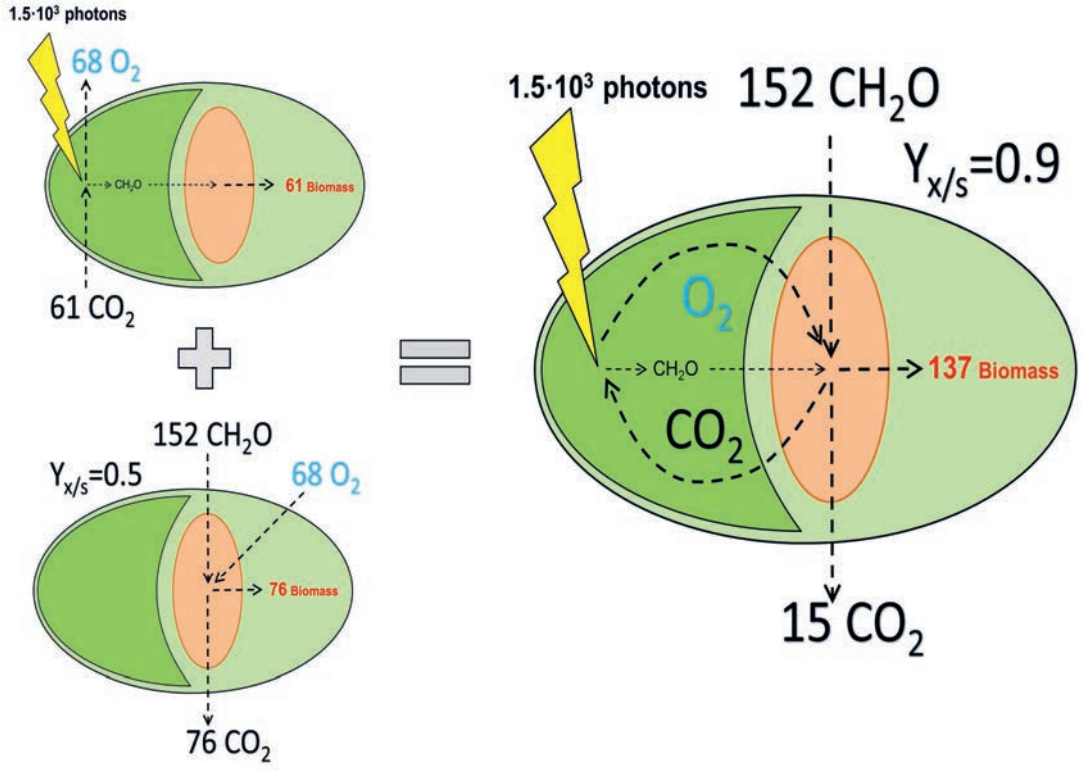
1.5·10³ photons
68 O₂
CH₂O
61 Biomass
61 CO₂
152 CH₂O
Y_x/s=0.5
68 O₂
76 Biomass
76 CO₂
1.5·10³ photons
152 CH₂O
Y_x/s=0.9
O₂
CH₂O
137 Biomass
CO₂
15 CO₂

Chapter 2

Doubling of microalgae productivity by oxygen balanced mixotrophy

This chapter has been published as:
Fabian Abiusi, Rene H. Wijffels, Marcel Janssen.
Doubling of microalgae productivity by oxygen balanced mixotrophy

ACS Sustainable Chem. Eng. 2020, 8, 6065−6074

ABSTRACT

Microalgae productivity was doubled by designing an innovative mixotrophic cultivation strategy that does not require gas-liquid transfer of oxygen or carbon dioxide. *Chlorella sorokiniana* SAG 211-8K was cultivated under continuous operation in a 2 L stirred-tank-photobioreactor re-designed such that respiratory oxygen consumption a was controlled by tuning the acetic acid supply.

In this mixotrophic set-up, the reactor was first operated with aeration and no net oxygen production was measured at a fixed acetic acid supply rate. Then the aeration was stopped and the acetic acid supply rate was automatically regulated to maintain a constant dissolved oxygen level using a process control software. Respiratory oxygen consumption was balanced by phototrophic oxygen production and the reactor was operated without any gas-liquid exchange. The carbon dioxide required for photosynthesis was completely covered by the aerobic conversion of acetic acid. Under this condition the biomass/substrate yield was 0.94 C-mol$_x$·C-mols^{-1}. Under chemostat conditions both reactor productivity and algal biomass concentration were doubled in comparison to a photoautotrophic reference culture.

Mixotrophic cultivation did not affect the photosystem II maximum quantum yield (F_v/F_m) and the average dry weight-specific optical cross section of the microalgal cells. Only light absorption by chlorophylls over carotenoids decreased by 9% in the mixotrophic culture in comparison to the photoautotrophic reference. Our results demonstrate that photoautotrophic and chemoorganotrophic metabolism operate concurrently and that the overall yield is the sum of the two metabolic modes. At the expense of supplying an organic carbon source, photobioreactor productivity can be doubled while preventing energy intensive aeration.

Keywords: Microalgae productivity, biomass yield on substrate, oxygen balance, carbon balance, mixotrophic cultivation.

INTRODUCTION

The growing demand for food and fossil-derived products is placing increasing pressure on our current resources. This has resulted in an ongoing search for renewable resources and more environmentally friendly production processes (Amulya et al., 2016). In this scenario, microalgae are regarded as a high potential renewable feedstock (Moncada et al., 2014; Ruiz et al., 2016). The most common procedure for cultivating microalgae is photoautotrophic culture (henceforth referred to as autotrophic) (Lin & Wu, 2015), in which cells harvest light energy, use carbon dioxide (CO_2) as a carbon source, and release oxygen (O_2) as a by-product.

Despite the advantage of CO_2 mitigation and use of solar energy, autotrophic cultures have limitations. In autotrophic culture light availability is the main growth limiting factor. Cellular self-shading hinders light availability limiting biomass production. To overcome this problem, generally low biomass concentrations are maintained in autotrophic cultures reducing the volumetric productivity. Another limitation of autotrophic culture is the need for gassing demanding substantial energy. Gas-liquid transfer is necessary to avoid O_2 accumulation in the liquid culture and to provide the CO_2 required to run photosynthesis.

CO_2 supply is a frequently overlooked challenge in microalgae commercialization. Atmospheric CO_2 levels (~0.04% v/v) are not sufficient to support high biomass productivities because the driving force for gas-liquid transfer is too small and too high gas flows would be required (Langley et al., 2012). For this reason, CO_2-enriched gas streams are provided to achieve high biomass productivity. Not all CO_2 provided is taken up and in open ponds up to the 97% of the provided CO_2 might be lost to the atmosphere (Ganuza & Tonkovich, 2016). Even in optimized photobioreactors, CO_2 loses minimally are 25% in closed photobioreactors *(PBRs)* (Acién et al., 2012), and 50% in open ponds (Doucha et al., 2005). Anthropogenic CO_2-enriched gas (e.g. flue-gas with 10-15% CO_2) are envisioned to meet the requirement for large scale production. However, considering the high CO_2 demand of a large scale facility, without

an extensive and costly infrastructure of CO_2 capture and transportation, only a limited amount of areas are suitable for large scale production (Smith et al., 2015).

An alternative to autotrophic culture are chemoorganotrophic (henceforth referred to as heterotrophic) culture in which organic carbons, such as sugars and organic acids, are used as carbon sources in the absence of light. In contrast to autotrophic culture, heterotrophic culture can be performed in conventional fermenters, requiring O_2 by intensive aeration, reaching higher concentration and productivity. Despite the high productivity, heterotrophic growth has been observed in a few microalgal species only. Moreover, darkness can lead to reduced pigmentation limiting the potential of heterotrophic cultivation for the large-scale production of these phytochemicals (Lee, 2001).

Autotrophic and heterotrophic cultivation of microalgae can be combined in mixotrophic cultivation. In this trophic mode, light and organic carbons are simultaneously exploited and both heterotrophic and autotrophic metabolism operate concurrently within a single microalgal monoculture. Mixotrophic cultivation offers several advantages that can overcome both autotrophic and heterotrophic limitations. In mixotrophic cultivation, the simultaneous presence of two energy sources (light and reduced organic carbon) can significantly increase biomass productivity (Turon et al., 2015c; Wang et al., 2014). Moreover, higher biomass concentration can be reached at a given light intensity reducing downstream processing cost (Chandra et al., 2014; Deschênes et al., 2015). Recent studies also indicated that mixotrophic cultivation has the potential to drastically reduce the need of gas-liquid exchange (Grama et al., 2016; Smith et al., 2015) since the O_2 required by aerobic heterotrophic growth can be covered by oxygenic photosynthesis. Vice versa, the CO_2 needed to carry on photosynthesis can be provided by the heterotrophic metabolism. This internal CO_2 recirculation will maximize the biomass yield on substrate (Turon et al., 2015c) making the process close to carbon neutrality. As a comparison in a heterotrophic culture typically 40 to 60 % of the carbon is lost (Blanken et al., 2016).

Moreover, preventing any gas-liquid exchange of oxygen and carbon dioxide greatly reduces the power required for the mixotrophic production process, as compared to either a photoautotrophic or a chemoheterotrophic production process.

In order to minimize gas exchange, the heterotrophic and autotrophic contribution to the overall mixotrophic growth needs to be equilibrated. Such balanced mixotrophic growth can only be obtained if the organic carbon supply rate is controlled. Unfortunately, batch experiments are dominant in the literature on mixotrophic cultivation of microalgae. In such dynamic batch processes, the dominance of the autotrophic and heterotrophic metabolism changes over time (Smith et al., 2015), making balanced mixotrophic cultivation impossible. These batch dynamics might be a reason for contradictory conclusions in previous studies. Part of the studies agree on the fact that during mixotrophic cultivation, autotrophic and heterotrophic metabolism can proceed non-competitively and that the overall growth is the sum of the two metabolisms (Acién et al., 2012; Lee, 2001; Wang et al., 2014). In other studies both positive (Grama et al., 2016; Villarejo et al., 1995) and negative (Kamiya & Kowallik, 1987a; Kamiya & Kowallik, 1987b) interactions between the two metabolisms are reported.

The aim of the study is to design an oxygen balanced mixotrophic process that does not require any gas exchange. To this end, the model strain *C. sorokiniana* SAG 211-8K was cultivated in a closed *PBR*, under continuous operation, trying to maintain constant dissolved oxygen concentration *(DO)* by tuning the acetic acid supply rate to the rate of photosynthesis. Special attention was given the carbon balance to investigate the hypothesis that the mixotrophic metabolism is the sum of the heterotrophic and autotrophic metabolisms.

MATERIALS AND METHODS

Organism, media and cultivation conditions

Chlorella sorokiniana SAG 211-8K was obtained from the algae culture collection at Göttingen University (SAG) and cultivated in modified M-8 medium (Mandalam & Palsson, 1998). Medium composition can be found in supporting information 1. Axenic algal cultures were cryopreserved and stored in liquid nitrogen. Before reactor inoculation, cryopreserved cultures were defrosted and used to inoculate 250 mL flasks with 100 mL volume in an incubator operated at 37˚ C, 4.5% v/v CO_2, and stirring at 100 rpm with a magnetic rod. In this incubator the flasks were illuminated 24h/24h from below with a warm-white LED (BXRAW1200, Bridgelux, USA) at a photon flux density (*PFD*, µmol m^{-2} s^{-1}) of 500 µmol m^{-2} s^{-1}. The *PFD* was measured with a LI-COR 190-SA 2π sensor (PAR-range: 400–700 nm). Based on this procedure two inocula were prepared: an autotrophic inoculum on M8a medium, and a mixotrophic inoculum on M8a supplemented with 3.41 g·L-1 of sodium acetate.

In the heterotrophic flask experiments glucose, acetate and glycerol were supplemented to the modified M8a medium. The heterotrophic experiments were started by using an autotrophic inoculum and this culture was adapted to heterotrophic growth for at least 2 weeks using the three different substrates. Flasks were incubated at 37˚C in darkness while being shaken at 250 rpm. The acclimated heterotrophic cultures were diluted the day before the experiment using the same M8a medium with organic carbon resulting in exponentially growing cultures, which were used as inoculum for the experiment.

Heterotrophic flask experiments

The heterotrophic biomass yield on substrate ($Y^{het}_{x/s}$, C-mol_x·C-mol_s^{-1}) was determined in dark batch experiments. Glucose, acetate, and glycerol were supplemented to the M8a medium based on their carbon molarity (C-mol·L^{-1}). In order to provide 83.3 C-mmol·L^{-1}, 2.75g·L^{-1}, 3.4 g·L^{-}

^{1}, and 2.56 g·L^{-1} of glucose monohydrate, sodium acetate, and glycerol were used. Sodium acetate was tested also at double concentration (167 C-mmol·L^{-1}). Glucose and glycerol were sterilized by autoclaving while acetate was sterilized by filtration. The pH was stabilized by adding 0.1 mol·L^{-1}of HEPES. The experiments were started at an optical density at 750 nm (OD_{750}) between 0.3 and 0.5.

During the experiments, samples were taken every 2 hours until steady values were reached indicating substrate depletion. The microalgae concentration was quantified measuring OD_{750}. For each sample, first OD_{750} was measured and then 1 mL was centrifuged, and the supernatant was extracted and stored at -20˚C prior to analysis of substrate concentration by (U)HPLC.

The OD_{750} was converted into dry weight (C_x, $g_x \cdot L^{-1}$) using a linear regression (see analytical methods). At the end of each experiment, the C_x was measured to verify that the correlation was still valid. The heterotrophic biomass yield on substrate $Y^{het}_{x/s}$ was calculated as follow:

$$Y^{het}_{x/s} = -\frac{(C_{xe}-C_{x0})}{MW_x \cdot (S_e-S_0)} \qquad (1)$$

where C_{x0}/C_{xe} and S_0/S_e are respectively the biomass and the substrate concentrations (C-mol·L^{-1}) at the start and the end of the exponential phase while MWx ($g_x \cdot mol_x^{-1}$) is the weight of 1 carbon mole of biomass. The MWx was determined at the end of the experiment and it was assumed to be constant during the batch.

The specific growth rate (μ, h^{-1}) during exponential growth was calculated according to:

$$\mu = \frac{ln(C_{xe})-ln\,(C_{x0})}{t_e-t_0} \qquad (2)$$

where t_0/t_e and C_{x0}/C_{xe} are respectively the time and the biomass concentration at the start and the end of the exponential phase. Experiments were performed in biological duplicates. The averages and standard deviations will be shown in graphs and tables.

Photobioreactor set-up and experiments

Chlorella sorokiniana SAG 211-8K was grown in chemostat mode in a 3 L bioreactor (Applikon, The Netherlands) depicted in figure 1. The fermenter had a working volume (V_{PBR}) of 1.923 L when aeration was provided and 1.975 L without aeration.

Figure 1. *Top view (A) and side view (B) of the photobioreactor used in the study.*

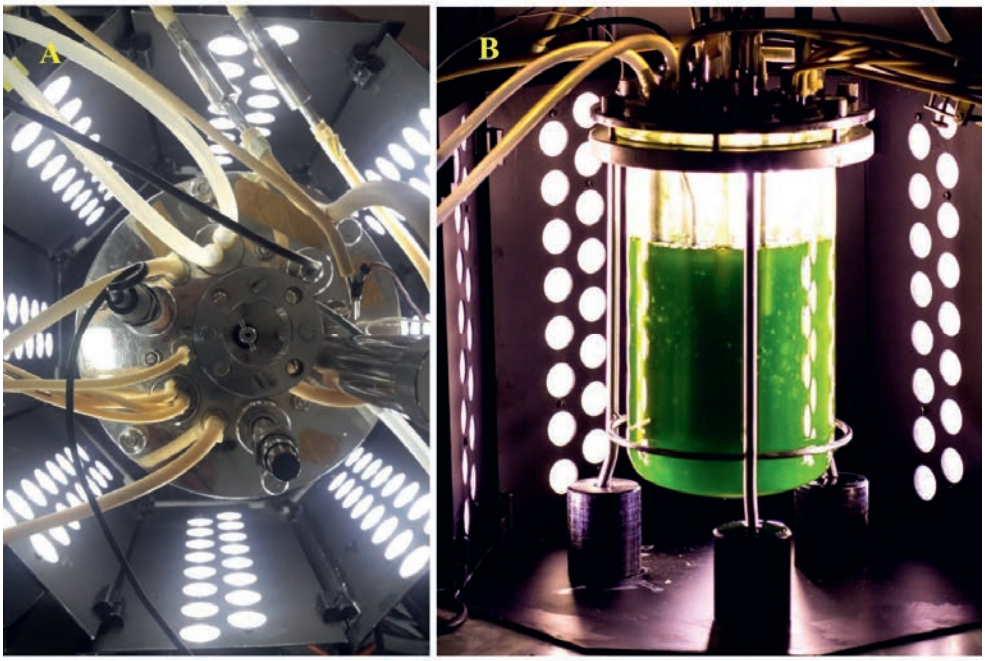

The internal diameter was 0.130 m, while the culture height was maintained at 0.165 m by a level probe, resulting in an illuminated area (A_{PBR}) of 0.067 m^2. The cylindrical reactor was illuminated from all sides resulting in a homogenous light field over the vertical reactor surface. More specifically, a circular light source was constructed, consisting of 8 vertical light panels placed around the fermenter as an octagon. Each panel was composed of 16 warm-white 3 Watt LEDs (Avago ASMT-MY22-NMP00, Broadcom, USA) equipped with a plastic lens with

FHWM of 25.5˚ (Part no. 10393, Carclo-optics, UK). Light intensity on the reactor surface was measured at 16 fixed points inside the empty reactor prior to each experiment. The measured light intensities at all 16 points were averaged obtaining an average *PFD* of 498±17 μmol m^{-2} s^{-1}.

The reactor was equipped with a dissolved oxygen (*DO*) sensor (VisiFerm DO ECS 225, Hamilton, US). This *DO* sensor was calibrated inside the reactor filled with growth medium and sparged with dinitrogen gas, or air, to give a *DO* level of respectively 0 and 100%. The reactor was kept at 37°C by a heat exchanger inside the reactor vessel. To prevent evaporation, the reactor was equipped with a condenser connected to a cryostat feeding cold water of 2°C. Continuous stirring at 500 rpm was applied during all experiments. When aerated, air enriched with 2% v/v carbon dioxide was provided at a flow rate of 1 $L \cdot min^{-1}$ using mass flow controllers (Smart TMF 5850S, Brooks Instruments, USA). The pH was continuously measured and controlled at 6.7 by automatic base addition (1 M, NaOH).

Two reactor experiments were performed. In the first experiment the reactor was operated mixotrophically inoculated at a density of 0.3 $g_x \cdot L^{-1}$ with a mixture of phototrophic and mixotrophic cultures. A 5% w/w acetic acid solution was supplied at a fixed rate while gassing the reactor with air enriched with CO_2 (‘mixo with gas exchange’). After this phase, the aeration was stopped resulting in a mixotrophic cultivation without gas exchange (‘mixo without gas exchange’) where the supply rate of acetic acid was automatically adjusted to maintain a *DO* of 135%. Before ending this first experiment, the acetic acid supply was stopped, the aeration re-established, and the reactor was operated autotrophically (‘autotrophic 1’). In the second experiment the reactor was operated autotrophically (‘autotrophic 2’) inoculated with an autotrophic culture at a density of 0.3 $g_x \cdot L^{-1}$.

The base solution, the acetic acid solution and the harvest bottles were placed on analytic balances. Balances, *DO* sensor, temperature, pH sensor, and mass flow controllers were

connected to a data acquisition system interfaced via a computer by means of a virtual instrument (Lab View, National Instruments, USA) allowing for continuous data logging and process control. Culture samples for off-line measurements were taken aseptically from the middle of the reactor through a dedicated port. The complete set-up, including all the solutions, where sterilized by autoclaving for 60 min at 121˚C. After inoculation, the reactor was operated in batch until a biomass density of about 1.5 $g_x \cdot L^{-1}$ was reached and then it was operated as chemostat at a dilution rate of about 2 day^{-1}. Once the steady state was obtained, it was maintained for a least 4 consecutive days during which samples were taken for off-line measurements.

Photobioreactor calculations

In the chemostat experiments, the volumetric biomass production rate (r_x, $g_x \cdot L^{-1} \cdot day^{-1}$) was calculated multiplying the measured biomass concentration (C_x, $g_x \cdot L^{-1}$) with the measured dilution rate (D, day^{-1}). The r_x was also converted into its carbon equivalent (r_c, $C\text{-}mol_x \cdot L^{-1} \cdot day^{-1}$) by dividing r_x by the molecular weight of 1 C-mol of biomass (MWx, $g_x \cdot C\text{-}mol_x^{-1}$). The MWx was determined in each sample taken from the reactor. In the two autotrophic experiments r_c was used to determine the biomass yield on light ($Y_{x/ph}$, $C\text{-}mol_x \cdot mol_{ph}^{-1}$) according to the formula:

$$Y_{x/ph} = \frac{r_{c,auto} \cdot V_{PBR}}{\mathrm{PFD} \cdot A_{PBR}} \quad (3)$$

In the mixotrophic experiments, the volumetric substrate consumption rate (r_s, $C\text{-}mols \cdot L^{-1} \cdot day^{-1}$) was calculated as follows, assuming ideal mixing:

$$r_s = \frac{F_{AA} \cdot C_{sAA} - D \cdot V_{PBR} \cdot C_s}{V_{PBR}} \quad (4)$$

Where F_{AA} ($L \cdot day^{-1}$) and C_{sAA} ($C\text{-}mol_s \cdot L^{-1}$) represent respectively the supply rate of the acetic acid solution rate and the concentration of the acetic acid solution while Cs ($C\text{-}mol_s \cdot L^{-1}$) is the acetic acid concentration in the reactor ($C\text{-}mol_s \cdot L^{-1}$).

The mixotrophic yield on substrate ($Y^{mixo}_{x/s}$, C-mol$_x$·mol$_s^{-1}$) was calculated dividing r_c by r_s.

Analytical methods

Culture sampling and off-line measurements

Samples were taken aseptically multiple times per day for off line measurements. Two 1 mL aliquots were centrifuged at 20238 RCF for 10 minutes. The supernatant fractions were stored at -20 ˚C until analysis, while the pellet was washed with demineralized water and cooled to -20 °C, lyophilized and stored. Extra aliquots of sample were taken from the reactor to quantify the total inorganic carbon concentration (*TIC*) in the medium. To avoid CO_2 stripping, immediately after centrifugation, 950 µL of the supernatant fraction was alkalized by addition of 50 µL of base (2 M, NaOH). Alkalized samples were stored at -20 ˚C until analysis.

Dry weight concentration

Culture growth was estimated by biomass dry weight (C_x, g$_x$·L^{-1}) determination: aliquots of the culture (2.5-5 mL) were diluted to 25 mL with demineralized water and filtered over pre-weighed Whatman GF/F glass microfiber filters (diameter of 55 mm, pore size 0.7 µm).The filters were washed with deionized water (25 mL) and dried at 105° C until constant weight.

Optical density

The optical density was measured in duplicate on a spectrophotometer (DR6000, Hach-Lange, US) at 680 and 750 nm. The relationship between C_x and OD_{750} was determined with biomass grown heterotrophically in a range of 0.1 to 2 g$_x$·L^{-1} by filtering at least 5 mg of algal dry biomass onto pre-weighed glass fiber filters (Whatman GF/F, GE Healthcare UK Ltd., UK) which were dried overnight at 105 °C until constant weight. This resulted in the following correlation:

C_x ($g_x \cdot L^{-1}$) = 0.48·OD_{750} (R^2=0.98)

Cell concentration and bio-volume

Cell bio-volume and concentration were measured using the Multisizer III (Beckman Coulter Inc., USA) with a 50 µm aperture tube. Samples were diluted in ISOTON II diluent. The measured cellular biovolume was converted to cell diameter assuming spherical cells.

Average dry weight-specific optical cross section

The average dry weight-specific optical cross section (a_x, $m^2 \cdot Kg^{-1}$) was measured and calculated according to de Mooij et al. (de Mooij et al., 2015) using the absorbance from 400 to 750 nm with a step size of 1 nm. The absorbance was measured in UV-VIS/double beam spectrophotometer (Shimadzu UV-2600, Japan) equipped with integrating sphere (ISR-2600). Cuvettes with an optical path of 2 mm were used.

Photosystem II quantum yield

The photosystem II maximum quantum yield (*QY*, F_v/F_m) was measured at 455 nm with an AquaPen-C AP-C 100 (Photon Systems Instruments, Czech Republic). Prior to the measurement, samples were adapted to darkness for 15 min at room temperature and diluted to an *OD750* between 0.3 and 0.5.

Acetic acid and glucose determination

Acetic acid and glucose concentrations were determined using an Agilent 1290 Infinity (U)HPLC equipped with a guard column (Security Guard Cartridge System, Phenomenex, USA). The compounds were separated on an organic acid column (Rezex ROA-Organic acid H^+ 8% column, Phenomenex, USA) at 55 °C with a flow of 0.5 mL/min 0.005 M H_2SO_4 as eluent. A final concentration of 50 mM propionic acid was used as internal standard.

Total organic and total inorganic carbon

The organic carbon content in the pellet was measured as total carbon ($g_c \cdot L^{-1}$) using a TOC-L analyzer (Shimadzu, Japan). Possible traces of inorganic carbon in the lyophilized pellet were removed by resuspending the pellet in 1 mL of HCl (1M) and sonicating the solution at 80 kHz 40˚C for 30 minutes. After this treatment samples were diluted ten times in demi water and immediately placed in the TOC-L analyzer. The biomass carbon content ($C_{\%}$, % $w_c \cdot w_x^{-1}$) was calculated by dividing the obtained total carbon by the C_x determined on the same sample. The $C_{\%}$ was used to determine the biomass molecular weight (MW_x, $g_x \cdot C\text{-}mol_x^{-1}$). MW_x was determined by dividing the carbon molecular weight (12.011 $g_c \cdot C\text{-}mol^{-1}$) by $C_{\%}$. The *TIC* was measured in the undiluted supernatant with the TOC-L analyzer.

Assessment bacterial contaminant

During the experiment, axenicity was checked daily by DNA staining of culture samples with SYBER Green I (Sigma-Aldrich, US) and fluorescence microscopy (EVOS FL auto, Thermo Fisher Scientific, US).

Statistical analysis

Propagation of errors was calculated according to Eq. (5) and Eq. (6) for sum and multiplication operations, respectively, to obtain the error.

$$\Delta z = \sqrt{\Delta x^2 + \Delta y^2 + \ldots} \qquad (5)$$

$$\frac{\Delta z}{x} = \sqrt{\frac{\Delta x^2}{x} + \frac{\Delta y^2}{y} + \cdots} \quad (6)$$

where Δx is the absolute error associated to the value x and so on.

Reproducibility of duplicates was perform by *t* test. Significant differences between different conditions was analyzed by one-way ANOVA, followed by Tukey's multiple comparison test, using the software Graph Pad Prism 5.00 (GraphPad Prism® Software, San Diego, US). The significance level was $P<0.05$.

RESULTS AND DISCUSSIONS

Heterotrophic reference experiments

Strict heterotrophic and autotrophic reference experiments were conducted to determine the heterotrophic biomass yield on substrate ($Y^{het}_{x/s}$) and the biomass yield on photons ($Y_{x/ph}$).

The $Y^{het}_{x/s}$ was determined in heterotrophic batch experiments where *C. sorokiniana* was grown in darkness in modified M8a medium supplemented with three organic substrates: glucose, glycerol and acetate. Since the inoculum was obtained from an autotrophic culture, the culture expressed a lag phase of about 48 h (data not shown). After this lag phase, the cultures on glucose or acetate grew exponentially while no growth was observed on glycerol (data not shown).

Heterotrophic biomass production and substrate consumption are reported in figure 2. At 100 C-mmol$_s$·L^{-1}, cultures grew exponentially until the substrate was completely consumed. Both substrates, glucose and acetate, resulted in a biomass concentration of 57 C-mmol$_x$·L^{-1} corresponding to a $Y_{x/s}$ of 0.49±0.06 (C-mol$_s$·C-mol$_s^{-1}$). A significant ($P<0.05$) difference in the specific growth rate (μ) was found for growth on glucose and acetate: on glucose, μ was 0.14±0.00 h^{-1} whereas on acetate it was 0.18±0.00 h^{-1}. Given its better performance, acetate was also tested at 200 C-mmol$_s$·L^{-1} (Figure 2). At this concentration, the culture grew exponentially for 14 h and a slightly higher $Y_{x/s}$ was found (0.51±0.05 C-mol$_x$·C-mol$_s^{-1}$) although it was not statistically significant ($P>0.05$).The specific growth rate μ (0.15±0.00 h^{-1}) was comparable with the μ obtained using glucose but significantly lower than the one obtained at 100 C-mmol$_s$·L^{-1}of acetate ($P<0.05$). In summary, a $Y_{x/s}$ of 0.50±0.04C-mol$_x$·C-mol$_s^{-1}$ was obtained on both glucose and acetate. This value falls in the middle of the range 0.40-0.63 C-mol$_x$·C-mol$_s^{-1}$ reported for this microalgal species (Blanken et al., 2016) and it will be used for further calculations. The maximal $Y^{het}_{x/s}$ for aerobic heterotrophic organisms is 0.7 mol$_x$ mol$_s^{-1}$ and it is bound by thermodynamic constraints (Heijnen, 1994). A yield of 0.7 C-mol$_x$·C-mol$_s^{-1}$ has also

been found in *Chlamydomonas reinhardtii* (Chen & Johns, 1996) and in *Scenedesmus acuminatus* (Jin et al., 2020), indicating that microalgae are as efficient as other heterotrophic organisms (bacteria and yeasts) in the aerobiotic conversion of substrate into biomass.

Autotrophic reference experiments

The $Y_{x/ph}$ was determined in two strictly autotrophic cultures. The first autotrophic culture was performed after two week of mixotrophic cultivation, called autotrophic 1, while the second experiment, called autotrophic 2, was performed in an independent experiment. All the experiments, including the mixotrophic cultures, were conducted in chemostat at the same dilution rate and light regime.

The two autotrophic cultures reached a stable and identical biomass concentration (C_x) of 0.7 $g \cdot L^{-1}$ and a volumetric biomass production rate (r_c) of 61.4 C-$mmol_x \cdot L^{-1} \cdot day^{-1}$ (Figure 2, table 1). Likewise, all the other parameters measured (table 1) did not shown any statistical difference ($P<0.05$) between the two cultures. These results indicate that the autotrophic 1 was not affected by the previous two weeks of mixotrophic cultivation and that the experimental setup and routines were reproducible. The only exception was the average dry weight-specific optical cross section (a_x) that was the 16% higher in the autotrophic 2 compared to the autotrophic 1. *C. sorokiniana* is known to adjust his a_x in few hours in response to changes in the light regimes (de Mooij et al., 2017), for this reason the difference in a_x between the two autotrophic cultures might have been caused by unknown batch to batch variation rather than to the shift between mixotrophic and phototrophic metabolism.

Figure 2. *Heterotrophic biomass production (dark) and substrate consumption (open) of C. sorokiniana SAG 211-8K cultivated in M8a medium with 100 C-mmol·L^{-1} sodium acetate (circles), and 200 C-mmol·L^{-1} sodium acetate (squares), and 100 C-mmol·L^{-1} glucose (triangles).*

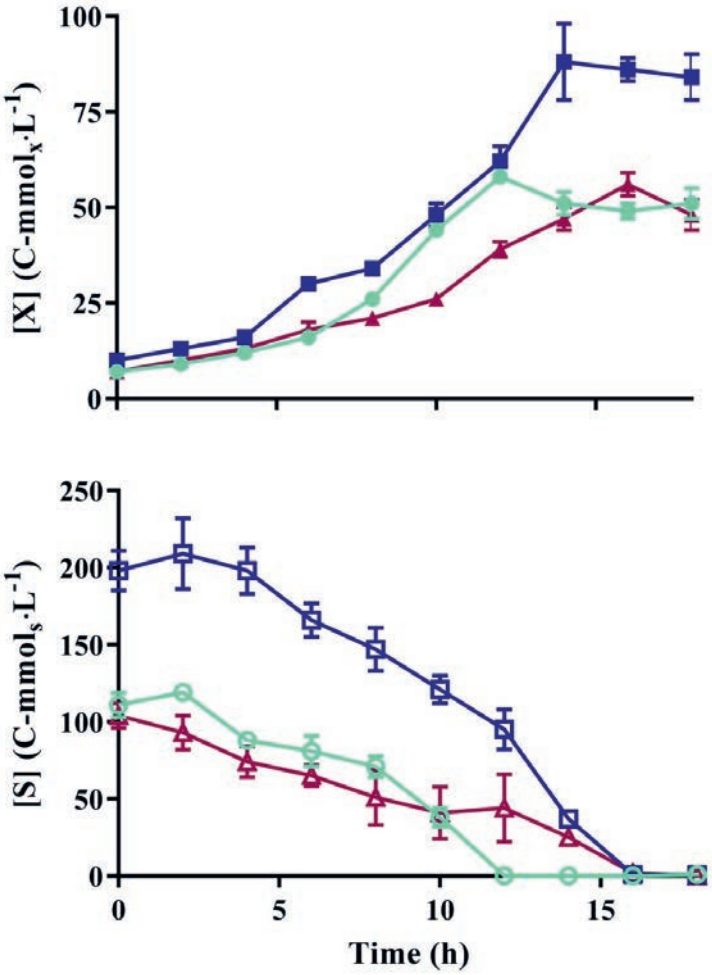

In summary, a $Y_{x/ph}$ of 40.7±0.0 C-mmol$_x$·mol$_{ph}^{-1}$ was obtained in the two autotrophic experiments, which is equivalent to 0.98 g$_x$·mol$_{ph}^{-1}$. This $Y_{x/ph}$ is 33% lower than the maximum reported value (54.2 C-mmol$_x$·C-mol$_{ph}^{-1}$) for this strain (Cuaresma et al., 2011b). We used the light model developed by Evers for cylindrical vessels (Evers, 1991) to estimate the attenuation of the light intensity, caused by cellular light absorption, from the reactor surface toward the reactor center. Details of this calculation are presented in supporting information 2. The model requires as input the biomass concentration (C_x) and a_x. The values reported in table 1 were used to calculate the light gradient for each condition tested. The model clearly indicates that, in all the conditions tested, over 64% of culture volume was experiencing a light level below 10 μmol m^{-2} s^{-1} which we assumed to be the compensation point of photosynthesis (Blanken et al., 2016). Under this light regime suboptimal $Y_{x/ph}$ is expected since the culture spends a relevant part of the light absorbed for maintenance purposes rather than for growth, lowering the overall biomass yield on light. Despite being suboptimal, this light regime is within the range of light conditions prevalent within outdoor *PBRs*. For example, tubular *PBRs* have diameters between 5 and 9 cm and are operated at biomass concentrations of 1.3 to 2.1 g$_x$·L^{-1} (Acién et al., 2012; Ruiz et al., 2016). In *PBRs*, yields of 0.6 to 0.8 g$_x$·mol$_{ph}^{-1}$ have been obtained, similar to the one reported in this study. Furthermore, outdoor vertical *PBRs*, experience maximal incident light intensities close to the light intensity tested in our study (Cuaresma et al., 2011b), making our study comparable to outdoor microalgae production. Nevertheless, a direct extrapolation of the present work to large scale outdoor production is complicated and is beyond the scope of this study.

Mixotrophic growth and oxygen balance

In the two mixotrophic experiments the carbon based volumetric biomass production rate (r_c) was the double of the autotrophic references (Figure 3, table 1). We indeed expected that in a

mixotrophic culture the presence of two energy sources (light and reduced organic carbon) would lead to a significant increase of productivity (Turon et al., 2015c; Wang et al., 2014). The extent of this increase can be quantified assuming that in mixotrophy, the autotrophic and the heterotrophic metabolism can proceed non-competitively and that the overall growth is the sum of the two metabolisms. In the next section we will elucidate in detail this hypothesis.

The volumetric biomass production rate in mass units (r_x) also doubled under mixotrophy in comparison to autotrophy because the biomass carbon content was constant under all conditions tested (51-54 % $w_c \cdot w_x^{-1}$, Table 1). Biomass productivity is the product of biomass concentration

Figure 3. *Volumetric carbon based biomass production rate (r_c) of C. sorokiniana SAG 211-8K grown mixotrophically with gas exchange (diamonds) and without gas exchange (triangles). Also included are two autotrophic reference cultures: autotrophic 1 (squares), which was carried out immediately after 2 weeks of mixotrophic growth, and autotrophic 2 (circles), which was carried out as a second independent experiment. The dashed line indicates the average r_c in mixotrophic cultivation (top) and in the two autotrophic cultures (bottom).*

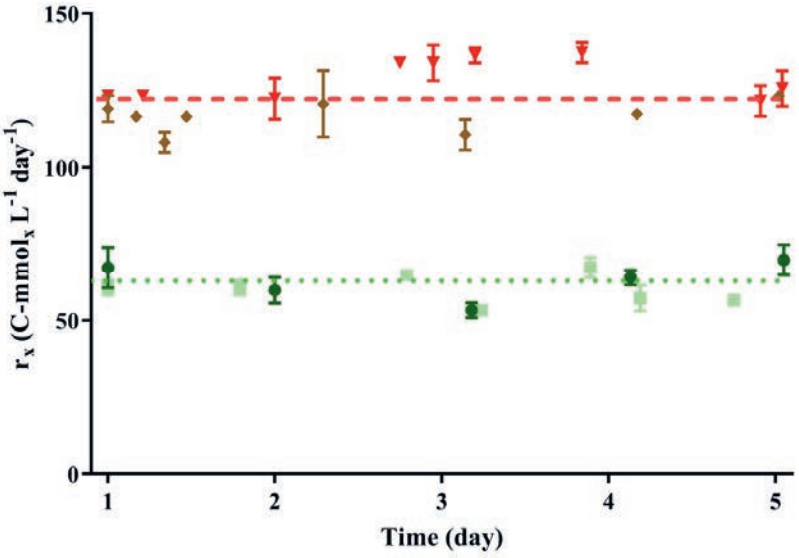

and dilution rate. This implies that at steady state and constant dilution rate, biomass productivity can only be doubled by doubling biomass concentration. The mixotrophic experiment with gas exchange and the two autotrophic experiments were performed at an identical dilution rate and, as expected, the biomass concentration of the mixotrophic experiment with gas exchange was about the double the autotrophic cultures. Unfortunately, this was not the case in the mixotrophic culture without gas exchange were the biomass productivity was doubled but the biomass concentration was only 46% higher than the autotrophic reference. This discrepancy can be explained having a close look to the dilution rate (*D)*. The *D* was comparable among the cultures with gas exchange, while it was 22% higher in the mixotrophic culture without gas exchange (table 1). The different *D* has been caused by the outlet pump that operated at constant rpm. In the culture with gas exchange the outlet pump was removing a mixture of liquid and gas. Instead, without gas exchange, only the liquid phase was pumped out of the reactor, increasing the volume removed from the reactor per rpm of the outlet pump. Dissolved oxygen and biomass concentration over the entire experiment 1 and 2 are reported in supporting information 3.

A surprising result was that in the two mixotrophic experiments all the substrate was completely converted into biomass, resulting in a mixotrophic biomass yield on substrate ($Y^{mixo}_{x/s}$) of 1 (table 2). This finding implies the absence of CO_2 production. Such hypothesis was verified in the mixotrophic experiment without gas exchange, where the CO_2 production rate (r_{CO2}, C-mol·L^{-1}·day^{-1}) can be estimated by measuring the total inorganic carbon concentration (*TIC*, C-mol·L^{-1}) in the liquid phase:

$$r_{CO2} = (TIC_{out} - TIC_{in}) \cdot D \quad (7)$$

Table 1. *Overview of the off-line, DO, D measurements on the cultivation of C. sorokiniana SAG 211-8K under autotrophic conditions, and under mixotrophic conditions with and without gas exchange.*

	Unit	Mixo with gas exchange	Mixo without gas exchange	Autotrophic 1	Autotrophic 2
DO	Air saturation %	92.3±1.9^{a}	141.8±5.4^{b}	135.7±2.6^{c}	132.7±1.6^{c}
TIC_{in}	C-mmol L^{-1}	n.d.	0.04±0.02	n.d.	n.d.
TIC_{out}	C-mmol L^{-1}	n.d.	3.73±0.45	n.d.	n.d.
Cx	$g_x \cdot L^{-1}$	1.41±0.07^{a}	1.16±0.06^{b}	0.70±0.07^{c}	0.70±0.06^{c}
D	day^{-1}	1.94±0.00^{a}	2.44±0.00^{b}	2.07±0.00^{a}	2.11±0.00^{a}
r_x	$g \cdot L^{-1} \cdot day^{-1}$	2.74±0.07^{a}	2.78±0.06^{a}	1.41±0.07^{b}	1.48±0.06^{b}
$C_{\%}$	% $w_c \cdot w_x^{-1}$	51.0±2.8^{a}	54.2±2.5^{b}	51.1±1.4^{a}	50.8±2.4^{a}
Cell volume	$\mu m^3 \cdot cell^{-1}$	23.6±1.1^{a}	22.8±3.3^{a}	39.5±5.7^{b}	33.5±3.0^{b}
a_x	$m^2 \cdot kg^{-1}$	249±11^{a}	271±13^{a,b}	272±11^{b}	323±30^{c}
Chl/Car		0.53±0.00^{a}	0.55±0.00^{b}	0.60±0.00^{c}	0.60±0.00^{c}
QY	F_v/F_m	0.70±0.00^{a}	0.77±0.01^{b}	0.77±0.01^{b}	0.77±0.01^{b}

Along the rows the same letter indicates no significant differences (P>0.05).
Not determined (n.d.)

Table 2. *Carbon mass balance of C. sorokiniana SAG 211-8K grown mixotrophically with and without gas exchange. The value predicted by the summation of autotrophic and heterotrophic stoichiometry assuming oxygen balance are reported as comparison. Yields are expressed as C-mol$_x$·C-mol$_s^{-1}$ while all the other parameters are expressed as C-mmol·L^{-1}·day^{-1}.*

	Mixo with gas exchange	Mixo without gas exchange	Prediction
$r_{c,mixo}$	116.3±0.0	127.9±0.0	136.9
$Cs \cdot D$	3.2±0.2	0.0±0.0	-
r_s	-111.5±0.2	-126.5±3.3	-151.8
$r_{c,het'}$	54.8±0.0	66.5±0.0	75.9
$Y^{het'}_{x/s}$	0.46±0.00	0.53±0.00	0.5
r_{CO2}	n.d.	9.0±0.0	14.9
$Y^{mixo}_{x/s}$	1.04±0.00	1.01±0.00	0.90
$Y^{mixo'}_{x/s}$	n.d.	0.94±0.00	

Not determined (n.d.)

Where (TIC_{in}) and (TIC_{out}) are the total inorganic carbon concentration in the inlet and outlet medium. The TIC_{in} was measured once in medium in equilibrium with air and assumed constant over the whole experiment, while the TIC_{out} was measured daily. The TIC_{in} was about 2 orders of magnitude smaller than the TIC_{out} (table 1), clearly indicating CO_2 production (table 2). The r_{CO2} calculated was used to correct the mixotrophic yield on substrate ($Y^{mixo*}_{x/s}$, C-mol$_x$·C-mol$_s^{-1}$) according to the following formula:

$$Y_{x/s}^{mixo*} = \frac{P_c - P_{co2}}{P_s} \quad (8)$$

Using this correction, the $Y^{mixo}_{x/s}$ in the mixotrophic culture without gas exchange decreased from 1 to 0.94 C-mol$_x$·C-mol$_s^{-1}$, which fits with our expectations as explained later

Complete substrate conversion cannot be excluded in the mixotrophic experiment with gas exchange. A close look to the volumetric substrate consumption rate (r_s) (table 2) reveals that in the mixotrophic experiment with gas exchange r_s was 16% lower than in the mixotrophic without gas exchange. In the experiment with gas exchange r_s was empirically adjusted to maintain the *DO* constant around the value measured in the same conditions with only medium. In this empirical approach, the provided feeding rate might not have been enough to balance

the photosynthetic oxygen production rate, but instead it might have balanced photosynthetic carbon dioxide consumption. Using the stochiometric equations 9, 10 and 11 that will be presented in next section, it is possible to predict the net oxygen production rate in the scenario case of CO_2 balance. We calculated a rate of 13.3 mmol O_2 L^{-1} day^{-1}. Although this is a plausible scenario, oxygen production did not result in a significant increase of the *DO*. Possibly the increase in *DO* was too low to be detected.

In our mixotrophic experiments, we were able to reach almost complete substrate to biomass conversion. This is much higher than the biomass yield on substrate ($Y^{mixo}_{x/s}$) of 0.5-0.7 C-mol_x·C-mol_s^{-1} that are generally reported in mixotrophic experiments operated in batch (Li et al., 2014; Sforza et al., 2018). Our higher performance can be explained looking at the mixotrophic stoichiometry (see next section). In an oxygen balanced mixotrophic culture, the autotrophic and the heterotrophic metabolisms are operating concurrently almost at the same rate, equally contributing to the overall energetics of the cell. Previous studies on mixotrophic cultivation (Li et al., 2014; Sforza et al., 2018) were often unbalanced with a larger heterotrophic contribution to the mixotrophic growth in comparison to autotrophic metabolism. Under this condition, the heterotrophic metabolism dominates, and the culture produces CO_2 at a higher rate compared to the photosynthetic needs. In contrast to these batch approaches, Barros et al. (Barros et al., 2017) applied a fed-batch and reached a higher $Y^{mixo}_{x/s}$. In this work the acetic acid supply was added stepwise and coupled to the incident solar radiation to ensure that excess organic carbon substrate did not accumulate in the culture medium. Using this approach, the authors obtained a $Y^{mixo}_{x/s}$ of 0.94 C-$mmol_x$·C-mol_s^{-1}, which is equal to the yield found in our mixotrophic culture without gas exchange.

In the mixotrophic experiment without gas exchange we demonstrated that is possible to regulate and maintain constant dissolved oxygen (*DO*) levels by automatically regulating substrate feeding. Using this approach, the reactor was operated for several days without any

gas exchange. Furthermore, in automated feeding the substrate was completely consumed, while when the substrate was fed at a constant rate the 3% of the supplied substrate was not consumed (table 2). The better performance of the automatic feeding can be explained by looking at the regular fluctuations of the *DO* around the pre-set value (supporting information 3). These fluctuations were caused by the variation in the substrate feeding rate (r_S), that increased when the *DO* exceeded the pre-set value. Most likely this increase in *DO* was a sign of complete substrate consumption.

The *DO* is often used to dose the substrate supply in heterotrophic fed-batch cultivations (Schmidt et al., 2005), but this feeding strategy is not commonly used in mixotrophic cultivation of microalgae. Ganuza et al. in a patent application (Ganuza et al., 2015) claimed to automatically control *DO* and pH by adjusting the acetic acid and the CO_2 feeding rate. The authors claimed to couple *DO* and pH control by feeding acetic acid when *DO* and pH simultaneously exceeded the set point, while CO_2 was provided to lower the pH when only the pH exceeded the set pH. Although the *DO* can be successfully controlled using this strategy, coupling pH and *DO* control has some limitations. For example, this strategy can only be applied when the overall stoichiometry of the process consumes protons (e.g. when nitrate is used as nitrogen source). In addition, the substrate must be an organic acid with a pKa lower than the pH of the culture (e.g. acetic acid to control the pH around neutrality). In our process, by decoupling pH and *DO* control, these limitations are solved allowing to use any type of substrate (e.g. glucose) and to cultivate any type of mixotrophic microalgae (e.g. acidophilic strains).

Mixotrophic growth stoichiometry and interaction between heterotrophic and autotrophic metabolism

In this section we will describe mixotrophic growth stoichiometry and we will investigate the hypothesis that the mixotrophic metabolism is the sum of the heterotrophic and autotrophic metabolisms. According to this hypothesis mixotrophic stoichiometry can be split in two components:

1) A heterotrophic component in which an organic substrate is partly oxidized to derive energy to support biomass growth (catabolism), and partly used as a building block for growth (anabolism). In the overall reaction CO_2 is produced and O_2 consumed
2) An autotrophic component in which light is used as energy source, CO_2 is consumed and used as a building block, while O_2 is produced as a waste product

To describe the stoichiometry of autotrophic and heterotrophic cultivations, the biomass elemental composition, the heterotrophic biomass yield on substrate ($Y^{het}_{x/s}$), and the autotrophic biomass yield on light ($Y_{x/ph}$) need to be known. If the mixotrophic metabolism is the sum of the heterotrophic and autotrophic metabolisms, the yield factors can be assumed to be constant regardless of the trophic mode. The elemental biomass composition of $CH_{1.62}O_{0.41}N_{0.14}P_{0.01}$ reported by Kliphuis et al. (Kliphuis et al., 2012) was used as reference. The $Y^{het}_{x/s}$ and $Y_{x/ph}$ were measured in this study and were respectively 0.50±0.04C-$mol_x \cdot$C-$mol_s^{-1}$and 40.7±0.0 C-$mmol_x \cdot mol_{ph}^{-1}$.

It has to be stressed that these numbers reflect nutrient replete growth conditions using ammonia as nitrogen source. Under nitrogen limited conditions storage compounds such as carbohydrates and lipids accumulate and the relative contribution of proteins in algal biomass decreases. Consequently the elemental composition and the growth stoichiometry will change. At the same time algal growth rates decline. An analysis of mixotrophy under these specific conditions were outside of the scope of our study.

The autotrophic stoichiometry, given a light input of 1.5 $mol_{ph}\cdot L^{-1}\cdot day^{-1}$can be written as:

$$61.0 \cdot CO_2 + 8.5 \cdot NH_4^+ + 0.7 \cdot H_2PO_4^- + 35.6 \cdot H_2O + 1.5 \cdot 10^3 \cdot photons \rightarrow$$

$$61.0\ CH_{1.62}O_{0.41}N_{0.14}P_{0.011} + 67.7 \cdot O_2 + 7.9 \cdot H^+ \qquad (9)$$

Where all stoichiometric coefficients reflect volumetric rates in $mmol\cdot L^{-1}\cdot day^{-1}$ observed in the photobioreactor (*PBR*). Similarly, the heterotrophic stoichiometry can be set up where the oxygen consumption is set equal to the oxygen production according to the autotrophic part of the metabolism shown above:

$$151.8 \cdot CH_2O + 67.7 \cdot O_2 + 10.6 \cdot NH_4^+ + 0.8 \cdot H_2PO_4^- \rightarrow 75.9\ CH_{1.62}O_{0.41}N_{0.14}P_{0.011} + 107.5 \cdot H_2O + 75.9 \cdot CO_2 + 9.8 \cdot H^+ \quad (10)$$

Adding up the autotrophic to the heterotrophic stoichiometry the following overall reaction equation is obtained reflecting mixotrophic growth under O_2 balance:

$$151.8 \cdot CH_2O + 19.2 \cdot NH_4^+ + 1.5 \cdot H_2PO_4^- + 1.5 \cdot 10^3 \cdot photons \rightarrow 136.9\ CH_{1.62}O_{0.41}N_{0.14}P_{0.011} + 71.9 \cdot H_2O + 14.9 \cdot CO_2 + 17.7 \cdot H^+ \quad (11)$$

Also, in this equation the stoichiometric coefficients reflect the volumetric rates in $mmol\cdot L^{-1}\cdot day^{-1}$ expected in the *PBR*.

According to the mixotrophic stoichiometry the volumetric biomass production rate ($r_{c,mixo}$) was expected to be 136.9 $mmol\cdot L^{-1}\cdot day^{-1}$. This value closely matches the $r_{c,mixo}$ of 127.9 $mmol\cdot L^{-1}\cdot day^{-1}$ found in the mixotrophic culture without gas exchange. In the mixotrophic with gas exchange the biomass production rate was 116.3 $mmol\cdot L^{-1}\cdot day^{-1}$, which is 15% lower than the expected value (table 2). The lower performance of the mixotrophic with gas exchange can be explained by a lower substrate consumption rate (r_s), which can be attributed to the empirical approach used to set the feeding rate, as discussed in the previous section.

In order to correct for the different r_s, we calculated the fraction of biomass heterotrophically produced during the mixotrophic growth ($r_{c,het'}$, $C\text{-}mol_x\cdot L^{-1}\cdot day^{-1}$). The $r_{c,het'}$ was calculated by subtracting the autotrophic biomass productivity ($r_{c,auto}$) to $r_{c,mixo}$. The $r_{c,het'}$ was then used to

calculate the heterotrophic yield on substrate occurring in mixotrophy ($Y^{het'}_{x/s}$) according to the equation:

$$Y^{het\prime}_{x/s} = \frac{r_{C,het}}{S_c} \quad (12)$$

A close look at the numbers in table 2 reveals that $Y^{het'}_{x/s}$ in both the mixotrophic experiments was equal to the biomass yield on substrate found in the heterotrophic reference experiment, supporting our hypothesis that the mixotrophic stoichiometry is the sum of the heterotrophic and autotrophic metabolism.

The finding that mixotrophy can be described as the sum of heterotrophic and autotrophic metabolisms, implies that photosynthesis is not affected by the presence of organic substrate. In our experiments the effect of organic carbon on photosynthesis was assessed by measuring the photosynthetic efficiency of PSII directly as the quantum yield (QY) and by measuring the average dry weight-specific optical cross section (a_x). In the mixotrophic culture without gas exchange the QY was 0.77, the same value found in the two autotrophic cultures (table 1), indicating that photosynthesis is not affected by the presence of organic substrate. In the mixotrophic culture with gas exchange the QY was 0.70. Despite this value is lower than the QY under the other conditions a QY of 0.70 still indicate optimal PSII performance (de Mooij et al., 2017).

The average dry weight-specific optical cross section (a_x) obtained in all the experiments falls in the range that is normally observed in mass culture for this strain (de Mooij et al., 2017). Also, a_x was constant along the all experiments regardless of the trophic mode; a further indication that the heterotrophic and autotrophic metabolism can operate concurrently without affecting each other.

The absorption spectra recorded to calculate the average dry weight-specific optical cross section were also used to detect possible changes in pigment ratios when shifting from autotrophy to mixotrophy. Chlorophylls have an absorption maximum at both 400-500 nm and

600-700 nm, while carotenoids only have an absorption maximum between 400-500 nm. Thus the ratio between light absorbed at 600-700 nm (Chlorophylls) and at 400-500 nm (Carotenoids) (*Chl/Car*) can be used as a proxy for the relative chlorophyll abundance within the pigment pool. The mixotrophic cultures had a lower *Chl/Car* than the autotrophic cultures, this might indicate either a lower chlorophyll abundance in total pigments or a higher carotenoids content. In conclusion, we do not exclude that the presence of organic carbon might have some effect on pigment composition as reported in other studies (Grama et al., 2016; Wilken et al., 2014; Yang et al., 2000), but according to our results these changes are not affecting the overall photosynthetic activity.

The finding that mixotrophy can be described as the sum of the heterotrophic and autotrophic metabolism allowed us to conduct a sensitivity analysis on the effect of the elemental biomass composition, $Y_{x/ph}$ and $Y^{het}_{x/s}$ on the oxygen balanced mixotrophic productivity. The effect on an increase of $Y_{x/ph}$ and $Y^{het}_{x/s}$ on the volumetric biomass productivity (r_C) is reported in the figure 4. The results indicate that an increase in $Y_{x/ph}$ is not affecting the ratio between $r_{c,auto}$ and $r_{c,het}$ and leads to a linear increase of $r_{c,mixo}$. On the contrary, an increment in $Y^{het}_{x/s}$ changes the ratio between $r_{c,auto}$ and $r_{c,het}$ and dramatically increases the contribution of $r_{c,het}$ on the overall oxygen balanced mixotrophic growth leading to an exponential increase of $r_{c,mixo}$. According to our sensitivity analysis, the cultivation of a microalgal strain with high $Y^{het}_{x/s}$ might lead to quadruplicate $r_{c,mixo}$ that is the maximum biomass increase expected in an oxygen balanced mixotrophic culture.

Figure 4. *Sensitivity analysis on the effect of (a) the biomass yield on photons ($Y_{x/ph}$) and (b) the heterotrophic biomass yield on substrate ($Y^{het}_{x/s}$) on the oxygen balanced mixotrophic biomass productivity ($r_{c,mixo}$, square). The contributions of autotrophic ($r_{c,auto}$, circle) and heterotrophic ($r_{c,het}$, triagle) metabolisms to the mixotrophic volumetric biomass productivity are reported separatly. A constant $Y^{het}_{x/s}$ was assumed in the simulation of the effect on an increase in $Y_{x/ph}$. Vice versa, a constant $Y_{x/ph}$ was assumed in the simulation of the effect of on an increase in $Y^{het}_{x/s}$. As starting point, the $Y^{het}_{x/s}$ and $Y_{x/ph}$ found in this work were used.*

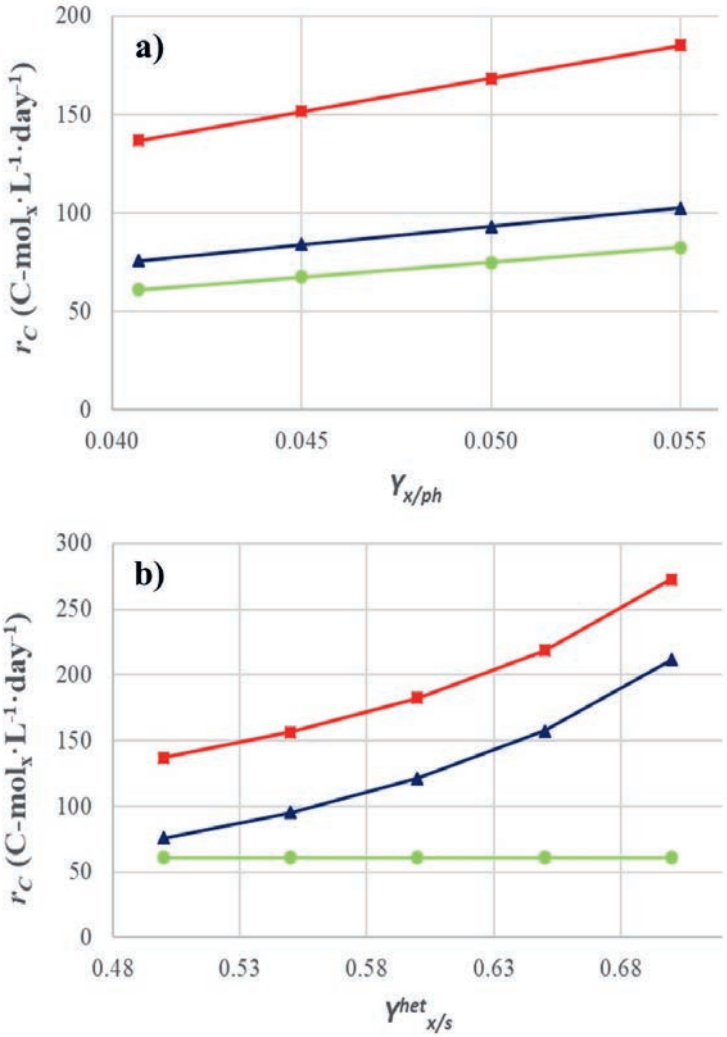

CONCLUSIONS

In the present work, and to the best of our knowledge, a mixotrophic microalgae monoculture was grown for the first time for several days in a closed *PBR* without net oxygen production and CO_2 consumption, allowing the system to operate without any gas exchange. Under this condition, mixotrophic stoichiometry could be described as the sum of heterotrophic and autotrophic stoichiometry and the overall biomass productivity was the exactly the sum of the two metabolisms. The presence of two complementary growth modes within a microalgal monoculture led to doubled biomass productivity and doubled biomass concentration in comparison to an autotrophic reference. Furthermore, the 94% of the substrate was converted into biomass, making the process close to carbon neutral. Our results indicate that mixotrophy is a successful strategy to increase microalgae biomass concentration.

NOMENCLATURE

Abbreviations	
DO	Dissolved oxygen concentration (% air saturation)
PBR	Photobioreactor
PFD	Photon flux density ($\mu mol \cdot m^{-2} \cdot s^{-1}$)
PAR	Photo active radiation, 400-700 nm
TIC	Total inorganic carbon ($C\text{-}mol \cdot L^{-1}$)
Symbols	
$Y_{x/s}$	Biomass yield on substrate ($C\text{-}mol_x \cdot C\text{-}mol_s^{-1}$)
OD_{750}	Optical density at 750 nm
C_x	Biomass dry weight concentration ($g_x \cdot L^{-1}$)
MW_x	Biomass molecular weight ($g_x \cdot C\text{-}mol_x^{-1}$)
μ	Specific growth rate (h^{-1})
V_{PBR}	Photobioreactor working volume (L)
A_{PBR}	Photobioreactor illuminated area (m^2)
r_x	Volumetric biomass production rate ($g_x \cdot L^{-1} \cdot day^{-1}$)
r_c	Carbon based volumetric biomass production rate ($C\text{-}mol_x \cdot L^{-1} \cdot day^{-1}$)
D	Dilution rate (day^{-1})
$Y_{x/ph}$	Biomass yield on light ($C\text{-}mol_x \cdot mol_{ph}^{-1}$)
r_s	Substrate consumption rate ($C\text{-}mol_s \cdot L^{-1} \cdot day^{-1}$)
F_{AA}	Acetic acid supply rate ($L \cdot day^{-1}$)
$C_{s,AA}$	Acetic acid concentration in the stock solution ($C\text{-}mol_s \cdot L^{-1}$)
C_s	Acetic acid concentration in the reactor ($C\text{-}mol_s \cdot L^{-1}$)
a_x	Average dry weight-specific optical cross section ($m^2 \cdot g^{-1}$)
$C_{\%}$	Biomass carbon content ($\%\ w_c \cdot w_x^{-1}$)
r_{CO2}	CO_2 production rate ($C\text{-}mol \cdot L^{-1} \cdot day^{-1}$)
Chl/Car	Ratio between light absorbed at 600-700 nm (Chlorophylls) and at 400-500 nm (Carotenoids)
Sub/super script	
auto	autotrophic
het	heterotrophic
het'	heterotrophic fraction of the mixotrophic biomass
mixo	mixotrophic
ph	PAR photons
x	Biomass
s	Substrate

SUPPORTIN INFORMATIONS

Supporting information 1: Medium composition

Modified M-8 medium was prepared as follows (composition expressed in mmol·L^{-1}): 5.4 KH_2PO_4; 1.5 $Na_2HPO_4 \cdot 2\ H_2O$; 1.6 $MgSO_4 \cdot 7H_2O$; 0.09 $CaCl_2 \cdot 2H_2O$; 28.8 $ClNH_4$; 0.3 EDTA ferric sodium salt; 0.1 $Na_2EDTA \cdot 2\ H_2O$; $1 \cdot 10^{-3}$ H_3BO_3; $65.6 \cdot 10^{-3}$ $MnCl_2 \cdot 4\ H_2O$; $11.1 \cdot 10^{-3}$ $ZnSO_4 \cdot 7\ H_2O$; $7.3 \cdot 10^{-3}$ $CuSO_4 \cdot 5H_2O$. To prevent foaming, we added 0.05% v/v Antifoam B silicone emulsion (Mallinckrodt Baker B.V, The Netherlands). The pH was adjusted to 6.7 with a concentrated solution of NaOH.

Supporting information 2: Calculation of light gradient in the photobioreactor

The light gradient inside the photobioreactor was estimated using Lambert Beers' law and the geometrical relationship derived for cylindrical vessels by Evers (1991). The cylindrical vessel was considered evenly illuminated and the light field was considered to isotropic. The spectral composition of the light is not incorporated in the model and we used the spectrally averaged absorption coefficient. Attenuation of light intensity at a given point of the reactor ($I_{ph}(r)$, µmol·m^{-2}·s^{-1}) caused by cellular light absorption was calculated as follow:

$$I_{ph}(r) = \frac{I_{phin}}{\pi} \left[\int_0^{\pi} exp\left[-a_x \cdot C_x \cdot [(R-r) \cdot \cos(\Theta) + (R^2 - (R-r)^2 \cdot \sin(\Theta)^2]^{0.5}\right]\right] d\Theta] \qquad (S1)$$

Where I_{in} is light intensity at the surface of the cylindrical vessel (µmol·m^{-2}·s^{-1}), r the distance from vessel surface (m), R the vessel radius (m), Θ is the angle of light path with line trough vessel center, a_x the average dry weight-specific optical cross section ($m^2 \cdot g^{-1}$) and C_x the biomass dry weight concentration ($g_x \cdot L^{-1}$). The light gradient in the mixotrophic culture with and without gas exchange and in the two autotrophic cultures was calculated using the C_x and a_x originated from the actual experiments described in this paper (Table 1). The light gradient was used to calculated at which radial position of the photobioreactor (r_{dark}, m) the light intensity drops below the compensation point. The r_{dark} was used to calculate the volume

fraction of the vessel in the photic zone with net growth (V_{light}, L), and the dark zone with biomass loss because of maintenance respiration (V_{dark}, L), according to:

$$V_{light} = \frac{[\pi \cdot R^2 - \pi \cdot (R - r_{dark})^2]}{\pi \cdot R^2} \quad \text{(S2)}$$

$$V_{dark} = 1 - V_{light} \quad \text{(S3)}$$

According to equations S1, S2 and S3, V_{dark} was estimated to be 64%, 70%, 78% and 80% respectively in the autotrophic 1, autotrophic 2, mixotrophic without gas exchange and in the mixotrophic with gas exchange.

Supporting information 3: Dissolved oxygen and biomass concentration over the entire experiment 1 and 2

Dissolved oxygen (*DO*, % air saturation, blue line) and biomass concertation (C_x, $g_x \cdot L^{-1}$, red circles) over the entire experiment 1 and 2. The boxes indicated adaptation periods excluded from the calculations.

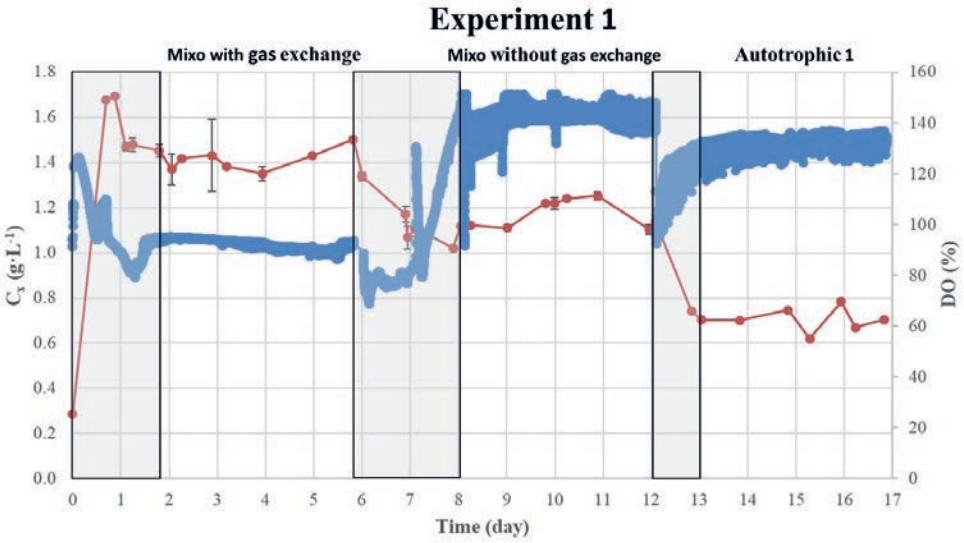

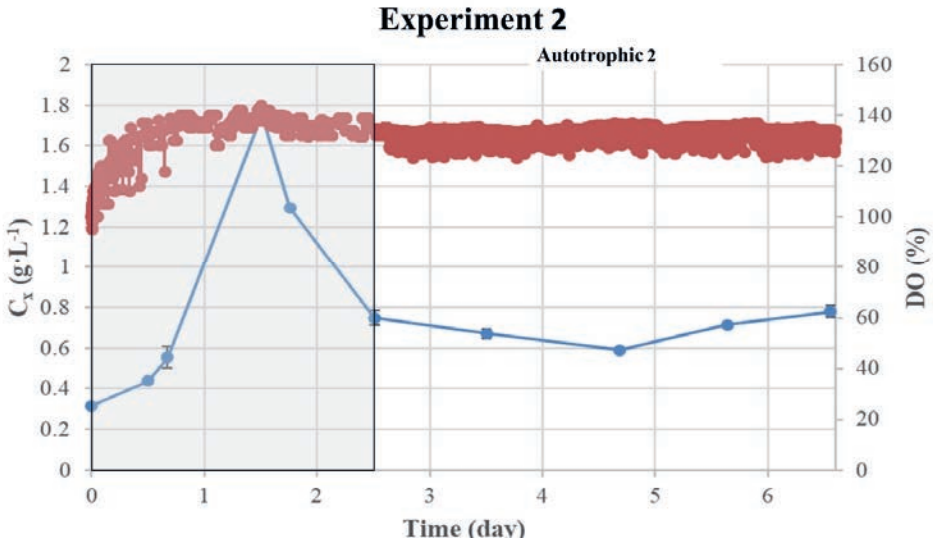

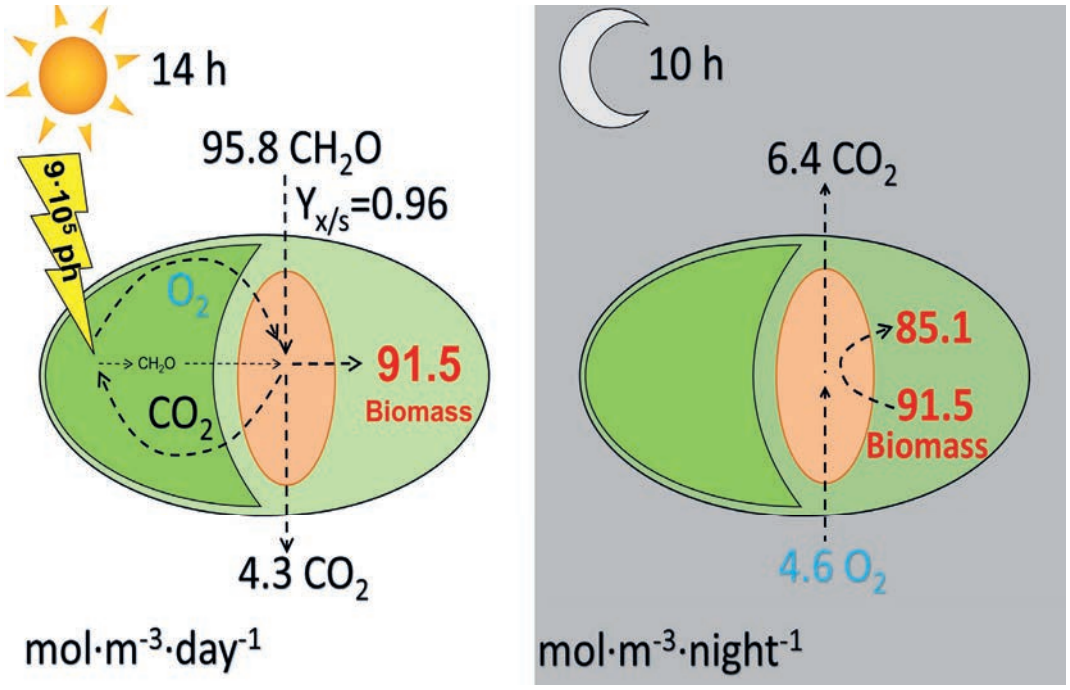
14 h
95.8 CH_2O
$Y_{x/s}$=0.96
9.10^5 J/h
O_2
CH_2O
CO_2
91.5
Biomass
4.3 CO_2
mol·m^{-3}·day^{-1}
10 h
6.4 CO_2
85.1
91.5
Biomass
4.6 O_2
mol·m^{-3}·night^{-1}

Chapter 3

Oxygen Balanced Mixotrophy Under Day-Night Cycles

This chapter has been published as:
Fabian Abiusi, Rene H. Wijffels, Marcel Janssen.
Oxygen Balanced Mixotrophy Under Day-Night Cycles

ACS Sustainable Chem. Eng. 2020, 8, 11682−11691

ABSTRACT

Using sunlight to fuel photosynthesis exposes microalgae to day-night cycles. Under day-night cycles microalgae tend to synchronize their metabolism by optimizing light utilization during daytime. During night storage compounds are consumed, leading to biomass losses and demand of O_2. We investigated 'oxygen balanced' mixotrophy under14:10 day: night cycles. In this mixotrophic setup, photosynthetic O_2 production was balanced by respiratory oxygen consumption and CO_2 required for photosynthesis was provided by aerobic conversion of acetic acid. This strategy allowed operation of the reactor without any gas-liquid exchange during daytime. Under these conditions *Chlorella sorokiniana* SAG 211-8K converted 96% of the substrate into biomass. Mixotrophic cultivation did not affect the photosystem II maximum quantum yield (F_v/F_m) or pigment contents of the microalgal cells. Mixotrophic biomass contained 50% w/w of protein and 7.3 $mg \cdot g^{-1}$ of lutein.

Acetic acid feeding was discontinued at night and aeration initiated. Respiration was monitored by on-line off-gas analysis and O_2 consumption and CO_2 production rates were determined. Biomass night losses were around 7% on carbon basis with no significant difference between mixotrophic and photoautotrophic cultures. Over 24 h, the mixotrophic culture required 61 times less gaseous substrate and its biomass productivity was doubled compared to the photoautotrophic counterpart.

Keywords: Circadian rhythms, lutein, microalgae productivity, biomass yield on substrate, photosynthetic efficiency, gas-liquid transfer, oxygen balance, carbon balance.

INTRODUCTION

The continuous growth of the human population is placing an increasing pressure on our limited natural resources. Producers are facing more challenges to meet the growing food demand, there is competition for arable land, fresh water, and energy while simultaneously an urgent need to reduce the negative impact of agriculture on the environment (Godfray et al., 2010).

Microalgae are regarded as one of the most nutritious foods known to man (García et al., 2017). Microalgae can provide a significant number of essential nutrients, such as vitamins, minerals, pigments and essential fatty acids and amino acids, to support human health (García et al., 2017; Lupatini et al., 2017). The high protein content (even >70%) (Lupatini et al., 2017) and quality, especially in relation to the composition and digestibility of amino acids (Becker, 2007) makes microalgae a promising novel source of proteins.

Microalgae can reach higher areal productivity than terrestrial plants, do not require arable land or fresh water (Wijffels & Barbosa, 2010), and they can use fertilizers with almost 100% efficiency (Tredici, 2010). Further research is needed to better understand the microalgal metabolic flexibility to be able to improve the production process aiming for a higher productivity, simpler reactor design, and lower energy requirement.

One of the strategies to decrease microalgae production costs is utilizing mixotrophic cultivation. In this trophic mode, light and organic carbons are simultaneously exploited and both chemoheterotrophic (henceforth referred to as heterotrophic) and photoautotrophic (henceforth referred to as autotrophic) metabolisms operate concurrently within a single microalgal monoculture. We recently designed an ‘oxygen balanced’ mixotrophic cultivation method which doubled microalgae productivity under continuous light and operation (Abiusi et al., 2020a). We demonstrated that dissolved oxygen concentration (*DO*) can be controlled by adjusting acetic acid supply rate with the rate of photosynthesis. In ‘oxygen balanced’ mixotrophy the O_2 required for aerobic heterotrophic growth was supplied by oxygenic

photosynthesis. Vice versa, the CO_2 needed to carry out photosynthesis was provided by the heterotrophic metabolism. This internal CO_2 recirculation converted 94% of substrate into biomass, making the process close to carbon neutrality. Due to internal gas recirculation the photobioreactor (*PBR*) was operated without any gas-liquid exchange therefore saving the power otherwise needed for aeration. Moreover, presence of two energy sources, light and reduced organic carbon, doubled biomass productivity and concentration.

The light energy needed to fuel photosynthesis can be provided by the sun or with the employment of lamps. Cultivation of microalgae on artificial light requires substantial energy input that increases production costs and decreases sustainability of the process (Blanken et al., 2013). Sunlight is free and abundant. However, the use of sunlight exposes microalgae to day-night cycles and seasonal change on the light pattern.

In most photosynthetic organisms, part of the carbon fixed during the light period, is accumulated in storage compounds (e.g. carbohydrates or lipids). During the night, in absence of light, storage compounds are used to support cell division (León-Saiki et al., 2017). The metabolic energy required is created by respiration and, for this reason, oxygen must be supplied in the night. Cell division is usually completed during the first hours after sunset (de Winter et al., 2017a; León-Saiki et al., 2017), after which energy is expected to be mainly consumed for non-growth related processes defined as maintenance (Pirt & Hinshelwood, 1965). Thus, microalgal energy consumption, and with it microalgal oxygen demand, is not expected to be constant throughout the night. Furthermore, the consumption of cellular components leads to a decrease in cell weight, often referred to as biomass losses. Biomass losses in autotrophic culture are typically reported to be between 3 and 8% (Edmundson & Huesemann, 2015; Michels et al., 2014; Ogbonna & Tanaka, 1996) of the biomass produced during the daytime, although losses up to 34% have been reported (Torzillo et al., 1991).

No studies have been carried out to elucidate possible differences on night losses between autotrophic and mixotrophic culture. In a mixotrophic culture, when the organic substrate is completely consumed during daytime, night biomass losses will lead to a decrease of the biomass yield on substrate. Furthermore, respiration requires O_2 and at nighttime aeration is needed to avoid anaerobic conditions. The amount of oxygen that needs to be provided to support nighttime metabolism is essential information for the scale-up of mixotrophic cultivation. The aim of this work therefore is to evaluate the effect of day-night cycles on the 'oxygen balanced' mixotrophy. Specifically, we wanted to investigate the effects of these cycles on the biomass yield on light and the biomass yield on the organic substrate during daytime, and the oxygen consumption and biomass losses during nighttime.

In order to achieve our goals, the model strain *C. sorokiniana* SAG 211-8K was cultivated under day-night cycles and a mixotrophic culture was compared to its autotrophic counterpart. The two cultures were grown in continuous mode with a fixed dilution rate (i.e. chemostat) where the culture was only diluted during daytime and not during the night (cyclostat). During daytime the dissolved oxygen concentration in the mixotrophic culture was controlled by tuning acetic acid supply rate to the rate of photosynthesis. During nighttime, no acetic acid was fed to the mixotrophic culture. In both the mixotrophic and autotrophic cultures the oxygen consumption related to night respiration was measured. Biomass productivity was assessed over the entire day and also the biomass loss during the night was measured. Finally, the protein and pigment contents of the mixotrophic and autotrophic cultures were compared.

MATERIALS AND METHODS

Organism, Media and Cultivation Conditions

Chlorella sorokiniana SAG 211-8K was obtained from the algae culture collection of Göttingen University (SAG) and cultivated in modified M-8 medium (Abiusi et al., 2020a) using ammonium as nitrogen source. Axenic algal cultures were cryopreserved and stored in liquid nitrogen. Before reactor inoculation, cryopreserved cultures were used to inoculate 100 mL of medium in 250 ml flasks placed in an incubator operated at 37° C, 4.5% v/v CO_2 and stirring at 100 rpm with a magnetic rod. In this incubator the flasks were illuminated 24h/24h from below with a warm-white LED (BXRAW1200, Bridgelux, USA) at a photon flux density (*PFD*, µmol m^{-2} s^{-1}) of 500 µmol m^{-2} s^{-1}. The *PFD* was measured with a LI-COR 190-SA 2π PAR quantum sensor.

Photobioreactor Setup and Experiments

Chlorella sorokiniana SAG 211-8K was grown in a 3 L bioreactor (Applikon, The Netherlands) described in more detail in Abiusi et al. (Abiusi et al., 2020a). This reactor had a working volume (V_{PBR}) of 1.946 L. The internal diameter was 0.130 m, while the liquid height was maintained at 0.166 m by a level sensor, resulting in a cylindrical illuminated area (A_{PBR}) of 0.068 m^2. The reactor was operated in cyclical steady state (cyclostat) under day-night cycle. At daytime the reactor was diluted at fixed rate, while the cultures were not diluted during the night. During daytime we aimed to reproduce the dilution rate (D, day^{-1}) of our previous work (Abiusi et al., 2020a). We aimed for a D of 2 day^{-1} when considering only daylight hours, which is equivalent to 1.1 day^{-1} when referencing to the 24 hours day-night period.

The reactor was illuminated from all sides creating a homogenous light field over the cylindrical reactor surface. Light intensity on the reactor surface was measured at 16 fixed points inside the empty reactor obtaining an average *PFD* of 514±17 µmol m^{-2} s^{-1}. Light was provided in

day-night cycle of 14D:10N in 'block' with constant illumination during the day. Previous work (de Winter et al., 2017a) indicated that light provided in 'block' resulted in the same biomass yield on light ($Y_{x/ph}$, C-mol$_x$·C-mol$_s^{-1}$) as in 'sine' wave form. The block approach was preferred over sine due to easier operation and comparison to our previous study.

The reactor was equipped with a dissolved oxygen (*DO*) sensor (VisiFerm DO ECS 225, Hamilton, US). This *DO* sensor was calibrated inside the reactor filled with growth medium at operation temperature (37°C) and pH (6.7). Calibration was done by sparging dinitrogen gas to obtain the 0% *DO* level, and sparging air to obtain the 100% *DO* level. A *DO* of 100% corresponds to 224 μmol·L^{-1} at 37°C. The reactor was kept at 37°C by a heat exchanger inside the reactor vessel. To prevent evaporation, the reactor was equipped with a condenser connected to a cryostat feeding cold water of 2°C. Continuous stirring with a marine impeller at 500 rpm was applied during all experiments. During day, the autotrophic culture was aerated with compressed air enriched with 2% v/v carbon dioxide at a flow rate of 0.5 L·L^{-1}·min^{-1} using mass flow controllers (Smart TMF 5850S, Brooks Instruments, USA) while the mixotrophic culture was not aerated. During night both cultures were aerated with compressed air at a flow rate of 0.1 L·L^{-1}·min^{-1}. The CO_2 content of the compressed air was reduced below detection limit by zeolite adsorption. The pH was controlled at 6.7 during day by automatic base addition (1 M, NaOH) and at 6.8 during night by automatic addition of acid (0.5 M, H_2SO_4).

The reactor was inoculated with an autotrophic culture at a density of 1.0 g$_x$·L^{-1}. A 5% w/w acetic acid solution was supplied at a fixed rate while gassing the reactor with CO_2 enriched air for 5 hours. After this start-up phase the aeration was stopped during daytime resulting in a mixotrophic cultivation without gas exchange, where the supply rate of acetic acid was automatically adjusted to maintain a *DO* of 105%. At nighttime the feeding of acetic acid was stopped. The reactor was operated under these conditions for 9 consecutive days. For the last 4 days, a harvesting vessel was placed into an ice-cooled water bath. The harvesting vessel was

changed daily at the end of the light phase. The harvested culture was mixed well, 10 mL of it was used for dry weight determination, while the remaining culture was collected for pigment analysis. During these 4 days, reactor samples were taken for off-line measurements multiple times a day.

After the first 9 days, acetic acid supply was stopped, aeration re-established, and reactor was operated autotrophically. The autotrophic experiment also lasted for 9 days and during the last 4 days again samples were taken using the same procedure as for the mixotrophic experiment. Cultures were considered at cyclical steady state (cyclostat) when the daily change in biomass concentration over the day:night cycle was constant for at least 3 days. In our previous work (Abiusi et al., 2020a) we demonstrated that a mixotrophic culture can switch to autotrophic metabolism with no effect on photosynthesis. This finding simplified our experimental design as we had no need to stop and restart the experiment to switch between trophic states.

The acid and base solutions, acetic acid solution, and the harvest bottle were placed on analytic balances. The balances, *DO* sensor, temperature probe, pH sensor, mass flow controllers and gas analyzer (see next section) were connected to a data acquisition system interfaced via a computer by means of a virtual instrument (Lab View, National Instruments, USA) allowing for continuous data logging and process control. Culture samples for off-line measurements were taken aseptically from the reactor through a dedicated port. The complete setup, including all the solutions, were sterilized prior the experiment by autoclaving for 60 min at 121˚C.

On-Line Gas Analysis

Oxygen and carbon dioxide concentrations in the off-gas were measured online using a gas analyzer (Servomex 4100, The Netherlands). The gas analyzer was fitted with two sensor modules, a paramagnetic purity transducer to measure oxygen and an infrared 1500 transducer

to measure carbon dioxide. Data from the gas analyzer and the mass flow controllers were collected every 4 seconds and these data were stored per minute as moving average of 15 points. Before the experiment, two wet and dry baselines were measured: one under nighttime conditions (0.1 $L \cdot L^{-1} \cdot min^{-1}$ of air) and one under autotrophic daytime conditions (2/98% v/v CO_2/air at a flow rate of 0.5 $L \cdot L^{-1} \cdot min^{-1}$). The dry baseline was measured by leading the gas inlet directly over the gas analyzer. For the wet baseline the gas inlet was first sparged through the reactor filled with medium and maintained at the same temperature and pH as during the experiment. To minimize water vapor, the off -gas was passed through a condenser which was maintained at 2 °C. After passing the condenser the reactor off-gas was led through a membrane module (gas dryer model MD-110-24P, Perma Pure, USA) in which the reactor gas was further dried before being analyzed. The total gas flow leaving the reactor ($F_{g,out}$, $mol \cdot min^{-1}$) including remaining water vapor (≈ 0.5% v/v) was then calculated as follow:

$$F_{g,out} = F_{g,in} \cdot \left(\frac{X_{O2,db}}{X_{O2,wb}}\right) \qquad (1)$$

where $F_{g,in}$ is the total gas inlet flow and $X_{O2,db}$ and $X_{O2,dw}$ are the molar fractions of O_2 respectively measured in the dry and wet baseline.

The total gas inlet flow ($F_{g,in}$, $mol \cdot min^{-1}$) was calculated by summing the air ($F_{air,in}$) and CO_2 inlet flow ($F_{CO2,in}$). The resulting $F_{g,out}$ was used to calculate the oxygen (r_{O2}, $mol_{O2} \cdot L^{-1} \cdot min^{-1}$) and carbon dioxide ($r_{CO2}$, $mol_{O2} \cdot L^{-1} \cdot min^{-1}$) production or consumption rate at a resolution of one minute according to:

$$r_{O2} = F_{g,out} \cdot \left(X_{O2,out} - X_{O2,wb}\right) \qquad (2)$$

$$r_{CO2} = F_{g,out} \cdot \left(X_{CO2,out} - X_{CO2,wb}\right) \qquad (3)$$

where $X_{O2,out}$ and $X_{CO2,out}$ are the molar fractions of O_2 and CO_2, respectively, measured during the experiment and $X_{O2,b}$ and $X_{CO2,wb}$ are the molar fractions of O_2 and CO_2 measured in the wet baseline.

Photobioreactor Calculations

The biomass production rate over 24 h (r_{x24}, $g_x \cdot L^{-1} \cdot day^{-1}$) was calculated multiplying the biomass concentration in the harvesting vessel (C_x, $g_x \cdot L^{-1}$), collected after a complete day:night cycle, times the dilution rate (D, day^{-1}). In the mixotrophic culture, we also calculated the r_x during daylight period (r_{x14}, $g_x \cdot L^{-1} \cdot day^{-1}$) by correcting for the night biomass loss.

$$r_{x14,mixo} = r_{x24,} + \frac{C_{x14} - C_{x0}}{t_{14} - t_0} \qquad (4)$$

where C_{x0} and C_{x14} are the biomass concentrations at the beginning and the end of the day respectively. The r_x was also converted into its carbon equivalent (r_c, $C\text{-mol}_x \cdot L^{-1} \cdot day^{-1}$) by dividing r_x by the molecular weight of 1 C-mol of biomass (MWx, $g_x \cdot C\text{-mol}_x^{-1}$). MWx was determined in all off-line samples taken from the reactor and the average of those values was used to calculate the mixotrophic and the autotrophic MWx. In the autotrophic culture r_{c14} was calculated based on the CO_2 uptake rate ($r_{CO2,}$ $C\text{-mol}_{CO2} \cdot L^{-1}$) and both $r_{c,14}$ and $r_{c,24}$ were used to determine the biomass yield on light ($Y_{x/ph}$, $C\text{-mol}_x \cdot mol_{ph}^{-1}$) over 24 h and during daytime only according to the formula:

$$Y_{x/ph} = \frac{r_{c,auto} \cdot V_{PBR} \cdot}{\text{PFD} \cdot A_{PBR}} \qquad (5)$$

In the mixotrophic experiments, the volumetric substrate consumption rate (r_s, $C\text{-mols} \cdot L^{-1} \cdot day^{-1}$) was calculated as follows:

$$r_s = \frac{F_{AA} \cdot C_{sAA} - D \cdot V_{PBR} \cdot C_s}{V_{PBR}} \qquad (6)$$

Where F_{AA} ($L \cdot day^{-1}$) and C_{sAA} ($C\text{-mol}_s \cdot L^{-1}$) represent respectively the supply rate and the concentration of the acetic acid (AA) solution while Cs ($C\text{-mol}_s \cdot L^{-1}$) is the acetic acid concentration in the reactor ($C\text{-mol}_s \cdot L^{-1}$). The mixotrophic biomass yield on substrate ($Y^{mixo}_{x/s}$, $C\text{-mol}_x \cdot mol_s^{-1}$) was calculated dividing r_c by r_s. The r_s was used also to estimate the fraction of biomass heterotrophically produced during the mixotrophic growth ($r_{c,het'}$, $C\text{-mol}x \cdot L^{-1} \cdot day^{-1}$). This was done by multiplying r_s for the heterotrophic biomass yield on substrate ($Y_{x/s}$, C-

$mol_x \cdot C\text{-}mol_s^{-1}$). A $Y_{x/s}$ value of 0.5 $C\text{-}mol_x \cdot C\text{-}mol_s^{-1}$ was used for this purpose (Abiusi et al., 2020a). The resulting $r_{c,het'}$ was subtracted from the overall mixotrophic r_c to estimate the fraction of biomass autotrophically produced during mixotrophic growth ($r_{c,auto'}$, $C\text{-}mol_x \cdot L^{-1} \cdot day^{-1}$).

Nighttime losses were quantified measuring the difference in dry weight concentration (C_x, $g_x \cdot L^{-1}$) and the difference in total organic carbon content (TOC, $g_c \cdot L^{-1}$) between samples taken at the beginning and at the end of the night. The third method used to quantify nighttime losses was the CO_2 production rate ($r_{CO2,}$ $C\text{-}mol_{CO2} \cdot L^{-1}$) over the whole night, which was derived from the off-gas analysis.

ANALYTICAL METHODS

Culture Sampling and Off-Line Measurements

Samples were taken aseptically multiple times per day for off-line measurements. Two 1 mL aliquots were centrifuged at 20238 RCF for 10 min. The supernatant was stored at -20 ˚C until analysis, while the pellet was washed twice with demineralized water and cooled to -20 °C, lyophilized and stored at room temperature in the dark. Extra samples were taken from the reactor to quantify the dissolved inorganic carbon concentration (*DIC,* C-mol·L^{-1}) in the medium. This was done daily at the beginning and at the end of the night. To avoid CO_2 stripping, 950 µL of the supernatant fraction was alkalized immediately after centrifugation by the addition of 50 µL of base (2 M, NaOH). Alkalized samples were stored at -20 ˚C until analysis. During the last 4 days of the mixotrophic and the autotrophic experiment, 1 L of the harvested culture was centrifuged at 1200 RCF for 30 min. The supernatant was discharged while the pellet was washed twice with demineralized water and cooled to -20 °C, lyophilized and stored.

Dry Weight Concentration

Culture growth was estimated by biomass dry weight (*Cx*, $g_x \cdot L^{-1}$) determination: aliquots of the culture (5 mL) were diluted to 25 mL with demineralized water and filtered over pre-weighed Whatman GF/F glass microfiber filters (diameter of 55 mm, pore size 0.7 µm). The filters were washed with deionized water (25 mL) and dried at 105° C until constant weight.

Cell Concentration

Cell concentration was measured using a Multisizer III (Beckman Coulter Inc., USA) with a 50 µm aperture tube. Samples were diluted in ISOTON II diluent. The measured cellular biovolume was converted to cell diameter assuming spherical cells.

Average Absorption Cross Section

Average absorption cross section (a_x, $m^2 \cdot kg^{-1}$) in the PAR region (400-700 nm) of the spectrum was measured and calculated according to de Mooij et al. (de Mooij et al., 2015). The absorbance was measured in UV-VIS/double beam spectrophotometer (Shimadzu UV-2600, Japan) equipped with integrating sphere (ISR-2600). Cuvettes with an optical path of 2 mm were used.

Photosystem II Quantum Yield

The photosystem II maximum quantum yield (*QY*, F_v/F_m) was measured at 455 nm with an AquaPen-C AP-C 100 (Photon Systems Instruments, Czech Republic). Prior to the measurement, samples were adapted to darkness for 15 min at room temperature and diluted to optical density at 750 nm between 0.3 and 0.5.

Acetic Acid determination

Acetic acid concentrations was determined using an Agilent 1290 Infinity (U)HPLC equipped with a guard column (Security Guard Cartridge System, Phenomenex, USA). The compounds were separated on an organic acid column (Rezex ROA-Organic acid H^+ 8% column, Phenomenex, USA) at 55 °C with a flow of 0.5 mL/min 0.005 M H_2SO_4 as eluent. A final concentration of 50 mM propionic acid was used as internal standard.

Pigment Analysis

Pigment extract were obtained by a sequence of mechanical cell disruption and solvent based (methanol) pigment extraction using 10 mg of lyophilized biomass. Cells were disrupted by beat beating (Precellys 24, Bertin Technologies, France) at 5000 rpm for 3 cycles of 60 seconds with 120 seconds breaks on ice between each cycle. The extraction was done through five

washing steps with methanol. Separation, identification and quantification of pigments was performed using a Shimadzu (U)HPLC system (Nexera X2, Shimadzu, Japan), equipped with pump, degasser, oven (25 °C), cooled autosampler (4 °C), and photodiode array detector (PDA). Samples (20 uL) were quantitatively injected on a YMC Carotenoid C30 column (250 x 4.6 mm) coupled to a YMC C30 guard column (20 x4 mm) (YMC, Japan) at 25 °C, flow 1 ml·min^{-1}. The mobile phases consisted of Methanol (A), water/methanol (20/80 by volume) containing 0.2% ammonium acetate (B) and tert-methyl butyl ether (C). The gradient of elution used with this column was 95% A, 5% B isocratically for 12 min, a step to 80% A, 5% B, 15% C at 12 min, followed by 18 min of linear gradient to 30% A, 5% B, 65% C. A conditioning phase (30-40 min) was then used to return the column to the initial concentrations of A and B.

Total Organic and Total Inorganic Carbon and Nitrogen

The dissolved inorganic carbon (*DIC)* concentration was measured in the undiluted supernatant with a TOC-L analyzer (Shimadzu, Japan). The organic carbon and nitrogen content in the pellet were measured as total carbon (*TOC*, $g_c \cdot L^{-1}$) and total nitrogen (*TON*, $g_N \cdot L^{-1}$) respectively using the TOC-L analyzer. Possible traces of inorganic carbon in the lyophilized pellet were removed by resuspending the pellet in 1 mL of HCl (1M) and sonicating the solution at 80 kHz 40˚C for 30 minutes. After this treatment samples were diluted ten times in demi water and immediately placed in the TOC-L analyzer. The biomass carbon content (*C%*, % $w_c \cdot w_x^{-1}$) and nitrogen content (*N%*, % $w_N \cdot w_x^{-1}$) was calculated by dividing the obtained total carbon and total nitrogen by the dry weight determined on the same sample. The *C%* was used to determine the biomass molecular weight (*MWx*, $g_x \cdot C\text{-}mol_x^{-1}$). *MWx* was determined by dividing the carbon molecular weight (12.011 $g_c \cdot C\text{-}mol^{-1}$) by *C%*. The *N%* was used to determine the biomass protein content using a protein-nitrogen fraction (0.168 g-N·g-protein^{-1}) (Kliphuis et al., 2012).

Assessment of Bacterial Contaminant

During the experiment, axenicity was checked daily by DNA staining of culture samples with SYBR Green I (Sigma-Aldrich, US) and fluorescence microscopy (EVOS FL auto, Thermo Fisher Scientific, US).

Statistical Analysis

Propagation of errors was calculated according to Eq. (7) and Eq. (8) for sum and multiplication operations, respectively, to obtain the error.

$$\Delta z = \sqrt{\Delta x^2 + \Delta y^2 + \dots} \qquad (7)$$

$$\frac{\Delta z}{z} = \sqrt{\frac{\Delta x^2}{x} + \frac{\Delta y^2}{y} + \cdots} \qquad (8)$$

where Δx is the absolute error associated to the value x and so on.

In the comparison between the mixotrophic and the autotrophic cultures each day was considered as a replicate during the last four days of cyclostat. Figures and tables reports the standard deviation of these 4 replicates (n=4). Significant differences between those two conditions were analyzed by one-way ANOVA. The significance level was $P<0.05$.

RESULTS AND DISCUSSION

Oxygen Balanced Mixotrophy Under Day-Night Cycles

We previously demonstrated that a mixotrophic culture can operate without any gas-liquid transfer of oxygen or carbon dioxide (Abiusi et al., 2020a). We proposed to control respiratory oxygen consumption by tuning acetic acid supply. However, envisioning outdoor scale-up, this strategy needed to be tested under day-night cycles. In this study, a mixotrophic and an autotrophic culture grown under the same light-dark conditions were compared. First, we will describe the overall biomass productivity and biomass composition over a 24 h period. Next, we will zoom in on daytime and nighttime metabolisms.

Before going to the actual results, we will first discuss how off-gas analysis was applied in this study. On-line off-gas analysis was used to calculate the oxygen (r_{O2}, $mol_{O2} \cdot L^{-1} \cdot day^{-1}$) and carbon dioxide ($r_{CO2}$, $mol_{O2} \cdot L^{-1} \cdot day^{-1}$) production or consumption rates. Day-night transitions, however, were followed by a change in the aeration rate and gas composition, which led to rapid changes in the chemical-physical equilibria of dissolved O_2 and CO_2. These chemical-physical artefacts necessitated further data treatment.

During the transition from day to night the r_{O2} was positive for a few minutes according to our raw data, meaning that oxygen was produced, which is impossible from a biological point of view (Supporting Information 1). This phenomenon is caused by the step-wise reduction in the aeration rate at the beginning of the night. In addition, especially in the autotrophic culture, the dissolved oxygen (*DO*, % air saturation) was higher than 100% during the day. When the night began, part of the oxygen dissolved in the liquid phase was stripped from the culture, giving an apparent positive r_{O2}. This experimental artefact was removed by re-calculating the r_{O2} based on the dissolved oxygen (*DO*) and the general relations used to describe transfer of gaseous compounds between liquid and gas. The detailed procedure is explained in supporting information 1. Following these procedures, we calculated the oxygen gas-liquid transfer

coefficient (k_La, h^{-1}) adopting the steady state method (supporting information 1) while still using r_{O2} determined from off-gas analysis outside of the time with the day-night transition phenomena. More specifically, we calculated the k_La, during a long period at the end of the day, and at the end of the night, where gas analysis was not affected by transition events and where the system was in a steady state.

Similar to the r_{O2}, the carbon dioxide production or consumption rate (r_{CO2}) showed a peak during day-night transition (supporting information 2) which was too high to be merely due to biological activity. This overestimation is related to the fact that at the beginning of the day dissolved inorganic carbon (*DIC*, C-mol·L^{-1}) accumulates in the liquid phase until it reaches its chemical-physical equilibrium. This *DIC* is then stripped from the culture as CO_2 at the beginning of the night. *DIC* measured at the end of the day is reported in table 1, and this *DIC* was completely removed by the end of the night. For this reason, to calculate the real r_{CO2} , the *DIC* was subtracted from the cumulative amount of the CO_2 exchange measured during the day and night (table 2). Consequently, the r_{CO2} presents a nighttime average and we do not have insight of the dynamics of CO_2 production during the night.

Mixotrophic and Autotrophic Productivity and Composition over 24 h

The oxygen balanced mixotrophic strategy confirmed that microalgae productivity and concentration can be doubled (table 1). Furthermore, we established that mixotrophic stoichiometry is the sum of the heterotrophic and autotrophic metabolism (table 3). In fact, subtracting the fraction of biomass heterotrophically produced during the mixotrophic growth ($r_{c,\ het}$, C-mol_x·L^{-1}·day^{-1}) from overall mixotrophic productivity ($r_{c,mixo}$, C-mol_x·L^{-1}·day^{-1}), allowed us to calculate the fraction of biomass produced autotrophically ($r_{c,auto'}$). The $r_{c,auto'}$, and therefore the biomass yield on light ($Y_{x/ph}$, C-mol_x·mol_{ph}^{-1}), was not significantly ($P>0.05$) different from the r_c of the autotrophic culture. Surprisingly, despite the 10 h of darkness, $Y_{x/ph}$

was identical to the 40.7 C-mmol$_x$·mol$_{ph}^{-1}$ reported in our previous study under continuous light (Abiusi et al., 2020a). Therefore, under day-night cycle, where some biomass is lost during the night, the daytime $Y_{x/ph}$ is expected to be higher than under continuous light, and this higher yield compensates for night biomass losses (de Winter et al., 2017a). Those findings will be elucidated in more detail in the next sections. Thanks to the higher $Y_{x/ph}$ and despite the 10 h of darkness, the mixotrophic biomass yield on substrate under day-night cycle ($Y^{mixo}_{x/s}$, C-mol$_x$·C-mol$_s^{-1}$) was 0.88 C-mol$_x$·C-mol$_s^{-1}$ (table 3) only 6% lower than previously reported under continuous light (Abiusi et al., 2020a).

Similar $Y_{x/ph}$ of the mixotrophic and the autotrophic cultures indicate that photosynthesis is not affected by the presence of organic substrate. In our experiment the effect of organic carbon on photosynthesis was assessed by measuring photosynthetic efficiency of PSII directly as quantum yield (QY), by measuring the average specific absorption cross section (a_x), and by measuring the total chlorophyll (a+b) and lutein contents (table 1). These values did not vary between the mixotrophic and autotrophic cultures.

These results confirm our previous finding (Abiusi et al., 2020a) but are in contrast with most of the existing literature where a decrease in pigment content is reported (Grama et al., 2016; Wilken et al., 2014; Yang et al., 2000). A possible explanation is that in order to balance oxygen production, the heterotrophic ($r_{c,het'}$) and the autotrophic ($r_{c,auto'}$) metabolisms are equally contributing to the overall mixotrophic growth (table 3). Most of the previous work were conducted in batch or in repeated batch[17,18] with high initial substrate concentration and low light intensity, therefore the rate of heterotrophic metabolism was much higher than the rate of autotrophic metabolism. The dominance of heterotrophy in these studies might have resulted in a lower pigment content in comparison to our study.

***Table 1**. Overview of the off-line, DO, D measurements on the cultivation of C. sorokiniana SAG 211-8K under mixotrophic and autotrophic conditions. The data presented are the average of 4 consecutive days at* cyclostat *(n=4) and reported with the standard deviation of measurements.*

	Unit	Mixotrophic	Autotrophic
DO (daytime)	Air saturation %	98±33	146±5*
DIC_{out} *(end of the day)*	C-mmol L^{-1}	3.75±1.2	1.67±0.6*
Cx (end of the day)	$g_x \cdot L^{-1}$	1.90±0.02	0.88±0.03*
Cx (harvesting)	$g_x \cdot L^{-1}$	1.82±0.02	0.90±0.01*
D	day^{-1}	1.12±0.00	1.08±0.00
r_x	$g \cdot L^{-1} \cdot day^{-1}$	2.03±0.04	0.96±0.03*
$C_{\%}$	% $w_C \cdot w_x^{-1}$	50.4±0.6%	47.9±0.8%*
$N_{\%}$	% $w_N \cdot w_x^{-1}$	8.9±0.6%	8.0±0.1%*
QY (end of the day)	F_v/F_m	0.77±0.01	0.77±0.01
a_x *(end of the day)*	$m^2 \cdot kg^{-1}$	258±4	277±17
Protein (end of the day)	% $w_P \cdot w_x^{-1}$	50.1±2.2%	45.1±1.8%*
Lutein (harvesting)	mg g_x^{-1}	7.3±0.5	7.7±0.5
Chlrophyll a+b	mg g_x^{-1}	35.4±1.7	37.1±7.1

* Significant differences (P>0.05).

***Table 2**. Average mixotrophic and autotrophic specific oxygen (q_{O2}) and carbon dioxide (q_{CO2}) consumption/production rate over the day and night. The data presented are the average of 4 consecutive days at* cyclostat *(n=4) and reported with the standard deviation of measurements.*

	Mixotrophic		Autotrophic	
	Day	Night	Day	Night
q_{O2} ($mol_{O2} \cdot C\text{-}mol_x^{-1} \cdot day^{-1}$)	0	$-40.5 \cdot 10^{-3} \pm 4.8$	1.30±0.04	$-44.6 \cdot 10^{-3} \pm 2.4$
q_{CO2} ($mol_{CO2} \cdot C\text{-}mol_x^{-1} \cdot day^{-1}$)	$4.7 \cdot 10^{-6} \pm 0.3$*	$56.6 \cdot 10^{-3} \pm 6.8$	-1.15±0.04	$73.2 \cdot 10^{-3} \pm 3.9$

***Table 3**. Carbon mass balance of C. sorokiniana SAG 211-8K grown mixotrophically over the 14 hours of the day-light period and over 24 hours. In the table the overall mixotrophic productivity ($r_{c,mixo}$) was split in the fraction of biomass heterotrophically produced ($r_{c,het'}$) and the fraction of biomass produced autotrophically ($r_{c,auto'}$). As comparison isthe autotrophic productivity ($r_{c,auto}$) also reported. The data presented are the average of 4 consecutive days at* cyclostat *(n=4) and reported with the standard deviation of measurements.*

	Unit	Mixotrophic		Autotrophic	
		24 h	14 h	24 h	14 h
r_s	C-mmol$_s$·L^{-1}·day^{-1}	-95.8±3.4	-95.8±3.4	n.a	n.a
$r_{c,mixo}$	C-mmol$_x$·L^{-1}·day^{-1}	84.8±2.7	91.5±3.5	n.a	n.a
$Y^{mixo}_{x/s}$	C-mol$_x$·C-mol$_s^{-1}$	0.88±0.04	0.96±0.05	n.a	n.a
$r_{c,het'}$	mmol$_x$·L^{-1}·day^{-1}	47.9±4.2	47.9±2.2	n.a	n.a
$r_{c,auto'}$ / $r_{c,auto}$	C-mmol$_x$·L^{-1}·day^{-1}	36.9±5.0	43.16±5.5	39.5±1.1	42.4±0.8
$Y_{x/ph}$	C-mol$_x$·C-mol$_{ph}^{-1}$	40.9±5.8	48.3±6.4	43.8±2.1	47.1±2.0

Not applicable (n.a.)

A chlorophyll content between 20 and 40 mg·g$_x^{-1}$ is commonly found in this species (Mandalam & Palsson, 1998; Myers & Graham, 1971; Van Wagenen et al., 2015) and our results are on the high side of this range (table 1). The high chlorophyll content indicates that our cultures were photo-limited. In our previous work we used a light model to estimate the attenuation of light intensity, caused by cellular light absorption, from the reactor surface towards the reactor center (Abiusi et al., 2020a). Applying this model to the present work, we estimated that 85% of mixotrophic and 71% of autotrophic cultures were experiencing a light level below 10 µmol m^{-2} s^{-1} which we assumed to be the compensation point of photosynthesis (Blanken et al., 2016). Microalgae acclimate to the light regime they experience. In case the algae are light limited they are known to increase their pigmentation (Dubinsky & Stambler, 2009).

The lutein content found in our cultures was 7 to 8 mg g$_x^{-1}$, one of the highest ever reported for microalgae. Previous studies have reported lutein content commonly being in the range of 1 - 4.3 mg·g$_x^{-1}$ and values above this range are considered rare. In this strain, a maximum lutein content of 6 mg·g$_x^{-1}$ has been previously reported (Cuaresma, 2011) while up to 15 mg·g$_x^{-1}$ has

been obtained in *C. vulgaris* (Gong et al., 2018). Understanding the biological reason behind this high lutein content might have important commercial applications. However, the scope of this work was primarily to compare mixotrophic and autotrophic cultures, and we can clearly conclude that pigments were not ill-affected by the presence of an organic substrate.

C. sorokiniana has been proposed as a sustainable source of food given its high protein content and nutritional value (Safi et al., 2014). We measured a protein content of 50.1%±2.2 w/w in the mixotrophic and 45.1%±1.8 w/w in the autotrophic culture. These values are within the range reported for these species (Mandalam & Palsson, 1998) (Kumar et al., 2014). The higher protein content of the mixotrophic culture can partially explain its higher carbon content ($C_{\%}$) (table 1). This hypothesis was confirmed by Kumar et al. (Kumar et al., 2014) in another *C. sorokiniana* strain.

Daytime Metabolism in Mixotrophic and Autotrophic Cultures

Under day-night cycles, the application of automatic feeding of acetic acid to control *DO* proved to be more challenging than under continuous light (figure 1) and some settings needed adjustment. In the initial configuration, the process was designed to provide acetic acid to the culture only if *DO* was exceeding a set point (DO 105%). Therefore, feeding of acetic acid would have started only after an initial oxygen production had begun. Surprisingly, without an initial addition of acetic acid, the culture did not start producing oxygen (data not shown). This phenomenon might have been caused by an insufficient level of dissolved inorganic carbon (*DIC*) present in the medium after the night, and without CO_2, photosynthesis could not start. For this reason, a small and constant acetic acid supply rate (F_{AA}, $L \cdot min^{-1}$) was maintained between 0.1 and 0.3 $mL \cdot min^{-1}$. Thus, the substrate was provided even when *DO* did not reach the setpoint yet. Introducing this basal F_{AA} led to a decrease in *DO* during the first 1.5 hours, where the *DO* reached a minimum of 20%, after which *DO* rose again to the setpoint (*DO*

105%), which was reached after 3 h (Figure 1). Once the setpoint was reached, automatic feeding began to adjust F_{AA} based on the *DO* and succeeded in maintaining *DO* at the setpoint.

***Figure 1**. Daytime dissolved oxygen (DO) of C. sorokiniana SAG 211-8K grown mixotrophically without aeration. The data presented are the average of 4 consecutive days at* cyclostat *(n=4) and the shaded area represents the standard deviation of measurements.*

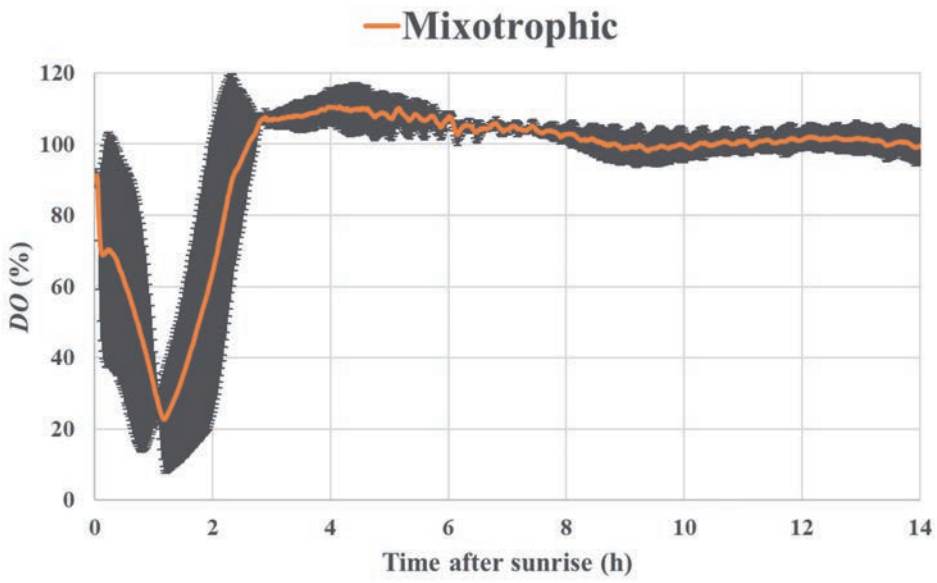

The autotrophic culture also needed about 3 h before reaching its full photosynthetic capacity corresponding to an r_{O2} of 62 µmol·O_2·L^{-1}·min^{-1} (Figure 2). It has been reported that in the first hours of the day algae need to restart photosynthesis and adjust the photosynthetic apparatus to the light intensity by increasing, or decreasing, their pigment content, among others (Strenkert et al., 2019). After this period, r_{O2} further increased reaching the maximum value of 63 µmol·O_2·L^{-1}·min^{-1} 5 h after the sunrise (Figure 2). Maximum r_{O2} was maintained for about 5 h, after which r_{O2} declined in the last 4 h of the daytime. Similar trends have been reported in other microalgal species (de Winter et al., 2017a; de Winter et al., 2017b; León-Saiki et al., 2017) and although the precise mechanisms behind these circadian variations have not been

discovered yet, it is well known that photosynthesis is controlled by the circadian clock (Post et al., 1985). Cell division might reduce photosynthetic efficiency (de Winter et al., 2017a; de Winter et al., 2017b) which could have been the case in our culture at the end of the day (Figure 3) explaining the r_{O2} decline in the last 4 h of the daytime (Figure 2).

Synchronized cultures, where cell division occurs mainly at night, might have a higher daytime biomass yield on light ($Y_{x/ph}$, C-mol$_x$·mol$_{ph}^{-1}$) compared with continuous light culture, where cell division occurs randomly (de Winter et al., 2017a; León-Saiki et al., 2017). This was the case in our experiment, where the average of daytime biomass yield on light for both the mixotrophic and autotrophic cultures was 48 C-mol$_x$·mol$_{ph}^{-1}$ (table 3), while in our previous experiment in continuous light culture it was 41 C-mol$_x$·mol$_{ph}^{-1}$ (Abiusi et al., 2020a). However, in order to confirm that the beginning of the cell division corresponded exactly with the decline in photosynthetic activity, cell counting should have been measured over 24 h, while our study we mainly focused on cell division at nighttime (see next section).

In this study the autotrophic carbon uptake rate (r_{CO2}) (supporting information 2) equals the biomass production rate r_C (r_C, C-mol$_x$·L^{-1}·day^{-1}) (table 3). The accuracy of this method was also confirmed by the ratio between r_{O2} and r_{CO2} that matched the value of 1.1 expected from autotrophic stoichiometry (Abiusi et al., 2020a) using ammonium as nitrogen source. Off-gas analysis was also used to calculate the amount of CO_2 taken up from the reactor, on the total amount provided during the daytime (supporting information 3). Our results indicate that 90% of the ingoing CO_2 was lost in the autotrophic reference culture. Similar CO_2 losses are commonly reported (Smith et al., 2015, Kim et al., 2019). Low CO_2 uptake efficiency might have a dramatic impact on microalgae production cost and carbon footprint (Kim et al., 2019; Smith et al., 2015). Several studies have been conducted to decrease CO_2 losses but even in

***Figure 2**. Daytime oxygen production rate (r_{O2}) of C. sorokiniana SAG 211-8K grown autotrophically. The data presented are the average of 4 consecutive days at* cyclostat *(n=4) and the shaded area represents the standard deviation of measurements.*

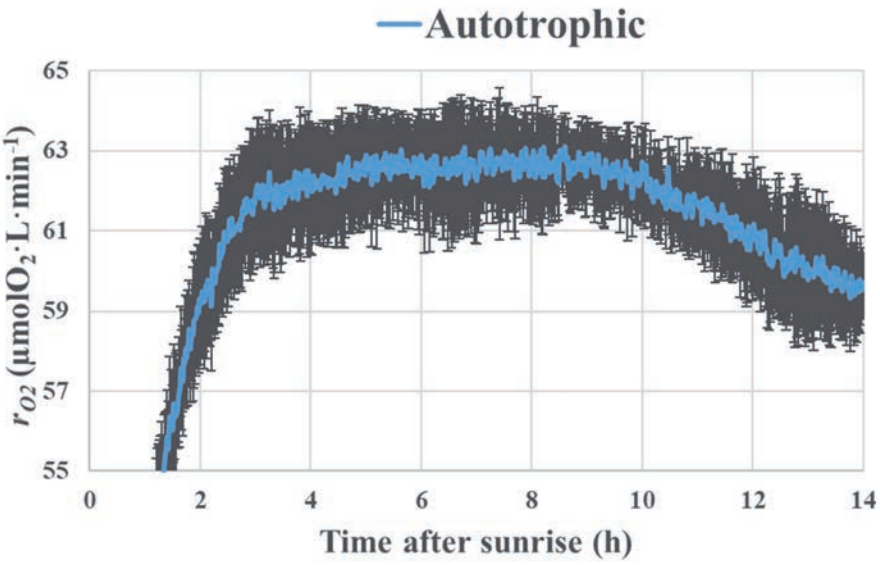

***Figure 3**. Nighttime cell number of C. sorokiniana SAG 211-8K that during the daytime was grown either mixotrophically (orange) or autotrophically (blue). The data presented are the average of 4 consecutive days at* cyclostat *(n=4) and reported with the standard deviation of measurements.*

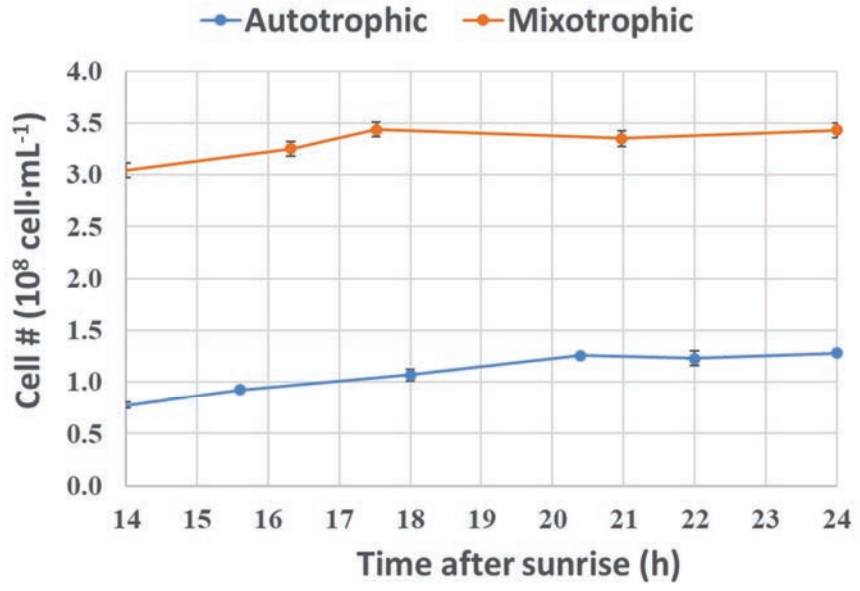

optimized photobioreactors ***(PBRs)***, CO_2 losses are 25% at minimum in closed ***PBRs*** (Acién et al., 2012) and 50% in open ponds (Doucha et al., 2005), indicating that CO_2 uptake efficiency is one of the challenges in autotrophic cultivation of microalgae.

Nighttime Metabolism in Mixotrophic and Autotrophic Cultures

The average volumetric oxygen consumption rate (r_{O2}) was measured for 4 consecutive days and used to calculate the biomass specific oxygen consumption rate (q_{O2}, $mol_{O2} \cdot C\text{-}mol_x \cdot day^{-1}$). We will use these specific rates because in the mixotrophic culture the biomass concentration was roughly double the concentration of the autotrophic culture (table 1).

Mixotrophic and autotrophic cultures expressed a similar trend of q_{O2} in time (figure 4) with higher oxygen consumption at the beginning of the night decreasing to a low and constant rate towards the end of the night. Calculations show that 50% of the oxygen was consumed within the first 3 hours. A closer look at the graph reveals that q_{O2} decreased more rapidly in the mixotrophic culture compared to the autotrophic culture, while towards the end of the night the two cultures had a similar q_{O2}. As a consequence of the more rapid decline, the average q_{O2} during the night was slightly lower in the mixotrophic culture than in the autotrophic culture (table 2).

Few studies have employed on-line off-gas analysis in microalgae to study dynamics in metabolism during the day-night cycle (Cuaresma et al., 2011b; de Winter et al., 2017a; Norsker et al., 2019). Most of these studies were conducted only during the day in an autotrophic culture, with the goal of quantifying biomass production rate based on r_{O2}. During the night, carbohydrate reserves are consumed to produce energy. In the case of aerobic respiration of sugar for energy production (catabolism), 1 mol of sugar (CH_2O) is respired, consuming 1 mol of O_2 and producing 1 mol CO_2. In a situation where part of the sugar is used as molecular building block for the formation of functional biomass (e.g. proteins, pigments) in anabolic

pathways, the ratio between r_{O2} and r_{CO2} is lower than 1. Thus, the ratio between q_{O2} and q_{CO2} gives information on the relative contribution of catabolic and anabolic pathways. In our experiment this ratio was 0.71 for the mixotrophic culture during the night, and 0.61 for the autotrophic culture (table 2). The difference suggests that in the autotrophic culture anabolic processes were more dominant.

***Figure 4**: Nighttime specific oxygen consumption rate (q_{O2}) of C. sorokiniana SAG 211-8K that during the daytime was grown either mixotrophically (orange) or autotrophically (blue). The data presented are the average of 4 consecutive days at* cyclostat *(n=4) and the shaded area represents the standard deviation of measurements. The dotted line indicates the time in which half of the total r_{O2} is reached.*

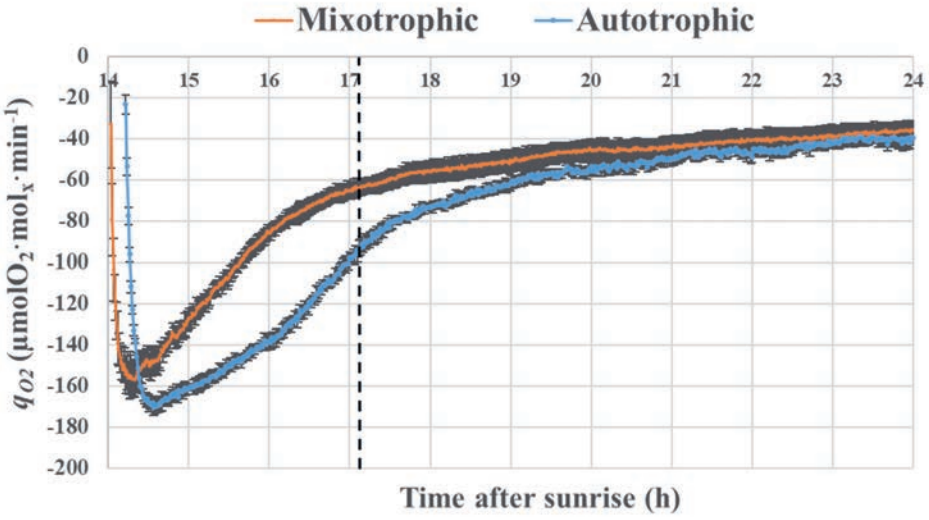

The finding that anabolic processes were more dominant in the autotrophic culture than in the mixotrophic culture, was confirmed by nighttime cell division (Figure 3). In the autotrophic culture cell number increased by 62% while in the mixotrophic culture only by 13%. However, neither of the cultures doubled their cell number during the night, indicating that cell division must have already started during the day as discussed in previous section. In the mixotrophic

culture cell division was completed after 3.5 hours while in the autotrophic culture it lasted for 6.5 hours.

Not surprisingly q_{O2} declined after cell division (Figure 4) and this decline was faster in the mixotrophic culture than in the autotrophic culture. Cells need energy for growth related process, such as cell division, and less so for non-growth related process defined as maintenance (Pirt & Hinshelwood, 1965). At night, after cell division, the cells enter in a metabolically quiescent stage of the cell cycle known as G_0 (Strenkert et al., 2019). In this stage energy is spent mainly for maintenance, and the energy for maintenance was constant in both cultures. The specific oxygen consumption for maintenance in this strain has been reported (Kliphuis et al., 2011; Zijffers et al., 2010) to be 0.3 $mmolO_2 \cdot g_x^{-1} \cdot h^{-1}$, which is in the same order the 0.1 $mmolO_2 \cdot g_x^{-1} \cdot h^{-1}$ measured in our study.

The most relevant question with respect to scale-up of mixotrophic cultivation is the amount of oxygen that needs to be provided to support night time aerobic heterotrophic metabolism (i.e. respiration). The amount of oxygen consumed during the night was similar between the two cultures, with mixotrophic culture requiring slightly less oxygen at night (table 2). Moreover, most of the oxygen was consumed in the first hours of the night, so it is advisable to tune the aeration based on the *DO*, rather than aerate the culture at a constant rate. In fact, the oxygen requirement at night is only a minimal part of the overall daily gaseous substrate demand under autotrophy. Averaged over 24 hours the mixotrophic culture required 61 times less gaseous substrates than the autotrophic culture (table 3), confirming that the energy required for gassing under mixotrophy is almost negligible.

Another relevant question regarding scale-up is the amount of nighttime biomass losses. Nighttime losses were quantified using three methods: biomass dry weight concentration (C_x, $g_x \cdot L^{-1}$), total organic carbon content (*TOC*, $C\text{-}mol_s \cdot L^{-1}$), and CO_2 production rate (r_{CO2}, $C\text{-}mol_s \cdot L^{-1}$). The results obtained with these three different methods are reported in table 4.

The three methods did not show any significant difference ($P<0.05$) with the exception of Cx of the autotrophic culture. The C_x based method failed to quantify nighttime losses of the autotrophic culture, probably because it was not sensitive enough, and for this reason the night losses of the autotrophic culture were calculated using the other two methods. Excluding the C_x and making an average of $r_{CO2,}$ and TOC, no significant difference in the nighttime losses were found between the two cultures. Nighttime losses were around 7% on carbon basis. This value is within the typical range of 3-8% reported for autotrophic cultures (Edmundson & Huesemann, 2015; Michels et al., 2014; Ogbonna & Tanaka, 1996). Previous studies (Michels et al., 2014; Ogbonna & Tanaka, 1996) indicated that nighttime losses depend on the growth rate of the day. In our experiment the cultures were grown in a cyclostat at a constant dilution rate during the day, and therefore expressed the same specific growth rate. This equivalent specific growth rate might explain the similar nighttime losses for both cultures. Total organic nitrogen content (TON, $g_N \cdot L^{-1}$) did not change significantly along the night (supporting information 4). Absence of nitrogen uptake has been previously reported in other green algae (Boelee et al., 2014; Voltolina et al., 2005) and is consistent with the hypothesis of a quiescent stage (Strenkert et al., 2019). The protein fraction contains 90% of microalgal nitrogen (Becker, 2004), therefore an absence of nitrogen uptake might be associated with a lack of protein synthesis. Other studies however reported that part of the carbon accumulated during the day in the form of starch or lipids, is consumed during the night for protein synthesis (Blanken et al., 2017; Ogbonna & Tanaka, 1996). Even so, whether or not protein synthesis occurs during the night is unclear and goes beyond the scope of this study. Neither mixotrophic or autotrophic cultures expressed significant nitrogen uptake nitrogen during the night, and we can safely conclude that night time nitrogen uptake is not affected by mixotrophy.

***Table 4**. Nighttime losses in a mixotrophic and an autotrophic culture, according to biomass dry weight concentration (C_x, $g_x \cdot L^{-1}$), total organic carbon content (TOC, C-$mol_s \cdot L^{-1}$) and CO_2 production rate (r_{CO2}, C-$mol_s \cdot L^{-1}$). The data presented are the average of 4 consecutive days at* cyclostat *(n=4) and reported with the standard deviation of measurements.*

Method	Mixotrophic	Autotrophic
C_x	-8.7%±1.5%	0.7%±7.0%*
TOC	-6.8%±1.6%	-6.9%±2.9%
r_{CO2}	-5.4%±0.1%	-7.9%±0.5%

* Significant differences (P>0.05).

Practical Application of Oxygen Balanced Mixotrophy

In this study we demonstrated that oxygen balanced mixotrophy allows for complete removal of day-time gas-liquid exchange and that the oxygenation required in the night period is very low. In several photobioreactor (*PBR*) designs, however, gassing is an integral part of the mixing of the microalgal culture. In vertical panel or column type *PBRs* mixing is exclusively provided by gassing, but in tubular *PBRs* mixing and gassing are separated. In tubular *PBRs* mixing is ensured via a liquid pump, while oxygen and carbon dioxide gas-liquid exchange is supported by a dedicated unit usually in the form of a bubble column. In tubular *PBRs* the energy for gassing is 25% of the operational energy cost (Acién et al., 2012). Our process might allow for the complete removal of the bubble column saving the related energy consumption and dramatically decreasing the complexity of the system. Also the rate of mixing (liquid circulation through the tubes) potentially can be decreased as no accumulation or depletion of oxygen or carbon dioxide is expected.

One of the major challenges of mixotrophic outdoor cultivation is the undesired contamination of heterotrophic microorganism, mainly bacteria and fungi (Unnithan et al., 2014), that compete with microalgae for the assimilation of organic carbon. Bacteria have a growth rate that is an

order of magnitude higher than microalgae and they can easily outcompete microalgae for organic carbon uptake. However, since the start of commercial production of Chlorella in 1964 the pioneers involved already replaced CO_2 by acetic acid in open ponds (Iwamoto, 2004), without serious contamination of the culture. A similar approach has been recently embraced by Heliae Development LLC (Ganuza & Tonkovich, 2016).

In search of strategy to prevent bacterial contamination, Deschênes et al. (Deschênes et al., 2015) demonstrated the possibility to control bacterial contamination under mixotrophic conditions by preventing the simultaneous presence of nitrogen and organic carbon in the culture medium. The main idea behind this cultivation strategy was that microalgae can grow when either nitrogen or organic carbon are not present in the culture medium by consuming the internal quota of nitrogen and by photosynthesis, respectively, whereas most bacteria can grow only if all nutrients are simultaneously present in the culture medium. A similar strategy has been successfully adopted for microalgae heterotrophic growth in non-axenic condition (Di Caprio et al., 2019).

Another possible solution to avoid bacteria contamination is to employ acidophilic microalgae that have a pH optima below 3, where most of the bacteria cannot grow. This strategy has been used to cultivate *Galdieria sulphuraria* in unsterilized primary effluent (Delanka-Pedige, 2018). The authors reported that at pH 2 the initial bacterial population was reduced by 98% and lowering the pH resulted in a complete removal of pathogen.

We strongly believe that although it might be technically feasible to run a closed photobioreactor, without aeration, with minimal infection risk, contaminations can be further controlled by employing one of the above mentioned strategies.

CONCLUSIONS

In the present work, a mixotrophic microalgal monoculture was grown without gas exchange during the day, and with minimal aeration during the night. In mixotrophy biomass productivity and concentration doubled compared to an autotrophic reference culture. In the mixotrophic culture, due to efficient light utilization, 88% of the substrate was converted into biomass, making the process close to carbon neutrality. Mixotrophic and autotrophic cultures had similar nighttime oxygen consumption patterns, with most of the oxygen consumed within the first 3 hours of the night. Overall, mixotrophy required 61 times less gaseous substrates compared to autotrophy. Thus, mixotrophy is an effective strategy for reducing the requirement for gassing by at least 98 %. Biomass nighttime losses were about 7% regardless of the trophic mode. The mixotrophic culture had 5% more protein and the same lutein content as the autotrophic culture. Our results indicate that mixotrophy is a successful strategy for producing protein and lutein, while still maintaining the same efficiency of light utilization as an autotrophic culture.

NOMENCLATURE

Abbreviations	
DO	Dissolved oxygen concentration (% air saturation)
PBR	Photobioreactor
PFD	Photon flux density ($\mu mol \cdot m^{-2} \cdot s^{-1}$)
PAR	Photo active radiation, 400-700 nm
TOC	Total organic carbon ($g_c \cdot L^{-1}$)
DIC	Dissolved inorganic carbon ($C\text{-}mol \cdot L^{-1}$)
TON	Total organic nitrogen ($g_N \cdot L^{-1}$)
Symbols	
V_{PBR}	Photobioreactor working volume (L)
A_{PBR}	Photobioreactor illuminated area (m^2)
D	Dilution rate (day^{-1})
$Y_{x/ph}$	Biomass yield on light ($C\text{-}mol_x \cdot mol_{ph}^{-1}$)
F	Flow ($mol \cdot min^{-1}$)
r	Volumetric production/consumption rate ($mol \cdot L^{-1} \cdot min^{-1}$)
X	Gas molar fraction (%)
C	Concentration ($mol \cdot L^{-1}$)
$Y_{x/s}$	Biomass yield on substrate ($C\text{-}mol_x \cdot C\text{-}mol_s^{-1}$)
MW	Molecular weight ($g \cdot C\text{-}mol^{-1}$)
a_x	Average absorption cross section ($m^2 \cdot Kg^{-1}$)
QY	Quantum yield (F_v/F_m)
$C_{\%}$	Biomass carbon content ($\%\ w_c \cdot w_x^{-1}$)
$N_{\%}$	Biomass nitrogen content ($\%\ w_N \cdot w_x^{-1}$)
K_La	O_2 gas-liquid transfer coefficient (h^{-1})
q	Biomass specific production/consumption rate ($mol \cdot C\text{-}mol_x \cdot day^{-1}$)
Sub/super script	
mixo	Mixotrophic
auto	Autotrophic
auto'	Autotrophic fraction of the mixotrophic biomass
het'	Heterotrophic fraction of the mixotrophic biomass
g	Gas
in/out	Inlet/outlet
ph	PAR photons
x	Biomass
c	Carbon based biomass
s	Substrate
AA	Acetic acid

SUPPORTING INFORMATION

Supporting information 1: O_2 Production/Consumption Rate

In our study, on-line off-gas analysis was used to calculate the oxygen (r_{O2}, $mol_{O2}\cdot L^{-1}\cdot day^{-1}$) and carbon dioxide ($r_{CO2}$, $mol_{O2}\cdot L^{-1}\cdot day^{-1}$) production or consumption rates. Day-night transitions, however, were followed by a change in the aeration rate and gas composition (Figure S1 and S2), which led to rapid changes in the chemical-physical equilibria of dissolved O_2 and CO_2. These chemical-physical artefacts necessitated further data treatment.

During the transition from day to night the r_{O2} was positive for a few minutes (Figure S1), meaning that oxygen was produced, which is impossible from a biological point of view. This phenomenon is caused by a stepwise reduction of the aeration rate at the beginning of the night. In addition, especially in the autotrophic culture, the dissolved oxygen (*DO*, % air saturation) at the end of the day was 150%. When the night began, part of the oxygen dissolved in the liquid phase was stripped from the culture, giving an apparent positive r_{O2}. This experimental artefact was removed by re-calculating the r_{O2} based on the *DO* and the general relations used to describe transfer of gaseous compounds between liquid and gas. More specifically, we calculated the oxygen gas-liquid transfer coefficient (k_La, h^{-1}) using the steady state method. In order to do that, we first determined from the off-gas analysis a period at the end of the day and at the end of the night where r_{O2} was not affected by day-night transition phenomena. We considered r_{O2} to be at steady state for the last 2 h of the night (Figure S1), and between 4.8 and 14 h after sunrise for the daytime in the autotrophic culture (Figure S2). These two periods were used to calculate the k_La, according to:

$$K_La(t) = \frac{r_{O2}(t)}{C^*_{O2} - C_{O2}(t)} \qquad \text{(Eq. S1)}$$

where C_{O2}^* and C_{O2} are the concentration of dissolved oxygen at 100% air saturation and at a specific time point respectively. A *DO* of 100% corresponds to 224 $\mu mol\cdot L^{-1}$ at 37°C. Using this procedure, we estimated a k_La value of 8.6±1.2 and 28.8±1.2 h^{-1} when the aeration rate was 0.1 and 0.5 $L\cdot L^{-1}\cdot min^{-1}$ respectively. These values are in the range reported by the

manufacturing company (https://www.applikon-biotechnology.com/files/applikon-poster-scalability-in-lab-bioreactors-kla.pdf).

These two k_La were used to recalculate r_{O2} (figures S3 and S4) and it was used for further calculations as presented in the main text.

Figure S1. *Night time raw data of the oxygen consumption rate (r_{O2}) and dissolved oxygen (DO) of C. sorokiniana SAG 211-8K that during the daytime was grown either mixotrophically (orange) or autotrophically (blue). The red box indicates the steady state period used to calculate the oxygen gas-liquid transfer coefficient (k_La, h^{-1}). The data presented are the average of 4 consecutive days at cyclostat (n=4) and reported with their standard deviation.*

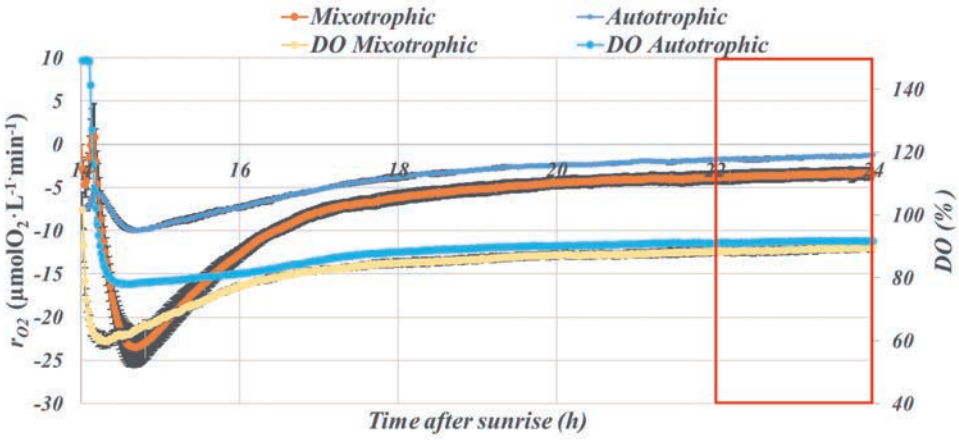

Figure S2. *Daytime raw data of oxygen production rate (r_{O2}) and dissolved oxygen (DO) of C. sorokiniana SAG 211-8K grown autotrophically. The red box indicates the steady state period used to calculate the oxygen gas-liquid transfer coefficient (k_La, h^{-1}). The data presented are the average of consecutive days at steady state and the shaded area represents the standard deviation of measurements.*

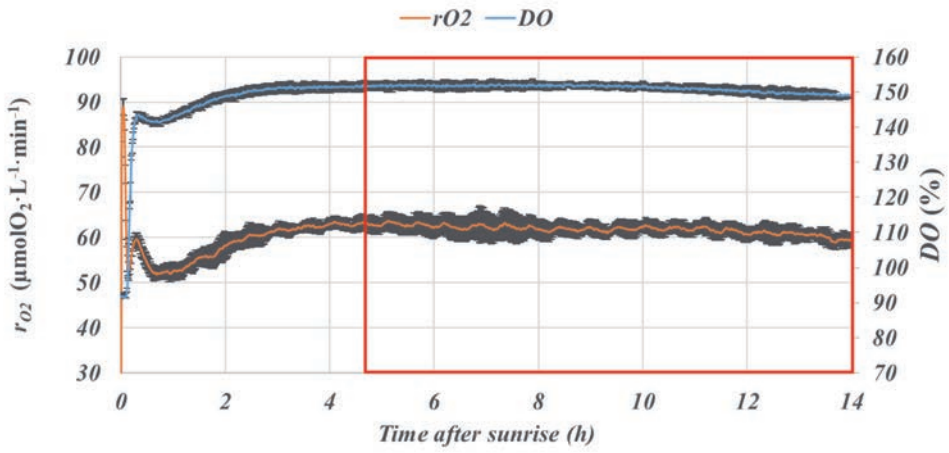

Figure S3. *Night time oxygen consumption rate (r_{O2}) of C. sorokiniana SAG 211-8K that during the daytime was grown either mixotrophically (orange) or autotrophically (blue). The data presented are the average of 4 consecutive days at cyclostat (n=4) and the shaded area represents the standard deviation of measurements.*

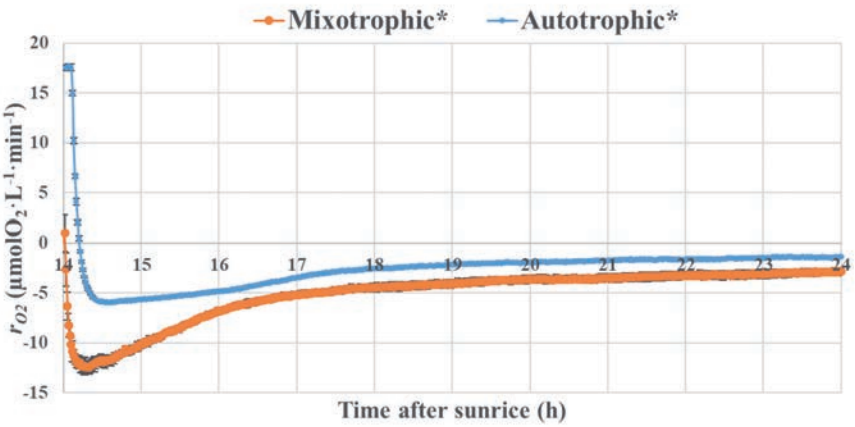

Figure S4. *Daytime oxygen production rate (r_{O2}) of C. sorokiniana SAG 211-8K grown autotrophically. The data presented are the average of 4 consecutive days at cyclostat (n=4) and the shaded area represents the standard deviation of measurements*

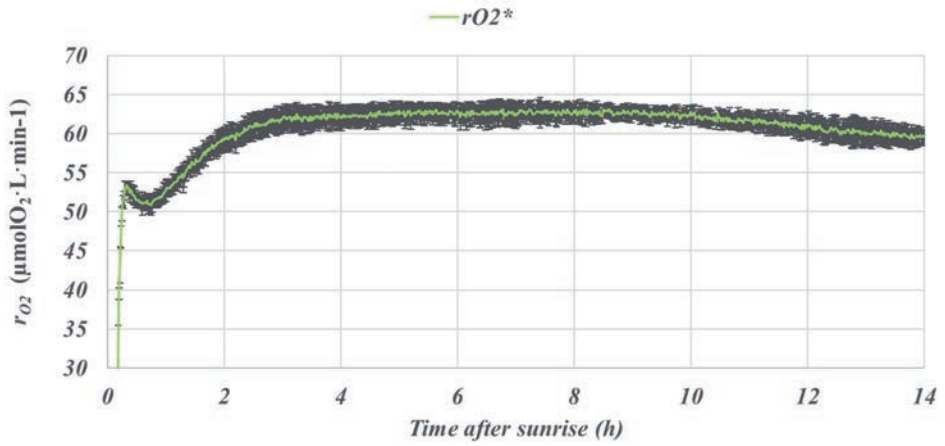

Supporting information 2: Raw Data of CO_2 Production/Consumption Rate

Similar to the oxygen production rate, carbon dioxide production/consumption rates (r_{CO2}) showed a peak during day-night transitions (figure S5 and S6) which were too high to be merely due to biological activity. At the beginning of the day dissolved inorganic carbon (*DIC*, C-mol·L^{-1}) accumulates in the liquid phase until it reaches its chemical-physical equilibrium. This *DIC* is then stripped from the culture as CO_2 at the beginning of the night resulting in an over estimation of r_{CO2}. For this reason, r_{CO2} was corrected for *DIC*. Employing this correction, the daytime r_{CO2} in the autotrophic culture was -42.4±0.8 C-mmol$_x$·L^{-1}·day^{-1} while during the night time the autotrophic and mixotrophic had a of 2.7±0.1 and 4.3±0.5 C-mmol$_x$·L^{-1}·day^{-1} respectively. The net carbon uptake equals the biomass production rate r_C (table 3) confirming the accuracy of this method

***Figure S5**. Daytime carbon dioxide consumption rate (r_{O2}) of C. sorokiniana SAG 211-8K grown autotrophically. The data presented are the average of 4 consecutive days at cyclostat (n=4) and the shaded area represents the standard deviation of measurements.*

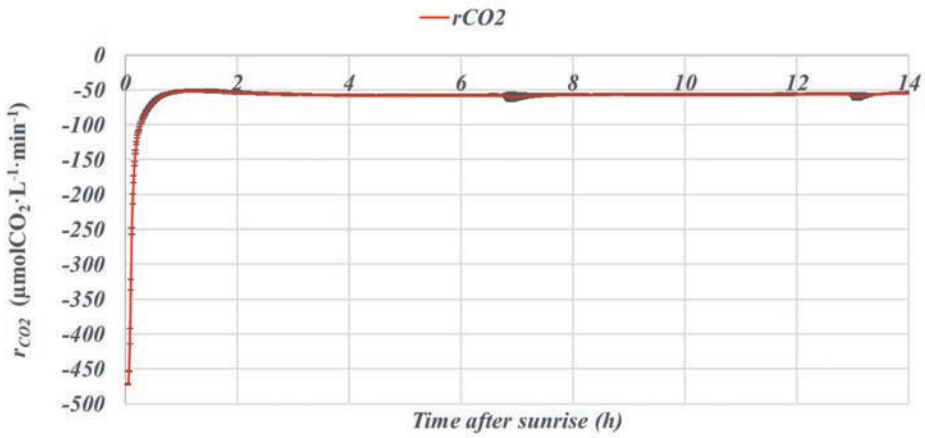

***Figure S6**. Night time raw data of the carbon dioxide production rate (r_{CO2}) of C. sorokiniana SAG 211-8K that during the daytime was grown either mixotrophically (orange) or autotrophically (blue). The data presented are the average of 4 consecutive days at cyclostat (n=4) and the shaded area represents the standard deviation of measurements.*

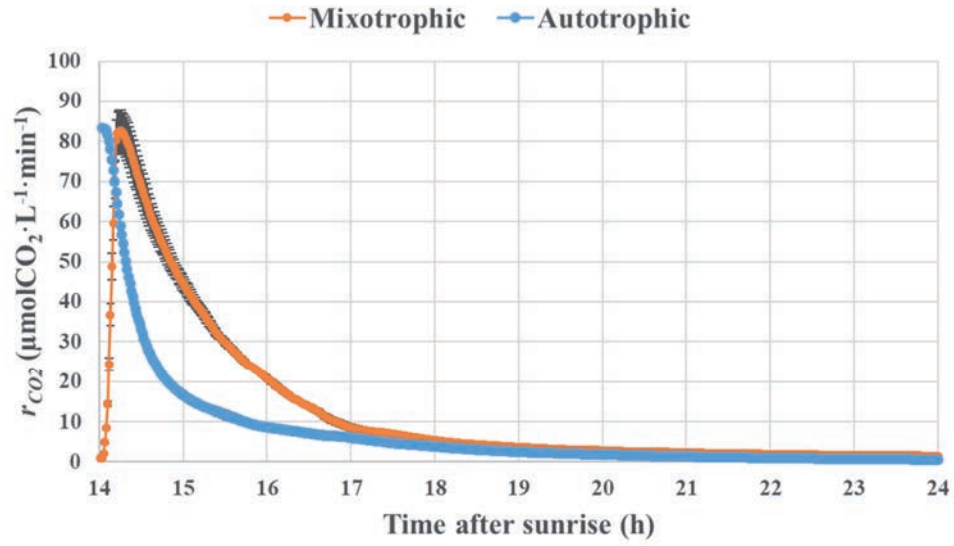

Supporting information 3: CO_2 Fraction in the Gas Inlet and Outlet

***Figure S7**. Molar fraction of the CO_2 (X_{CO2}) in the inlet (CO_2,in) and outlet (CO_2,out) gas measured in the autotrophic culture of C. sorokiniana SAG 211-8K during daytime.*

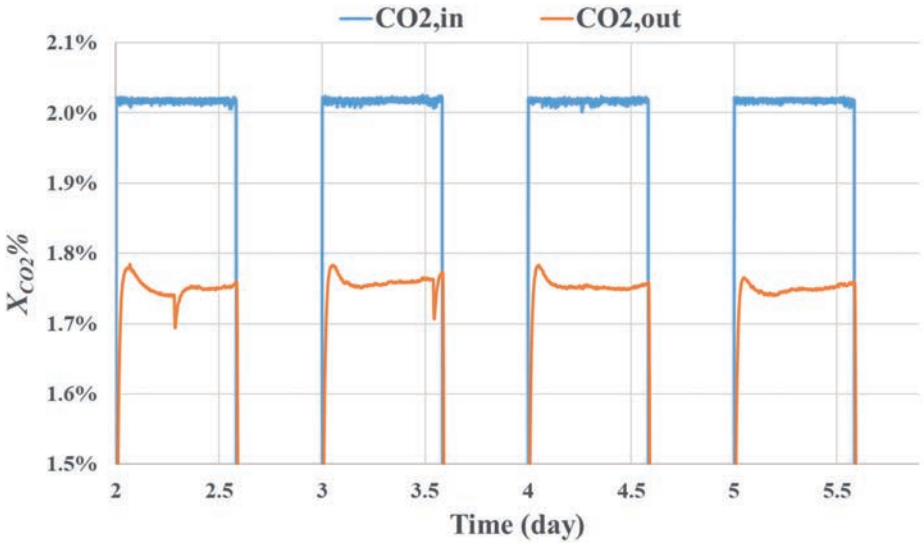

Supporting information 4: Total Organic Nitrogen Content at Nighttime

***Figure S8**. Nighttime total organic nitrogen content (TN, $g_N \cdot L^{-1}$) of C. sorokiniana SAG 211-8K biomass, that during the daytime was grown either mixotrophically (orange) or autotrophically (blue). The data presented are the average of 4 consecutive days at cyclostat (n=4) and the shaded area represents the standard deviation of measurements.*

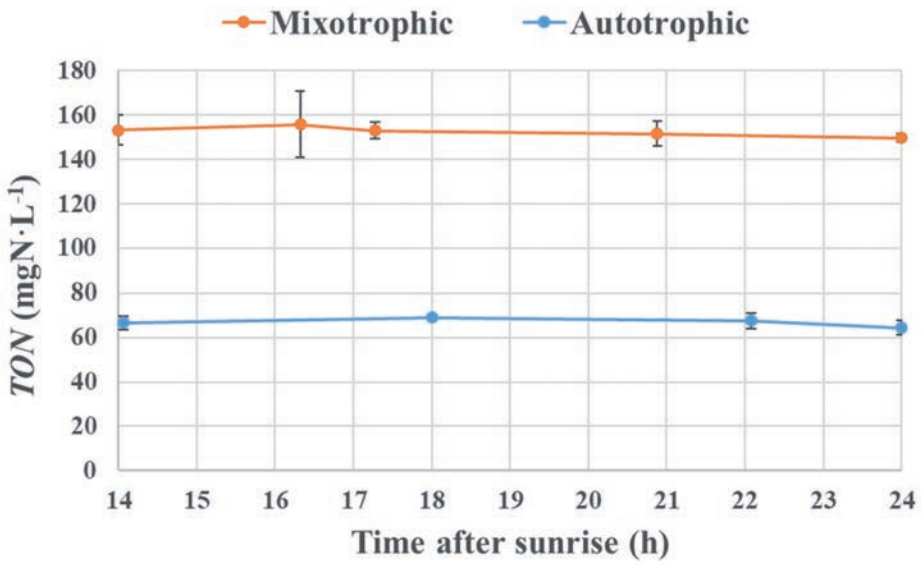

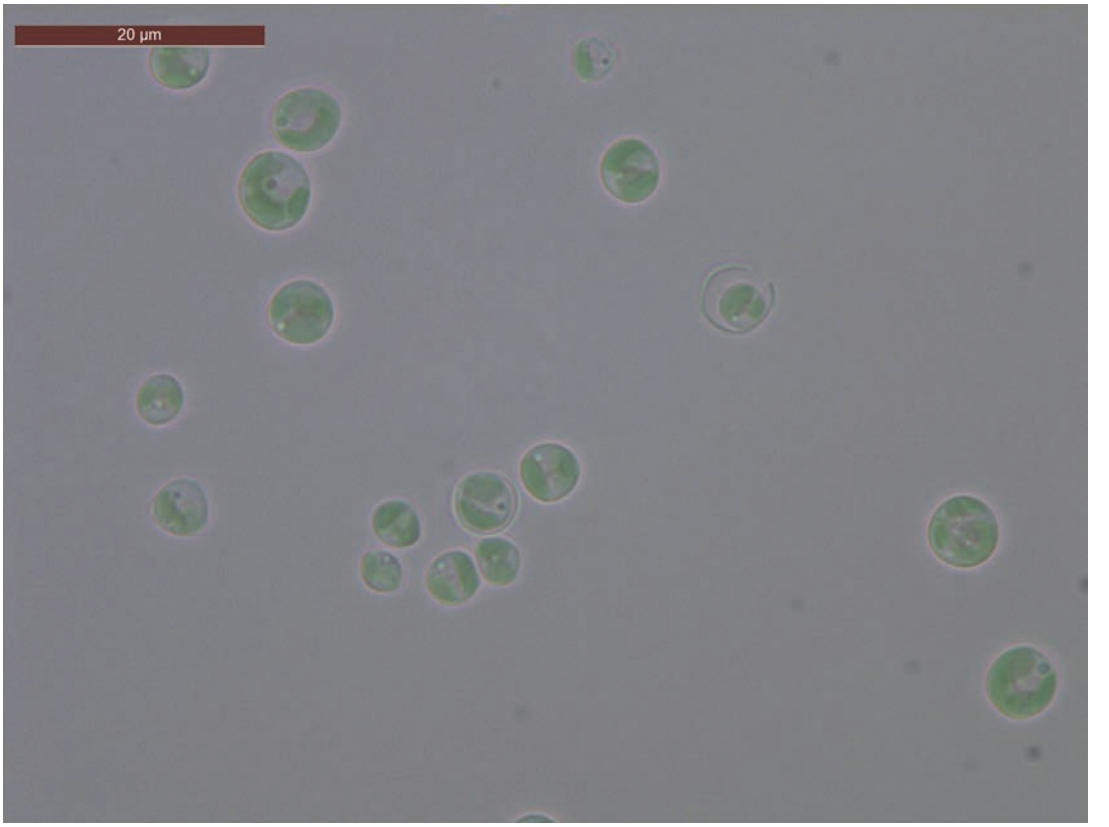
20 µm

Chapter 4

Autotrophic and mixotrophic biomass production of the acidophilic *Galdieria sulphuraria* ACUF 64

This chapter has been submitted for publication as:
Fabian Abiusi, Egbert Trompetter, Hugo Hoenink, Rene H. Wijffels, Marcel Janssen. Autotrophic and mixotrophic biomass production of the acidophilic *Galdieria sulphuraria* ACUF 64

Submitted

ABSTRACT

G. sulphuraria is an acidophilic microalga isolated in proximity of sulfuric ponds where pH is below 3 and most organisms cannot grow. We cultivated *G.sulphuraria* ACUF 64 free of contamination for over 2 months in a media containing organic carbon at pH 1.7 with continuous, high intensity, lighting. We compared biomass productivity of chemostat and repeated batch cultivations. The optimal biomass density in autotrophic and mixotrophic cultures were identified. In autotrophy biomass productivity was 28.3 $g_x \cdot m^{-2} \cdot day^{-1}$, 1.8 to 7.7-fold higher than previously reported. Autotrophy was compared to 'oxygen balanced' mixotrophy where intracellular recirculation of O_2 and CO_2 take place. Aeration was not needed and 91% of the substrate carbon was converted into biomass. In mixotrophy biomass productivity was 1.8 times higher than autotrophic culture and linear growth was maintained at high biomass concentration (9.7 $g_x \cdot L^{-1}$). Light tolerance and high productivity in dense culture make our strain promising for mixotrophic outdoor cultivation.

Keywords: Photoinhibition, biomass yield on substrate, oxygen balance, high density, acidophilic microalgae.

INTRODUCTION

Microalgae are oxygenic photoautotrophic microorganisms (henceforth referred to as autotrophic), meaning that they harvest light energy, use carbon dioxide (CO_2) as a carbon source, and release oxygen (O_2) as a by-product. Microalgae can reach high areal productivity, do not require arable land or fresh water for growth (Wijffels & Barbosa, 2010), and they can use fertilizers with almost 100% efficiency (Tredici, 2010). These unique traits make microalgae a promising sustainable source of food and feed (Ruiz et al., 2016).

Some microalgal species are able to exploit light and organic carbons simultaneously resulting in a mixotrophic metabolism. In mixotrophic cultivation, the simultaneous presence of two energy sources (light and reduced organic carbon) can significantly increase biomass productivity (Turon et al., 2015c; Wang et al., 2014). We recently designed an 'oxygen balanced' mixotrophic cultivation method in which the dissolved oxygen concentration (*DO*) was kept constant by coupling the substrate supply rate with the rate of photosynthesis (Abiusi et al., 2020a). This method allowed internal O_2 and CO_2 recirculation between photosynthesis and respiration avoiding (Abiusi et al., 2020a), or minimizing (Abiusi et al., 2020b), gas exchange. Furthermore, under these conditions biomass productivity and biomass concentration were doubled and 96% of the substrate carbon was converted into biomass carbon.

Contamination by bacteria and fungi is a notable challenge when microalgae are cultivated in a medium that contains a source of organic carbon, as microalgae have a growth rate one order of magnitude lower than its competitors. Cultivation of extremophilic microalgae has been proposed as a strategy to reduce the risk of bacterial contamination (Delanka-Pedige, 2018). These algae are able to grow in conditions defined as "extremes" such as very acidic or alkaline pH, unusually high or low temperatures, or high salinity which are all unfavorable to most other micro-organisms.

The microalgal genus *Galdieria* emerged as a promising extremophile (Sydney et al., 2019). Among the *Galdieria* genus, *G. sulphuraria* is the most studied species. *G. sulphuraria* is a polyextremophile that can tolerate low pH (1–4) (Sloth et al., 2006), high temperature (up to 57 °C) (Ott & Seckbach, 1994) and high osmotic pressure (up to 400 $g \cdot L^{-1}$ of sugar and 2-3 M of salt) (Schmidt et al., 2005). Due to these exceptional traits, *G. sulphuraria* is often the only organism able to colonize acidic hot springs where it forms mats of a deep blue-green color (Pinto et al., 2007). The peculiar color is due to a presence of the blue pigment phycocyanin and of chlorophyll a (Albertano et al., 2000). In addition to phycocyanin, *G. sulphuraria* is rich proteins (Cheng et al., 2019), insoluble dietary fibres (Graziani et al., 2013), and antioxidants (Carfagna et al., 2016). Given its high nutritional value *G. sulphuraria* may be a suitable component in foods (Graziani et al., 2013) .

Given its benthonic nature, *G. sulphuraria* has been considered extremely photosensitive with light inhibition occurring at intensities above 200 $\mu mol \cdot m^{-2} \cdot s^{-1}$ (Brock, 1978; Sloth et al., 2006). Due to photosensitivity, most of the research on *G. sulphuraria* has focused on heterotrophic cultivation. *G. sulphuraria* has been successfully grown heterotrophically using 27 organic substrates (Graziani et al., 2013; Gross & Schnarrenberger, 1995) although most of *G. sulphuraria* strains completely lose their pigmentation when grown in the dark (Graziani et al., 2013; Gross & Schnarrenberger, 1995). Previous studies also indicated that the presence of organic substrates in the light strongly reduced photosynthesis of *G. sulphuraria* (Mozaffari et al., 2019; Stadnichuk et al., 1998). Oesterhelt et al (Oesterhelt et al., 2007) reported that if glucose is available *G. sulphuraria* prefers heterotrophic metabolism over autotrophic growth, repressing O_2 production and CO_2 fixation.

A screening performed by the Algal Collection of the University Federico II (ACUF) on 43 *G. sulphuraria* strains (Graziani et al., 2013), identified the strain *G. sulphuraria* ACUF 64 as the most promising autotrophic strain. The aim of our work was to assess if the strain *G.*

sulphuraria ACUF 64 could be cultivated under 'oxygen balanced' mixotrophy and therefore grow without any gas exchange in a closed photobioreactor (***PBR***). The strain was cultivated at pH 1.7 and we investigated the potential of such acidic environment to prevent bacterial contamination. In addition, we studied both autotrophic and mixotrophic cultivation of ***G. sulphuraria*** ACUF 64 at a high light intensity to identify the cell concentration resulting in maximal biomass productivity. We explored the hypothesis that in ***G. sulphuraria*** ACUF 64 the mixotrophic metabolism is the sum of the heterotrophic and autotrophic metabolisms paying special attention to the carbon balance.

MATERIALS AND METHODS

Organism, Media and Cultivation Conditions

Galdieria sulphuraria ACUF 64 (http://www.acuf.net) was kindly donated by Prof A. Pollio (University Federico II, Naples, Italy). The culture medium was prepared as following (composition expressed in $mol \cdot L^{-1}$): $2.2 \cdot 10^{-3}$ KH_2PO_4, $20.0 \cdot 10^{-3}$ $(NH_4)_2SO_4$, $1.6 \cdot 10^{-3}$ $MgSO_4 \cdot 7 \cdot H_2O$, $0.1 \cdot 10^{-3} \cdot CaCl_2$, $0.16 \cdot 10^{-3}$ EDTA ferric sodium salt, $0.05 \cdot 10^{-3}$ $Na_2EDTA \cdot 2H_2O$, $0.9 \cdot 10^{-3}$ NaCl, $0.2 \cdot 10^{-3} \cdot H_3BO_3$, $20.2 \cdot 10^{-6}$ $MnCl_2 \cdot 4H_2O$, $20.6 \cdot 10^{-6}$ $ZnCl_2$, $8.0 \cdot 10^{-6}$ $CuSO_4 \cdot 5H_2O$, $4.1 \cdot 10^{-6}$ $Na_2MoO_4 \cdot 2H_2O$, $4.2 \cdot 10^{-6} CoCl_2 \cdot 6H_2O$. The pH was adjusted to 1.7±0.1 with about 18 $mL \cdot L^{-1}$ of 2.5 M of H_2SO_4. During photobioreactor experiments all concentrations were increased fourfold with exception of EDTA ferric sodium salt and $Na_2EDTA \cdot 2H_2O$ that were doubled, and NaCl that was not increased. Axenic algal cultures were maintained in 250 ml flasks containing 100 mL medium. Cultures were maintained in light-limited linear growth by weekly dilution. They were incubated at 37° C, 4.5% v/v CO_2 and stirring at 100 rpm with a magnetic rod. The flasks were illuminated 24h/24h from below with a warm-white LED (BXRAW1200, Bridgelux, USA) at a photon flux density (*PFD*, μmol m^{-2} s^{-1}) of 300±35 μmol m^{-2} s^{-1}.

Heterotrophic flask experiments

The heterotrophic biomass yield on substrate ($Y^{het}_{x/s}$, $C\text{-}mol_x \cdot C\text{-}mol_s^{-1}$) was determined in dark batch experiments. The heterotrophic experiments were conducted in flasks adding glucose monohydrate at 0.3 $C\text{-}mol_s \cdot L^{-1}$ to the autotrophic medium. The heterotrophic experiments were started using an inoculum that was acclimated to the heterotrophic growth for at least 2 weeks. Cultures were maintained in exponential growth by diluting the culture with fresh medium every 3-5 days. Flasks were were wrapped in aluminum foil and incubated at 37°C in darkness while being shaken at 250 rpm. The experiments were started at an optical density at 750 nm

(OD_{750}) of 0.24. During the experiments, multiple samples per day were taken until glucose was depleted. The microalgae concentration was quantified measuring OD_{750}. For each sample, first OD_{750} was measured, 1 mL was centrifuged and the supernatant was stored at -20˚C prior to analysis of glucose concentration.

The OD_{750} was converted into dry weight (C_x, $g_x \cdot L^{-1}$) using a linear regression (see analytical methods). At the end of each experiment, the C_x was measured to verify that the correlation was still valid. The heterotrophic biomass yield on substrate $Y^{het}_{x/s}$ was calculated as follow:

$$Y^{het}_{x/s} = -\frac{(C_{xe}-C_{x0})}{MW_x \cdot (S_e-S_0)} \qquad (1)$$

where C_{x0}/C_{xe} and S_0/S_e respectively are the biomass and the substrate concentrations (C-mol·L^{-1}) at the start and the end of the exponential phase while MW_x ($g_x \cdot mol_x^{-1}$) is the weight of 1 carbon mole of biomass. The MW_x was determined at the end of the experiment and it was assumed to be constant during the batch.

The specific growth rate (μ, h^{-1}) during exponential growth was calculated according to:

$$\mu = \frac{ln(C_{xe})-ln\,(C_{x0})}{t_e-t_0} \qquad (2)$$

where t_0/t_e and C_{x0}/C_{xe} are respectively the time and the biomass concentration at the start and the end of the exponential phase. Experiments were performed in biological duplicates. The averages and standard error will be shown in graphs and tables.

Photobioreactor Setup and Experiments

Galdieria sulphuraria ACUF 64 was grown in a 3 L bioreactor (Applikon, The Netherlands) described in more detail in Abiusi et al., 2020a. This reactor had a working volume (V_{PBR}) of 2 L. The internal diameter was 0.130 m, while the liquid height was maintained at 0.166 m by a level sensor, resulting in a cylindrical illuminated area (A_{PBR}) of 0.068 m^2.

The reactor was operated under continuous lighting provided by warm white LEDs that were configured around the reactor creating a homogenous light field over the cylindrical reactor surface at an average *PFD* of 514±17 μmol m^{-2} s^{-1}.

The reactor was equipped with a dissolved oxygen (*DO*) sensor (VisiFerm DO ECS 225, Hamilton, US). This *DO* sensor was calibrated inside the reactor filled with growth medium and sparged with dinitrogen gas, or air, to give a *DO* level of respectively 0 and 100%. The reactor was kept at 37°C by a heat exchanger inside the reactor vessel. To prevent evaporation, the reactor was equipped with a condenser connected to a cryostat feeding cold water of 2°C. Continuous stirring at 500 rpm was applied during all experiments. When aerated, air enriched with 2% v/v carbon dioxide was provided at a flow rate of 1 L·min^{-1} using mass flow controllers (Smart TMF 5850S, Brooks Instruments, USA). The pH was continuously measured and controlled at 1.7 by automatic base (2 M, NaOH) or acid (2 M H_2SO_4) addition.

The acid and base solutions, glucose solution, and the harvest bottle were placed on analytic balances. The balances, *DO* sensor, temperature probe, pH sensor and mass flow controllers were connected to a data acquisition system interfaced via a computer by means of a virtual instrument (Lab View, National Instruments, USA) allowing for continuous data logging and process control. Culture samples for off-line measurements were taken aseptically from the reactor through a dedicated port. The complete setup, including all the solutions, were sterilized prior the experiment by autoclaving for 60 min at 121˚C.

In one experiment the reactor was operated in chemostat while in another experiment it was operated in repeated batch. The chemostat experiment was performed at a dilution rate (*D*, day^{-1}) of 0.5 day^{-1}. The culture was first grown autotrophically for two weeks. For the 4 last days of this period the harvest bottle was placed in ice water. The harvested culture was collected daily. A 10 mL aliquot was used for dry weight determination. Other measurements (see section culture sampling and off-line measurements) were taken multiple times per day directly from

the reactor during these 4 days. After these first 14 days oxygen balanced mixotrophy was initiated at a *DO* of 90%. In this period the reactor was not aerated and a glucose solution was automatically supplied when the *DO* exceeded the set-point of 90%. Mixotrophic cultivation was maintained for 14 days and during the last 4 days samples were taken again according to the same procedures as described for the autotrophic experiment.

In another experiment the photobioreactor was operated in repeated batch mode. The experiment was started inoculating the reactor with an autotrophic culture at 0.4 $g_x \cdot L^{-1}$. The microalgal culture in the reactor was diluted every 5-9 days for three times (batches I-III) for an overall cultivation period of 21 days. After the first 21 days, the glucose solution was supplied at a constant rate while maintaining gassing with CO_2 enriched air resulting in a mixotrophic culture. After 2 days we switched to oxygen balanced mixotrophy as we stopped gassing and switched to the automatic supply of glucose to maintain the DO at 90% air saturation. The culture was diluted every 6-8 days for three times (batches IV-VI) for an overall cultivation period of 23 days. During each batch daily samples were taken daily for different analyses.

Photobioreactor Calculations

In the chemostat experiments, the volumetric biomass production rate (r_x, $g_x \cdot L^{-1} \cdot day^{-1}$) was calculated multiplying the measured biomass concentration (C_x, $g_x \cdot L^{-1}$) with the dilution rate (D, day^{-1}). In the repeated batch experiment r_x was calculated from a linear regression of the increase of C_x over time. The r_x was also converted into its carbon equivalent (r_c, $C\text{-}mol_x \cdot L^{-1} \cdot day^{-1}$) by dividing r_x by the molecular weight of 1 C-mol of biomass (MWx, $g_x \cdot C\text{-}mol_x^{-1}$). The MWx was determined in each sample taken from the reactor. In the autotrophic cultures r_c was used to determine the biomass yield on light ($Y_{x/ph}$, $C\text{-}mol_x \cdot mol_{ph}^{-1}$) according to the formula:

$$Y_{x/ph} = \frac{r_{c,auto} \cdot V_{PBR}}{\text{PFD} \cdot A_{PBR}} \quad (1)$$

In the mixotrophic experiments, the volumetric substrate consumption rate (r_s, C-mols·L^{-1}·day^{-1}) was calculated as follows, assuming ideal mixing:

$$r_s = \frac{F_{glu} \cdot C_{s,glu} - D \cdot V_{PBR} \cdot C_s}{V_{PBR}} \qquad (2)$$

Where F_{glu} (L·day^{-1}) and $C_{s,glu}$ represent respectively the supply rate of the glucose solution and the concentration in the glucose solution while Cs (C-mol_s·L^{-1}) is the glucose concentration measured in the reactor (C-mol_s·L^{-1}). The mixotrophic yield on substrate ($Y^{mixo}_{x/s}$, C-mol_x·mol_s^{-1}) was calculated dividing r_c by r_s.

The specific light supply rate (q_{ph}, μmol_{ph}·g_x^{-1}·s^{-1}) was calculated as follow:

$$q_{ph} = \frac{PFD \cdot A_{PBR}}{C_x \cdot V_{PBR}} \qquad (3)$$

ANALYTICAL METHODS

Photo Flux Density Measurements

The photo flux density *PFD* was measured with a LI-COR 190-SA 2π PAR quantum sensor. Light intensity on the reactor surface was measured at 16 fixed points inside the empty reactor.

Culture Sampling and Off-Line Measurements

Samples were taken aseptically multiple times per day for off-line measurements. Two 1 mL aliquots were centrifuged at 20238 RCF for 10 min. When needed, the supernatant was immediately analyzed for glucose or phosphorus content. The pellet was washed twice with demineralized water and cooled to -20 °C, lyophilized and stored at room temperature in the dark.

Dry Weight Concentration

Culture growth was estimated by biomass dry weight (C_x, $g_x \cdot L^{-1}$) determination: aliquots of the culture (2-5 mL) were diluted to 25 mL with demineralized water and filtered over pre-weighed Whatman GF/F glass microfiber filters (diameter of 55 mm, pore size 0.7 µm). The filters were washed with deionized water (25 mL) and dried at 105° C until constant weight.

Optical density

The optical density was measured in duplicate on a spectrophotometer (DR6000, Hach-Lange, US) at 680 and 750 nm. The relationship between C_x and OD_{750} was determined with biomass grown heterotrophically in a range of 0.3 to 5 $g_x \cdot L^{-1}$ by filtering at least 5 mg of algal dry biomass onto pre-weighed glass fiber filters (Whatman GF/F, GE Healthcare UK Ltd., UK) which were dried overnight at 105 °C until constant weight. This resulted in the following correlation:

C_x ($g_x \cdot L^{-1}$) = $0.55 \cdot OD_{750} + 0.06$ ($R^2 = 1.00$)

Average Absorption Cross Section

Average absorption cross section (a_x, $m^2 \cdot Kg^{-1}$) in the PAR region (400-700 nm) of the spectrum was measured and calculated according to de Mooij et al. (de Mooij et al., 2015). The absorbance was measured in UV-VIS/double beam spectrophotometer (Shimadzu UV-2600, Japan) equipped with integrating sphere (ISR-2600). Cuvettes with an optical path of 2 mm were used.

Photosystem II Quantum Yield

The photosystem II maximum quantum yield (*QY*, F_v/F_m) was measured at 455 nm with an AquaPen-C AP-C 100 (Photon Systems Instruments, Czech Republic). Prior to the measurement, samples were adapted to darkness for 15 min at room temperature and diluted to optical density at 750 nm between 0.3 and 0.5.

Glucose and phosphorus determination

In the mixotrophic culture, glucose concentrations were daily measured using an YSI analyzer (YSI 2700, YSI Life Sciences, Yellow Springs, OH, USA). Total phosphorus was quantified with a spectrophotometric phosphorus detection kit (LCK 349/350, Hach Lange, Germany).

Total Organic and Carbon and Nitrogen

The organic carbon and nitrogen content in the pellet were measured as total carbon (*TOC*, $g_c \cdot L^{-1}$) and total nitrogen (*TON*, $g_N \cdot L^{-1}$) respectively using the TOC-L analyzer. The biomass carbon content ($C_{\%}$, % $w_c \cdot w_x^{-1}$) and nitrogen content ($N_{\%}$, % $w_N \cdot w_x^{-1}$) was calculated by dividing the obtained total carbon and total nitrogen by the dry weight determined on the same sample. The $C_{\%}$ was used to determine the biomass molecular weight (*MWx*, $g_x \cdot C\text{-}mol_x^{-1}$). *MWx* was

determined by dividing the carbon molecular weight (12.011 $g_c \cdot C\text{-}mol^{-1}$) by *C%*. The $N_{\%}$ was used to determine the biomass protein content using a protein-nitrogen fraction (0.168 $g\text{-}N \cdot g\text{-}protein^{-1}$). (Kliphuis et al., 2012)

Assessment of Bacterial Contamination

During the experiment, axenicity was checked daily by DNA staining of culture samples with SYBR Green I (Sigma-Aldrich, US) and fluorescence microscopy (EVOS FL auto, Thermo Fisher Scientific, US).

Statistical Analysis

Propagation of errors by summation and multiplication of individual measurements were calculated according to Abiusi et al., 2020a. In the chemostat experiment each day of the steady state was considered as a replicate (n=4). In the autotrophic repeated batch experiment, batch I and III were considered as replicates (n=2) while in the mixotrophic experiment each batch was considered as a replicate (n=3). In each experiment autotrophic and mixotrophic cultures were compared and significant differences were analyzed by one-way ANOVA ($P<0.05$).

RESULTS AND DISCUSSIONS

Contamination of algal cultures at low pH

One of the major challenges of mixotrophic outdoor cultivation is the undesired contamination by heterotrophic microorganisms, mainly bacteria and fungi (Unnithan et al., 2014), which compete with microalgae for the assimilation of organic carbon. In the present work *G. sulphuraria* was cultivated at pH 1.7±0.1 and fluorescence DNA staining did not show contaminations neither during the several weeks of heterotrophic cultivation in flasks, nor in our closed photobioreactor (*PBR*) for 33 days and for 42 days.

Prior studies (Delanka-Pedige, 2018) demonstrated that low pH reduced the initial bacterial population by 98% and resulted in complete removal of pathogens when *G. sulphuraria* was cultivated in unsterilized primary effluent at pH 2. However, *G. sulphuraria* has been reported to be prone to fungal contamination when grown mixotrophically in open biofilms (Carbone et al., 2020). In the current work, we employed a closed cultivation vessel and all the inputs and outputs used in our experiments were filter sterilized. This reactor configuration combined with the low pH was effective in preventing contaminations.

Heterotrophic reference experiments

Strict heterotrophic experiments were conducted to determine the heterotrophic biomass yield on substrate ($Y^{het}_{x/s}$). The $Y^{het}_{x/s}$ was determined in a heterotrophic batch experiment performed in flasks. *G. sulphuraria* ACUF 64 was grown in darkness in a medium supplemented with glucose. Since the inoculum was obtained from an autotrophic culture, the culture was allowed to adapt to heterotrophic growth conditions for two weeks. During this pre-cultivation period, the culture lost most of its pigments (fig. S1). This was verified by measuring the absorption cross section spectrum (fig. S2). The loss of pigmentation during heterotrophic cultivation of this strain has been previously reported (Graziani et al., 2013).

Figure 1. *Heterotrophic biomass production (squares) and substrate consumption (triangle) of G. sulphuraria ACUF 64 cultivated at pH 1.6 with 330 C-mmol·L^{-1} glucose.*

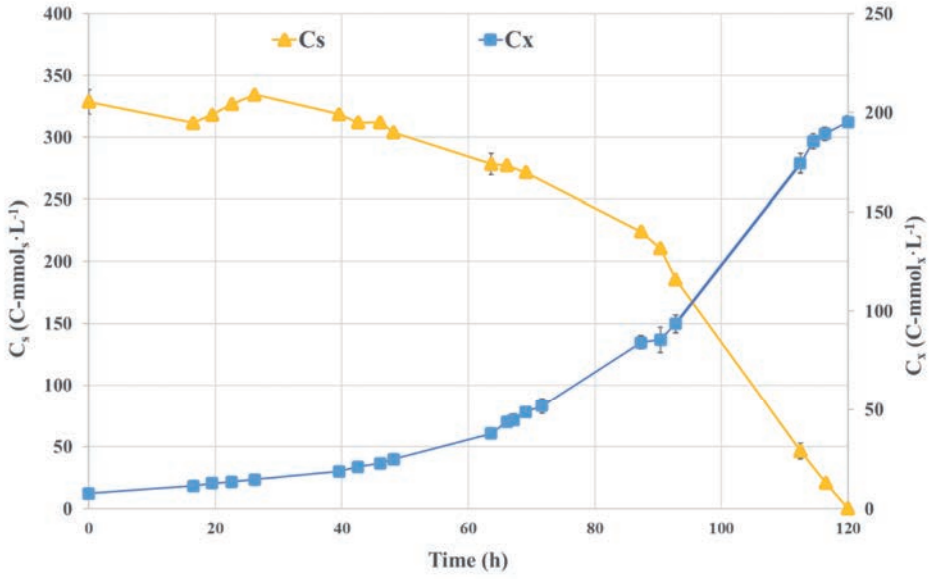

Heterotrophic biomass production and substrate consumption are reported in figure 1. At 330 C-mmol$_s$·L^{-1}, cultures grew exponentially for 116 h at a specific growth rate (μ) of 0.74 day^{-1}. The only published heterotrophic experiment performed with *G. sulphuraria* ACUF 64 (Graziani et al., 2013) reported a specific growth rate of 1.0 day^{-1} which is in line with the most studied *G. sulphuraria* 74G (Graverholt & Eriksen, 2007). The final biomass concentration was 195 C-mmol$_x$·L^{-1} corresponding to $Y_{x/s}$ of 0.59±0.02 (C-mol$_s$·C-mol$_s^{-1}$). Previously, heterotrophic substrate yields of 0.53–0.63 C-mol$_s$·C-mol$_s^{-1}$ have been reported for *G. sulphuraria* 74G grown in aerobic fermenters (Graverholt & Eriksen, 2007). The maximal $Y^{het}_{x/s}$ for aerobic heterotrophic organisms is 0.7 mol$_x$ mol$_s^{-1}$ and it is bound by thermodynamic constraints (Heijnen, 1994). Our results indicate that, despite the low pH, when grown heterotrophically *G. sulphuraria* can efficiently convert organic substrate into biomass but at a

maximal growth rate which is 4 and 9 times lower than the most studied *Chlamydomonas* and *Chlorella* species, respectively. (Blanken et al., 2016)

Oxygen Balanced Mixotrophy in Galdieria sulphuraria ACUF 64

We previously demonstrated with *Chlorella sorokiniana* that a mixotrophic culture can operate without any gas-liquid transfer of oxygen or carbon dioxide (Abiusi et al., 2020a) by coupling the substrate supply rate to the rate of photosynthesis. In the present study the same concept was applied to *Galdieria,* and we compared biomass productivity of chemostat and repeated batch cultivations. In both operating strategies the cultures were also grown under autotrophic conditions without the addition of organic carbon but with continuous gassing with CO_2 enriched air. These autotrophic cultures where used as reference to determine the biomass yield on photons ($Y_{x/ph}$).

Oxygen balanced mixotrophy in chemostat

Oxygen balanced mixotrophy was applied successfully to *G. sulphuraria* ACUF 64 and the *PBR* was operated without any gas exchange for 14 days. Under these conditions the biomass concentration and productivity were 3.6 times higher than with the autotrophic reference (table 1). The result clearly indicated that, at least in our strain, the presence of an organic substrate does not inhibit oxygen production as was previously suggested (Mozaffari et al., 2019; Oesterhelt et al., 2007). Subtracting the estimated fraction of the biomass heterotrophically produced ($r_{c,\,het}$) from the overall mixotrophic productivity ($r_{c,mixo}$), allowed us to calculate the fraction of biomass produced autotrophically ($r_{c,auto'}$). The $r_{c,auto'}$, and therefore the biomass yield on light ($Y_{x/ph}$), was not significantly ($P>0.05$) different from the $r_{c,auto}$ of the autotrophic culture leading us to conclude that the mixotrophic stoichiometry was the sum of the heterotrophic and autotrophic metabolisms (table 1).

The pigmentation of the mixotrophic and autotrophic cultures were found to be different. The average absorption cross section (a_x) of the autotrophic culture was double the mixotrophic culture a_x (table 1). A recent study on *G. sulphuraria* ACUF 64 found a lower chlorophyll a content in a mixotrophic culture compared to an autotrophic culture grown under otherwise similar conditions (Salbitani et al., 2020). This indicates that the addition of organic substrate has an impact on pigmentation, which is not surprising considering the complete loss of pigments when *G. sulphuraria* was cultivated in darkness (see previous section).

In the chemostat culture of *G. sulphuraria* ACUF 64 cultivated in autotrophy without the addition of organic carbon, but with continuous gassing with CO_2 enriched air, the biomass yield on light ($Y_{x/ph}$) was 12.3 C-mmol$_x$·mol$_{ph}^{-1}$, approximately 3.3 times lower than $Y_{x/ph}$ found in *C. sorokiniana* under similar experimental conditions (Abiusi et al., 2020a). The lower autotrophic performance can be partially explained by photoinhibition. *G. sulphuraria* is well known to be photosensitive with light inhibition occurring at intensities above 200 µmol·m^{-2}·s^{-1} (Oesterhelt et al., 2007; Sloth et al., 2006). Light inhibition was confirmed by measuring the dark-adapted quantum yield of PSII photochemistry (*QY*). The *QY* was 0.22 in autotrophic culture, significantly ($P<0.05$) lower than the value of 0.32 measured in the mixotrophic culture, and both definitely lower than 0.72 generally reported in *C. sorokiniana* (Abiusi et al., 2020b; de Mooij et al., 2017). The low *QY* confirms the lower autotrophic performance of *G. sulphuraria* compared to *C. sorokiniana.* Moreover, the mixotrophic culture displayed a higher *QY* than the autotrophic culture, indicating a lower degree of photoinhibition. This higher *QY* is potentially explained by a 3.5 times lower specific light supply rate (q_{ph}) in the mixotrophic culture compared to the autotrophic culture (Table 1).

Table 1. *Overview of the off-line, DO, D measurements on the chemostat cultivation of G. sulphuraria ACUF 64 under mixotrophic and autotrophic conditions.*

	Unit	Autotrophic	Mixotrophic
C_x	$g_x \cdot L^{-1}$	0.86±0.05[a]/7.4±0.2*	3.06±0.16[b]
D	day^{-1}	0.51±0.04 [a]	0.50±0.01 [a]
$C_{\%}$	% $w_C \cdot w_x^{-1}$	49.0±1.1 [a]	49.1±1.1 [a]
$N_{\%}$	% $w_N \cdot w_x^{-1}$	9.8±0.3 [a]	9.3±0.1 [b]
r_x	$g_x \cdot L^{-1} \cdot day^{-1}$	0.45±0.02 [a]	1.62±0.07 [b]
$r_{c,mixo}$	$C\text{-}mmol_x \cdot L^{-1} \cdot day^{-1}$	n.a	66.0±2.9
r_s	$C\text{-}mmol_s \cdot L^{-1} \cdot day^{-1}$	n.a	-82.6±3.8
$Y^{mixo}_{x/s}$	$C\text{-}mol_x \cdot C\text{-}mol_s^{-1}$	n.a	0.80±0.04
$r_{c,het'}$	$mmol_x \cdot L^{-1} \cdot day^{-1}$	n.a	48.7±2.2
$r_{c,auto'}$ / $r_{c,auto}$	$C\text{-}mmol_x \cdot L^{-1} \cdot day^{-1}$	18.5±1.0 [a]	17.3±3.1 [a]
$Y_{x/ph}$	$C\text{-}mol_x \cdot C\text{-}mol_{ph}^{-1}$	12.3±0.6 [a]	11.5±2.0 [a]
a_x	$m^2 \cdot kg^{-1}$	114±6 [a]/180±3* [b]	62±7 [c]
q_{ph}	$\mu mol_{ph} \cdot g_x^{-1} \cdot s^{-1}$	20.2±1.8 [a]/2.3±0.1* [b]	5.7±0.5 [c]
QY	Fm/Fv	0.22±0.01 [a] /0.48±0.02* [b]	0.32±0.02 [c]

*Values obtained in the flasks used as inoculum.

Along the rows, the same letter indicates no significant differences (P > 0.05).

In the autotrophic inoculum QY was 0.48, indicating that not only the autotrophic culture in the *PBR* but probably even the mixotrophic culture was experiencing light stress. The inoculum was grown in batch at 300 $\mu mol \cdot m^{-2} \cdot s^{-1}$ and at the time of QY and a_x measurements, just prior to inoculation, a biomass concentration (C_x) of 7.4 $g_x \cdot L^{-1}$ was reached (data not shown). Assuming the flaks used for the inoculum were illuminated solely from the bottom, the inoculum had a volumetric light supply rate similar to the one observed in the reactor (17 $\mu mol \cdot L^{-1} \cdot s^{-1}$). However, given the high C_x, the specific light supply rate (q_{ph}) was 2.3 $\mu mol \cdot g_x^{-1} \cdot s^{-1}$. Therefore, low q_{ph} explains the higher a_x and QY measured in the inoculum compared to the autotrophic culture (table 1).

Despite low $Y_{x/ph}$ and photoinhibition, the autotrophic culture reached a steady state which was maintained for more than a week. In a chemostat culture, once a steady state was obtained, the specific growth rate (μ) equaled the dilution rate, therefore making μ 0.50 day^{-1}. A similar autotrophic μ has been reported in our strain earlier (Graziani et al., 2013) and it is about double the autotrophic μ reported in other *Galdieria* strains (Oesterhelt et al., 2007; Sentsova, 1988) pointing towards potential of this strain in autotrophic biomass production. The observed effect of q_{ph} on photosynthetic performance strongly suggests that high C_x, and therefore low q_{ph}, is an effective strategy to minimize photoinhibition in *G. sulphuraria*. In this study such an optimization was done through repeated batch experiments where the specific light supply rate continuously decreases during the batch phase because of an increasing biomass concentration.

Oxygen balanced mixotrophy in repeated batch

The purpose of the repeated batch experiment was to identify the biomass concentration (C_x) that results in an optimal light regime maximizing biomass productivity of *G. sulphuraria* ACUF 64 under our experimental settings. The repeated batch approach also provided information on the effect of a sudden change of the specific light supply rate (q_{ph},) on the autotrophic and mixotrophic metabolism after culture dilution. Six consecutive batches were performed: three autotrophic batches (I, II, III), and three mixotrophic batches (IV, V, VI).

Referring to figure 2, it can be observed that in the autotrophic cultures linear growth was obtained between 2 and 5 $g_x \cdot L^{-1}$ and, at lower C_x the culture was photoinhibited while at higher C_x light limitation became more evident and biomass productivity (r_x) decreased. In batches I and III during the linear phase the r_x was 0.97±0.2 $g_x \cdot L^{-1} \cdot day^{-1} \cdot$and the biomass yield on light (Yx/ph) was 24.8±1.3. Those values are about double the values of the autotrophic culture operated in chemostat confirming that in our chemostat experiment the autotrophic culture was light inhibited. Biomass productivity and yield on light in *G. sulphuraria* were comparable to

other commercially relevant microalgae such as *Isocrysis lutea* (Gao et al., 2020), *Rhodomonas sp.* (Oostlander et al., 2020), *Nannochloropsis sp* (Benvenuti et al., 2016), indicating the potential of this strain for autotrophic biomass production.

Figure 2. *Autotrophic (I-III) and mixotrophic (IV-VI) repeated batches. Dotted lines indicate the time of dilution. Black arrow indicates the end of aeration. Orange area indicates pH 0.2. In the graph are reported biomass concentration (C_x dotes), specific light supply rate (q_{ph}, triangles), photosystem II maximum quantum yield (QY, squares) and average absorption cross section (a_x, diamonds).*

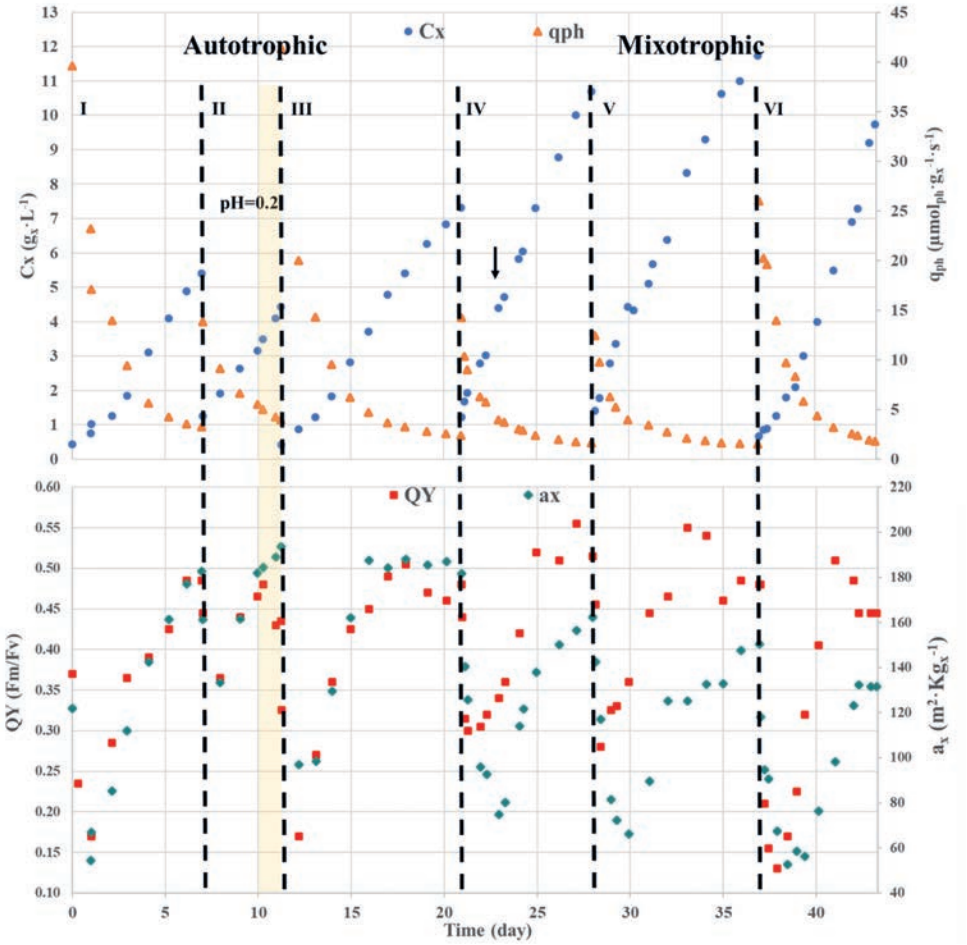

In three mixotrophic repeated batches (IV, V, VI) linear growth started at 2.8 $g_x \cdot L^{-1}$ and it was maintained until a biomass concentration (C_x) between 7.3 to 9.7 $g_x \cdot L^{-1}$ was reached (Figure 2, table 2). The upper biomass limit, at which linear growth rate was still maintained and optimal biomass productivity (r_x) observed, progressively increased during each batch (Figure 2, table 2). The same trend was observed for the mixotrophic biomass yield on substrate ($Y^{mixo}_{x/s}$), while the maximum absorption cross section area (a_x) at the end of each batch progressively decreased. Together these four observations indicate adjustment of metabolism from autotrophy to mixotrophy over time, resulting in a culture that in the last batch (VI) was more acclimated to the presence of glucose. The three mixotrophic batches lasted 22 days in total. The fact that the cultures kept adapting to mixotrophy over such a long time was unexpected. A recent study (Salbitani et al., 2020) investigated the cellular changes occurring in *Galdieria phlegrea* during the switch to mixotrophic metabolism from an heterotrophic culture. The study suggested that 7-10 days were needed to fully recover the photosynthetic capacity lost during the heterotrophic growth. In our experiment the culture was switched from autotrophy to mixotrophy. In our previous experiment in chemostat (see previous section) steady state was observed after one week and maintained over 7 days. A possible explanation for the slow adaptation time observed in the mixotrophic repeated batch is that the sudden increase in the photon supply rate (q_{ph}), after dilution interfered with the heterotrophic metabolism, destabilizing the culture and increasing the adaptation time. Inhibition of glucose uptake observed after each dilution (Figure 3) validates this hypothesis and will be discussed later.

In the comparison between mixotrophic and autotrophic cultures, we will focus mainly on mixotrophic batch VI and on the average between autotrophic batches I and III. The autotrophic batch II was excluded from the comparison because the culture grew at pH 0.2 (see next section). In the mixotrophic culture (VI) biomass productivity (r_x) was 1.8-fold higher than in the autotrophic cultures (I and III) and optimal r_x was maintained at a biomass concentration

(C_x) that was double the biomass concentration in the autotrophic culture. Moreover, it was possible to operate the mixotrophic culture without any gas-liquid transfer of oxygen or carbon dioxide for 20 days. The internal carbon dioxide recirculation led to a mixotrophic biomass yield on substrate of 0.91 ($Y^{mixo}_{x/s}$, $C\text{-}mol_x \cdot C\text{-}mol_s^{-1}$) making the process close to carbon neutral. These results are in line with our previous finding obtained with *Chlorella* (Abiusi et al., 2020a; Abiusi et al., 2020b) suggesting that 'oxygen balanced' mixotrophy can, be applied to other mixotrophic algae.

In the three mixotrophic repeated batches (IV, V, VI) the stoichiometry was not the sum of the autotrophic and heterotrophic metabolism (table 2). Subtracting the estimated fraction of the biomass produced heterotrophically ($r_{c,het}$) from the overall mixotrophic productivity ($r_{c,mixo}$), allowed us to calculate the fraction of biomass produced autotrophically ($r_{c,auto'}$). This $r_{c,auto'}$, was 2.6, 2.3, and 1.5 fold lower than the autotrophic reference (batches I and III) respectively in batch IV, V and VI. It must be highlighted that in the estimation of the autotrophic fraction

Table 2. *Overview of the off-line measurements on the repeated batch cultivation of G. sulphuraria ACUF 64 under mixotrophic and autotrophic conditions.*

		Autotrophic			Mixotrophic		
	Unit	I	II	III	IV	V	VI
C_x	$g_x \cdot L^{-1}$	1.9-4.9	1.9-4.4	1.8-4.8	2.8-7.3	2.8-8.3	3.0-9.7
$C_{\%}$	$\%\ w_C \cdot w_x^{-1}$	45.4	46.1	47.5	48.3	47.0	47.6
$N_{\%}$	$\%\ w_N \cdot w_x^{-1}$	10.3	10.4	10.0	9.8	9.1	9.4
r_x	$g_x \cdot L^{-1} \cdot day^{-1}$	0.95	0.76	0.98	1.50	1.59	1.72
$r_{c,mixo}$	$C\text{-}mmol_x \cdot L^{-1} \cdot day^{-1}$	-	-	-	60.3	62.2	68.2
r_s	$C\text{-}mmol_s \cdot L^{-1} \cdot day^{-1}$	-	-	-	84.2	78.4	74.5
$Y^{mixo}_{x/s}$	$C\text{-}mol_x \cdot C\text{-}mol_s^{-1}$	-	-	-	0.72	0.79	0.91
$r_{c,het'}$	$mmol_x \cdot L^{-1} \cdot day^{-1}$	-	-	-	49.4	46.0	43.7
$r_{c,auto'}$ / $r_{c,auto}$	$C\text{-}mmol_x \cdot L^{-1} \cdot day^{-1}$	35.9	29.2	38.8	10.9	16.2	24.4
$Y_{x/ph}$	$C\text{-}mmol_x \cdot mol_{ph}^{-1}$	23.9	19.4	25.8	7.23	10.77	16.25
a_x	$m^2 \cdot kg^{-1}$	177	194	184	138	125	132
q_{ph}	$\mu mol_{ph} \cdot g^{-1} \cdot s^{-1}$	9.4-3.6	9.1-3.9	9.5-3.6	6.3-2.4	6.3-2.1	5.8-1.8
QY	Fm/Fv	0.37-0.49	0.37-0.44	0.36-0.49	0.31-0.52	0.33-0.55	0.32-0.45

of the mixotrophic biomass productivity ($r_{c,auto'}$) we assumed that the heterotrophic biomass yield on substrate ($Y_{x/s}$), measured in the heterotrophic experiment, did not change in the presence of light. This calculation shows that the yield of biomass on light (autotrophy) or, possibly, the yield of biomass on glucose (heterotrophy) are affected by either the presence of glucose, or the presence of light. As a result, mixotrophy cannot be approached as the sum of the heterotrophic and the autotrophic metabolism and there appears to be an interaction between these metabolic pathways. The negative interaction between the heterotrophic and the autotrophic metabolism decreased over time. However, even in batch VI the hypothetical autotrophic rate under mixotrophy was still 1.5 lower than the autotrophic rate without the addition of organic carbon.

Interaction between autotrophic and heterotrophic metabolisms were also noticed in the dissolved oxygen (*DO*) control by means of substrate addition (Figure 3). After each dilution, the sudden increase in specific light supply rate (q_{ph}) partially inhibited glucose uptake and it was not possible to control the *DO*. Since the substrate was supplied to the culture without being consumed, substrate accumulated in the reactor. In order to deplete the accumulated substrate (C_s), we manually interrupted the glucose supply (*Fs*). The initial accumulation of substrate, followed by its depletion, provoked unstable *DO*, that lasted the first 2-4 days after dilution and resulted in *DO* fluctuations from 30 to 230 %. After this initial phase, the *DO* was successfully maintained in the desired range by automatic substrate addition at an average feed rate *Fs* of -2.95±0.59 $Cmmol_s \cdot L^{-1} \cdot h^{-1}$.

Previous studies indicated reduced photosynthetic performance and even suppression of oxygen evolution in other *G. sulphuraria* strains cultivated under mixotrophic conditions with glucose supplementation (Mozaffari et al., 2019; Oesterhelt et al., 2007). According to our results, rather than glucose affecting photosynthesis, it was the sudden increase in q_{ph} that inhibited glucose uptake. This hypothesis is supported by measuring the dark-adapted quantum yield of PSII

Figure 3. *Mixotrophic repeated batches. Dotted lines indicate the time of dilution. Red arrows indicates substrate depletion. In the graph are reported biomass concentration (C_x dotes), dissolved oxygen (DO, triangles), substrate concentration in the reactor (C_s, squares) and substrate supply rate (F_s, diamonds)*

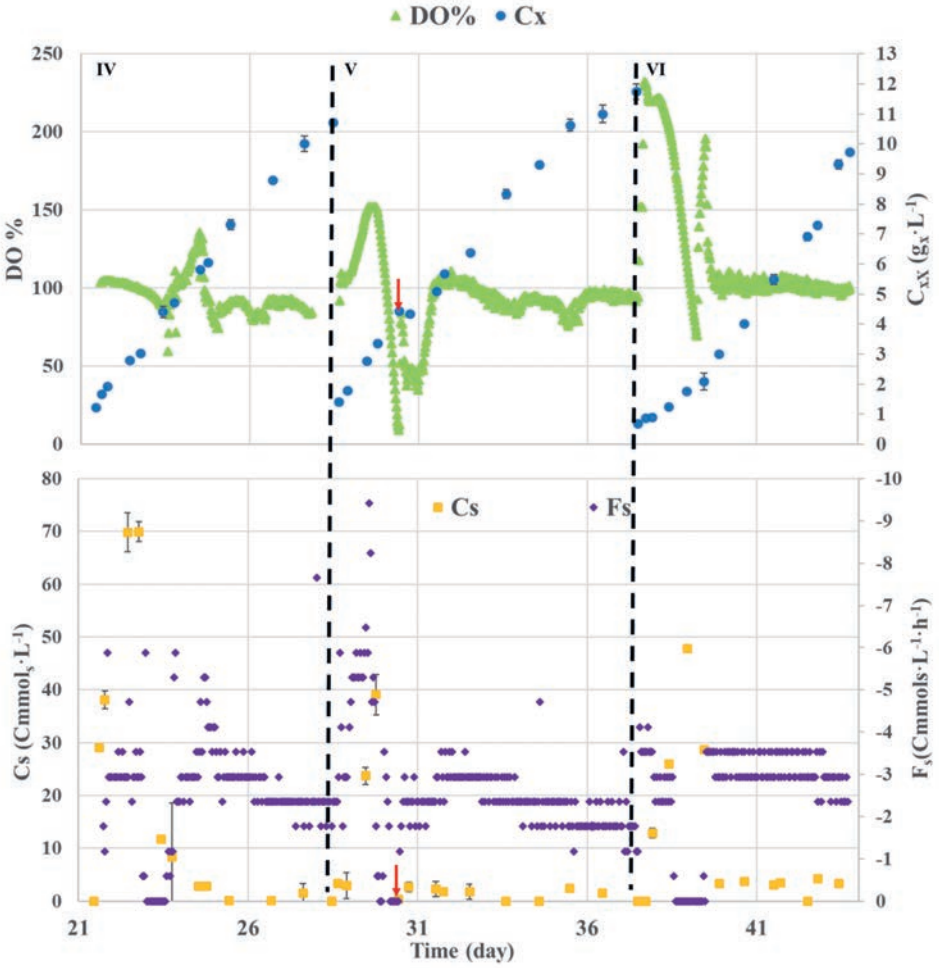

photochemistry (*QY*), that in mixotrophic cultures was equal to, or higher than. the autotrophic cultures, indicating that photosynthesis was not negatively affected by glucose.

Another sign of interaction between autotrophic and heterotrophic metabolism was the reduction in pigmentation observed in the mixotrophic repeated batches (IV, V, VI) when

compared to the autotrophic culture grown under the same conditions. In mixotrophic repeated batches, at the end of the linear growth phase, a_x was 132±6 $m^2 \cdot Kg^{-1}$, 27% less than the autotrophic culture under the same condition. This decrease in pigmentation was much less severe than in the mixotrophic cultivated in chemostat where a_x decreased by half compared to the autotrophic culture grown under the same conditions (table 1). The dramatic reduction in pigments observed in the mixotrophic culture grown in chemostat therefore is most likely related to the low C_x resulting in light inhibition instead of glucose inhibition of photosynthesis. The repeated batch clearly indicated that the optimization of the light regime is a key point for successful cultivation of light sensitive *G. sulphuraria*. In the autotrophic repeated batch the optimal specific light supply rate (q_{ph}) was 3.6-9.5 $\mu mol_{ph} \cdot g_x^{-1} \cdot s^{-1}$ (Table 2). Under this light regime biomass production rate (r_x) was the double of the autotrophic culture in chemostat cultivated under the same incident light intensity but at 20.2 $\mu mol_{ph} \cdot g_x^{-1} \cdot s^{-1}$ (Table 1, Table 2). This result clearly suggests that photoinhibition can be mitigated by finding the range of biomass concentration (C_x) which results in optimal q_{ph}. At an optimal q_{ph} *G. sulphuraria* can successfully grow even at a high incident light intensity.

The present work is the first report of an autotrophic *G. sulphuraria* culture grown in a photobioreactor (*PBR*) at incident light intensity above 200 $\mu mol \cdot m^{-2} \cdot s^{-1}$. Reports on other trophic mode at this high light intensity are scarce (Table 3). In a mixotrophy culture a of *G. sulphuraria* 74G in operated in chemostat at a dilution rate of 0.63 day^{-1}, Sloth et al (Sloth et al., 2006) reported that at an incident light intensity of 395 $\mu mol \cdot m^{-2} \cdot s^{-1}$ photoinhibition affected the culture so much that the culture couldn't reach a steady state. The specific growth rate reported by Sloth et al was 0.49 day^{-1} and it was calculated as the sum of the wash out rate and the dilution rate. We estimated the initial q_{ph} of their culture to be 9.0 $\mu mol_{ph} \cdot g_x^{-1} \cdot s^{-1}$, on the high side of the range found in our autotrophic culture. However, in the study of (Sloth et al.,

2006 the culture was washed out at a rate of 0.14 day^{-1} which rapidly increased q_{ph} causing photoinhibition.

With the intent of avoiding photoinhibition, Wan et al (Wan et al., 2016) proposed a two-phase cultivation strategy where *G. sulphuraria* 74G is firstly grown heterotrophically for biomass production. During heterotrophic growth pigmentation is lost. In the second phase, this heterotrophic culture is used as an inoculum for an autotrophic phase (photoinduction) in *PBRs* for phycocyanin accumulation. Photoinduction has been recently scaled up outdoors in *PBRs* at light intensity reaching up to 2000 $\mu mol \cdot m^{-2} \cdot s^{-1}$ at solar noon (Wang et al., 2020). During photoinduction, cultures started without pigmentation (heterotrophic inoculum) needed up to 14 days to fully regain their pigmentation. The initial low pigmentation improved light tolerance, in fact using this strategy the authors cultivated *G. sulphuraria* in bubble columns at an initial q_{ph} of 35.3-47.6 $\mu mol_{ph} \cdot g_x^{-1} \cdot s^{-1}$. Moreover the authors demonstrated that the initial biomass concentration (C_x), and therefore the initial q_{ph}, is crucial to successfully cultivate *G. sulphuraria* at high light intensity.

In order to compare our work with other *PBR* designs, we converted the volumetric biomass concentration (C_x) and productivity (r_x) into areal biomass concentration (C_A, $g \cdot m^{-2}$) and areal productivity (r_A, $g_x \cdot m^{-2} \cdot day^{-1}$). This was done using a correction factor α (m):

$$\alpha = \frac{V_{PBR}}{A_{PBR}} \qquad (6)$$

Where V_{PBR} (m^3) and A_{PBR} (m^2) represent the volume and the illuminated area of the photobioreactor respectively. Volumetric biomass concentration (C_x) and productivity (r_x) can be converted in their areal equivalent multiplying C_x and r_x for the correction factor α.

***Table 3**. Comparison of final biomass concentration (C_x), biomass productivity, specific light supply rate (q_{ph}), volumetric (r_C) and areal (r_A) biomass productivity among this study and other reports. STR: stirred tank reactor; BC: bubbled column; ITL: immobilized twin layer; RWP: race way pond.*

Strain	*PBR*	Operation mode	Trophic mode	A_{PBR} (m^2)	I_0 ($\mu mol_{ph} \cdot m^{-2} \cdot s^{-1}$)	C_x ($g_x \cdot L^{-1}$)	q_{ph} ($\mu mol_{ph} \cdot g_x^{-1} \cdot s^{-1}$)	r_x ($g_x \cdot L^{-1} \cdot day^{-1}$)	r_A ($g_x \cdot m^{-2} \cdot day^{-1}$)	Reference
G. sulphuraria ACUF 64	STR	Chemostat	Autotrophic	0.068	514	0.86	20.2	0.45	13.3	This study
G. sulphuraria ACUF 64	STR	Chemostat	Mixotrophic	0.068	514	3.07	5.7	1.62	47.8	This study
G. sulphuraria ACUF 64	STR	Repeated Batch	Autotrophic	0.068	514	1.9-4.9	9.5-3.6	0.97	28.6	This study
G. sulphuraria ACUF 64	STR	Repeated Batch	Mixotrophic	0.068	514	3.0-9.7	5.8-1.8	1.72	50.7	This study
G. sulphuraria ACUF 64	BC	Batch	Autotrophic	0.190	150	0.4-5.7	17.8-1.3	0.18	3.7	(Graziani et al., 2013)
G. sulphuraria ACUF 64	ITL	Batch	Autotrophic	n.a.	50	10-107*	5.0-0.5	n.a.	5.2	(Carbone et al., 2020)
G. sulphuraria ACUF 64	ITL	Batch	Autotrophic	n.a.	100	10-185*	10-0.5	n.a.	6.8	(Carbone et al., 2020)
G. sulphuraria ACUF 64	ITL	Batch	Autotrophic	n.a.	200	10-195*	20-1.0	n.a.	10.4	(Carbone et al., 2020)
G. sulphuraria 74G	STR	Chemostat	Mixotrophic	0.071	125	0.78	5.2	0.49	14.5	(Sloth et al., 2006)
G. sulphuraria 74G	STR	Chemostat	Mixotrophic	0.071	175	0.84	7.1	0.53	15.6	(Sloth et al., 2006)
G. sulphuraria 74G	STR	Chemostat	Mixotrophic	0.071	395	0.85**	9.0	0	0	(Sloth et al., 2006)
G. sulphuraria 74G	BC	Batch	Photo-induction	0.057	250	0.6-6.0	23.8-2.4	0.77	13.0	(Wan et al., 2016)
G. sulphuraria 74G	BC	Batch	Photo-induction	0.029	1092	0.9-5.5	35.3-5.8	0.38	13.0	(Wang et al., 2020)
G. sulphuraria 74G	RWP	Batch	Photo-induction	1.35	641***	0.7-2.4	8.5-2.5	0.13	10.0	(Wang et al., 2020)

*Biomass concentration (C_x) expressed as $g \cdot m^{-2}$

** Initial biomass concentration. It was not possible to obtain a steady state and the culture was washed out of the reactor

*** The culture was grown outdoor with at a light intensity of 30 $MJ \cdot m^{-2} \cdot day^{-1}$. This value was converted into average PFD

In our study the autotrophic areal biomass production rate (r_A) obtained in repeated batch was 28.6 $g_x \cdot m^{-2} \cdot day^{-1}$. This areal productivity was 1.8 to 7.7 times higher than previously reported (Table 3). Moreover, the mixotrophic r_A was 1.8 and 1.7 times higher than the autotrophic r_A in the repeated batch (VI) and in chemostat respectively, making the present study the highest r_A ever obtained in a photosynthetic culture of *G. sulphuraria*.

G. sulphuraria ACUF 64 displayed an outstanding capacity to maintain linear growth at low specific light supply rate (q_{ph}) (figure 2, table 2). In the mixotrophic batch (VI) linear growth was maintained at 1.8 $\mu mol_{ph} \cdot g_x^{-1} \cdot s^{-1}$, corresponding to 9.7 $g_x \cdot L^{-1}$ or 340 $g_x \cdot m^{-2}$. In the autotrophic culture linear growth was maintained until 3.6 $\mu mol_{ph} \cdot g_x^{-1} \cdot s^{-1}$, corresponding to 4.8 $g_x \cdot L^{-1}$ or 170 $g_x \cdot m^{-2}$. These values were half of those obtained in the mixotrophic culture. Linear growth at high areal biomass densities have been recently reported by Carbone et at (Carbone et al., 2020). The authors cultivated *G. sulphuraria* ACUF 64 autotrophically in a biofilm at 200 $\mu mol \cdot m^{-2} \cdot s^{-1}$ obtaining linear growth until 195 $g_x \cdot m^{-2}$. Despite the higher density, r_A was 2.8 times lower than in our autotrophic culture in repeated batch. The ability of *G. sulphuraria* to efficiently perform photosynthesis in dense culture will lead to a significant reduction in downstream processing costs, making this a promising candidate for large scale cultivation

Biomass productivity at pH 0.2

Most *G. sulphuraria* strains have been isolated from highly acidic hot springs where the pH is close to zero (Pinto et al., 2007). Although optimal pH for *G. sulphuraria* is reported to be between pH 1 and 4 (Graziani et al., 2013; Oesterhelt et al., 2007; Selvaratnam et al., 2014; Sloth et al., 2006) only two of those studies (Schmidt et al., 2005)·(Brock, 1978) investigated pH below 1. During autotrophic batch II at day 9.9, the pH suddenly dropped from 1.8 to 0.2 (Fig S3) and we stopped the automatic pH control. After a few hours, we confirmed pH to be 0.2 by taking several samples from the reactor and measuring the pH with an external probe.

The culture was maintained at pH 0.2 for 1.3 days (Figure 2, yellow area). The pH in our medium was buffered by $H_3PO_4 \rightleftharpoons H_2PO_4^- + H+$ ($pKa_1 = 2.14$) and $H_2SO_4+H_2O \rightleftharpoons H^+ + HSO^-_4$ ($pK_{a1}=1.92$). Since H_2SO_4 was used as titrant we excluded sulfur depletion and we analyzed phosphorus (P) content in the culture. The measurements indicated that P was completely depleted at the point in time where the pH dropped. This finding was unexpected, because even considering a high biomass P content of 1.5% w_P/w_x, the P concentration in the medium should have been sufficient to sustain the growth up to 18 $g \cdot L^{-1}$ of biomass, while in batch II only 4 $g \cdot L^{-1}$ of biomass was produced. We used the software MINTEQ 3.1 (https://vminteq.lwr.kth.se) to estimate possible salt precipitation and the calculations allowed us to reject any risk of precipitation. Therefore, the only possible explanation was an error in the medium preparation. For this reason, after batch II the medium was changed and H_3PO_4 was chosen as P source. This change allowed a reduction from 88 to 14 $mL \cdot L^{-1}$ of the addition of 2.5 M H_2SO_4 to set the pH at 1.6. In the new medium pH was constant for the remainder of the experiment without the addition of any titrant. Interestingly, phosphorus starvation had seemed to increase pigment content (a_x). The absorption cross sector area (a_x) in batch II was significantly higher ($p<0.05$) than in batches I and III. This finding matches with the claim of the patent of Cagnac et al. (Cagnac et al., 2016) which reported phycocyanin accumulation under P limitation.

Despite being an unintentional event, this is the first report of *G. sulphuraria* grown in a *PBR* at pH 0.2. In previous studies no growth (Schmidt et al., 2005) or 30% reduction in μ grow has been reported (Brock, 1978) when *G. sulphuraria* was grown below pH 0.5. Nevertheless, pH optima and tolerance are strain specific and it might be that our *G. sulphuraria* strain is more tolerant to low pH than others. Surprisingly, in our study during the 2 days of growth at pH 0.2 r_x was not significantly different ($p>0.05$) from the value found in batch I and III (table 2). Further studies, where pH 0.2 will be maintained for a longer time and without P starvation are

needed to confirm this finding. Tolerance to extremely low pH might further decrease the risk of contamination.

CONCLUSIONS

In the present study *G. sulphuraria* ACUF 64 was cultivated at high incident light intensity autotrophically and under oxygen balanced mixotrophy. The autotrophic biomass productivity surpassed by far all other ever reported in literature. Under oxygen balanced mixotrophy the acidophilic condition prevented bacterial contamination, the reactor operated without any gassing and biomass productivity and concentration were almost double the autotrophic culture grown under similar conditions. All of these characteristics make *G. sulphuraria* ACUF 64 a promising candidate for outdoor cultivation.

NOMENCLATURE

Abbreviations	
DO	Dissolved oxygen concentration (% air saturation)
PBR	Photobioreactor
PFD	Photon flux density ($\mu mol \cdot m^{-2} \cdot s^{-1}$)
PAR	Photo active radiation, 400-700 nm
Symbols	
V_{PBR}	Photobioreactor working volume (L)
A_{PBR}	Photobioreactor illuminated area (m^2)
D	Dilution rate (day^{-1})
$Y_{x/ph}$	Biomass yield on light ($C\text{-}mol_x \cdot mol_{ph}^{-1}$)
F	Flow ($mol \cdot min^{-1}$)
r	Volumetric production/consumption rate ($mol \cdot L^{-1} \cdot day^{-1}$)
C	Concentration ($mol \cdot L^{-1}$)
$Y_{x/s}$	Biomass yield on substrate ($C\text{-}mol_x \cdot C\text{-}mol_s^{-1}$)
MW	Molecular weight ($g \cdot C\text{-}mol^{-1}$)
a_x	Average absorption cross section ($m^2 \cdot Kg^{-1}$)
QY	Quantum yield (F_v/F_m)
$C_{\%}$	Biomass carbon content ($\%\ w_c \cdot w_x^{-1}$)
$N_{\%}$	Biomass nitrogen content ($\%\ w_N \cdot w_x^{-1}$)
q	Biomass specific production/consumption rate ($mol \cdot C\text{-}mol_x \cdot day^{-1}$)
Sub/super script	
mixo	Mixotrophic
auto	Autotrophic
auto'	Autotrophic fraction of the mixotrophic biomass
het'	Heterotrophic fraction of the mixotrophic biomass
ph	PAR photons
x	Biomass
c	Carbon based biomass
s	Substrate
A	Areal

SUPPORTING INFORMATION

Figure S1*: Photograph of a sample of G. sulphuraria ACUF 64 taken from an autotrophic (left) and an heterotrophic (right) culture.*

***Figure S2**. Absorption cross section spectrum of a sample of G. sulphuraria ACUF 64 taken from an autotrophic (green) and an heterotrophic (black) culture.*

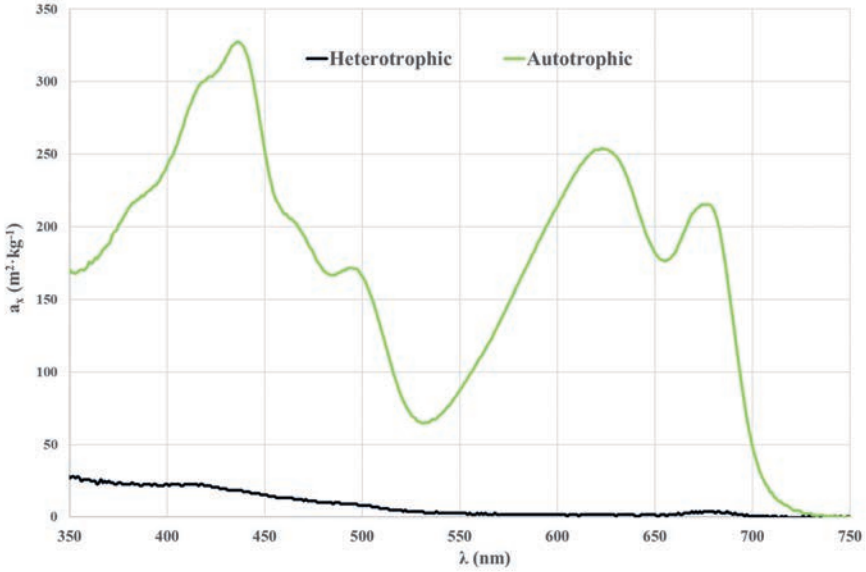

***Figure S3.** Sudden pH drop during the autotrophic batch II. After batch II the medium was changed and H_3PO_4, rather than KH_2PO_4, was chosen as phosphorus source. In the new medium pH was constant for the remainder of the experiment without the addition of any titrant.*

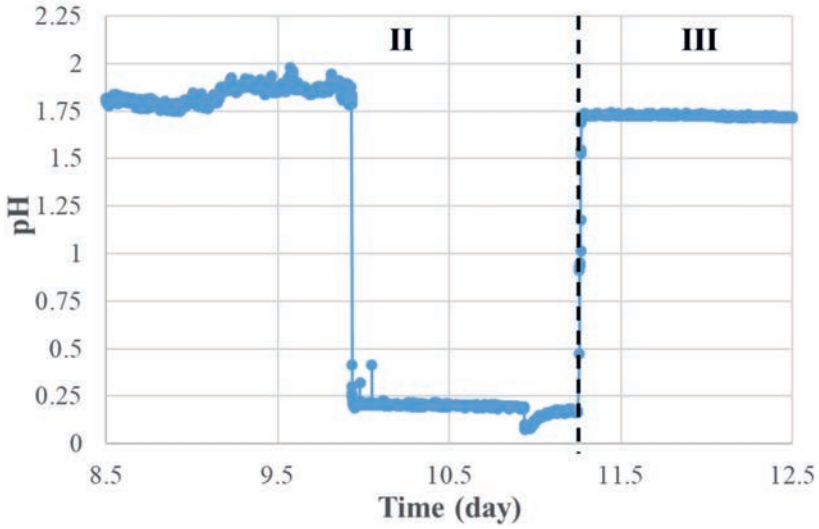

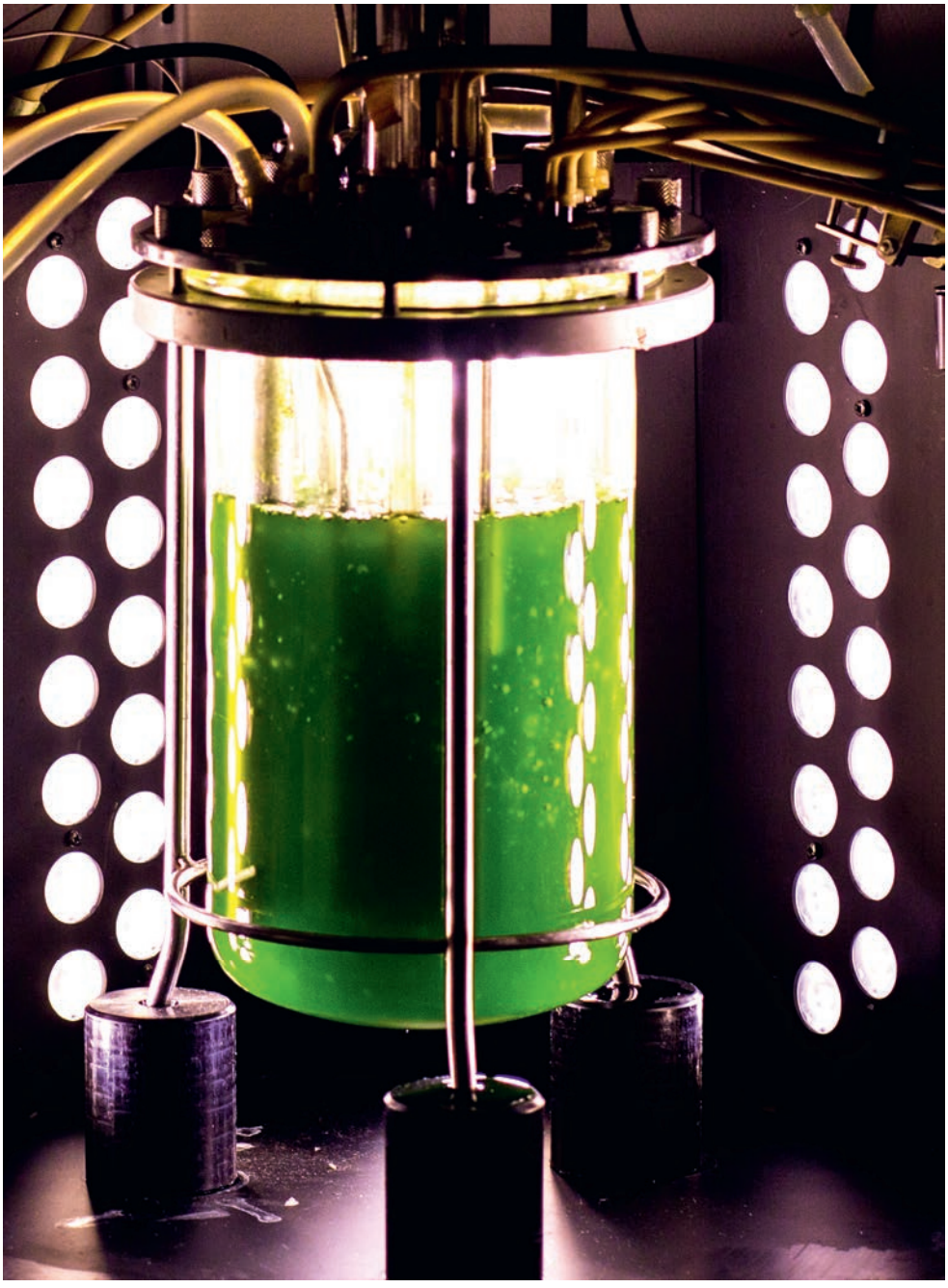

Chapter 5

Algae blues: Is *Galdieria* the new *Spirulina*?

This chapter has been submitted for publication as:
Fabian Abiusi[§], Pedro Moñino Fernández[§], Stefano Canziani, Marcel Janssen, René H. Wijffels, Maria Barbosa. Algae blues: Is *Galdieria* the new *Spirulina*?

[§] Authors contributed equally

Submitted

ABSTRACT

G. sulphuraria is a polyextremophilic microalga that can tolerate low pH, high temperature and high osmotic pressure. We cultivated *G. sulphuraria* ACUF 64 in chemostat at high biomass concentration (134 – 243 $g \cdot m^{-2}$) aiming for maximal pigment content without compromising biomass productivity. Autotrophy was compared to 'oxygen balanced' mixotrophy with intracellular recirculation of oxygen and carbon dioxide. No differences were found in C-phycocyanin (*C-PC*) and protein content between autotrophic and mixotrophic cultures. In mixotrophy the biomass productivity and concentration were doubled compared to the photoautotrophic counterpart. In mixotrophy aeration was not needed and 89% of the substrate carbon was converted into biomass.

Mixotrophically grown biomass contained 10% w/w *C-PC* which, combined with its high areal biomass productivity (49 $g \cdot m^{-2} \cdot day^{-1}$), sums up as one of the highest *C-PC* areal productivities ever reported (5 $g \cdot m^{-2} \cdot day^{-1}$) under 24h/24h illumination. *C-PC* extracted from *G. sulphuraria* was more stable than the currently used *C-PC* extracts from *Spirulina*. No significant loss of color was observed down to a pH of 3 and up to a temperature of 55 °C. *G. sulphuraria* had a protein content of 62% w/w and compared favorably with FAO dietary recommendation of adults regarding amino acid composition. *G. sulphuraria* contains a high proportion of essential, sulfur amino acids compared to *Chlorella*, *Spirulina* and soybean protein.

Due to its attractive amino acid profile and high protein content, *G. sulphuraria* is a good candidate for food and feed applications to overcome sulfur amino acid deficiencies. In addition, oxygen balanced mixotrophy allows for efficient and productive cultivation of *G. sulphuraria* biomass.

Keywords: Amino acid profile, protein production, oxygen balance, acid stable phycocyanin, thermo stable phycocyanin, phycocyanin productivity.

INTRODUCTION

Galdieria sulphuraria is a polyextremophile microalgae able to tolerate low pH (as low as 0.2) (Chapter 4), high temperature (up to 57 °C) (Ott & Seckbach, 1994) and high osmotic pressure (up to 400 $g \cdot L^{-1}$ of sugar and 2-3 M of salt) (Schmidt et al., 2005). Due to these exceptional traits, *G. sulphuraria* is often the only organism able to colonize acidic hot springs where it forms mats of deep blue-green color (Pinto et al., 2007). This peculiar color is due to the presence of blue phycobiliproteins C-phycocyanin (*C-PC*), allophycocyanin, and chlorophyll a (Albertano et al., 2000). Phycocyanins are used in diagnostic histochemistry and as colorants in cosmetics and foods. Phycocyanins have also been found to have antioxidant properties and may have potential as therapeutic agents (Pagels et al., 2019).

When cultivated autotrophically, *G. sulphuraria* expresses a *C-PC* content of 10% w/w, similar to the *C-PC* content commonly reported in *Arthrospira platensis* (Hirooka & Miyagishima, 2016; Tredici & Zittelli, 1998; Wan et al., 2016; Wang et al., 2020), henceforth referred to with its commercial name *Spirulina*. Compared to the *C-PC* extracted from *Spirulina, C-PC* extracted from *Galdieria* has shown greater stability at low pH and at high temperature, increasing the possible industrial applications of this pigment (Carfagna et al., 2018; Moon et al., 2014).

Nowadays commercial production of *C-PC* is almost exclusively based on *Spirulina* cultivation and extraction. *Spirulina* extracts have been approved for use in candy, chewing gum and other types of confection in the US in 2013 and 2014 (U.S.F.D.A., 2016). In EU *Spirulina* extracts have been approved in 2013 as coloring food (European-Commission, 2013). While Spirulina has been consumed for centuries (Sili et al., 2012) and its consumption is approved and considered safe worldwide, *G. sulphuraria* has no previous history of use in feed or foods. Recent studies indicated that *G. sulphuraria* could be safe as food ingredient or supplements

(Abdelmoteleb et al., 2021; Modeste et al., 2019), but *G. sulphuraria* still needs to be approved as novel food before it can be used as such.

G. sulphuraria is also considered as a promising source for protein (Modeste et al., 2019). The protein content of *G. sulphuraria* has been reported in several studies resulting in a range from as little as 22% to an impressive 72% of total biomass dry weight (Cheng et al., 2019; Graziani et al., 2013; Massa et al., 2019; Wan et al., 2016). In addition to bulk protein content, protein quality in terms of amino acid composition, is a core marker for nutritional value. Humans have a limited ability to (bio)synthesize amino acids, out of the 20 common amino acids, nine "essential" amino acids must be provided through food. Therefore, the amount of essential amino acids is key in determining the quality of a protein source. To the best of our knowledge, there have been no studies on the amino acid profile of *G. sulphuraria*.

We recently designed an 'oxygen balanced' mixotrophic cultivation method that allows operation of a closed photobioreactor without any gas exchange (Abiusi et al., 2020a, Abiusi et al., 2020b). We succefully applied this cultivation strategy to *G. sulphuraria* and due to the low pH, the reactor was operated for over two months without contamination (Chapter 4). *G. sulphuraria* proved to be photosensitive, which is the reason why optimization of the light regime was a key point for successful cultivation. In order to find the optimal specific light supply rate (q_{ph}, $\mu mol_{ph} \cdot g_x^{-1} \cdot s^{-1}$) in our previous work, we cultivated *G. sulphuraria* autotrophically and mixotrophically in repeated batch (Chapter 4). After each dilution, the sudden change in the q_{ph} caused photoinhibition that was manifested as a drop of the photosystem II maximum quantum yield (QY, F_v/F_m), and as a reduction on biomass productivity. Photoinhibition was followed by a period of photo-acclimation, during which pigmentation of the culture was reduced and QY recovered its initial value. Once the autotrophic culture reached a biomass concentration of 2 $g_x \cdot L^{-1}$, corresponding to a q_{ph} of 9.5 $\mu mol_{ph} \cdot g_x^{-1} \cdot s^{-1}$, the volumetric biomass productivity reached 0.97 $g_x \cdot L^{-1} \cdot day^{-1}$. This productivity was

maintained until a biomass concentration of 5 $g_x \cdot L^{-1}$ was achieved, corresponding to a q_{ph} of 3.6 $\mu mol_{ph} \cdot g_x^{-1} \cdot s^{-1}$, after which light limitation became more evident and biomass productivity decreased. In mixotrophic repeated batch operation biomass productivity progressively increased during each batch. In a third and last batch linear growth could be maintained until a biomass concentration of 9.7 $g_x \cdot L^{-1}$ resulting in a biomass productivity of 1.72 $g_x \cdot L^{-1} \cdot day^{-1}$. Despite this high productivity it was concluded that ideally *G. sulphuraria* is cultivated under a constant light regime without stepwise reductions of biomass concentration as in repeated batch.

In this work we cultivated *G. sulphuraria* in chemostat, in which the specific light supply rate q_{ph} can be maintained constant to obtain stable biomass and pigment production. In order to reach this goal, we estimated a dilution rate based on our previous work (Chapter 4), in which maximal pigment content could be achieved without negatively affecting biomass productivity. Once the steady state was reached, C-phycocyanin (*C-PC*) and protein content, as well as amino acid profile of the produced biomass were determined. The produced *C-PC* was tested for its thermal- and acid-stability. In addition, autotrophic and oxygen balanced mixotrophic cultures were compared with respect to biomass productivity.

MATERIALS AND METHODS

Strain, growth conditions and medium

Galdieria sulphuraria ACUF 64 (http://www.acuf.net) was kindly provided by Prof. A. Pollio (University of Naples, Italy) while *Arthrospira platensis* (Gomont) Geitler A1 was provided by Algreen B.V (The Netherlands). Axenic stock cultures of *G. sulphuraria* were incubated in 250 mL flasks containing 100 mL of culture at 37ºC, 2% v/v CO_2, 120 rpm, and under a photon flux density (PFD) of 75 µmol m^{-2} s^{-1}. These cultures were used to inoculate the photobioreactor for the experiments described below. The medium contained the following components at the concentration given (mol·L^{-1}): $12.2 \cdot 10^{-3}$ H_3PO_4, $20.0 \cdot 10^{-3}$ $(NH_4)_2SO_4$, $1.6 \cdot 10^{-3}$ $MgSO_4 \cdot 7H_2O$, $0.1 \cdot 10^{-3}$ $CaCl_2$, $0.2 \cdot 10^{-3}$ FeNaEDTA, $0.05 \cdot 10^{-3}$ $Na_2EDTA \cdot 2H_2O$, $1.7 \cdot 10^{-3}$ NaCl, $8.0 \cdot 10^{-4}$ H_3BO_3, $8.1 \cdot 10^{-5}$ $MnCl_2 \cdot 4H_2O$, $8.2 \cdot 10^{-5}$ $ZnCl_2$, $3.2 \cdot 10^{-5}$ $CuSO_4 \cdot 5H_2O$, $1.7 \cdot 10^{-5}$ $Na_2MoO_4 \cdot 2H_2O$ and $1.7 \cdot 10^{-5}$ $CoCl_2 \cdot 6H_2O$. pH was adjusted to 1.8 with 10M H_2SO_4.

A. platensis cultures were incubated in 250 mL flasks containing 100 mL of Zarrouk medium (Zarrouk, 1966) at pH 9.2, 25 °C, 2% v/v CO_2, 120 rpm and under a PFD of 75 µmol m^{-2} s^{-1}.

Photobioreactor setup and experiments

Autotrophic and mixotrophic cultures were carried out in a 3 L stirred-tank bioreactor (Applikon, The Netherlands) with a working volume (V_{PBR}) of 2 L. The internal diameter was 0.130 m and the liquid height was maintained at 0.166 m, which results in a cylindrical illuminated surface (*IS*) of 0.068 m^2. The reactor was continuously stirred at 500 rpm and homogeneously illuminated over the cylindrical vessel surface, as described in detail in Abiusi et al. 2020a. The average PFD was 511 µmol·m^{-2}·s^{-1}. The temperature was maintained at 37ºC by a heat exchanger inside the reactor. Water evaporation was prevented with a condenser connected to a cryostat that fed water at 2ºC. The pH was controlled at 1.8 by automatic base addition (2 M NaOH). Dissolved oxygen (*DO*) was measured by a *DO* sensor (VisiFerm DO

ECS 225, Hamilton, USA). The sensor was calibrated inside the reactor containing medium at aforesaid working temperature and pH. Dinitrogen gas (N_2) and air sparging were applied to obtain 0% and 100% *DO* reads, respectively. For autotrophic operation the reactor was sparged with air enriched with 2% v/v CO_2 at a flow rate of 1 $L \cdot min^{-1}$ using mass flow controllers (Smart TMF 5850S, Brooks Instruments, USA).

The reactor was inoculated with an initial biomass concentration of 1.25 $g_x \cdot L^{-1}$. It was operated in batch until a biomass concentration (C_x) of 4 $g_x \cdot L^{-1}$ was reached after which the system was operated in autotrophic chemostat mode. Reactor volume was maintained constant by a level-probe based control system. A dilution rate (D) of 0.2 day^{-1} was chosen as optimal for *G. sulphuraria* ACUF 64 based on our previous study (Chapter 4):

$$D = \frac{r_{x,opt}}{C_{x,opt}} \quad (1)$$

Where $C_{x,opt}$ (4.8 $g_x \cdot L^{-1}$) represents the maximal concentration within the range of linear growth during autotrophic repeated batch and $r_{x,opt}$ (0.97 $g_x \cdot L^{-1} \cdot day^{-1}$) the volumetric productivity achieved at that range. After steady state was reached under such autotrophic conditions, the harvest bottle was placed in ice-cooled water bath and collected and analyzed daily for 3 consecutive days. Dry weight and phycocyanin contents were measured, and amino acid composition was determined. Additional samples were taken aseptically from the reactor for measurements of photosystem II maximum quantum, absorption cross section and carbon and nitrogen content of the biomass.

After the autotrophic chemostat, the reactor was operated in batch for 1.5 days with constant glucose addition and sparging with 2% CO_2 enriched air. A 10% w/w glucose solution was added at a rate of 3.7 $g \cdot h^{-1}$. Then, aeration was switched off and the dissolved oxygen level (*DO*) was controlled at 90% air saturation by glucose addition (i.e. oxygen-balanced mixotrophy). Only when a C_x of 8 $g_x \cdot L^{-1}$ was reached, chemostat operation was activated again. Also in the mixotrophic culture a dilution rate (D) of 0.2 day^{-1} was chosen as optimal. The D

was calculated using equation 1 and a value of 8.6 $g_x \cdot L^{-1}$ and .72 $g_x \cdot L^{-1} \cdot day^{-1}$ were used for $C_{x,opt}$ and $r_{x,opt}$ respectively. After steady state was reached under oxygen-balanced mixotrophic conditions, culture was harvested daily for 4 days. Identical analyses as under the autotrophic reference condition were done and in addition glucose analysis from the reactor was performed several times per day.

Photobioreactor calculations

Volumetric biomass productivity r^V_x (r^V_x, $g_x \cdot L^{-1} \cdot day^{-1}$) was determined by multiplying the measured C_x in the harvest with the measured reactor dilution rate D. Areal biomass productivity (r^A_x, $g_x \cdot L^{-1} \cdot day^{-1}$) was calculated as follows:

$$r_X^A = \frac{r_X^V \cdot V_{PBR}}{IS} (2)$$

Where IS is the illuminated reactor surface (m^2). In the autotrophic chemostat, r^V_x was used to calculate the autotrophic yield of biomass on photons ($Y_{x/ph}$, $g_x \cdot mol_{ph}^{-1}$) according to the formula:

$$Y_{X/ph} = \frac{r_X^V \cdot V_{PBR}}{PFD \cdot IS} (3)$$

In the mixotrophic chemostat, first the volumetric substrate consumption rate (r_s, $g_s \cdot L^{-1} \cdot day^{-1}$) was calculated:

$$r_S = \frac{F_{glu} \cdot C_{S,glu} - D \cdot V_{PBR} \cdot C_S}{V_{PBR}} (4)$$

Where F_{glu} ($L \cdot day^{-1}$) and $C_{S,glu}$ (C-$g_s \cdot L^{-1}$) stand for the glucose feeding rate and the carbon concentration in the solution. C_s (C-$g_s \cdot L^{-1}$) represents the carbon substrate concentration measured in the reactor. Then, the mixotrophic biomass yield on substrate ($Y_{x/s}$, C-$g_x \cdot g_s^{-1}$) was derived as follows:

$$Y_{X/S}^{mixo} = \frac{r_X^V \cdot C_{\%}}{r_S} (5)$$

Where $C_{\%}$ (% $W_C \cdot W_x^{-1}$) represents the carbon content in the harvested biomass. C-phycocyanin volumetric $r^V_{C\text{-}PC}$ ($r^V_{C\text{-}PC}$, $g_{C\text{-}PC} \cdot L^{-1} \cdot day^{-1}$) and areal ($r^A_{C\text{-}PC}$, $g_{C\text{-}PC} \cdot m^{-2} \cdot day^{-1}$) productivities were calculated by multiplying r^V_x and r^A_x by the phycocyanin content in the biomass (% $W_{C\text{-}PC} \cdot W_x^{-1}$).

ANALYTICAL METHODS

Photon flux density measurements

PFD was measured with a Li-Cor 190-SA 2π PAR quantum sensor (LI-COR Biosciences, USA). Incident light intensity on the reactor surface was determined at 16 points inside the empty reactor vessel, as explained in detail in Abiusi et al. 2020a.

Dry weight concentration

C_X was estimated by biomass dry weight determination. Aliquots of culture (1-5 mL) were diluted to 30 mL with demineralized water and filtered over pre-weighed Whatman GF/F glass microfiber filters (diameter of 55 mm, pore size 0.7 μm). The filters were washed with 30 mL of deionized water and dried at 100ºC for at least 3 hours.

Average absorption cross section

Average absorption cross section (a_x, $m^2 \cdot Kg_x^{-1}$) in the PAR region (400-700 nm) of the spectrum was determined as meticulously described in de Mooij *et al*. (de Mooij et al., 2015). In short, the absorbance was measured with a UV-VIS/double beam spectrophotometer (Shimadzu, Japan) equipped with an integrating sphere (ISR-2600) and using cuvettes with an optical path of 2 mm.

Photosystem II Quantum Yield

The photosystem II maximum quantum yield (*QY*, F_v/F_m) was measured at 455 nm with an AquaPen-C AP-C 100 (Photon Systems Instruments, Czech Republic). Prior to the measurement, samples were adapted to darkness for 15 min at room temperature and diluted to optical density at 750 nm between 0.3 and 0.5.

Glucose concentration, total organic carbon and total organic nitrogen determination

During the steady state, two 1-mL aliquots of culture were sampled daily from the reactor and centrifuged for 10 minutes at >20,000 RCF. The supernatant was used for estimation of glucose concentration with a YSI analyzer (YSI 2700, YSI Life Sciences, USA). The pellets were washed twice with deionized water following the aforesaid centrifugation procedure. Then, they were used for total carbon (*TC*, $g_C \cdot L^{-1}$) and total nitrogen (*TN*, $g_N \cdot L^{-1}$) determination using a TOC-L analyzer (Shimadzu, Japan). The biomass carbon (*C%*,% $W_C \cdot W_x^{-1}$) and nitrogen (*N%*, % $W_N \cdot W_x^{-1}$) content was calculated dividing the obtained *TC* and *TN* by the C_X of the same sample.

Extraction of phycocyanin and quantification

Phycocyanins were quantitatively extracted by bead beating (Precellys 24, Bertin Technologies, France) 10 mg of lyophilized biomass. Cell were resuspended in 50 mM Na-acetate at pH 5.5 and exposed to 5 beating cycles of 60 s with 300 s breaks on ice between each cycle. Cell debris was removed through centrifugation at 10,000 rpm for 10 min and the supernatant was collected in fresh tubes. This extract is called crude extract. The C-phycocyanin (*C-PC*) and allo-phycocyanin contents were calculated measuring the absorbance at 620 nm and 652 and converting the measured absorbance to concentration using the Kursar and Alberte equation (Kursar & Alberte, 1983).

Temperature and pH stability of C-phycocyanin

The effects of temperature and pH on the stability of *C-PC* were investigated on crude extracts. The crude extracts from cultures grown in auto- and mixotrophic conditions were divided into aliquots and diluted in 50 mM Na-acetate pH 5.5 buffer. This *C-PC* solution was incubated for 30 min in a water bath at 45°C, 55°C, 65°C, and 75°C. After the heat treatment, absorbance at 620 nm was measured and the residual absorbance at 620 nm ($C\text{-}PC_R$) was calculated as a percentage of the initial absorbance in samples kept at room temperature (20 °C). To determine the pH stability, 200 µL of *C-PC* crude extracts added with 800 µL 50 mM Na-acetate at different pH ranging from 1.2 to 5.5 were incubated for 30 min. The pH of each solution was measured. After the pH treatment, absorbance at 620 nm was measured and the residual absorbance at 620 nm ($C\text{-}PC_R$) was calculated as a percentage of the initial absorbance in samples at pH 5.5.

Amino acid composition

Biomass samples obtained during autotrophic and mixotrophic steady states were freeze-dried in a Sublimator 2x3x3-5 (Zirbus Technology, Germany). The amino acid content of the freeze-dried biomass was then analyzed following the standardized method ISO 13903:2005 for animal feedstuffs (ISO, 2005) based on the procedure developed by Llames and Fontaine (Llames & Fontaine, 1994). Tryptophan content was determined by the method ISO 13904:2016 for animal feedstuffs (ISO, 2016). The analyses were performed in duplicate.

Statistical analyses and procedures

Significant differences between autotrophic and mixotrophic cultures were analyzed by unpaired t test and two-tailed P value with a confidence level of 95% in GraphPad Prism 5.03 (GraphPad Prism Software, USA).

Propagation of errors for addition operations was calculated according to Eq. (6) to determine the error.

$$\Delta z = \sqrt{\Delta x^2 + \Delta y^2 + \ldots} \qquad (6)$$

Where Δx is the absolute error related to the value x, etc.

When comparing the mixotrophic and the autotrophic cultures each day at steady state was considered a replicate. Three and four days of steady state were maintained for the autotrophic (n=3) and mixotrophic (n=4) cultures respectively.

RESULTS AND DISCUSSION

High density chemostat cultivation of G. sulphuraria ACUF 64

We previously demonstrated that *G. sulphuraria* can be successfully cultivated without any gas exchange by making use of oxygen balanced mixotrophy (Chapter 4). However, our strain, as most *Galdiera* strains, turned out to be photosensitive, which is why optimization of the light regime was a key point for successful cultivation. In this work we cultivated *G. sulphuraria* in chemostat at high biomass concentration aiming for maximum pigment content without affecting biomass productivity.

Biomass productivity

Chemostat production of *G. sulphuraria* at high concentration proved to be a successful strategy for constant biomass production with a high pigment content under both autotrophic and mixotrophic conditions (Figure 1, table 1). High C-phycocyanin (*C-PC*) (table 2) content and high PSII maximum quantum yield (*QY,* F_v/F_m) indicated that neither the autotrophic nor the mixotrophic culture were photo-inhibited. It must be noted that even under optimal conditions F_v/F_m of *Galdieria* is at most 0.5 which is intrinsically lower than green algae expressing a maximum F_v/F_m of 0.7 or more. In our previous repeated batch experiment high biomass productivity was obtained only under optimal specific light supply rate (q_{ph}) (chapter 4). After each dilution the sudden change in q_{ph} caused photo-inhibition that strongly decreased biomass productivity in the 1-2 days following the dilution, reducing the overall performance of each batch. We confirmed that by adjusting the biomass concentration, thus reaching optimal light regime, *G. sulphuraria* can be continuously cultivated at high light intensity without signs of photo-inhibition. Therefore, while in our previous repeated batch experiment high biomass productivity was obtained only for a few days, in chemostat high biomass productivity can be maintained.

Figure 1. *Volumetric biomass production rate (r_x) (circles) and concentration (C_x) (triangles) of G. sulphuraria ACUF 64 grown autotrophically (green) and mixotrophically (blue).*

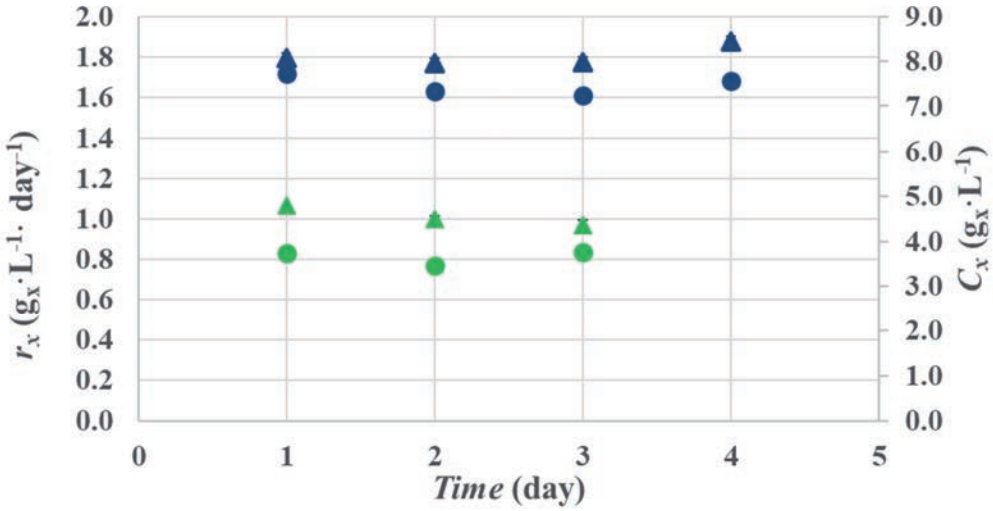

Table 1*. Overview of the offline measurements and process parameters of Galdieria sulphuraria ACUF 64 under autotrophic and oxygen-balanced mixotrophic conditions in chemostat (this study) and the best values determined in repeated batch (batches I and III under autotrophic and VI under mixotrophic conditions) (chapter 4). Values expressed as averages ± standard deviation.*

	Unit	Autotrophic (this study)	Mixotrophic (this study)	Autotrophic (Chapter 4)	Mixotrophic (Chapter 4)
C_x	$g_x \cdot L^{-1}$	4.6 ± 0.2^a	8.1 ± 0.2^b	4.9	9.7
D	day^{-1}	0.18 ± 0.00^a	0.21 ± 0.00^b	-	-
r_x	$g_x \cdot L^{-1} \cdot day^{-1}$	0.81 ± 0.03^a	1.66 ± 0.04^b	0.97	1.72
C-PC	% $w_{C\text{-}PC} \cdot w_x^{-1}$	9.6 ± 0.8^a	10.1 ± 0.5^a	-	-
$C_{\%}$	% $w_C \cdot w_x^{-1}$	47.5 ± 1.7^a	47.3 ± 2.2^a	46.6	47.6
$N_{\%}$	% $w_N \cdot w_x^{-1}$	9.9 ± 0.0^a	9.7 ± 0.0^a	10.2	9.4
a_x	$m^2 \cdot kg_x^{-1}$	231 ± 5^a	184 ± 45^b	181	132
QY	(F_v/F_m)	0.38 ± 0.06^a	0.44 ± 0.03^a	0.49	0.45
$Y^{mixo}_{X/S}$	$C\text{-}g_x \cdot C\text{-}gs^{-1}$	-	0.89 ± 0.02	-	0.91
$Y_{x/ph}$	$g_x \cdot mol_{ph}^{-1}$	0.55 ± 0.02	-	0.65	-

Among the rows the same letter indicates no significant differences (P>0.05).

***Table 2**. Comparison of biomass and C-PC volumetric- and areal productivities of this study and other values under 24h/24h illumination reported in literature.*

Reference	Trophic mode	Strain	*IS* (m^2)	C^V_x ($g \cdot L^{-1}$)	C^A_x ($g \cdot m^{-2}$)	r^V_x ($g \cdot L^{-1} \cdot day^{-1}$)	r^A_x ($g \cdot m^{-2} \cdot day^{-1}$)	*C-PC* (% w/w)	$r^V_{C\text{-}PC}$ ($mg \cdot L^{-1} \cdot day^{-1}$)	$r^A_{C\text{-}PC}$ ($g \cdot m^{-2} \cdot day^{-1}$)
This study	Autotrophic	*G. sulphuraria* ACUF 64	0.067	4.5	134	0.81	24.1	9.6	78	2.3
This study	Mixotrophic	*G. sulphuraria* ACUF 64	0.067	8.0	243	1.66	49.3	10.1	168	5.0
Sloth *et al.*, 2006	Mixotrophic	*G. sulphuraria* 74G	0.084	0.8	24	0.50	15.0	2.81	14	0.4
Wan et al., 2016	Photoinduction	*G. sulphuraria* 74G	0.057	0.6 – 6.0	11 – 105	0.90	15.8	13.2	119	2.1
Wang *et al.*, 2020	Photoinduction	*G. sulphuraria* 74G	0.029	0.9 – 5.5	31 – 188	0.38	13.1	12.3	46	1.6
Carbone *et al.*, 2020	Autotrophic	*G. sulphuraria* ACUF 64	-	-	10 - 225	-	7.2	3.2	-	0.2
Graverholt *et al.*, 2007	Heterotrophic	*G. sulphuraria* 74G	-	51.6 – 83.1	-	50	-	1.6	861	-
Tredici & Chini Zittelli 1998	Autotrophic	*A. platensis M2 (Spirulina)*	0.192	3.2	80	1.9	45.6	9.3	179	4.2

The high biomass concentration (8.0 $g \cdot L^{-1}$) obtained in the mixotrophic culture did not affect biomass areal productivity (49.3 $g \cdot m^{-2} \cdot day^{-1}$) (table 2) that was not significantly different from the areal productivity obtained in our previous batch experiment. Such high areal biomass productivity (r^A_x, $g \cdot m^{-2} \cdot day^{-1}$) is 3 times to 7 times greater than previously reported in a 24h/24h illuminated culture of *G. sulphuraria*. The mixotrophic r^A_X was similar to one of the highest r^A_X reported in an autotrophic culture of *Spirulina* (Tredici & Zittelli, 1998). This maximal biomass productivity of *Spirulina* was obtained at a light intensity twice as high as used in this study and a thin layer photobioreactor was used. *Spirulina* has been the focus of extensive research for almost a century; therefore its biomass productivity is optimized and no significant increase in production has been reported during the last 20 years. Meanwhile, the genus *Galdiera* was discovered in 1981, but it wasn't until 2005 that a high cell density culture was reported (Sydney et al., 2019). We believe that further research on *Galdiera* will lead to a further improvement of biomass productivity.

In our mixotrophic experiment, volumetric biomass productivity (r^V_X, $g \cdot L^{-1} \cdot day^{-1}$) was 30 times lower than the highest heterotrophic r^V_X productivity reported in literature for *G. sulphuraria* (Graverholt & Eriksen, 2007). The authors reported a maximum biomass yield on substrate of 0.52 g of biomass per gram of glucose ($g_x \cdot g_s^{-1}$) while under oxygen balanced mixotrophy we obtained 0.75 $g_x \cdot g_s^{-1}$. Heterotrophic high biomass yield on substrate can only be obtained through aerobic respiration requiring active aeration, while in our culture gas exchange was completely avoided. Our mixotrophic culture had a carbon content of 47.3% (table 1) resulting in a $Y_{x/s}$ of 0.89 $C\text{-}g_x \cdot C\text{-}g_s^{-1}$. This means that in our culture 89% of the carbon in the substrate was transformed into biomass carbon and only 11% lost in the form of CO_2. This result is equivalent to the maximum $Y_{x/s}$ obtained in our previous work in repeated batch (Chapter 4). While our previous work $Y_{x/s}$ was not stable between batches, in the present work $Y_{x/s}$ was constant over the whole steady state.

In one of the few works, in which ***G. sulphuraria*** was cultivated mixotrophically in chemostat, with aeration, a maximum biomass yield of 0.84 $g_x \cdot g_s^{-1}$ on substrate was obtained (Sloth et al., 2006), representing a 12% increment to our current reported yield. For a fair comparison, the biomass yield on substrate should be estimated based on carbon content ($Y_{x/s}$, C-$g_x \cdot$C-g_s^{-1}). Such comparison was not possible with the works mentioned above (Graverholt & Eriksen, 2007; Sloth et al., 2006). Assuming a carbon content similar to our culture (47.3%) Sloth et al. (Sloth et al., 2006) might have succeeded in converting 100% of the substrate (glucose) into biomass, obtaining a carbon balanced culture. Since the ratio between O_2 produced per mol of CO_2 consumed is always higher than 1 (Abiusi et al., 2020a), a carbon balanced culture needs aeration to prevent O_2 accumulation while oxygen balanced mixotrophy operates without aeration.

Autotrophic biomass productivity and concentration were half of the mixotrophic cultures values (table 1). Average biomass concentration (C_x) at steady state was 4.50 $g \cdot L^{-1}$ and the average volumetric productivity (r^V_x) was 0.81 $g \cdot L^{-1} \cdot day^{-1}$ (Table 1). In comparison, the average productivity obtained in the optimal range during the autotrophic repeated batches was 0.97 $g \cdot L^{-1} \cdot day^{-1}$, the highest biomass productivity ever reported in autotrophic culture of ***G. sulphuraria***. This 20% reduction in r^V_x in the current experiment was unexpected, as we applied a similar light regime as in the optimal range of the batches. When looking at the C_x, 4.50 $g_x \cdot L^{-1}$ is on upper limit of the linear growth range in batch (Chapter 4). Moreover, in the current work the absorption cross section (a_x, $g \cdot m^{-2}$) was 28% higher than the maximum value in the previous work (see next section). High a_x decreases the light penetration within the culture accentuating possible light limitation. In an autotrophic culture operated in chemostat at a lower C_x we expected to obtain similar productivity as in repeated batch. Despite the lower performance compared to our previous experiment, the obtained autotrophic areal productivity is still 1.5 times to 3.4 times higher than previously reported in ***G. sulphuraria*** (table 2) and

comparable to other commercially relevant microalgae such as *Isocrysis lutea* (Gao et al., 2020), *Rhodomonas sp.* (Oostlander et al., 2020), *Nannochloropsis sp* (Benvenuti et al., 2016), indicating the potential of this strain for autotrophic biomass production.

Phycocyanin productivity

Chemostat production of *G. sulphuraria* at high concentration proved to be a successful strategy to achieve high pigment productivity under both autotrophic and mixotrophic conditions (table 2). We succeeded in increasing the absorption cross section (a_x, $g \cdot m^{-2}$), by 28% and 39% in the autotrophic and mixotrophic cultures respectively, compared to our previous maximal values in repeated batch (Table 1). Moreover, a_x was constant over the whole autotrophic and mixotrophic chemostat (data not shown) while in repeated batch pigmentation temporarily decreased after each dilution (Chapter 4). In the mixotrophic culture a_x was 20% lower than in the autotrophic culture, confirming that the addition of an organic carbon source does affect a_x of *G. sulphuraria*. In contrast, no differences in a_x were found between autotrophic and oxygen balanced mixotrophic cultures of *C. sorokiniana* (Abiusi et al., 2020a; Abiusi et al., 2020b).

Despite the lower a_x , the mixotrophic culture had one of the highest C-phycocyanin (*C-PC)* content and *C-PC* productivity reported in this species (table 2). No significant difference ($p>0.05$) was found in *C-PC* content between autotrophic and mixotrophic cultures (table 2) and both cultures had approximately 10% w/w of *C-PC* and 1.7% of allo-phycocyanin (data not shown). *C-PC* content of 10% w/w is the highest obtained in this strain (Carbone et al., 2020; Graziani et al., 2013). Moreover, in the mixotrophic culture high *C-PC* combined with high biomass productivity lead to a *C-PC* areal productivity ($r^A_{C\text{-}PC}$, $g \cdot m^{-2} \cdot day^{-1}$) of 5 $g \cdot m^{-2} \cdot day^{-1}$, 2.4 times to 25 times higher than previously reported in 24h/24h illuminated culture of *G. sulphuraria* (table 2). The mixotrophic $r^A_{C\text{-}PC}$ was even higher than reported in an autotrophic culture of *Spirulina* (Tredici & Zittelli, 1998), which reached 4.2 $g \cdot m^{-2} \cdot day^{-1}$.

In our mixotrophic experiment *C-PC* volumetric productivity ($r^{V}_{C\text{-}PC}$, $g \cdot L^{-1} \cdot day^{-1}$) was 5 times lower than the highest heterotrophic *C-PC* productivity reported in literature for ***G. sulphuraria*** (table 2). The superior heterotrophic *C-PC* productivity is due to its high biomass volumetric productivity (see previous section). Moreover, heterotrophic culture can be productive 24 h a day and does not suffer of seasonal variation on light intensity and photoperiod, making even greater the gap on biomass and *C-PC* productivity between the two cultivation strategies.

Despite the higher volumetric productivity compared to mixotrophic culture, the downside of heterotrophic pigment production is that the *C-PC* content is lower than 3% w/w (Graverholt & Eriksen, 2007; Sloth et al., 2006). The low *C-PC* content results in higher pigment extraction costs and limitations with the commercial application of this technology. Within the EU, the initial concentration of a pigment in the food of origin will determined if the extract can be considered a "food extracts with coloring properties" or "natural color additives" (Regulation(EC), 2008). Food extracts are considered a "food ingredients" and used in clean label products while natural additives requires an "E" number.

We determined thermal- and acid-stability of the *C-PC* extract. No significant differences ($p>0.5$) were found in *C-PC* stability between autotrophic and mixotrophic cultures (Figure 2 and Figure 3). *C-PC* produced in ***G. sulphuraria*** ACUF 64 proved to be stable at low pH (Figure 1). The absorbance at 620 nm remained high down to pH 3. A further reduction of pH, from 3 to 1.9, led to a linear decrease in *C-PC* content, until it reached 39% of the reference (pH 5.5) absorbance. *C-PC* extracted from ***Spirulina*** was significantly less acid stable. The absorbance at 620 nm with pH 3.5 was only 40% of the absorbance at pH 5.5. Similar results were obtained by Carfagna et al. (Carfagna et al., 2018) in autotrophic and heterotrophic cultures of ***G. fleagrea***. The authors reported similar *C-PC* stability in their autotrophic cultures with 80% of the color maintained from pH 4 to pH ,3 followed by a rapid drop below pH 3.

***Figure 2**. Effect of pH on the residual absorbance at 620 nm (C-CP$_R$) in G. sulphuraria ACUF 64 cultures grown autotrophically (GS auto) and mixotrophically (GS mixo). An autotrophic culture of A. platensis (Spirulina) is used as comparison. The extracts were incubated at the indicated pH for 30 min. The absorbance at pH 5.5 represents 100%.*

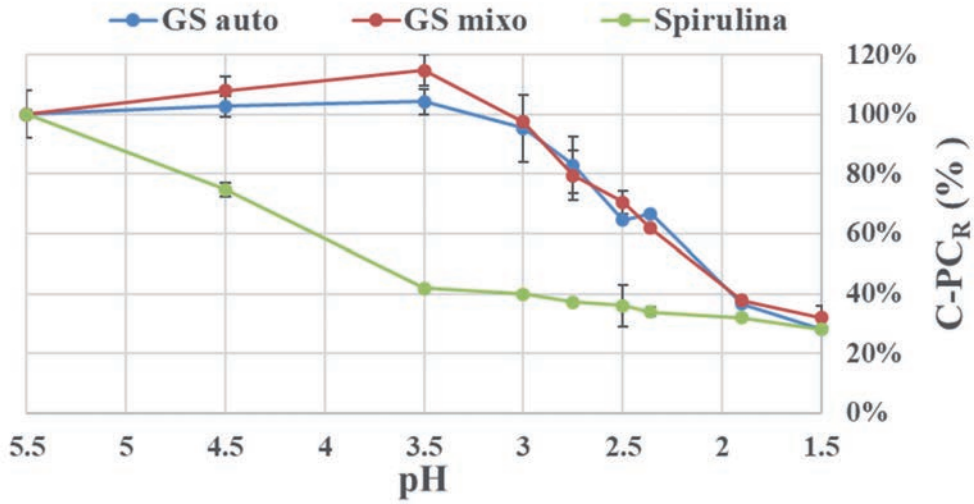

***Figure 3**. Effect of temperatures (T) on the residual absorbance at 620 nm (C-CP$_R$) in G. sulphuraria ACUF 64 cultures grown autotrophically (GS auto) and mixotrophically (GS mixo). An autotrophic culture of A. platensis (Spirulina) is used as comparison. The extracts were incubated at the indicated T for 30 min. The absorbance at 20°C represents 100%.*

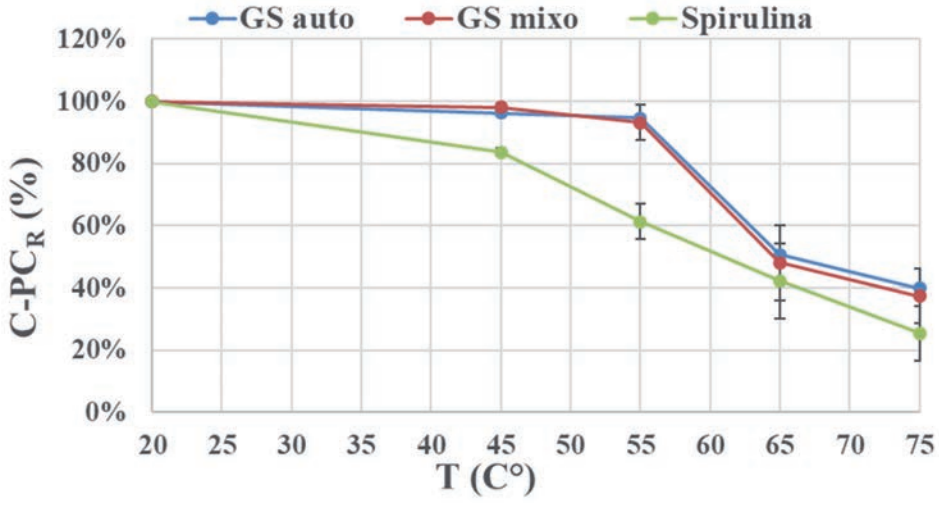

Acid stability is an import trait in natural colorants. Most commercial beverages have a pH of less than 4 (Reddy et al., 2016). Acids are added to beverages and compose a flavor profile giving the beverage a distinctive taste. Acids provide a tartness and tangy taste that helps to balance the sweetness of sugar present in the beverage; they are key factors in the taste of the beverage. Therefore, while the *C-PC* extracted from *Spirulina* will lose its blue color in most beverages, the *C-PC* of *G. sulphuraria* can be used in almost any beverage increasing the market size of this pigment.

Thermostability is another important characteristic of a natural pigment. We incubated *G. sulphuraria* and *Spirulina* extracts for 30 min at temperatures ranging from 25° to 75° C (Figure 3). In *G. sulphuraria* the absorbance at 620 nm remained stable until 55° C, maintaining 94% of its original color. Then when the temperature was elevated from 55° to 75° C, *C-PC*'s absorbance decreased steadily, until at 75° C it was 39% of the original. *Spirulina's C-PC* extracts started losing color already at 45° C having lost 18% of initial absorbance. The absorbance linearly decreased until 75° C, at which only 21% of initial absorbance was maintained. Our strain was more thermostable than the two *G. phlegrea* grown autotrophically by Carfagna et al. (Carfagna et al., 2018) but less stable than the *G. sulphuraria* strain described by Moon et al. (Moon et al., 2014). The latter reported a thermostable *C-PC* that maintained 62% and 60% of its initial absorbance at 620 nm at 75 °C and 85 °C respectively.

In conclusion, mixotrophic cultivation of G. sulphuraria ACUF 64 is a promising strategy to produce C-phycocyanin (*C-PC*). Areal mixotrophic *C-PC* productivity was the highest ever reported in a phototrophic or mixotrophic culture of this species, and slightly higher than the highest productivity obtained in autotrophic culture of *Spirulina* (Tredici & Zittelli, 1998). Moreover, the *C-PC* extracted from *G. sulphuraria* showed superior acid- and thermo- stability compared to *C-PC* extracted in Spirulina. These traits may increase the commercial application of this pigment.

Amino acid content of G. sulphuraria ACUF 64

In order to address the knowledge gap existing in the amino acid composition of *G. sulphuraria*, in this work we analyzed the total amino acid content of *G. sulphuraria* ACUF 64 in steady state under autotrophic and mixotrophic metabolic regimes.

The results of the amino acid analysis are displayed in Table 3. For most amino acids, there were no significant differences in content between autotrophy and mixotrophy. The exceptions are aspartate, threonine, glycine, alanine and methionine, which were found in slightly larger quantities in the autotrophic biomass. The most abundant amino acids in both metabolic regimes were glutamate, aspartate and leucine, constituting nearly 9%, 6% and 5% of the total biomass dry weight, in that order. Furthermore, the least abundant amino acids were tryptophan, cysteine and histidine, which accounted for less than 1.1% of the total biomass dry weight each. The remaining amino acids were found in concentrations ranging from 2 to 4% of total biomass dry weight.

These results are in line with the relative amino acid frequency found in several microalgal species and seaweeds (Kent et al., 2015; Lourenço et al., 2004; Mišurcová et al., 2014; Safi et al., 2014). The acidic amino acids predominate, partially influenced by the concurrent detection of their amides by most analytical procedures. As elicitors of the umami taste (Mouritsen et al., 2019), glutamate and aspartate are pivotal in the sensory perception of food. Moreover, leucine has also been found to be the most abundant of the essential amino acids in *Chlorella*, *Spirulina* and *Chlamydomonas reinhardtii* (Darwish et al., 2020). Brown et al. (Brown, 1991) analyzed the amino acid content of 16 microalgae and showed that the content of sulfur amino acids, histidine and tryptophan are generally the lowest of all amino acids. However, similar relative frequency does not mean that the total amino acid content is equivalent among different species,

***Table 3**. Amino acid composition of steady state autotrophic and mixotrophic G. sulphuraria ACUF 64 (% w/w). Values expressed as averages ± standard deviation.*

	Asp*	Thr	Ser	Glu*	Gly	Ala	Val	Ile	Leu	Tyr
Autotrophic	6.00 ± 0.02^{a}	3.71 ± 0.02^{a}	4.21 ± 0.06^{a}	9.25 ± 0.10^{a}	2.81 ± 0.00^{a}	4.09 ± 0.01^{a}	3.66 ± 0.00^{a}	3.62 ± 0.00^{a}	5.29 ± 0.07^{a}	4.14 ± 0.18^{a}
Mixotrophic	5.76 ± 0.02^{b}	3.60 ± 0.01^{b}	4.07 ± 0.03^{a}	9.14 ± 0.06^{a}	2.74 ± 0.01^{b}	3.89 ± 0.00^{b}	3.59 ± 0.05^{a}	3.51 ± 0.03^{a}	5.12 ± 0.00^{a}	4.10 ± 0.16^{a}
	Phe	His	Lys	Arg	Pro	Cys	Met	Trp	Tau	Total**
Autotrophic	2.95 ± 0.02^{a}	1.06 ± 0.02^{a}	3.89 ± 0.00^{a}	4.12 ± 0.06^{a}	2.83 ± 0.02^{a}	1.03 ± 0.02^{a}	1.59 ± 0.01^{a}	0.86 ± 0.00^{a}	0.48 ± 0.01^{a}	65.12 ± 0.24^{a}
Mixotrophic	2.89 ± 0.03^{a}	1.08 ± 0.04^{a}	3.88 ± 0.03^{a}	3.99 ± 0.03^{a}	2.73 ± 0.07^{a}	1.06 ± 0.02^{a}	1.51 ± 0.01^{b}	0.85 ± 0.01^{a}	0.37 ± 0.00^{b}	63.50 ± 0.21^{b}

Among the columns the same letter indicates no significant differences (P>0.05).

*Aspartate and glutamate results include their amides, asparagine and glutamine.

**Total protein content excluding the free amino acid-like taurine.

as absolute amino acid quantities are subject to great variability, even within the same species, under different experimental conditions (James et al., 1989).

Interestingly, our analysis also found taurine in the biomass of *G. sulphuraria* (Table 3). Taurine is a sulfur-containing β-amino acid that does not form peptide bonds and is common in animal tissues. While plants and fungi contain scarce amounts of taurine, algae have been proposed as an alternative source of this compound for application in the animal feed industry (Tevatia et al., 2019). We found significant differences in the content of taurine between autotrophy and mixotrophy, representing 0.48 and 0.37% of the total biomass dry weight, respectively. Taurine had been already identified in other rhodophytes (Flynn & Flynn, 1992) but never within the genus *Galdieria*. The role of this molecule in *G. sulphuraria* is unknown. Taurine contains sulfur, which is found in large quantities in the acidic hot springs where *G. sulphuraria* is commonly found. As such, it could play a role in sulfur metabolism. Tevatia *et al*. showed that sulfur supplementation increases the levels of intermediates in the synthesis pathway of taurine in other microalgae (Tevatia et al., 2015). Additionally, in the same study it was showed that taurine participated in the osmoregulation of *Tetraselmis* sp. and *C. reinhardtii*. High salt concentrations are also a characteristic of the natural habitat of *G. sulphuraria*, so taurine could also have a function as osmolyte in this species.

Protein content of G. sulphuraria ACUF 64

We calculated the total protein content of the biomass by adding up quantities of the individual 20 protein-forming amino acids (Table 3). This method could overestimate the amount of protein due to the inclusion of free amino acids within the cells. However, the potential overestimation does not affect the determination of the nutritional value of the biomass. The total protein content for the autotrophic biomass was 65.1% of the total biomass dry weight, whereas for the mixotrophic biomass it was 63.5%. This difference is derived from the

aforementioned higher content of certain amino acids during autotrophy and was found to be significant. In literature, the reported protein contents of autotrophic *G. sulphuraria* show a great variability, ranging from 22% to 72% of total biomass dry weight (Cheng et al., 2019; Graziani et al., 2013; Massa et al., 2019; Wan et al., 2016). From these studies, only Graziani *et al.* used *G. sulphuraria* ACUF 64. They analyzed the protein content under heterotrophy and autotrophy, obtaining protein content of 26.5% and 32.5% of the biomass dry weight, respectively. In comparison, our result from autotrophic culture is twofold larger.

The variability in *G. sulphuraria* protein content among different studies might be caused by differences in the physiological state of the culture. Different types of microalgal cell walls affect the solubilization of intracellular proteins in diverse manners thus influencing protein content determination (Safi et al., 2014). *G. sulphuraria* has a rigid cell wall that contains an unusual large fraction of proteins, up to 55% (Bailey & Staehelin, 1968). As a consequence, if the cell wall is not properly broken, neither the proteins of other parts of the cell nor the proteins that constitute the cell wall will be accurately accounted for. Several class III peroxidases that are involved in cell wall hardening have been identified in *G. sulphuraria* (Oesterhelt et al., 2008). Peroxidase activity was mainly detected during the stationary phase of cell growth. In contrast to batch processes, in chemostat this effect might be absent and consequently cell protein may be more accessible, explaining the differences between our study and Graziani et al., 2013.

Another reason for the variability in *G. sulphuraria* protein content among different studies could be the different extraction methods employed (Lourenço et al., 2004). In our study we determined the total protein both by adding up the individual amino acids and by the total nitrogen (*N%*) (table 1) obtaining similar results. The method applied in the amino acid quantification (ISO, 2005) is based on strong HCl oxidation and hydrolysis at 120° C followed by precise HPLC quantification. This method is successfully used for amino acid analyses in

complex feed stuff mixtures and in plants that are very resistant to hydrolysis (Panaite et al., 2015; Starchenko & Grytsyk, 2017).

Apart from our study, all the other reported values of protein content in *G. sulphuraria* were determined by multiplying the total nitrogen (*N%*) content of the sample by a nitrogen-to-protein factor of 6.25. N% was determined either by Kjeldahl (Graziani et al., 2013; Massa et al., 2019; Wan et al., 2016), or a similar method (Cheng et al., 2019), which are based on strong oxidation of organic nitrogen. Multiplying the *N%* by a factor of 6.25 is generally thought to lead to an overestimation of the total amount of proteins in plant biomass, as a considerable fraction of the *N%* is non-proteinic (Sáez-Plaza et al., 2013). Moreover, the factor 6.25 is based on the assumption that the nitrogen content of protein is 16%, which is not correct for several protein sources. Species-specific factors have been published for several microalgae based on their amino acid composition (González López et al., 2010; Lourenço et al., 2004). Yet, it is a common practice to use 6.25 when a specific factor has not been determined for a certain species, as is the case for *G. sulphuraria*. Therefore, the reported results using this method can expected to overestimate the real protein content. In our study, we also determined nitrogen content (Table 1), resulting in 9.9% and 9.7% of the total biomass dry weight for autotrophy and mixotrophy, respectively. If we multiply those *N%* by a factor of 6.25, we obtain 62% and 61% protein content for said trophic modes. On the one hand, these values are close to the sum of all the individual amino acids. On the other hand, the *N%* based value is slightly lower than summing all amino acids while a higher values was expected. The combination of the unique amino acid profile and proportion of non-proteinic nitrogen of *G. sulphuraria* may result in an underestimation of protein when using 6.25 as a factor. Further insight is needed with respect to the small discrepancy between the resulting protein content following both approaches.

The highest protein content of *G. sulphuraria* reported in literature is 71.6% in autotrophy (Cheng et al., 2019) . However, this protein content was corrected for ash content. We can undo

this correction by multiplying their reported nitrogen content, 9.8%, by 6.25. The result then is 61%, which is the same as in our study. Wan ***et al***. (Wan et al., 2016) reported a protein content of 58% under an autotrophic regime. All in all, the protein contents obtained in autotrophic and mixotrophic chemostat in our current study are among the highest reported in ***G. sulphuraria.*** A protein content of 60% is on the high side of values ever reported for all microalgae (Becker, 2007), highlighting the potential of ***G. sulphuraria*** as a protein source.

Heterotrophic metabolism could be the reason why lower protein contents are reported in certain studies. Studies that compared protein content under autotrophic and heterotrophic growth reported higher protein contents under autotrophy (Graziani et al., 2013; Wan et al., 2016). In fact, the highest protein content reported under heterotrophic metabolism is only 32% (Massa et al., 2019). Among other factors, the reduction of phycocyanin levels in the heterotrophic cells (Schmidt et al., 2005) and their higher content in carbohydrates (Graziani et al., 2013; Wan et al., 2016) could explain this observation.

Essential amino acid profile of G. sulphuraria ACUF 64

In order to assess the nutritional value of ***G. sulphuraria***, the amino acid content not only needs to be analyzed quantitatively but also qualitatively. That is, focusing on the relative proportion of the essential amino acids in the proteins. For that reason, we compared the essential amino acid profile determined in this study with the FAO dietary requirements for adults (WHO, 2007) in Table 4. Moreover, we also included the essential amino acid profiles of the currently main industrial microalgae used in food applications, ***Spirulina*** and ***Chlorella***, and of the main vegetable protein source worldwide, soybean (Hughes et al., 2011; Muys et al., 2019). We chose reported values in literature that correspond to commercially available ingredients for human nutrition. For the microalgae, the commercial products were constituted by the whole biomass, while in soybean they were protein isolates (>90% protein) and concentrates (>70% protein).

Table 4. *Essential amino acid comparison of autotrophic and mixotrophic G. sulphuraria ACUF 64, commercial Chlorella and Spirulina and FAO requirements (mg AA/g protein). Values expressed as averages ± standard deviation.*

	His	Ile	Leu	Lys	Thr	Val	SAAs[b]	AAAs[c]	Trp	Reference
Requirement[a]	15	30	59	45	23	39	22	38	6	FAO (2007)
Autotrophic	16.3 ± 0.4	55.6 ± 0.0	81.1 ± 1.1	59.6 ± 0.0	56.9 ± 0.0	56.1 ± 0.1	40.2 ± 0.4	108.8 ± 2.4	13.2 ± 0.1	This study
Mixotrophic	17.0 ± 0.6	55.4 ± 0.5	80.9 ± 0.0	61.3 ± 0.5	56.8 ± 0.2	56.7 ± 0.8	40.6 ± 0.4	110.5 ± 2.0	13.4 ± 0.1	This study
Chlorella	10.4 ± 2.1	35.0 ± 5.4	83.4 ± 8.3	45.1 ± 7.4	29.5 ± 2.8	50.4 ± 5.0	12.7 ± 4.3	56.9 ± 3.7	n. d.[d]	Muys (2018)
Spirulina	10.4 ± 2.4	57.3 ± 5.1	92.2 ± 9.1	53.3 ± 6.0	34.1 ± 3.8	56.7 ± 5.3	16.9 ± 5.3	59.3 ± 13.6	n. d.[d]	Muys (2018)
Soybean	24.7 ± 0.2	46.4 ± 0.9	79.0 ± 1.9	62.3 ± 0.3	36.5 ± 0.2	49.4 ± 1.3	26.0 ± 1.1	88.4 ± 1.2	12.7 ± 0.2	Hughes (2011)

[a] Indispensable amino acid requirement for adults.

[b] Sulfur-containing amino acids, namely cysteine and methionine.

[c] Aromatic amino acids, namely phenylalanine and tyrosine.

[d] Not determined.

The comparison includes the 9 essential amino acids: histidine, isoleucine, leucine, lysine, methionine, phenylalanine, threonine, tryptophan and valine but also two conditionally essential ones, cysteine and tyrosine. Cysteine is added together to methionine under the denomination of sulfur amino acids (SAAs) and tyrosine is added to phenylalanine under the denomination of aromatic amino acids (AAAs).

G. sulphuraria ACUF 64 compared favorably to the FAO requirements for every amino acid, in both autotrophic and mixotrophic biomass. Even if threonine and methionine showed a lower content in mixotrophy than in autotrophy, these small differences did not affect the nutritional value of the mixotrophic biomass. Histidine exhibited the lowest margin above the nutritional requirement, and thus can be considered the most limiting essential amino acid in *G. sulphuraria* proteins. In comparison, *Chlorella* is deficient in histidine and SAAs while the average lysine content is just at the limit. *Chlorella* SAAs content showed the largest difference with the FAO requirement and they are the limiting factor for this chlorophyte. *Spirulina* on average is also below the requirements for histidine and SAAs, although the limiting amino acid is histidine instead of SAAs. Tryptophan was not analyzed in the study that we used for comparison and thus was not taken into account in these two microalgae. Soybean protein contains a balanced amino acid profile, surpassing the requirement for every essential amino acid, but compares unfavorably with *G. sulphuraria*. *G. sulphuraria* contains higher contents of every essential amino acid with the exception of lysine, that is equivalent to soybean, and histidine, in which soybean is superior. Average soybean content of SAAs, 26 mg/g protein, is just above the requirement of 22 mg/g protein and hence SAAs are the most limiting essential amino acid in this protein source. In fact, there have been several efforts to increase SAAs content in soybean (Krishnan & Jez, 2018a).

Besides the overall superior amino acid profile of *G. sulphuraria,* special attention must be given to SAAs content. *G. sulphuraria* contains a high proportion of SAAs compared with

Chlorella, *Spirulina* and soybean protein. Methionine and cysteine cannot be synthesized de novo by animals and therefore their supply is dependent on the diet. Most plant biomasses contain scarce amounts of these sulfur compounds (Day, 2013) and they have to be provided by other sources, mostly animal protein in the case of human nutrition and external SAAs supplementation or excess protein addition in the case of animal feed. Due to its remarkable amino acid profile and high protein content, *G. sulphuraria* is a good candidate to overcome SAAs deficiencies for food and feed applications. Nevertheless, amino acid composition and overall protein fraction are not the only characteristics that make a protein source suitable. Further research is needed to determine the digestibility and utilization of absorbed amino acids from *G. sulphuraria* biomass.

CONCLUSIONS

Chemostat production of *G. sulphuraria* ACUF 64 at high concentration proved to be a successful strategy for constant biomass production with high pigment content both under autotrophic and mixotrophic conditions. The biomass grown mixotrophically contained 10% w/w C-phycocyanin (*C-PC*). High *C-PC* content combined with high areal biomass productivity lead to the highest *C-PC* areal productivity reported under 24h/24h illumination in *Galdieria,* and even higher than with autotrophic culturing of *Spirulina*. The *C-PC* extracted from *G. sulphuraria* showed superior thermal- and acid-stability compared to *C-PC* extracted in *Spirulina*. *G. sulphuraria* had over 60% w/w protein content and compared favorably to the FAO dietary requirements for adults regarding every amino acid, in both autotrophic and mixotrophic biomass. Moreover *G. sulphuraria* contains a high proportion of sulphurated amino acid compared with *Chlorella*, *Spirulina* and soybean protein. Due to its attractive amino acid profile and high protein content, *G. sulphuraria* is a good candidate to overcome sulphurated amino acid deficiencies for food and feed applications.

Chapter 6

General discussion
Oxygen balanced mixotrophy: a look at the economics

INTRODUCTION

The continuous growth of the human population is placing increasing pressure on our limited natural resources. This has resulted in an ongoing search for renewable resources and more environmentally friendly production processes (Godfray et al., 2010). Microalgae can reach higher areal productivity than terrestrial plants, do not require arable land or fresh water, (Wijffels & Barbosa, 2010) and can use fertilizers with almost 100% efficiency (Tredici, 2010). Microalgae-derived products are considered a promising source of food and commodities (García et al., 2017; Wijffels et al., 2013).

Microalgae are commonly grown exploiting their photoautotrophic capacity (henceforth referred to as autotrophic), in which cells harvest light energy, use carbon dioxide (CO_2) as a carbon source, and release oxygen (O_2) as a byproduct. Despite the advantage of CO_2 mitigation and use of free solar energy, autotrophic cultures have limitations. In autotrophic cultures, light availability is the main growth limiting factor. Cellular self-shading hinders light availability therefore limiting biomass production. To limit self-shading, low biomass concentrations must be maintained in autotrophic cultures leading to a dilute harvest flow and a large volume of liquid to be handled. Another limitation of autotrophic cultivation is the need for gassing which demands a substantial amount of energy. Gas−liquid transfer is necessary to avoid O_2 accumulation in the liquid culture and to provide the CO_2 required for photosynthesis. The accumulation of O_2 might lead to a reduction of culture productivity (Kazbar et al., 2019; Sánchez Zurano et al.; Sousa et al., 2013).

In several photobioreactor (*PBR*) designs gassing is an integral part of the mixing of the microalgal culture. In vertical panel or column type *PBRs* mixing is exclusively provided by gassing, but in tubular *PBRs* mixing and gassing are separated. In tubular *PBRs* mixing is ensured via a liquid pump, while O_2 and CO_2 gas-liquid exchange is supported by a dedicated

unit called 'degasser' usually in the form of a bubble column. In tubular *PBRs* the energy for gassing has been reported to be 23% of the operational energy cost (Acién et al., 2012).

CO_2 supply is a frequently overlooked challenge in microalgae commercialization. Atmospheric CO_2 levels (~0.04% v/v) are not sufficient to support high biomass productivities because the driving force for gas-liquid transfer is too small and gas flows are required which are practically not achievable and/or would require excessive energy (Langley et al., 2012). For this reason, CO_2-enriched gas streams must be provided to achieve high biomass productivity. Not all CO_2 provided is taken up, and even in optimized closed photobioreactors, CO_2 losses are 25% at minimum (Acién et al., 2012; Moraes et al., 2020). When not efficiently utilized, CO_2 supply possibly represents a major contributor to production costs. Anthropogenic CO_2-enriched gas (e.g. flue-gas with 10-15% CO_2) is envisioned to meet the requirement for large scale production. However, considering the high CO_2 demand of a large scale facility, without an infrastructure for CO_2 capture and transportation, only a limited number of areas are suitable for large scale production (Smith et al., 2015).

Chemoorganotrophic (henceforth referred to as heterotrophic) cultures in which organic carbons, such as sugars and organic acids, are used as carbon sources in the absence of light could be alternatives to autotrophic cultures. In contrast to autotrophic cultivation, heterotrophic cultivation can be performed in conventional fermenters, requiring O_2 by intensive aeration, reaching higher concentration and productivity. However, darkness can lead to reduced pigmentation limiting the potential of heterotrophic cultivation for the large-scale production of these phytochemicals (Lee, 2001). Moreover, on average only half of the carbon substrate is converted into biomass while the other half is lost as CO_2 as reviewed by Blanken *et al.* (Blanken et al., 2016).

In this thesis I described a new cultivation method named 'oxygen balanced' mixotrophy. In this method the dissolved oxygen concentration (*DO*) is kept constant by coupling the substrate

supply rate with the rate of photosynthesis (Chapter 2). This method allowed O_2 and CO_2 cycling between photosynthesis and respiration within a single algal monoculture, avoiding (Chapters 2,4,5), or minimizing (Chapter 3), gas exchange. Furthermore, mixotrophic biomass productivity and biomass concentration was doubled in comparison to autotrophy and 88% to 94% of the substrate carbon was converted into biomass carbon (Chapters 2,3,4,5). We successfully applied this method to two industrially relevant microalgal species: *Chlorella sorokiniana* (chapters 2 and 3) and *Galdieria sulphuraria* (chapters 4 and 5) and demonstrated that oxygen balanced mixotrophy does not affect protein (50-60% w/w) and pigment content of those species: 7 $mg \cdot g_x^{-1}$ of lutein in *C. sorokiniana* and 101 $mg \cdot g_x^{-1}$ of C-phycocyanin in *G, sulphuraria* (chapters 3 and 5).

In this final chapter the insights obtained from this thesis are combined in a techno-economic model to allow for an objective evaluation of their cost-impacts . Projections are presented on the biomass production costs for a hypothetical 100-hectare facility located in southern Spain. The techno-economic model is used to compare the biomass production cost of autotrophic and "oxygen balanced" mixotrophic cultures of *Chlorella sorokiniana* and *Galdieria sulphuraria*. Finally, opportunities for future improvement of the mixotrophic process will be addressed.

MATERIALS AND METHODS

Autotrophic production of C. sorokiniana and G. sulphuraria in southern Spain: a techno-economic analysis

In the following section, a techno-economic analysis of autotrophic production of *C. sorokiniana* and *G. sulphuraria* is presented. This analysis will be used as base case and compared with oxygen balanced mixotrophic production of the same species. The techno-economic model originally developed by Ruiz et al. (2016) for autotrophic production of *Nannachloropsis sp* was adapted to the cultivation of our strains. A vertically stacked tubular photobioreactor was chosen as a cultivation system in the analysis because in this reactor type mixing and gassing are separated. The reactor design is identical to the vertically stacked tubular photobioreactor described by Ruiz et al. (2016): tube diameter 0.065 m; tube length 170 or 250 m. Projections are made for a 100-ha-scale plant located in southern Spain (37°15′ N 6° 56′ W).

Process description

The algal production chain (figure 1) begins with pumping (1) fresh water from a water reservoir, which is then mixed with nutrients (2) in an automatized mixing unit (3), filtered (4) and pumped into the photobioreactor (6). The freshwater medium enters the photobioreactor reactor only during daylight hours, and, concurrently, the same culture volume leaves the reactors. Harvesting is done by continuous pumping (10) of the culture harvest through a microfiltration (11) unit that concentrates the biomass to about 15 $g \cdot L^{-1}$. The concentrated fraction (retentate) is further processed with a centrifuge (12), obtaining an algal slurry (15% w/w) that is considered the final product of the current analysis. Part of the permeate coming from the ultrafiltration and part of the supernatant obtained by centrifugation is recirculated (9) back to the mixing unit. The water that is not recirculated is considered as wastewater and is

treated at a cost of 0.50 €·m^{-3} (Molina Grima et al., 2003), by an external party. The energy consumption of wastewater treatment is not included in the evaluation of the overall energy usage of the process. With respect to medium preparation the cost of nitrogen and phosphorus alone are considered in the analysis, being those with major influence on economics (Ruiz et al., 2016). Nitrogen and phosphorus losses are considered to be neglectable. During daytime, pure gaseous CO_2 (5) is injected at the tube inlet through a gas diffuser, while excess oxygen is removed from the culture by sparging ambient air (7) in a separate bubble column (degasser) (8). During night time oxygen is provided by sparging air at the tubes inlet (instead of CO_2) While the degasser vessel was not sparged. A combination of heat exchangers (14), pipes and pumps (13) is installed to control temperature. Deep sea water is directly used as cooling water and then discharged back to the sea.

***Figure 1**. Scheme of autotrophic microalgal production chain during day (top) and night time (bottom). 1) Fresh water pump, 2) Nitrogen and phosphorus supply unit, 3) mixing unit, 4) sterilization, 5) CO_2 supply unit, 6) vertical tubular photobioreactor, 7) blower, 8) degasser (bubble column), 9) recirculation pump,10) harvesting pump, 11) microfiltration unit, 12) centrifuge, 13) pump (cooling), 14) heat exchanger*

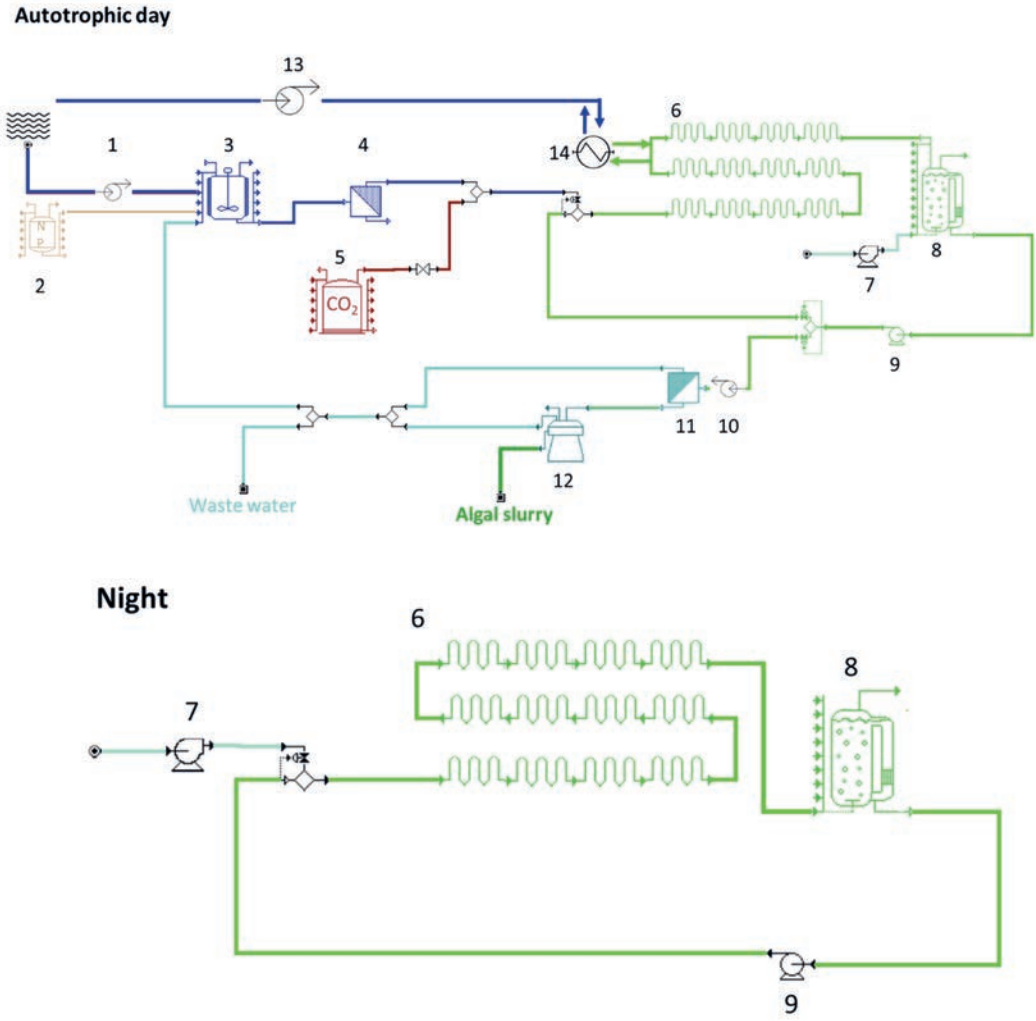

.

Selection operating conditions and estimated productivity

The amount of biomass produced per year was calculated according to the photosynthetic efficiency reported in outdoor studies. The photosynthetic efficiency is defined as the fraction of total sunlight energy converted into chemical energy (i.e. biomass) during photosynthesis. A photosynthetic efficiency on sunlight of 2.6% obtained by Doucha & Lívanský (2006), was used to estimate the production of *C. sorokiniana* while for *G. sulphuraria* half of this value was used. The factor half is based on our experimental results described in Chapter 5. Our data demonstrated that the biomass yield on light for *G. sulphuraria* was about half of the one obtained for *C. sorokiniana* under identical experimental conditions.

Different dilution rates were assumed for the cultivation of *C. sorokiniana* and *G. sulphuraria*. A dilution rate of 27% per day reported by de Vree et al (de Vree et al., 2015) in vertically stacked tubular photobioreactor, and used in the previous model (Ruiz et al., 2016), was adopted for *C. sorokiniana*. The dilution rate of *G. sulphuraria* was calculated such that the estimated biomass concentration results in a specific photon supply rate within the optimal rage reported in chapter 4 (supporting information 1). This resulted in a dilution rate of 13.5% per day. A liquid velocity in the tubes of 0.45 $m \cdot s^{-1}$ was used for both strains (de Vree et al., 2015, Ruiz et al., 2016).

In tubular photobioreactors the oxygen produced during photosynthesis accumulates along the tube and needs to be removed to prevent adverse effects that inhibit algal growth (e.g. photorespiration). The maximum dissolved oxygen concentration at the end of the tubes was set to 350% of oxygen saturation. The superficial gas velocity in the bubble column degassers was fixed (0.056 $m \cdot s^{-1}$) as well as the height of the bubble column (2.2 m) resulting in air flow rate of 1.52 vvm and a volumetric gas liquid mass transfer coefficient ($K_{LO2}a$) of 0.08 s^{-1} (Sánchez Mirón et al., 2000). Bubble columns were assumed to be perfectly mixed. The length of the tubes and the number of liquid pumps, and associated flow, were calculated based on the

maximal *DO* threshold of 350% air saturation at the end of the tube and a *DO* of 150% maintained in the bubble column. The number of bubble columns and associated gas flow was calculated based on the gas-liquid mass transfer coefficient and the oxygen concentration gradient between gas and liquid.

During the night, in absence of light, intracellular storage compounds (e.g. starch) are used to support cell division (León-Saiki et al., 2017). The metabolic energy required is created by respiration and, for this reason, oxygen must be supplied during the night. Oxygen is provided by injecting air at the inlet of the tube. The rate of air injection into the tubes was calculated based on the mass transfer model for an identical system described in Rubio et al (Rubio et al., 1999). During the night, the *DO* at the end of the tube was assumed to have 10% air saturation. Accordingly, the required air flow rate was calculated to match the volumetric oxygen transfer rate to the volumetric uptake rate of the culture. The volumetric oxygen uptake rate was calculated from the experimental results obtained under day-night mixotrophy (Chapter 3). In those experiments we found a night time O_2 requirement of 4.1 mmol O_2 per C-mol of biomass per h. This specific oxygen uptake rate was combined with the biomass concentration (4.6 $g \cdot L^{-1}$ for mixotrophy and 2.3 $g \cdot L^{-1}$ for autotrophy) to obtain the volumetric uptake rate.

The efficiency of CO_2 utilization (E_{CO2}, % $w \cdot w^{-1}$) is influenced by the pH of the culture. pH influences the chemical equilibrium according to:

$$CO_2(g) \leftrightarrow CO_2(aq) \leftrightarrow H_2CO_3 \leftrightarrow HCO_3^- \leftrightarrow CO_3^{2-} \quad (1)$$

Where $CO_2(g)$ is the CO_2 concentration in the gas phase, CO_2 (aq) is the CO_2 concentration in the aqueous phase, and all the other terms of the equation are the soluble form of CO_2. The difference between the CO_2 concentration in the liquid phase and that in equilibrium with the gas phase ($[CO_2^*]$—$[CO_2]$) represents the driving force for mass transfer of CO_2 from gas to water. The product of the driving force and the volumetric mass transfer coefficient ($K_{LCO2}a$) gives the transfer rate of CO_2 which ideally matches the CO_2 requirement of the algal biomass.

The mass transfer coefficient is independent of pH, but the driving force is pH dependent and it will increase with pH (Sugai-Guérios et al., 2014). Moraes et al. (Moraes et al., 2020) have shown that the efficiency of CO_2 utilization (E_{CO2}) can be improved from 8% to 75 % by increasing the pH from 6.5 to 7.8. Although in our experiments *C. sorokiniana* was cultivated at pH 6.7, several other *Chlorella* strains have been cultivated pH 7.5-8 (Guccione et al., 2014). Therefore, in this study we will assume that *C. sorokiniana* will be cultivated at pH 7.8 and a CO_2 use efficiency (E_{CO2}) of 75% will be used in the calculation. *G. sulphuraria* is an acidophilic strain with pH optima of 1-4 (Graziani et al., 2013; Oesterhelt et al., 2007; Selvaratnam et al., 2014; Sloth et al., 2006). Therefore 8% E_{CO2}, the lowest value reported by Moraes et al (Moraes et al., 2020), will be used in this study. All the gasses entering or leaving the reactor are filtered using air filters to prevent bacteria contaminations.

Tubular photobioreactors tend to accumulate algal films on the inner surface, restricting sunlight supply, and despite all the reactor entrances being protected by filters, in the long run also bacterial contamination might occur. Therefore, regular cleaning is essential for a reliable operation of a microalgae production facility. In the projections three cleaning cycles are performed per year. During a cleaning cycle, reactors are filled with 3% of cleaning solution composed of 35% H_2O_2 and 7.5% glycerin. To remove biofilms, also small plastic granulates (Bosma et al., 2014) are added into tubular systems at a concentration of 0.5 $Kg \cdot m^{-3}$. The granulates are recovered afterwards and can be reused up to 3 years. They are also used in the algal culture during cultivation in tubular systems to prevent biofilm formation.

Recycling the culture medium is key for sustainable microalgae cultivation. This is especially true for freshwater species. However, reused medium may accumulate inhibitory compounds. The subject has been recently reviewed by Lu et al. (2020). The response of *Chlorella* to medium recycling is contradictory: 3 studies reported medium reuse stimulates growth, 8 other studies indicated no effect of medium reuse, while 6 studies described growth inhibition after

medium reuse. Therefore, even though up to 100% of medium reuse has been reported not to affect growth over 63 days^{-1} (Hadj-Romdhane et al., 2013), in our study medium recycling of 80% is assumed. Medium recycling in *G. sulphuraria* has never been tested. In this analysis we will therefore apply the same water reuse percentage as with *Chlorella*. A fee of 0.023 €·m^{-3} is applied for fresh water required to make up fresh medium (Cornish et al., 2004).

Maximum culture temperature is maintained at 37°C by pumping cooling water through heat exchangers submerged into the culture. The heat flow in the photobioreactors and the expected temperature of the culture are calculated on an hourly basis. The temperature control units are active during those periods with an expected value above the setpoint. Cooling water from the sea comes from a depth of 200 m. The temperature of the water is 14.1 ±0.2 °C (NOAA). Energy consumption for temperature control represents the electrical power used by pumps and this was calculated according to Ruiz et al. (2016).

In our analysis, land is assumed to be purchased at the cost of unirrigated agricultural land in Huelva (Consejería-de-Agricultura-Pesca-y-Desarrollo-Rural-Junta-de-Andalucia, 2016). The extra land required, such as the space to place major equipment, buildings or roads, was considered to be 20% of the total photobioreactor area (100 hectares), the total land for the facility being 120 hectares. The value of purchased land was not depreciated, since its value does not decrease with time and use, therefore the price of land purchasing was only considered as part of the interest to pay on the initial investment and not as part of the CAPEX.

The model described by Ruiz et al. (2016) uses location-specific parameters such as climatic conditions, energy costs, labor costs and employer's contribution to labor costs as well as workweek hours. An account of the main model features is given in supporting information 2. The overview of the values used in this study are summarized in table 1. For further details, we refer to the original work (Ruiz et al., 2016).

***Table 1**. Overview of values used in the techno-economic evaluation of autotrophic production of C. sorokiniana and G. sulphuraria.*

Parameter	**Value**	**Unit**
Scale	100	ha
Chemostat operation-Dilution rate	0.27/0.09*	day^{-1}
Photosynthetic efficiency	2.6/1.3*	% (Sun light)
pH	7.8/1.6*	
CO_2 cost	184	$€\cdot ton^{-1}$
E_{CO2}	75/8*	$\% (w\cdot w^{-1})$
Culture temperature	37	°C
Temperature control	Deep sea water	
Liquid velocity in the tubes	0.45	$m\cdot s^{-1}$
Aeration rate day (degasser)	1.52	$VVM (L\cdot L^{-1}\cdot min^{-1})$
Aeration rate night (tubes)	0.006	$VVM (L\cdot L^{-1}\cdot min^{-1})$
$K_{LO2}a$ (degasser)	0.08	s^{-1}
$K_{LO2}a$ (tubular part reactor)	0.0003	s^{-1}
Water reuse	80	%
Freshwater cost	0.023	$€\cdot m^{-3}$
Wastewater cost	0.5	$€\cdot m^{-3}$
Land cost	12000	$€\cdot ha^{-1}$
Days of operation	300	day
Cleaning per year	3	
Area dedicated to inoculum production	10	%

* Value used for *G. sulphuraria*

Oxygen balanced mixotrophic production of C. sorokiniana and G. sulphuraria in southern Spain: a techno-economic analysis

In the following section, the techno-economic analysis of oxygen balanced mixotrophic production of *C. sorokiniana* and *G. sulphuraria* is presented. In this analysis the model described by Ruiz et al. (2016), with the modifications reported in the previous section, was adapted for the oxygen balanced mixotrophic production of our strains.

Process description

The process described in figure 1 was adapted for oxygen balanced mixotrophy. The CO_2 supply unit was removed from the process scheme and glucose is used as organic substrate (Figure 2). The glucose needed for 3 days of operations is stored in a feeding tank (5). Glucose is added to the mixing unit (3) and the volume of the mixing unit is therefore increased by 20%. No aeration is provided during daytime. During night time (Figure 1), air is provided through a diffuser at the entrance of the tube as already described for the autotrophic culture. The air injected in the tubes is allowed to escape in a small collection vessel (8) installed at tube outlet. This vessel is not actively sparged.

Empirical data

Glucose is purchased at 442 €·ton^{-1} according to the average cost reported by Sun et al. (Sun et al., 2019). The biomass yield on substrate of 0.88 C-mol$_x$·C-mol$_s^{-1}$ obtained under day-night cycle (Chapter 3) is used in this study. Biomass productivity and biomass concentration are the double of the autotrophic culture grown under the same conditions (Chapters 2,3,5).

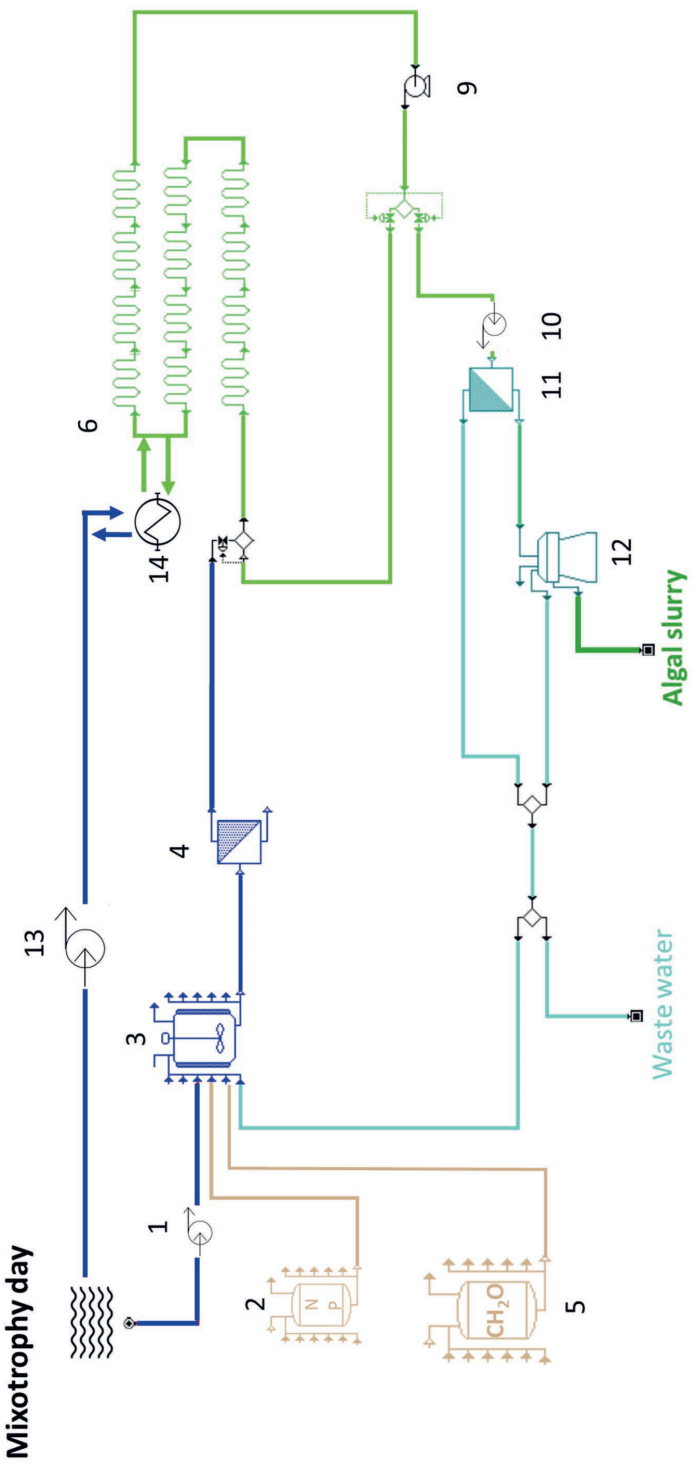

Figure 2. *Scheme of mixotrophic microalgal production chain during daytime. 1) Fresh water pump, 2) Nitrogen and phosphorus storage unit, 3) mixing unit, 4) sterilization, 5) Glucose storage unit, 6) vertical tubular photobioreactor, 9) recirculation pump, 10) harvesting pump, 11) microfiltration unit, 12) centrifuge, 13) pump (cooling), 14) heat exchanger.*

RESULTS AND DISCUSISON

Autotrophic and mixotrophic biomass production costs of C. sorokiniana

The techno-economic models for autotrophic and mixotrophic algae production were used to compare autotrophic and oxygen balanced mixotrophic biomass production costs of *C. sorokiniana*. According to our predictions, a 100 ha facility employing vertically stacked tubular photobioreactors located in south of Spain has a biomass capacity of $5.9 \cdot 10^3$ ton·year^{-1} and 11.7 10^3 ton·year^{-1} employing autotrophic cultivation and oxygen balanced mixotrophic cultivation, respectively. Our estimations indicate that the production cost of autotrophic cultures is 4.9 €·Kg^{-1} while mixotrophic production cost is 2.6 €·Kg^{-1}.

Breakdown of the contributors of the biomass production costs are reported in figure 3. The main contributor to the autotrophic production costs are the capital costs (32%). Among the capital costs, depreciation of the major equipment and the interest on the initial investments contribute 98.4% while the remaining 1.6% comprises of property taxes and insurances. Major equipment accounts for 20% while instrumentation and control take up 30% of the initial investment. Within the major equipment 44% of the costs are due to circulation pumps and 23% to air blower and bubble columns.

The second contributor to the autotrophic production costs are the raw materials (24%). Among the raw materials, the chemical disinfectant used for cleaning accounts for 55%, CO_2 accounts for 38%, while the cost for medium preparation accounts for 6% of raw materials. The process consumes 6.0 kWh per Kg of biomass, making energy the third contributor to the production costs (15%). The culture circulation pumps consume 79% of the total energy while 13% is spent in the aeration. This value is the half of previous reported by Acién et al. (2012). In their work (Acién et al., 2012) aeration was provided without distinction between day and night time. In our study we changed the aeration at night time to air injection at the tube inlet. We adopted

this change to use the same aeration procedure during night time for autotrophic and oxygen balanced mixotrophic culture allowing for an objective comparison of both strategies.

The main expenses for consumables (94%) are related to the borosilicate glass tubes that have a lifetime of 20 years. Other costs contribute for 12% of the total production cost, including general plant overheads, maintenance and contingency. Labor (5%) and waste water treatment costs (1%) had a minimal impact on the overall production costs.

Figure 3. *Breakdown of the contributors to autotrophic (left) and oxygen balanced mixotrophic (right) biomass production costs of C. sorokiniana.*

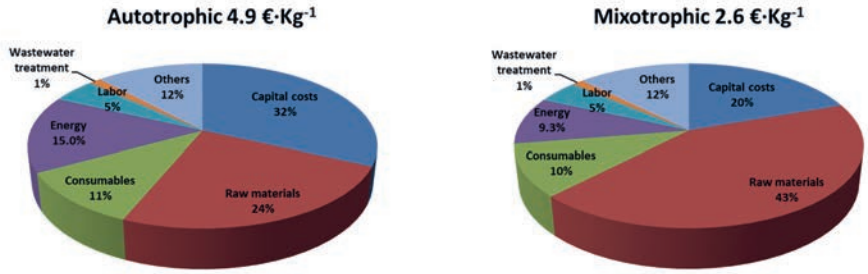

According to our projection, utilizing oxygen balanced mixotrophy will decrease biomass production costs by 47%, from 4.9 €·Kg^{-1} of the autotrophic cultivation to 2.6 €·Kg^{-1} for mixotrophic cultivation. In mixotrophy, the main contributor to the total cost is raw materials (43%), out of which glucose represents 59%, which comes down to 25% of the total biomass production costs (0.66 €·Kg^{-1}). The chemical disinfectant used for cleaning contributes 34% to the costs of raw materials and medium preparation contributes 7%. The other major contributor (19%) to the production costs are the capital costs, which have a similar cost distribution as for the autotrophic production. However, the absolute costs for major equipment needed for mixotrophy are 1.5-fold lower than for autotrophy (supporting information 2).

To construct a 100 ha facility for autotrophic cultivating would require an initial investment of 125 M€ while for the mixotrophic cultivation strategy this value would decrease to 82 M€. Since Lang - factors are used in the estimation of capital investment (Ruiz et al., 2016), a decrease in major equipment cost affects the overall capital costs. The investment needed to purchase major equipment is 25 M€ and 16 M€ for autotrophic and mixotrophic production, respectively.

The main causes of the cost reduction regarding major equipment of the mixotrophic culture are the savings obtained by decreasing the need for circulation pumps (4 M€), blowers (3 M€) and bubble columns (2 M€). The reduction in circulation pump numbers is due to the difference in tube lengths, 250 m in mixotrophy and 170 m in autotrophy. The average *DO* level at the end of the tube may not exceed 350%, thus the tube length is shorter under autotrophic growth conditions.

The reduction in major equipment is also affecting the energy consumption. In fact, a 100 ha facility for autotrophic microalgal production would consume 35 $GWh \cdot year^{-1}$ while the same facility operated mixotrophically would consume 23 $GWh \cdot year^{-1}$. The energy saving is caused by the reduction on the circulation pump electric consumption (-8.5 $MWh \cdot year^{-1}$) and omitting aeration during daytime (-4.2 $MWh \cdot year^{-1}$). However, the main reason for mixotrophy saving energy is because of the doubled biomass productivity and concentration, which reduces the overall energy consumption 3 times when expressed per Kg of biomass: 2 $kWh \cdot Kg^{-1}$ under mixotrophy as compared to 6 kWh under autotrophy.

In summary, despite oxygen balanced mixotrophic production of *C. sorokiniana* requiring less capital investments and consuming one third of the energy of the autotrophic culture, a 47% decrease in biomass production costs is mainly due to mixotrophic production doubling biomass productivity compared to autotrophic production.

Autotrophic and mixotrophic biomass production costs of G. sulphuraria

The model described above for *C. sorokiniana* was applied to estimate the biomass production cost of *G. sulphuraria* (figure 4). *G. sulphuraria* has half of the photosynthetic efficiency of *C. sorokiniana* (Chapter 5) and, given the low pH used for the cultivation, carbon uptake efficiency (E_{CO2}) in *G. sulphuraria* was assumed to be only 8%. The direct consequence of those assumptions is the high production cost of the autotrophic culture (11.8 €·Kg^{-1}) where the raw material represents 48% of the total costs. Since only 8% of the CO_2 entering the reactor is converted into biomass, CO_2 contributes to 76% of the raw material costs and to 36% of the total cost (4.3 €·Kg^{-1}), followed by cost for cleaning 22% and for medium preparation 2%. If the low E_{CO2} will be confirmed in a real tubular photobioreactor, the only possible solution for autotrophic cultivation of acidophilic microalgae will be to use flue gas as source of CO_2. Ruiz et al. (2016) estimated that flue gas can be conditioned and transported to an algae photobioreactor at a cost of 0.034 €·Kg^{-1}. Therefore, by employing flue gas rather than commercial CO_2, the autotrophic production cost of *G. sulphuraria* could drop to 6.9 €·Kg^{-1}.

The second contributor to the overall costs is capital costs (18%). The autotrophic production of *G. sulphuraria* requires 37% lower initial investments and 32% less electricity than autotrophic production of *C. sorokiniana*. These differences are related to the lower photosynthetic efficiency used in the model, and as consequence oxygen accumulates along the tube at a lower rate. Therefore, the number of major equipment (bubble columns and blowers) needed for oxygen removal degassing are decreased by 11%. Furthermore, longer tubes (up to 340 m) can be used, decreasing the number of circulation pumps needed. Despite the possibility of using longer tubes, we decided to set the maximum tube length to 250 m. This was done for an easier comparison between the mixotrophic performance of the two strains. Longer tubes in the autotrophic cultivation of *G. sulphuraria* allowed saving 15% of the capital costs and 26% of energy consumption of circulation pumps compared to autotrophic culture of *C. sorokiniana*.

In autotrophic cultivation *G. sulphuraria* energy requirement for degassing contributes only to 10% of the total energy costs.

However, all those savings are minimal considering the photosynthetic efficiency of *G. sulphuraria* being only half of *C. sorokiniana*'s and therefore the facility produces only half as much biomass (2.9 10^3 ton·year^{-1}) compared to *C. sorokiniana*. Because of the lower areal productivity, all of the capital and energy costs have a higher impact per kg of biomass produced. Lower productivity of *G. sulphuraria* also increases the autotrophic energy required per kg of biomass to 8.1 KWh·Kg^{-1}.

Oxygen balanced mixotrophic production *G. sulphuraria* is 3-fold cheaper than its autotrophic production. This is due to the high impact of CO_2 on the autotrophic production costs and to the doubling of the biomass productivity obtained in mixotrophy. In mixotrophy raw materials contribute to 35% of the total production costs. Among the raw materials, glucose accounts for 46% (0.64 €·Kg^{-1}), cleaning for 47% and medium preparation for 7% of the costs.

***Figure 4**. Breakdown of the contributors of autotrophic (left) and oxygen balanced mixotrophic (right) biomass production costs of G. sulphuraria.*

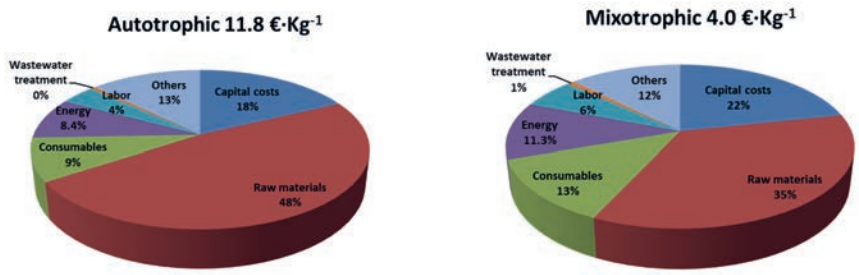

Mixotrophic cultivation strategy has a minimal impact (-9%) on the energy consumption of *G. sulphuraria*, compared to autotrophic cultivation. This is because under autotrophy the tubes can remain as long as under mixotrophy and therefore the amount of energy consumed by circulation pumps does not change. The only energy saving achieved is linked to the reduction

of aeration. Since mixotrophy doubled biomass productivity, the amount of energy required per kg of biomass drops considerably from 8.1 $KWh \cdot Kg^{-1}$ to 3.7 $KWh \cdot Kg^{-1}$. When compared to *C. sorokiniana*, we can conclude that mixotrophic energy consumption and biomass production costs of *G. sulphuraria* are strongly affected by its lower biomass productivity (twofold reduction) which increases the impact of each individual cost factor per Kg of biomass produced.

Sustainable protein production from microalgae

Cost assessment is not the only means to evaluate a production process. In this section we present the implications of oxygen balanced mixotrophy on land requirement and water consumption. Land and water required to produce 1 kg of proteins by autotrophic and mixotrophic cultivation of microalgae were compared to the requirements of soy beans, the largest global protein crop. Heterotrophic cultivation of microalgae and/or other possible single-cell protein producers (e.g. baker's yeast) were excluded from our comparison due to the lack of techno-economic models on heterotrophic biomass production costs in the public domain.

Water consumption of microalgae production was calculated considering only two sources of water losses: the volume of water that is treated as waste water (20% of the total water volume required for reactor dilution) and the volume of water consumed during cleaning of the reactors. According to our assumptions, the facility is cleaned three times per year, and each time the whole volume of the reactors is filled with clean water and disinfectant solution.

In the case of mixotrophic production of microalgae, land and water required to produce the sugar necessary for the process must be considered. We decided to use sugar beet produced in The Netherland as a source of hexose. Due to the joined efforts of the Dutch sugar industry, sugar beet yields have been increased from 10.6 $ton \cdot ha^{-1}$ in 2002-2006 to 13.8 $ton \cdot ha^{-1}$ in 2012-2016 (Hanse et al., 2018) and there are aims to reach 24 $ton \cdot ha^{-1}$ in the coming future (Hoffmann

& Kenter, 2018). Moreover, the production of this sugar requires only 358 m^3 of water per ton of sugar produced, making the water footprint of sugar production in The Netherland one of the lowest in the world (Scholten, 2009).

In 2018, European Union (EU) imported 93% of the soy beans consumed, out of which 50% originated from the United States of America (USA) (European-Soy-Monitor, 2017). Given the importance of the USA as a soy beans producer, we will focus our analysis on soy beans produced in the USA. Between 2015 and 2020 soy bean yield in the USA was 3.4 $ton \cdot ha^{-1}$ (USDA). The average soy bean protein content was 36% (Krishnan & Jez, 2018b) and on average 2757 m^3 of water are required per ton of soy beans produced (Field-to-Market, 2016). Comparison of land and water usage to produce 1 kg of protein from autotrophic and mixotrophic microalgae cultivation and soy bean farming is reported in table 2. Microalgal protein yield per hectare is 30-60 times higher than for soy beans. A closer look at the water requirements of algal protein production reveals the water footprint of microalgae to be 25-50 times lower than for soy beans. However, mixotrophic cultivation consumes glucose, the production of which leads to substantial water and land use. When counting in the land needed for sugar beet production, mixotrophic areal productivity decreases with roughly one order of magnitude, but it still remains 4 times more productive than soy beans. Moreover, mixotrophic cultivation still requires 7 times less water than soy beans. Envisioning a future of water and arable land scarcity, algae cultivation should not be done on arable lands and using fresh water should be avoided. Several *Chlorella* strains have been proven to grow on sea water (Guccione et al., 2014). No record of *Galdieria* on sea water has been reported in the literature. Galdieria, however, has been proven to tolerate high salt concentration (Schmidt et al., 2005), so it might be possible to cultivate this strain on sea water or brackish water. Another alternative to fresh water, is the cultivation of *Galdieria* on hot spring water (Hirooka & Miyagishima, 2016).

Mixotrophic algal protein production was 40% cheaper than autotrophic production. However, with soy beans at 0.36 €·Kg^{-1} , and microalgae at 2.5-6.1 €·Kg^{-1}, algae protein production as commodity source of protein seems currently out of reach (European-Commission, 2020). Nevertheless, ***G. sulphuraria*** has 2.6 times more sulphurated amino acid than soy beans (Chapter 5). Therefore, we believe, especially after a reduction of the production costs (see next section), ***G. sulphuraria*** to be promising as a food and feed supplement.

Algae biomass is not merely a source of protein. Microalgae are regarded as one of the most nutritious foods known to man (García et al., 2017). They can provide a significant number of essential nutrients, such as vitamins, minerals, essential fatty acids and pigments, to support human health (García et al., 2017; Lupatini et al., 2017). The two algae species studied in this thesis can both be used as a good source of pigments. When grown mixotrophically, ***C. sorokiniana*** biomass contained 7.3 mg lutein per g of biomass (chapter 3) while ***G. sulphuraria*** had 101 mg·g_x^{-1} of C-phycocyanin (chapter 5). Considering a commercial value of 490 €·Kg^{-1} and 130 €·Kg^{-1} respectively for lutein and C-phycocyanin (Algreen personal communication), these two pigments can generate an income of 3.6 €·Kg^{-1} and 13 €·Kg^{-1} respectively in ***C. sorokiniana*** and ***G. sulphuraria***. Ruiz et al. (2016) indicated that a complete biorefinery of autotrophic algae biomass is already profitable, and therefore since the biomass composition is not affected by mixotrophy (chapter 3 and 5), the decrease in the production costs will increase the net profits of algae production.

Besides a pure economic evaluation, the consumption of natural resources will assume even greater importance in the future (Tredici et al., 2016). A fair comparison between autotrophic and mixotrophic algal production and soy beans should take into account usage of non-renewable resources, such as phosphorus and fossil fuels, the impact of conventional agricultural practices on the environment and on human health, and the social and political implications of these practices.

Our simplified estimations highlight that in mixotrophic cultivation, water and land requirements are strictly related with agricultural practices needed to produce the organic substrate. Therefore, choosing the "right" organic substrate is key to the sustainability of the algal end-product. In this perspective, using agro-industrial side streams as organic substrate represents an attractive solution.

In recent years, coupling bacterial dark fermentation of organic waste stream with mixotrophic cultivation has been suggested as a promising approach to produce biofuel (H_2) and to decrease the production costs of microalgae (Turon et al., 2016). Several works demonstrate the feasibility of *C. sorokiniana* cultivation in acetic and butyric acid produced via dark fermentation (Turon et al., 2015a; Turon et al., 2015c). In one of these studies, heterotrophic cultivation of *C. sorokiniana* on unsterilized anaerobic effluent was demonstrated, and even if the bacterial community size increased during the experiment, bacteria did not have any significant impact on heterotrophic microalgal growth (Turon et al., 2015b).

Due to its capability to grow at an extremely low pH and the ability to use several organic substrates (Graziani et al., 2013; Gross & Schnarrenberger, 1995), *G. sulphuraria* has also been cultivated in unsterilized primary effluent (Delanka-Pedige, 2018). The authors reported that at pH 2 the initial bacterial population was reduced by 98% and complete removal of pathogens occurred. Other studies suggested that *G. sulphuraria* could be cultivated on food waste from restaurants and bakeries (Sloth et al., 2017).

In conclusion, coupling mixotrophic microalgal cultivation with the treatment of agro-industrial side streams is a promising strategy, not only to decrease microalgal production costs, but to also increase the overall sustainability of the process.

***Table 2.**. Comparison of land and water usage of autotrophic and mixotrophic microalgae cultivation with soy bean farming to produce 1 kg of protein.*

		Soy beans	**C. sorokiniana**		**G. sulphuraria**	
	Unit		Autotrophic	Mixotrophic	Autotrophic	Mixotrophic
Productivity	$ton_x \cdot ha^{-1} \cdot year^{-1}$	3.3	59	117	29	59
Sugar yield on biomass	$ton_s \cdot ton_x^{-1}$	n.a	n.a	1.49	n.a	1.49
Sugar consumption	$ton_s \cdot ha^{-1} \cdot year^{-1}$	n.a	n.a	175	n.a	87
Water footprint biomass	$m^3 \cdot ton_x^{-1}$	2757	152	76	176	88
Water footprint sugar	$m^3 \cdot ton_s^{-1}$	0	0	358	0	358
Water footprint biomass	$m^3 \cdot ha^{-1} \cdot year^{-1}$	9098	8943	8865	5176	5137
Mixotrophic water footprint for sugar	$m^3 \cdot ha^{-1} \cdot year^{-1}$	0	0	62523	0	31261
Total water footprint (biomass + sugar)	$m^3 \cdot ha^{-1} \cdot year^{-1}$	9098	8943	71387	5176	36398
Mixotrophic water footprint (biomass + sugar)	$m^3 \cdot ton_s^{-1}$	0	0	608	0	620
Land use of biomass production	$ha \cdot year^{-1}$	1	1	1	1	1
Mixotrophic land use of sugar production	$ha \cdot year^{-1}$	0	0	12.7	0	6.3
Total land use (biomass + sugar)	$ha \cdot year^{-1}$	1	1	13.7	1	7.3
Mixotrophic biomass productivity	$ton_x \cdot ha\text{-}total^{-1} \cdot year^{-1}$	0	0	8.6	0	8.0
Protein content	%	36%	50%	50%	60%	60%
Protein productivity	$ton_{prote} \cdot ha^{-1} \cdot year^{-1}$	1.2	29.3	58.7	17.6	35.2
Protein productivity mixotrophic	$ton_{prote} \cdot ha\text{-}total^{-1} \cdot year^{-1}$	0	0	4.3	0	4.8
Land used for protein produced	$ha\text{-}total \cdot ton_{prote}^{-1} \cdot year^{-}$	0.8	0.03	0.23	0.06	0.21
Protein water footprint (biomass)	$m^3 \cdot ton_{prote}^{-1}$	7658	305	151	294	146
Mixotrophic Protein water footprint (biomass + sugar)	$m^3 \cdot ton_{prote}^{-1}$	0	0	1217	0	1034
Biomass production cost	$€ \cdot ton_x^{-1}$	0.36	4.5	2.5	6.1	4.0
Protein production cost	$€ \cdot ton_{prote}^{-1}$	1.0	8.9	5.0	10.2	6.7

Future improvement: Increased biomass yield on light vs biomass yield on substrate

Biomass yield on light ($Y_{x/ph}$) and biomass yield on organic substrate ($Y^{het}_{x/s}$) are the two main parameters affecting the stoichiometry of oxygen balanced mixotrophy (chapter 2) and therefore they have an influence on the mixotrophic biomass production costs. In this section we combined the sensitivity analysis on the oxygen balanced mixotrophy stoichiometry (chapter 2) with the techno-economic model. This procedure allowed us to make projections on the effect of future improvements of $Y_{x/ph}$ and $Y^{het}_{x/s}$ on mixotrophic production costs.

The sensitivity analysis of mixotrophic stoichiometry (Chapter 2) is based on the assumption of mixotrophy being described as the sum of the heterotrophic and autotrophic metabolism. We demonstrated that such assumption was valid for *C. sorokiniana* (Chapter 2 and 3), while it was not valid for *G. sulphuraria* (Chapter 4). In this study we neglected this difference, and we applied the same analysis to both strains. Furthermore we assumed that both microalgae species have the biomass elemental composition of $CH_{1.62}O_{0.41}N_{0.14}P_{0.01}$ reported by Kliphuis et al. (2012).

We simulated the effect of increasing $Y_{x/ph}$ on the oxygen balanced mixotrophic stoichiometry, assuming a constant $Y^{het}_{x/s}$ (0.5 C-mol$_x$·C-mol$_s^{-1}$). The sensitivity analysis indicates that an increase in $Y_{x/ph}$ does not affect the relative contribution of the carbon based autotrophic metabolism ($r_{c,auto}$) to the overall mixotrophic metabolism ($r_{c,mixo}$) leading to a linear increase of $r_{c,mixo}$ (Figure 4). This implies that the ratio between carbon based autotrophic productivity ($r_{c,auto}$) and the carbon based heterotrophic productivity ($r_{c,het}$) is constant. Assuming a biomass yield on substrate ($Y^{het}_{x/s}$) of 0.5 C-mol$_x$·C-mol$_s^{-1}$, $r_{c,auto}$ and the $r_{c,het}$ almost equally contribute to $r_{c,mixo}$ and the expected $r_{c,mixo}$ is 2.2 fold higher than $r_{c,auto}$. This expectation was closely matched in our works (chapters 2,3,5). With *C. sorokiniana*, our estimation indicates that by increasing $Y_{x/ph}$ from 26 C-mol$_x$·C-mol$_{ph}^{-1}$, the value used in the techno-economic model, to 61 C-mmol$_x$·C-mol$_{ph}^{-1}$, the highest reported $Y_{x/ph}$ (Cuaresma et al., 2011a), biomass production will

drop to 1.8 €·kg^{-1} (Figure 6). In this case, 53% of total production costs are raw materials, of which 70% were the costs of the organic substrate (0.67 €·kg^{-1}).

As with *C. sorokiniana*, we simulated the effect of increasing $Y_{x/ph}$ on the biomass production cost with *G. sulphuraria* (Figure 6). Our estimation indicates that by increasing $Y_{x/ph}$ from 13 C-mol$_x$·C-mol$_{ph}^{-1}$, the value used in the techno-economic model, to 25 C-mmol$_x$·C-mol$_{ph}^{-1}$, the maximum value reported in *G. sulphuraria* (chapter 3), the biomass production costs will decrease to 2.7 €·kg^{-1} (Figure 6). In this case, 43% of the total production costs were raw materials, of which 58% was the organic substrate costs (0.67 €·kg^{-1}).

The $Y_{x/ph}$ of *C. sorokiniana* used in in the techno-economic model was based on real data obtained outdoors (Doucha & Lívanský, 2006). $Y_{x/ph}$ measured outdoors was 53% lower than the one reported in our experiments (chapters 2-3) and 2.3-fold lower than the maximum value observed in this strain (Cuaresma et al., 2011a). In *G. sulphuraria* the $Y_{x/ph}$ used in the model was 13 C-mmol$_x$·mol$_{ph}^{-1}$, corresponding to half of value used *C. sorokiniana* and about half of our highest value (chapter 4). *G. sulphuraria* has very little history of outdoor cultivation (Henkanatte-Gedera et al., 2017; Lu et al., 2020) and our work on light optimization is just a first attempt to increase its the autotrophic productivity.

Similarly to $Y_{x/ph}$, we simulated the effect on increasing biomass yield on substrate ($Y^{het}_{x/s}$) on carbon based mixotrophic productivity ($r_{c,mixo}$). We assumed a constant $Y_{x/ph}$ of 40.7 C-mmol$_x$·C-mol$_{ph}^{-1}$ for both strains. This biomass yield on light ($Y_{x/ph}$) is significantly higher than the $Y_{x/ph}$ obtained in *G. sulphuraria* (Chapters 4-5). However, the value of $Y_{x/ph}$ does not change the ratio between autotrophic ($r_{c,auto}$) and heterotrophic ($r_{c,het}$) contribution to $r_{c,mixo}$. Therefore, we decided to report only the effect of increasing $Y^{het}_{x/s}$ using one value of $Y_{x/ph}$ for both strains. The expected increase in biomass productivity between autotrophic and oxygen

Figure 5. *Sensitivity analysis on the effect of (top) the biomass yield on photons ($Y_{x/ph}$) and (bottom) the heterotrophic biomass yield on substrate ($Y^{het}_{x/s}$) on the oxygen balanced mixotrophic biomass productivity ($r_{,mixo}$, square). The contributions of autotrophic (r_{auto}, circle) and heterotrophic (r_{het}, triagle) metabolisms to the mixotrophic volumetric biomass productivity are reported separately. In the sensitivity analysis on $Y^{het}_{x/s}$, also the ratio between autotrophic (r_{auto}) and heterotrophic (r_{het}) is reported (r_{auto}/r_{het}, diamonds). In the sensitivity analysis on $Y_{x/ph}$ the filled arrows indicate the $Y_{x/ph}$ used for the current projections of the techno-economic model, while the dotted arrows indicated the one obtained in laboratory. Arrows indicate the maximum $Y_{x/ph}$ ever observed in C. sorokiniana (yellow), while $Y_{x/ph}$ observed in our experiments (dotted) or used in for the current projections the tecnoeconomic model (filled) are reported in green for C. sorokiniana and blue for G. sulphuraria.*

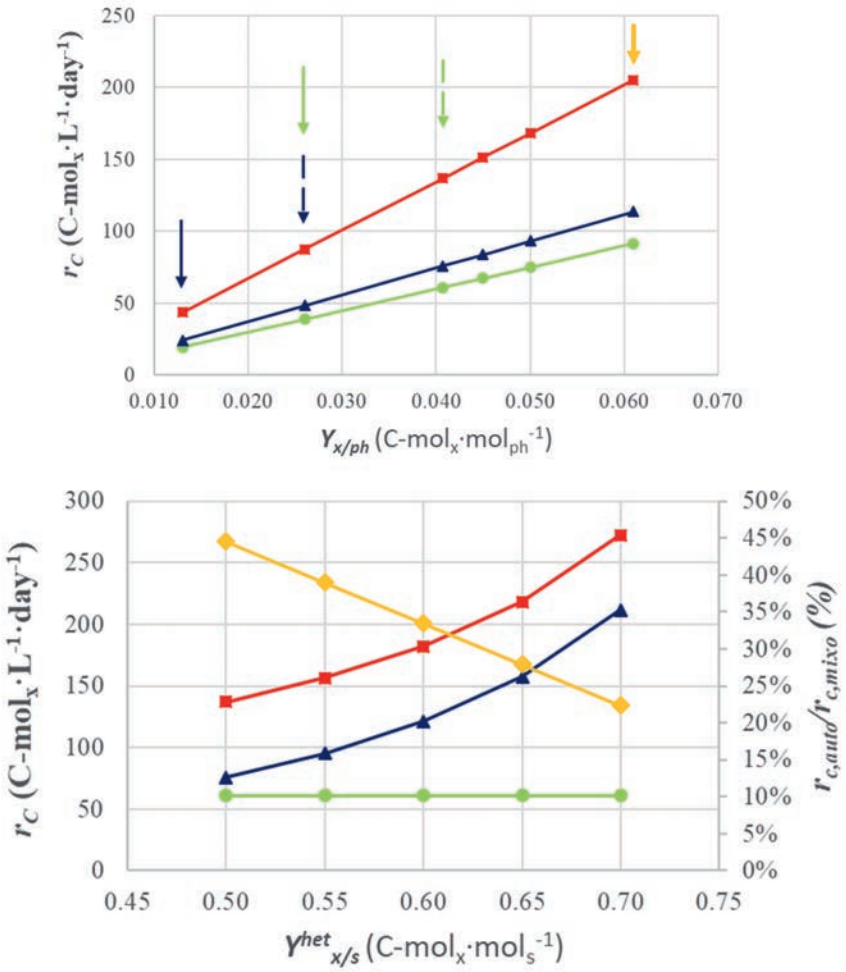

***Figure 6**. Breakdown of the contributors to biomass production costs of oxygen balanced mixotrophic cultivation of C. sorokiniana (left) and G. sulphuraria (right) assuming the highest ever reported photosynthetic efficiency ($Y_{x/ph}$).*

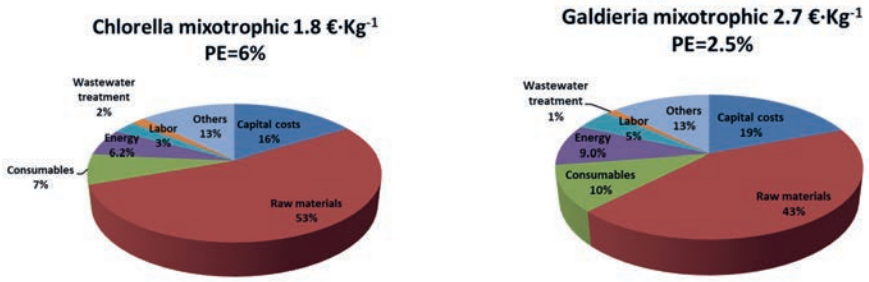

balanced mixotrophic cultivation was used in the tecno-economic model to simulate effect of these changes on the previously reported production costs.

$Y^{het}_{x/s}$ had a strong effect on the contribution of $r_{c,auto}$ and $r_{c,het}$ on overall mixotrophic metabolism ($r_{c,mixo}$), leading to a linear decrease of the ratio of autotrophy ($r_{c,auto}$) over heterotrophy ($r_{c,het}$) (Figure 7). When $Y^{het}_{x/s}$ was simulated to be 0.7 C-mol$_x$·C-mols^{-1}, which is the highest $Y^{het}_{x/s}$ ever reported in microalgae (Chen & Johns, 1996; Jin et al., 2020), the autotrophic metabolism ($r_{c,auto}$) is expected to contribute only for 22% to $r_{c,mixo}$ (Figure 7). Under these conditions, the productivity of an oxygen balanced mixotrophic culture is expected to be 4.5 times higher than an autotrophic culture.

The ability of a microalgae to maintain high $Y^{het}_{x/s}$ during mixotrophic growth is still to be proven. Under heterotrophic conditions *G. sulphuraria* expressed a yield of 0.6 C-mol$_x$·C-mols^{-1} (chapter 4). However when it was cultivated under oxygen balanced mixotrophy, $r_{c,mixo}$ was not the sum of autotrophic and heterotrophic metabolisms. Our measurements indicated that the photosynthetic apparatus was not affected by the addition of organic carbon (chapter 4), therefore a reduction in $Y^{het}_{x/s}$ rather than a reduction on $Y_{x/ph}$ seemed to be more plausible. Interestingly, when *G. sulphuraria* was grown autotrophically and mixotrophically in

chemostat, under optimal lighting (chapter 5), mixotrophic biomass productivity doubled in comparison to autotrophic productivity. According to our stochiometric model (chapter 2), if $Y_{x/ph}$ was not affected by the presence of organic substrate, $Y^{het}_{x/s}$ should have been 0.5 C-mol$_x$·C-mol$_s^{-1}$. To summarize, even if $Y^{het}_{x/s}$ higher than 0.5 C-mol$_x$·C-mol$_s^{-1}$ were obtained in pure heterotrophic cultivation, such high $Y^{het}_{x/s}$ could not be maintained under oxygen balanced mixotrophy. Further work is needed to elucidate the reason why heterotrophic yields are lower under mixotrophic conditions.

Following the hypothesis that it will be possible to find a strain that maintains high $Y^{het}_{x/s}$ under oxygen balanced mixotrophy, we simulated the effect of a mixotrophic culture with a yield of 0.7 C-mol$_x$·C-mol$_s^{-1}$ that is 4.5-times more productive than an autotrophic culture grown under the same conditions (Figure 7). Our estimations indicate that biomass production costs will drop to 1.8 and 2.3 €·kg^{-1} for *C. sorokiniana* and *G. sulphuraria* respectively (Figure 7). For both strains, raw materials account for around 50% of the total production costs, out of which the cost of the organic substrate is the main contributor(~65%).

Figure 7. *Breakdown of the contributors to biomass production costs of oxygen balanced mixotrophic cultivation of C. sorokiniana (left) and G. sulphuraria (right) assuming the highest ever reported biomass yield on substrate ($Y^{het}_{x/s}$).*

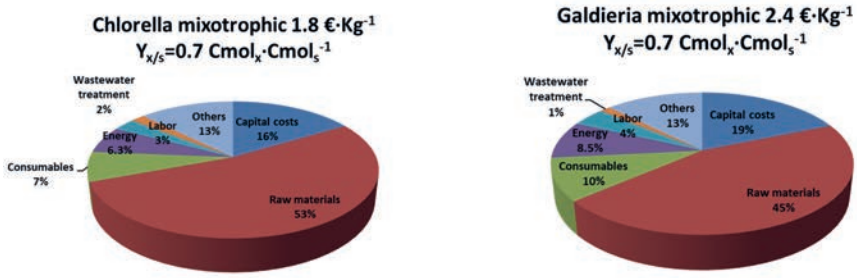

According to our projections, either by increasing the biomass yield on light ($Y_{x/ph}$) or biomass yield on organic substrate ($Y^{het}_{x/s}$), biomass production costs would substantially decrease making the organic substrate the main cost contributor (Figures 6 and 7). Therefore, if the cost of organic substrate would be removed by substituting glucose with an inexpensive and sustainable organic substrate derived from agro-industrial side stream (see previous section), the biomass production costs would be further reduced with around 0.66 €·kg^{-1} closing the gap between algae and soy beans regarding protein production costs. Considering the capability of *G. sulphuraria* to grow on several organic substrates, and the low risk of contaminations, this option seems feasible.

New opportunities for energy consumption reduction

Oxygen balanced mixotrophy provides more freedom with photobioreactor (*PBR*) design. Oxygen build-up is an important factor to consider with tubular *PBR* design. To prevent oxygen accumulation, liquid velocity and tube length are to be maintained within an appropriate range. Longer tubes and lower liquid velocity may, however, lead to a significant decrease in the energy requirement per kg of biomass produced. According to our projections, increasing the length of tubes in the mixotrophic culture of *C. sorokiniana* from 250 to 500 m, the energy consumption would be reduced from 1.9 to 1.1 KWh·Kg^{-1}. Alternatively, by reducing liquid velocity from 0.45 to 0.2 m·s^{-1} the energy consumption could be reduced from 1.9 to 0.9 KWh·Kg^{-1}. Combining these two strategies, energy consumption could drop to 0.5 KWh·Kg^{-1}. Energy consumption accounts for approximately 10% of the total production costs, therefore lowering energy consumption further would only have a minimal effect on the final production costs (-0.17 €·Kg^{-1}). However, the effect of longer tubes and lower liquid velocity would also reduce the major equipment costs (e.g. reduction on the number of circulation pumps) and save another 0.18 €·Kg^{-1}, leading to a final biomass production cost of 2.25 € Kg^{-1}.

Reducing the consumption of energy will have beneficial effects on the overall sustainability of the process. In 2016, in the EU 0.3 Kg of CO_2 were emitted per KWh^{-1} of electricity produced (www.eea.europa.eu). Lowering the electricity consumption from 1.9 to 0.5 $KWh \cdot Kg^{-1}$ would therefore save 0.42 Kg of CO_2 per Kg of biomass. Moreover, a reduction in electricity consumption is of primary importance envisioning future applications of oxygen balanced mixotrophy for bioenergy production.

Contamination of algal cultures

One of the major challenges of mixotrophic outdoor cultivation is the undesired contamination by heterotrophic microorganisms, mainly bacteria and fungi (Unnithan et al., 2014), which compete with microalgae for the assimilation of organic carbon. Bacteria have a growth rate an order of magnitude higher than microalgae and they can easily outcompete microalgae for organic carbon uptake. However, since the beginning of commercial *Chlorella* production in 1964, the pioneers already replaced CO_2 by acetic acid in open ponds (Iwamoto, 2004), leading to a very low bacterial contamination of the culture. The fraction of bacterial contaminant was then separated from *Chlorella* cells by centrifugation and further washing of the concentrated algae slurry with water. A similar approach has been recently embraced by Heliae Development LLC (Ganuza & Tonkovich, 2016).

Deschênes et al. (2015) proposed to prevent the simultaneous presence of nitrogen and organic carbon in the culture medium as a solution to limit bacteria contamination. The main idea behind this cultivation strategy is that microalgae can grow when either nitrogen or organic carbon are not present in the culture medium by consuming the internal quota of nitrogen and by photosynthesis, respectively, whereas most bacteria can grow only if all nutrients are simultaneously present in the culture medium. A similar strategy has been successfully adopted for microalgae heterotrophic growth in non-axenic condition (Di Caprio et al., 2019).

We believe that it might be technically feasible to run a closed photobioreactor, without aeration, with minimal infection risk, and that contaminations can be further controlled by employing one of the strategies mentioned above. We recognize, however, that controlling the bacterial population in large scale production and long- term operation might be challenging and requires further evaluation. It seems likely that a mixotrophic culture requires more frequent cleaning than an autotrophic culture, and this might have an impact on the economics of the process (e.g. less days of operation and/or higher reactor capacity needed for inoculum production).

Envisioning contaminations as a possible bottleneck of mixotrophy, we tested oxygen balanced mixotrophy on *G. sulphuraria* (chapter 4 and 5), the most studied acidophilic microalga. Even after 42 days of continuous operation we did not observe any contamination in our closed photobioreactor (*PBR*) (chapter 4). Previous studies demonstrated that low pH reduced the initial bacterial population by 98% and resulted in complete removal of pathogens when *G. sulphuraria* was cultivated in unsterilized primary effluent at pH 2 (Delanka-Pedige, 2018). We think it is realistic to assume that a closed photobioreactor in which all the inputs and outputs are filter sterilized, and which is operated a low pH, will not suffer from contaminations.

CONCLUSIONS

We have shown that oxygen balanced mixotrophy is a promising strategy for decreasing microalgal production costs. Our projections indicate mixotrophic cultivation of *C. sorokiniana* will half the autotrophic production cost. Such a price reduction is mainly related to the doubling of biomass productivity under mixotrophy. For *G. sulphuraria*, due to the expected low efficiency of CO_2 uptake, and due to the doubling of biomass productivity, the mixotrophic production costs are three times cheaper than autotrophic cultivation.

Microalgal protein yield per hectare is 30-60 times higher than for soy beans. A closer look at the water requirements reveals a 25-50 times smaller water footprint for microalgae. However, if glucose is used as a substrate for mixotrophic cultivation, the land and water consumption of sugar beet production substantially increases the overall water and land usage. Nevertheless, protein production by mixotrophic cultivation of microalgae remains 4 times more productive and requires 7 times less water than soy bean cultivation.

The choice of organic substrate is of great significance regarding the land and water footprints of the mixotrophic process. Usage of agro-industrial side streams rich in organic compounds is advisable for sustainable production. Furthermore, fresh water consumption could be completely avoided by using sea- or brackish water. Our projections indicate that oxygen balanced mixotrophy performed at a high photosynthetic efficiency, combined with the use of agro-industrial side streams as substrate, could make protein production from microalgae economically attractive and a sustainable alternative to soy beans.

SUPPORTING INFORMATION

Supporting information 1: Dilution rate in autotrophic and mixotrophic cultivation of G. sulphuraria

The dilution rate of *G. sulphuraria* was calculated such that the estimated biomass concentration (C_x, $g_x \cdot L^{-1}$) resulted in a specific photon supply rate (q_{ph}, $\mu molph \cdot g^{-1} \cdot s^{-1}$) within the optimal of range (chapter 4).

The daytime average light irradiation on the horizontal surface in December, the month with the lower irradiation ($I_{0,min}$, $\mu mol \cdot m^{-2} \cdot s^{-1}$) and July, the month with the highest irradiation ($I_{0,max}$), were used to calculate the range of biomass areal concentration for which q_{ph}. was in the optimal range:

$$A_x = \frac{q_{ph}}{I_{0,(min,max)}}$$

Where A_x is the areal biomass concentration ($g_x \cdot m^{-2}$), while $I_{o,(min,\ max)}$ are the daily average *PAR* light irradiation on the horizontal surface ($\mu mol_{ph} \cdot m^{-2} \cdot s^{-1}$) in December (min) and July (max). We estimated that by using an A_x between 74 and 108 $g \cdot m^{-2}$ in the autotrophic culture and between 148 and 216 $g \cdot m^{-2}$ in the mixotrophic culture, q_{ph} will be maintained within optimal range all over the year. Finally we divided the expected biomass volumetric productivity by the volumetric biomass concentration to obtain the daily dilution rate. This resulted in a dilution rate of 13.5% per day.

Supporting information 2: Major equipment used in the tecno-economic model.

Autotrophic cultivation of *Chlorella sorokiniana*.

N° in scheme	*Detail*	*Capacity(max)*		*€·unit^{-1}*	*Units*	*Total Cost (€)*	*Power cons. (kWh/Yr)*
1	Fresh water pump	200	$m^3 \cdot h^{-1}$	1.4E+04	5	6.8E+04	1.2.E+05
4	Sterilization	59.9	$m^3 \cdot h^{-1}$	1.4E+05	17	2.3E+06	0.0.E+00
3	Mixing unit	25	m^3	2.9E+05	1.0	2.9E+05	1.8.E+04
7	Culture circulation pump	28000	$m^3 \cdot h^{-1}$	6.0E+05	17	1.0E+07	2.7.E+07
5	CO_2 Supply Unit	5437	$€ \cdot ha^{-1}$	5.4E+03	100	5.4E+05	
7	Air blower (degasser)	2499	$m^3 \cdot h^{-1}$	1.1E+04	260.0	2.9E+06	4.4E+06
10	Harvest Pump	200	$m^3 \cdot h^{-1}$	1.4E+04	3	4.1E+04	1.2E+5
14	Heat exchanger					9.4E+05	
8	Degasser	6.6	m^3	2.5E+03	970	2.4E+06	
	Structure (Stand for the tubes)	336283	m	4.1E+00		1.4E+06	
	Pipe (cooling water)					1.6E+06	
13	Pump (cooling)	28000	$m^3 \cdot h^{-1}$	6.0E+05	1.0	6.0E+05	5.2E+04
	Head losses						2.4E+06
	Total					2.3E+07	3.3E+7
11	Microfiltration	18353	m^2	82 ($€ \cdot m^{-2}$)	1	1.5E+06	1.4E+6
12	Centrifugation	65	$m^3 \cdot h^{-1}$	3.0E+5	1	3.0E+5	3.7E+5
	Total harvesting					1.8E+6	1.8E+6
	Total					2.5E+07	2.3E+7

Oxygen balanced mixotrophic cultivation of *Chlorella sorokiniana*.

N° in scheme	*Detail*	*Capacity(max)*		*€·unit^{-1}*	*Units*	*Total Cost (€)*	*Power cons. (kWh/Yr)*
1	Fresh water pump	200	$m^3 \cdot h^{-1}$	1.4E+04	5	6.8E+04	1.2.E+05
4	Sterilization	59.9	$m^3 \cdot h^{-1}$	1.4E+05	17	2.3E+06	0.0.E+00
3	Mixing unit	25	m^3	2.9E+05	1	3.5E+05	1.8.E+04
9	Culture circulation pump	28000	$m^3 \cdot h^{-1}$	6.0E+05	11	6.6E+06	1.8.E+07
7	Air blower (night aeration)	200	$m^3 \cdot h^{-1}$	3.0E+03	8.0	8.9E+04	3.2E+05
10	Harvest Pump	200	$m^3 \cdot h^{-1}$	1.4E+04	3	4.1E+04	1.2E+5
14	Heat exchanger					9.4E+05	
	Structure (Stand for the tubes)	336283	m	4.1E+00		1.4E+06	
	Pipe (cooling water)					1.6E+06	
13	Pump (cooling)	28000	$m^3 \cdot h^{-1}$	6.0E+05	1	6.0E+05	1.2E+05
5	Tank for glucose storage	112	m^3	1.4E+05		1.4E+05	
8	Air collection vessel			1.9E+00	56637	1.1E+05	
	Head losses						2.4E+06
	Total production					1.4E+07	2.1E+7
11	Microfiltration	18353	m^2	82 ($€ \cdot m^{-2}$)	1	1.5E+06	1.4E+6
12	Centrifugation	65	$m^3 \cdot h^{-1}$	3.0E+5	2	6.0E+5	7.4E+5
	Total harvesting					2.1E+6	2.2E+6
	Total					1.6E+07	2.3E+7

Autotrophic cultivation of *Galdieria sulphuraria*.

N° in scheme	*Detail*	*Capacity(max)*		*€·unit^{-1}*	*Units*	*Total Cost (€)*	*Power cons. (kWh/Yr)*
1	Fresh water pump	200	$m^3 \cdot h^{-1}$	1.4E+04	5	4.1E+04	6.2.E+04
4	Sterilization	59.9	$m^3 \cdot h^{-1}$	1.4E+05	17	1.2E+06	0.0.E+00
3	Mixing unit	25	m^3	2.9E+05	1.0	2.4E+05	9.1.E+03
7	Culture circulation pump	28000	$m^3 \cdot h^{-1}$	6.0E+05	11	6.6E+06	1.8.E+07
5	CO_2 Supply Unit	5437	$€ \cdot ha^{-1}$	5.4E+03	100	5.4E+05	
7	Air blower (degasser)	200	$m^3 \cdot h^{-1}$	3.0E+03	94.0	1.5E+06	2.3E+06
10	Harvest Pump	200	$m^3 \cdot h^{-1}$	1.4E+04	3	2.7E+04	6.2E+6
14	Heat exchanger					9.4E+05	
8	Degasser	6.6	m^3	2.5E+03	1939	1.2E+06	
	Structure (Stand for the tubes)	336283	m	4.1E+00		1.4E+06	
	Pipe (cooling water)					1.6E+06	
13	Pump (cooling)	28000	$m^3 \cdot h^{-1}$	6.0E+05	1.0	6.0E+05	1.2E+05
	Head losses					1.6E+07	2.4E+06
	Total production					4.1E+04	2.3E+7
11	Microfiltration	943	m^2	82 ($€ \cdot m^{-2}$)	1	7.7E+04	7.3E+4
12	Centrifugation	65	$m^3 \cdot h^{-1}$	3.0E+5	1	3.0E+5	1.8E+5
	Total harvesting					1.1E+6	0.9E+6
	Total					1.7E+07	2.4E+7

Oxygen balanced mixotrophic cultivation of *Galdieria sulphuraria*.

N° in scheme	*Detail*	*Capacity(max)*		*€·unit^{-1}*	*Units*	*Total Cost (€)*	*Power cons. (kWh/Yr)*
1	Fresh water pump	200	$m^3 \cdot h^{-1}$	1.4E+04	3	4.1E+04	6.2.E+04
4	Sterilization	59.9	$m^3 \cdot h^{-1}$	1.4E+05	9	1.2E+06	0.0.E+00
3	Mixing unit	8	m^3	2.4E+05	1	2.9E+05	9.1.E+03
9	Culture circulation pump	28000	$m^3 \cdot h^{-1}$	6.0E+05	11	6.6E+06	1.8.E+07
7	Air blower (night aeration)	2499	$m^3 \cdot h^{-1}$	1.1E+04	8	8.9E+04	3.2E+05
10	Harvest Pump	200	$m^3 \cdot h^{-1}$	1.4E+04	2	2.7E+04	6.2E+4
14	Heat exchanger					9.4E+05	
	Structure (Stand for the tubes)	336283	m	4.1E+00		1.4E+06	
	Pipe (cooling water)					1.6E+06	
13	Pump (cooling)	28000	$m^3 \cdot h^{-1}$	6.0E+05	1	6.0E+05	5.2E+4
5	Tank for glucose storage	56	m^3	7.6E+04		7.6E+04	
8	Air collection vessel	200		1.9E+00	56637	1.1E+05	
	Head losses						2.4E+06
	Total production					1.3E+07	2.1E+7
11	Microfiltration	1887	m^2	82 ($€ \cdot m^{-2}$)	1	1.5E+05	1.5E+5
12	Centrifugation	65	$m^3 \cdot h^{-1}$	3.0E+5	1	3.0E+5	3.7E+5
	Total harvesting					1.1E+6	1.1E+6
	Total					1.4E+07	2.1E+7

References

Abdelmoteleb, M., Zhang, C., Furey, B., Kozubal, M., Griffiths, H., Champeaud, M., Goodman, R.E. 2021. Evaluating potential risks of food allergy of novel food sources based on comparison of proteins predicted from genomes and compared to www.AllergenOnline.org. *Food and Chemical Toxicology*, **147**, 111888.

Abiusi, F., Wijffels, R.H., Janssen, M. 2020a. Doubling of Microalgae Productivity by Oxygen Balanced Mixotrophy. *ACS Sustainable Chemistry & Engineering*, **8**(15), 6065-6074.

Abiusi, F., Wijffels, R.H., Janssen, M. 2020b. Oxygen Balanced Mixotrophy under Day–Night Cycles. *ACS Sustainable Chemistry & Engineering*, **8**(31), 11682-11691.

Acién, F.G., Fernández, J.M., Magán, J.J., Molina, E. 2012. Production cost of a real microalgae production plant and strategies to reduce it. *Biotechnology Advances*, **30**(6), 1344-1353.

Albertano, P., Ciniglia, C., Pinto, G., Pollio, A. 2000. The taxonomic position of Cyanidium, Cyanidioschyzon and Galdieria: an update. *Hydrobiologia*, **433**(1), 137-143.

Amulya, K., Shikha, D., Venkata Mohan, S. 2016. Building a bio-based economy through waste remediation: innovation towards sustainable future. *Bioremediation and Bioeconomy*, 497-521.

Bailey, R.W., Staehelin, L.A. 1968. The Chemical Composition of Isolated Cell Walls of Cyanidium caldarium. *Microbiology*, **54**(2), 269-276.

Barros, A., Guerra, L.T., Simões, M., Santos, E., Fonseca, D., Silva, J., Costa, L., Navalho, J. 2017. Mass balance analysis of carbon and nitrogen in industrial scale mixotrophic microalgae cultures. *Algal Research*, **21**, 35-41.

Becker, E.W. 2007. Micro-algae as a source of protein. *Biotechnology Advances*, **25**(2), 207-210.

Becker, E.W. 2004. Microalgae in human and animal nutrition. in: *Handbook of microalgal culture: biotechnology and applied phycology*, (Ed.) R. A, Oxford: Blackwell Science, pp. 312-351.

Benvenuti, G., Lamers, P.P., Breuer, G., Bosma, R., Cerar, A., Wijffels, R.H., Barbosa, M.J. 2016. Microalgal TAG production strategies: why batch beats repeated-batch. *Biotechnology for Biofuels*, **9**(1), 64.

Blanken, W., Cuaresma, M., Wijffels, R.H., Janssen, M. 2013. Cultivation of microalgae on artificial light comes at a cost. *Algal Research*, **2**(4), 333-340.

Blanken, W., Magalhães, A., Sebestyén, P., Rinzema, A., Wijffels, R.H., Janssen, M. 2017. Microalgal biofilm growth under day-night cycles. *Algal Research*, **21**, 16-26.

Blanken, W., Postma, P.R., de Winter, L., Wijffels, R.H., Janssen, M. 2016. Predicting microalgae growth. *Algal Research*, **14**, 28-38.

Boelee, N.C., Janssen, M., Temmink, H., Shrestha, R., Buisman, C.J.N., Wijffels, R.H. 2014. Nutrient Removal and Biomass Production in an Outdoor Pilot-Scale Phototrophic Biofilm Reactor for Effluent Polishing. *Applied Biochemistry and Biotechnology*, **172**(1), 405-422.

Bosma, R., de Vree, J.H., Slegers, P.M., Janssen, M., Wijffels, R.H., Barbosa, M.J. 2014. Design and construction of the microalgal pilot facility AlgaePARC. *Algal Research*, **6**, 160-169.

Brock, T.D. 1978. Thermophilic Microorganisms and Life at High Temperatures, Springer, pp. 255-302.

Brown, M.R. 1991. The amino-acid and sugar composition of 16 species of microalgae used in mariculture. *Journal of Experimental Marine Biology and Ecology*, **145**(1), 79-99.

Cagnac, O., Richard, L., Labro, J. 2016. Novel Method for the culture of unicellular red algae. *WO 2017/050917 Al*.

Carbone, D.A., Olivieri, G., Pollio, A., Melkonian, M. 2020. Biomass and phycobiliprotein production of Galdieria sulphuraria, immobilized on a twin-layer porous substrate photobioreactor. *Applied Microbiology and Biotechnology*, **104**(7), 3109-3119.

Carfagna, S., Bottone, C., Cataletto, P.R., Petriccione, M., Pinto, G., Salbitani, G., Vona, V., Pollio, A., Ciniglia, C. 2016. Impact of Sulfur Starvation in Autotrophic and Heterotrophic Cultures of the Extremophilic Microalga Galdieria phlegrea (Cyanidiophyceae). *Plant and Cell Physiology*, **57**(9), 1890-1898.

Carfagna, S., Landi, V., Coraggio, F., Salbitani, G., Vona, V., Pinto, G., Pollio, A., Ciniglia, C. 2018. Different characteristics of C-phycocyanin (C-PC) in two strains of the extremophilic Galdieria phlegrea. *Algal Research*, **31**, 406-412.

Chandra, R., Rohit, M.V., Swamy, Y.V., Venkata Mohan, S. 2014. Regulatory function of organic carbon supplementation on biodiesel production during growth and nutrient stress phases of mixotrophic microalgae cultivation. *Bioresource Technology*, **165**, 279-287.

Chen, F., Johns, M.R. 1996. Heterotrophic growth of Chlamydomonas reinhardtii on acetate in chemostat culture. *Process Biochemistry*, **31**(6), 601-604.

Cheng, F., Mallick, K., Henkanatte Gedara, S.M., Jarvis, J.M., Schaub, T., Jena, U., Nirmalakhandan, N., Brewer, C.E. 2019. Hydrothermal liquefaction of Galdieria sulphuraria grown on municipal wastewater. *Bioresource Technology*, **292**, 121884.

Consejería-de-Agricultura-Pesca-y-Desarrollo-Rural-Junta-de-Andalucia. 2016. Resultados de la encuesta de precios de la tierra en Andalucía. https://www.juntadeandalucia.es/export/drupaljda/Encuesta_Precios_Tierra_Andaluc%C3%ADa_2016_v2.pdf.

Cornish, G., Bosworth, B., Perry, C., Burke, J.J. 2004. *Water charging in irrigated agriculture: An analysis of international experience*. Food & Agriculture Org.

Cuaresma, M. 2011. Cultivation of microalgae in a high irradiance area, Wageningen University & Research, pp. 102-113.

Cuaresma, M., Janssen, M., van den End, E.J., Vílchez, C., Wijffels, R.H. 2011a. Luminostat operation: A tool to maximize microalgae photosynthetic efficiency in photobioreactors during the daily light cycle? *Bioresource Technology*, **102**(17), 7871-7878.
Cuaresma, M., Janssen, M., Vílchez, C., Wijffels, R.H. 2011b. Horizontal or vertical photobioreactors? How to improve microalgae photosynthetic efficiency. *Bioresource Technology*, **102**(8), 5129-5137.
Cuaresma, M., Janssen, M., Vílchez, C., Wijffels, R.H. 2009. Productivity of Chlorella sorokiniana in a short light-path (SLP) panel photobioreactor under high irradiance. *Biotechnology and bioengineering*, **104**(2), 352-359.
Darwish, R., Gedi, M.A., Eakpetch, P., Assaye, H., Zaky, A.S., Gray, D.A. 2020. Chlamydomonas reinhardtii Is a Potential Food Supplement with the Capacity to Outperform Chlorella and Spirulina. *Applied Sciences*, **10**(19), 6736.
Day, L. 2013. Proteins from land plants – Potential resources for human nutrition and food security. *Trends in Food Science & Technology*, **32**(1), 25-42.
de Mooij, T., Janssen, M., Cerezo-Chinarro, O., Mussgnug, J.H., Kruse, O., Ballottari, M., Bassi, R., Bujaldon, S., Wollman, F.-A., Wijffels, R.H. 2015. Antenna size reduction as a strategy to increase biomass productivity: a great potential not yet realized. *Journal of Applied Phycology*, **27**(3), 1063-1077.
de Mooij, T., Nejad, Z.R., van Buren, L., Wijffels, R.H., Janssen, M. 2017. Effect of photoacclimation on microalgae mass culture productivity. *Algal Research*, **22**, 56-67.
de Vree, J.H., Bosma, R., Janssen, M., Barbosa, M.J., Wijffels, R.H. 2015. Comparison of four outdoor pilot-scale photobioreactors. *Biotechnology for Biofuels*, **8**(1), 215.
de Winter, L., Cabanelas, I.T.D., Martens, D.E., Wijffels, R.H., Barbosa, M.J. 2017a. The influence of day/night cycles on biomass yield and composition of Neochloris oleoabundans. *Biotechnology for Biofuels*, **10**(1), 104.
de Winter, L., Cabanelas, I.T.D., Órfão, A.N., Vaessen, E., Martens, D.E., Wijffels, R.H., Barbosa, M.J. 2017b. The influence of day length on circadian rhythms of Neochloris oleoabundans. *Algal Research*, **22**, 31-38.
Delanka-Pedige, H.M. 2018. Algal-based wastewater treatment: assessment of pathogen removal and bacterial community profile of effluent, New Mexico State University.
Deschênes, J.-S., Boudreau, A., Tremblay, R. 2015. Mixotrophic production of microalgae in pilot-scale photobioreactors: Practicability and process considerations. *Algal Research*, **10**, 80-86.
Di Caprio, F., Altimari, P., Iaquaniello, G., Toro, L., Pagnanelli, F. 2019. Heterotrophic cultivation of T. obliquus under non-axenic conditions by uncoupled supply of nitrogen and glucose. *Biochemical Engineering Journal*, **145**, 127-136.
Doucha, J., Lívanský, K. 2006. Productivity, CO2/O2 exchange and hydraulics in outdoor open high density microalgal (Chlorella sp.) photobioreactors operated in a Middle and Southern European climate. *Journal of Applied Phycology*, **18**(6), 811-826.
Doucha, J., Straka, F., Lívanský, K. 2005. Utilization of flue gas for cultivation of microalgae Chlorella sp.) in an outdoor open thin-layer photobioreactor. *Journal of Applied Phycology*, **17**(5), 403-412.
Draaisma, R.B., Wijffels, R.H., Slegers, P.M., Brentner, L.B., Roy, A., Barbosa, M.J. 2013. Food commodities from microalgae. *Current Opinion in Biotechnology*, **24**(2), 169-177.
Dubinsky, Z., Stambler, N. 2009. Photoacclimation processes in phytoplankton: mechanisms, consequences, and applications. *Aquatic Microbial Ecology*, **56**(2-3), 163-176.
Edmundson, S.J., Huesemann, M.H. 2015. The dark side of algae cultivation: Characterizing night biomass loss in three photosynthetic algae, Chlorella sorokiniana, Nannochloropsis salina and Picochlorum sp. *Algal Research*, **12**, 470-476.
European-Commission. 2020. COMMODITY PRICE DASHBOARD. No 100 https://ec.europa.eu/info/sites/info/files/food-farming-fisheries/farming/documents/commodity-price-dashboard_092020_en.pdf.
European-Commission. 2013. Guidance Notes on the Classification of Food Extracts with Colouring Properties.
European-Soy-Monitor. 2017. Insights on the European supply chain and the use of responsible and deforestation-free soy in 2017. https://www.idhsustainabletrade.com/uploaded/2019/04/European-Soy-Monitor.pdf.
Evers, E.G. 1991. A model for light-limited continuous cultures: Growth, shading, and maintenance. *Biotechnology and Bioengineering*, **38**(3), 254-259.
Field-to-Market. 2016. Environmental and Socioeconomic Indicators for Measuring Outcomes of On-Farm Agricultural Production in the United States. http://fieldtomarket.org/media/2016/12/Field-to-Market_2016-National-Indicators-Report.pdf.
Flynn, K.J., Flynn, K. 1992. Non-protein free amines in microalgae: consequences for the measurement of intracellular amino acids and of the glutamine/glutamate ratio. *Marine ecology progress series. Oldendorf*, **89**(1), 73-79.
Ganuza, E., Licamele, J.D., Tonkovich, A.L., Bellefeuille, M.V., Wyatt, C., Kulaga, T.J., Galvez II, A. 2015. Balanced mixotrophy methods, US Patents 20150240199A1.
Ganuza, E., Tonkovich, A.L. 2016. Heliae Development, LLC: An Industrial Approach to Mixotrophy in Microalgae. in: *Industrial Biorenewables*, pp. 323-339.
Gao, F., Teles, I., Wijffels, R.H., Barbosa, M.J. 2020. Process optimization of fucoxanthin production with Tisochrysis lutea. *Bioresource Technology*, **315**, 123894.
García, J.L., de Vicente, M., Galán, B. 2017. Microalgae, old sustainable food and fashion nutraceuticals. *Microbial Biotechnology*, **10**(5), 1017-1024.
Godfray, H.C.J., Beddington, J.R., Crute, I.R., Haddad, L., Lawrence, D., Muir, J.F., Pretty, J., Robinson, S., Thomas, S.M., Toulmin, C. 2010. Food Security: The Challenge of Feeding 9 Billion People. *Science*, **327**(5967), 812-818.

Gong, M., Li, X., Bassi, A. 2018. Investigation of simultaneous lutein and lipid extraction from wet microalgae using Nile Red as solvatochromic shift probe. *Journal of Applied Phycology*, **30**(3), 1617-1627.
González López, C.V., García, M.d.C.C., Fernández, F.G.A., Bustos, C.S., Chisti, Y., Sevilla, J.M.F. 2010. Protein measurements of microalgal and cyanobacterial biomass. *Bioresource Technology*, **101**(19), 7587-7591.
Grama, B.S., Agathos, S.N., Jeffryes, C.S. 2016. Balancing photosynthesis and respiration increases microalgal biomass productivity during photoheterotrophy on glycerol. *ACS Sustainable Chemistry & Engineering*, **4**(3), 1611-1618.
Graverholt, O.S., Eriksen, N.T. 2007. Heterotrophic high-cell-density fed-batch and continuous-flow cultures of Galdieria sulphuraria and production of phycocyanin. *Applied Microbiology and Biotechnology*, **77**(1), 69-75.
Graziani, G., Schiavo, S., Nicolai, M.A., Buono, S., Fogliano, V., Pinto, G., Pollio, A. 2013. Microalgae as human food: chemical and nutritional characteristics of the thermo-acidophilic microalga Galdieria sulphuraria. *Food & function*, **4**(1), 144-152.
Gross, W., Schnarrenberger, C. 1995. Heterotrophic growth of two strains of the acido-thermophilic red alga Galdieria sulphuraria. *Plant and Cell Physiology*, **36**(4), 633-638.
Guccione, A., Biondi, N., Sampietro, G., Rodolfi, L., Bassi, N., Tredici, M.R. 2014. Chlorella for protein and biofuels: from strain selection to outdoor cultivation in a Green Wall Panel photobioreactor. *Biotechnology for Biofuels*, **7**(1), 84.
Hadj-Romdhane, F., Zheng, X., Jaouen, P., Pruvost, J., Grizeau, D., Croué, J.P., Bourseau, P. 2013. The culture of Chlorella vulgaris in a recycled supernatant: Effects on biomass production and medium quality. *Bioresource Technology*, **132**, 285-292.
Hanse, B., Tijink, F.G.J., Maassen, J., van Swaaij, N. 2018. Closing the Yield Gap of Sugar Beet in the Netherlands—A Joint Effort. *Frontiers in Plant Science*, **9**(184).
Heijnen, S.J. 1994. Thermodynamics of microbial growth and its implications for process design. *Trends in Biotechnology*, **12**(12), 483-492.
Henkanatte-Gedera, S.M., Selvaratnam, T., Karbakhshravari, M., Myint, M., Nirmalakhandan, N., Van Voorhies, W., Lammers, P.J. 2017. Removal of dissolved organic carbon and nutrients from urban wastewaters by Galdieria sulphuraria: Laboratory to field scale demonstration. *Algal Research*, **24**, 450-456.
Hirooka, S., Miyagishima, S.-y. 2016. Cultivation of Acidophilic Algae Galdieria sulphuraria and Pseudochlorella sp. YKT1 in Media Derived from Acidic Hot Springs. *Frontiers in Microbiology*, **7**(2022).
Hoffmann, C.M., Kenter, C. 2018. Yield Potential of Sugar Beet – Have We Hit the Ceiling? *Frontiers in Plant Science*, **9**(289).
Hughes, G.J., Ryan, D.J., Mukherjea, R., Schasteen, C.S. 2011. Protein Digestibility-Corrected Amino Acid Scores (PDCAAS) for Soy Protein Isolates and Concentrate: Criteria for Evaluation. *Journal of Agricultural and Food Chemistry*, **59**(23), 12707-12712.
ISO. 2005. Animal feeding stuffs — Determination of amino acids content (ISO 13903:2005). https://www.iso.org/standard/37258.html.
ISO. 2016. Animal feeding stuffs — Determination of tryptophan content (ISO 13904:2016). https://www.iso.org/standard/59955.html.
Iwamoto, H. 2004. 11 Industrial Production of Microalgal Cell-mass and Secondary Products–Major Industrial Species. *Handbook of microalgal culture: biotechnology and applied phycology*, 255-263.
James, C., Al-Hinty, S., Salman, A. 1989. Growth and ω3 fatty acid and amino acid composition of microalgae under different temperature regimes. *Aquaculture*, **77**(4), 337-351.
Jin, H., Zhang, H., Zhou, Z., Li, K., Hou, G., Xu, Q., Chuai, W., Zhang, C., Han, D., Hu, Q. 2020. Ultrahigh-cell-density heterotrophic cultivation of the unicellular green microalga Scenedesmus acuminatus and application of the cells to photoautotrophic culture enhance biomass and lipid production. *Biotechnology and Bioengineering*, **117**(1), 96-108.
Kamiya, A., Kowallik, W. 1987a. The inhibitory effect of light on proton-coupled hexose uptake in Chlorella. *Plant and cell physiology*, **28**(4), 621-625.
Kamiya, A., Kowallik, W. 1987b. Photoinhibition of glucose uptake in Chlorella. *Plant and cell physiology*, **28**(4), 611-619.
Kazbar, A., Cogne, G., Urbain, B., Marec, H., Le-Gouic, B., Tallec, J., Takache, H., Ismail, A., Pruvost, J. 2019. Effect of dissolved oxygen concentration on microalgal culture in photobioreactors. *Algal Research*, **39**, 101432.
Kent, M., Welladsen, H.M., Mangott, A., Li, Y. 2015. Nutritional evaluation of Australian microalgae as potential human health supplements. *PloS one*, **10**(2), e0118985.
Kim, G.-Y., Roh, K., Han, J.-I. 2019. The use of bicarbonate for microalgae cultivation and its carbon footprint analysis. *Green Chem*, **21**(18), 5053-5062.
Kliphuis, A.M.J., Janssen, M., van den End, E.J., Martens, D.E., Wijffels, R.H. 2011. Light respiration in Chlorella sorokiniana. *Journal of applied phycology*, **23**(6), 935-947.
Kliphuis, A.M.J., Klok, A.J., Martens, D.E., Lamers, P.P., Janssen, M., Wijffels, R.H. 2012. Metabolic modeling of Chlamydomonas reinhardtii: energy requirements for photoautotrophic growth and maintenance. *Journal of Applied Phycology*, **24**(2), 253-266.
Krishnan, H.B., Jez, J.M. 2018a. The promise and limits for enhancing sulfur-containing amino acid content of soybean seed. *Plant Science*, **272**, 14-21.
Krishnan, H.B., Jez, J.M. 2018b. Review: The promise and limits for enhancing sulfur-containing amino acid content of soybean seed. *Plant Science*, **272**, 14-21.
Kumar, K., Dasgupta, C.N., Das, D. 2014. Cell growth kinetics of Chlorella sorokiniana and nutritional values of its biomass. *Bioresource Technology*, **167**, 358-366.
Kursar, T.A., Alberte, R.S. 1983. Photosynthetic Unit Organization in a Red Alga : Relationships between Light-Harvesting Pigments and Reaction Centers. *Plant physiology*, **72**(2), 409-414.

Langley, N.M., Harrison, S.T.L., van Hille, R.P. 2012. A critical evaluation of CO2 supplementation to algal systems by direct injection. *Biochemical Engineering Journal*, **68**, 70-75.
Lee, Y.-K. 2001. Microalgal mass culture systems and methods: Their limitation and potential. *Journal of Applied Phycology*, **13**(4), 307-315.
León-Saiki, G.M., Remmers, I.M., Martens, D.E., Lamers, P.P., Wijffels, R.H., van der Veen, D. 2017. The role of starch as transient energy buffer in synchronized microalgal growth in Acutodesmus obliquus. *Algal Research*, **25**, 160-167.
León-Vaz, A., León, R., Díaz-Santos, E., Vigara, J., Raposo, S. 2019. Using agro-industrial wastes for mixotrophic growth and lipids production by the green microalga Chlorella sorokiniana. *New Biotechnology*, **51**, 31-38.
Li, T., Zheng, Y., Yu, L., Chen, S. 2014. Mixotrophic cultivation of a Chlorella sorokiniana strain for enhanced biomass and lipid production. *Biomass and Bioenergy*, **66**, 204-213.
Lin, T.-S., Wu, J.-Y. 2015. Effect of carbon sources on growth and lipid accumulation of newly isolated microalgae cultured under mixotrophic condition. *Bioresource Technology*, **184**, 100-107.
Llames, C.R., Fontaine, J. 1994. Determination of amino acids in feeds: collaborative study. *Journal of AOAC International*, **77**(6), 1362-1402.
Lourenço, S.O., Barbarino, E., Lavín, P.L., Lanfer Marquez, U.M., Aidar, E. 2004. Distribution of intracellular nitrogen in marine microalgae: calculation of new nitrogen-to-protein conversion factors. *European Journal of Phycology*, **39**(1), 17-32.
Lu, Z., Loftus, S., Sha, J., Wang, W., Park, M.S., Zhang, X., Johnson, Z.I., Hu, Q. 2020. Water reuse for sustainable microalgae cultivation: current knowledge and future directions. *Resources, Conservation and Recycling*, **161**, 104975.
Lupatini, A.L., Colla, L.M., Canan, C., Colla, E. 2017. Potential application of microalga Spirulina platensis as a protein source. *Journal of the Science of Food and Agriculture*, **97**(3), 724-732.
Mandalam, R.K., Palsson, B. 1998. Elemental balancing of biomass and medium composition enhances growth capacity in high-density Chlorella vulgaris cultures. *Biotechnology and Bioengineering*, **59**(5), 605-611.
Martínez, F., Orús, M.I. 1991. Interactions between glucose and inorganic carbon metabolism in Chlorella vulgaris strain UAM 101. *Plant physiology*, **95**(4), 1150-1155.
Massa, M., Buono, S., Langellotti, A.L., Martello, A., Russo, G.L., Troise, D.A., Sacchi, R., Vitaglione, P., Fogliano, V. 2019. Biochemical composition and in vitro digestibility of Galdieria sulphuraria grown on spent cherry-brine liquid. *New Biotechnology*, **53**, 9-15.
Michels, M.H.A., Camacho-Rodríguez, J., Vermuë, M.H., Wijffels, R.H. 2014. Effect of cooling in the night on the productivity and biochemical composition of Tetraselmis suecica. *Algal Research*, **6**, 145-151.
Mišurcová, L., Buňka, F., Vávra Ambrožová, J., Machů, L., Samek, D., Kráčmar, S. 2014. Amino acid composition of algal products and its contribution to RDI. *Food Chemistry*, **151**, 120-125.
Modeste, V., Brient, A., Thirion-Delalande, C., Forster, R., Aguenou, C., Griffiths, H., Cagnac, O. 2019. Safety evaluation of Galdieria high-protein microalgal biomass. *Toxicology Research and Application*, **3**, 2397847319879277.
Molina Grima, E., Belarbi, E.H., Acién Fernández, F.G., Robles Medina, A., Chisti, Y. 2003. Recovery of microalgal biomass and metabolites: process options and economics. *Biotechnology Advances*, **20**(7), 491-515.
Moncada, J., Tamayo, J.A., Cardona, C.A. 2014. Integrating first, second, and third generation biorefineries: Incorporating microalgae into the sugarcane biorefinery. *Chemical Engineering Science*, **118**, 126-140.
Moon, M., Mishra, S.K., Kim, C.W., Suh, W.I., Park, M.S., Yang, J.-W. 2014. Isolation and characterization of thermostable phycocyanin from Galdieria sulphuraria. *Korean Journal of Chemical Engineering*, **31**(3), 490-495.
Moraes, L., Rosa, G.M., Cara, I.M., Santos, L.O., Morais, M.G., Grima, E.M., Costa, J.A.V., Fernández, F.G.A. 2020. Bioprocess strategies for enhancing the outdoor production of Nannochloropsis gaditana: an evaluation of the effects of pH on culture performance in tubular photobioreactors. *Bioprocess and Biosystems Engineering*, **43**(10), 1823-1832.
Mouritsen, O.G., Duelund, L., Petersen, M.A., Hartmann, A.L., Frøst, M.B. 2019. Umami taste, free amino acid composition, and volatile compounds of brown seaweeds. *Journal of Applied Phycology*, **31**(2), 1213-1232.
Mozaffari, K., Seger, M., Dungan, B., Hanson, D.T., Lammers, P.J., Holguin, F.O. 2019. Alterations in photosynthesis and energy reserves in Galdieria sulphuraria during corn stover hydrolysate supplementation. *Bioresource Technology Reports*, **7**, 100269.
Muys, M., Sui, Y., Schwaiger, B., Lesueur, C., Vandenheuvel, D., Vermeir, P., Vlaeminck, S.E. 2019. High variability in nutritional value and safety of commercially available Chlorella and Spirulina biomass indicates the need for smart production strategies. *Bioresource Technology*, **275**, 247-257.
Myers, J., Graham, J.-R. 1971. The Photosynthetic Unit in Chlorella Measured by Repetitive Short Flashes *Plant Physiology*, **48**(3), 282.
NOAA. 2015. https://www.nodc.noaa.gov/, Vol. 2020.
Norsker, N.H., Michiels, M., Slegers, P.M., Swinkels, G.L.A.M., Barbosa, M.J., Wijffels, R.H. 2019. Productivity of Nannochloropsis oceanica in an industrial closely spaced flat panel photobioreactor. *Algal Research*, **43**, 101632.
Oesterhelt, C., Schmälzlin, E., Schmitt, J.M., Lokstein, H. 2007. Regulation of photosynthesis in the unicellular acidophilic red alga Galdieria sulphuraria†. *The Plant Journal*, **51**(3), 500-511.
Oesterhelt, C., Vogelbein, S., Shrestha, R., Stanke, M., Weber, A. 2008. The genome of the thermoacidophilic red microalga Galdieria sulphuraria encodes a small family of secreted class III peroxidases that might be involved in cell wall modification. *Planta*, **227**(2), 353-362.
Ogawa, T., Aiba, S. 1981. Bioenergetic analysis of mixotrophic growth in Chlorella vulgaris and Scenedesmus acutus. *Biotechnology and Bioengineering*, **23**(5), 1121-1132.

Ogbonna, J.C., Tanaka, H. 1996. Night biomass loss and changes in biochemical composition of cells during light/dark cyclic culture of Chlorella pyrenoidosa. *Journal of Fermentation and Bioengineering*, **82**(6), 558-564.

Oostlander, P.C., van Houcke, J., Wijffels, R.H., Barbosa, M.J. 2020. Optimization of Rhodomonas sp. under continuous cultivation for industrial applications in aquaculture. *Algal Research*, **47**, 101889.

Ott, F.D., Seckbach, J. 1994. A review on the taxonomic position of the algal genus Cyanidium Geitler 1933 and its ecological cohorts Galdieria Merola in Merola et al. 1981 and Cyanidioschyzon De Luca, Taddei and Varano 1978. in: *Evolutionary Pathways and Enigmatic Algae: Cyanidium caldarium (Rhodophyta) and Related Cells*, (Ed.) J. Seckbach, Springer Netherlands. Dordrecht, pp. 113-132.

Pagels, F., Guedes, A.C., Amaro, H.M., Kijjoa, A., Vasconcelos, V. 2019. Phycobiliproteins from cyanobacteria: Chemistry and biotechnological applications. *Biotechnology Advances*, **37**(3), 422-443.

Panaite, C., Dragatoiu, D., Marti, R., Panaite, T. 2015. Use of high-fibre feedstuffs in pullet diets starting with the starter stage. *Archiva Zootechnica*, **18**(1), 53.

Pinto, G., Ciniglia, C., Cascone, C., Pollio, A. 2007. *Species composition of cyanidiales assemblages in Pisciarelli (Campi Flegrei, Italy) and description of Galdieria Phlegrea sp. nov.*

Pirt, S.J., Hinshelwood, C.N. 1965. The maintenance energy of bacteria in growing cultures. *Proceedings of the Royal Society of London. Series B. Biological Sciences*, **163**(991), 224-231.

Post, A.F., Eijgenraam, F., Mur, L.R. 1985. Influence of light period length on photosynthesis and synchronous growth of the green alga Scenedesmus protuberans. *British Phycological Journal*, **20**(4), 391-397.

Reddy, A., Norris, D.F., Momeni, S.S., Waldo, B., Ruby, J.D. 2016. The pH of beverages in the United States. *The Journal of the American Dental Association*, **147**(4), 255-263.

Regulation(EC). 2008. No 333/2008 of the European Parliament and of the Council of 16 December 2008 on food additives. Official Journal of the European Union EN-6.11.2014-021.001.

Rodolfi, L., Zittelli, G.C., Bassi, N., Padovani, G., Biondi, N., Bonini, G., Tredici, M.R. 2009. Microalgae for Oil: Strain Selection, Induction of Lipid Synthesis and Outdoor Mass Cultivation in a Low-Cost Photobioreactor. *Biotechnology and Bioengineering*, **102**(1), 100-112.

Rubio, F.C., Fernández, F.G.A., Pérez, J.A.S., Camacho, F.G., Grima, E.M. 1999. Prediction of dissolved oxygen and carbon dioxide concentration profiles in tubular photobioreactors for microalgal culture. *Biotechnology and Bioengineering*, **62**(1), 71-86.

Ruiz, J., Olivieri, G., de Vree, J., Bosma, R., Willems, P., Reith, J.H., Eppink, M.H.M., Kleinegris, D.M.M., Wijffels, R.H., Barbosa, M.J. 2016. Towards industrial products from microalgae. *Energy Environ. Sci.*, **9**(10), 3036-3043.

Sáez-Plaza, P., Michałowski, T., Navas, M.J., Asuero, A.G., Wybraniec, S. 2013. An Overview of the Kjeldahl Method of Nitrogen Determination. Part I. Early History, Chemistry of the Procedure, and Titrimetric Finish. *Critical Reviews in Analytical Chemistry*, **43**(4), 178-223.

Safi, C., Zebib, B., Merah, O., Pontalier, P.-Y., Vaca-Garcia, C. 2014. Morphology, composition, production, processing and applications of Chlorella vulgaris: A review. *Renewable and Sustainable Energy Reviews*, **35**, 265-278.

Salbitani, G., Cipolletta, S., Vona, V., Di Martino, C., Carfagna, S. 2020. Heterotrophic Cultures of Galdieria phlegrea Shift to Autotrophy in the Presence or Absence of Glycerol. *Journal of Plant Growth Regulation*.

Sánchez Mirón, A., García Camacho, F., Contreras Gómez, A., Grima, E.M., Chisti, Y. 2000. Bubble-column and airlift photobioreactors for algal culture. *AIChE Journal*, **46**(9), 1872-1887.

Sánchez Zurano, A., Gómez Serrano, C., Acién-Fernández, F.G., Fernández-Sevilla, J.M., Molina-Grima, E. Modeling of photosynthesis and respiration rate for microalgae–bacteria consortia. *Biotechnology and Bioengineering*, **n/a**(n/a).

Schmidt, R.A., Wiebe, M.G., Eriksen, N.T. 2005. Heterotrophic high cell-density fed-batch cultures of the phycocyanin-producing red alga Galdieria sulphuraria. *Biotechnology and Bioengineering*, **90**(1), 77-84.

Scholten, W. 2009. The water footprint of sugar and sugar-based ethanol.

Selvaratnam, T., Pegallapati, A.K., Montelya, F., Rodriguez, G., Nirmalakhandan, N., Van Voorhies, W., Lammers, P.J. 2014. Evaluation of a thermo-tolerant acidophilic alga, Galdieria sulphuraria, for nutrient removal from urban wastewaters. *Bioresource Technology*, **156**, 395-399.

Sentsova, O.Y. 1988. Physiological-biochemical characteristics of the acidothermophilic algae Cyanidium caldarium and Galdieria sulfuraria, and growth of the algae during combined cultivation under photoautotrophic, mixotrophic, and heterotrophic conditions. *Sov. Plant Physiol.*, **35**, 516-525.

Sforza, E., Pastore, M., Spagni, A., Bertucco, A. 2018. Microalgae-bacteria gas exchange in wastewater: how mixotrophy may reduce the oxygen supply for bacteria. *Environmental Science and Pollution Research*, **25**(28), 28004-28014.

Sili, C., Torzillo, G., Vonshak, A. 2012. Arthrospira (Spirulina). in: *Ecology of Cyanobacteria II: Their Diversity in Space and Time*, (Ed.) B.A. Whitton, Springer Netherlands. Dordrecht, pp. 677-705.

Sloth, J.K., Jensen, H.C., Pleissner, D., Eriksen, N.T. 2017. Growth and phycocyanin synthesis in the heterotrophic microalga Galdieria sulphuraria on substrates made of food waste from restaurants and bakeries. *Bioresource Technology*, **238**, 296-305.

Sloth, J.K., Wiebe, M.G., Eriksen, N.T. 2006. Accumulation of phycocyanin in heterotrophic and mixotrophic cultures of the acidophilic red alga Galdieria sulphuraria. *Enzyme and Microbial Technology*, **38**(1), 168-175.

Smith, R.T., Bangert, K., Wilkinson, S.J., Gilmour, D.J. 2015. Synergistic carbon metabolism in a fast growing mixotrophic freshwater microalgal species Micractinium inermum. *Biomass and Bioenergy*, **82**, 73-86.

Sousa, C., Compadre, A., Vermuë, M.H., Wijffels, R.H. 2013. Effect of oxygen at low and high light intensities on the growth of Neochloris oleoabundans. *Algal Research*, **2**(2), 122-126.

Spolaore, P., Joannis-Cassan, C., Duran, E., Isambert, A. 2006. Commercial applications of microalgae. *Journal of Bioscience and Bioengineering*, **101**(2), 87-96.
Stadnichuk, I.N., Rakhimberdieva, M.G., Bolychevtseva, Y.V., Yurina, N.P., Karapetyan, N.V., Selyakh, I.O. 1998. Inhibition by glucose of chlorophyll a and phycocyanobilin biosynthesis in the unicellular red alga Galdieria partita at the stage of coproporphyrinogen III formation. *Plant Science*, **136**(1), 11-23.
Starchenko, G., Grytsyk, A. 2017. Analysis of amino acid composition of Calluna vulgaris L.(Hull.). *The Pharma Innovation*, **6**(3, Part B), 88.
Strenkert, D., Schmollinger, S., Gallaher, S.D., Salomé, P.A., Purvine, S.O., Nicora, C.D., Mettler-Altmann, T., Soubeyrand, E., Weber, A.P.M., Lipton, M.S., Basset, G.J., Merchant, S.S. 2019. Multiomics resolution of molecular events during a day in the life of Chlamydomonas. *PNAS*, **116**(6), 2374-2383.
Sugai-Guérios, M.H., Mariano, A.B., Vargas, J.V.C., de Lima Luz Jr., L.F., Mitchell, D.A. 2014. Mathematical model of the CO2 solubilisation reaction rates developed for the study of photobioreactors. *The Canadian Journal of Chemical Engineering*, **92**(5), 787-795.
Sun, Y., Xu, Z., Zheng, Y., Zhou, J., Xiu, Z. 2019. Efficient production of lactic acid from sugarcane molasses by a newly microbial consortium CEE-DL15. *Process Biochemistry*, **81**, 132-138.
Sydney, E.B., Schafranski, K., Barretti, B.R.V., Sydney, A.C.N., Zimmerman, J.F.D., Cerri, M.L., Mottin Demiate, I. 2019. Biomolecules from extremophile microalgae: From genetics to bioprocessing of a new candidate for large-scale production. *Process Biochemistry*, **87**, 37-44.
Tevatia, R., Allen, J., Rudrappa, D., White, D., Clemente, T.E., Cerutti, H., Demirel, Y., Blum, P. 2015. The taurine biosynthetic pathway of microalgae. *Algal Research*, **9**, 21-26.
Tevatia, R., Payne, S., Allen, J., White, D., Clemente, T.E., Cerutti, H., Demirel, Y., Blum, P. 2019. A synthetic cdo/csad taurine pathway in the green unicellular alga Chlamydomonas reinhardtii. *Algal Research*, **40**, 101491.
Torzillo, G., Sacchi, A., Materassi, R., Richmond, A. 1991. Effect of temperature on yield and night biomass loss in Spirulina platensis grown outdoors in tubular photobioreactors. *Journal of Applied Phycology*, **3**(2), 103-109.
Tredici, M.R. 2010. Photobiology of microalgae mass cultures: understanding the tools for the next green revolution. *Biofuels*, **1**(1), 143-162.
Tredici, M.R., Rodolfi, L., Biondi, N., Bassi, N., Sampietro, G. 2016. Techno-economic analysis of microalgal biomass production in a 1-ha Green Wall Panel (GWP®) plant. *Algal Research*, **19**, 253-263.
Tredici, M.R., Zittelli, G.C. 1998. Efficiency of sunlight utilization: Tubular versus flat photobioreactors. *Biotechnology and Bioengineering*, **57**(2), 187-197.
Turon, V., Baroukh, C., Trably, E., Latrille, E., Fouilland, E., Steyer, J.P. 2015a. Use of fermentative metabolites for heterotrophic microalgae growth: Yields and kinetics. *Bioresource Technology*, **175**, 342-349.
Turon, V., Trably, E., Fayet, A., Fouilland, E., Steyer, J.P. 2015b. Raw dark fermentation effluent to support heterotrophic microalgae growth: microalgae successfully outcompete bacteria for acetate. *Algal Research*, **12**, 119-125.
Turon, V., Trably, E., Fouilland, E., Steyer, J.P. 2015c. Growth of Chlorella sorokiniana on a mixture of volatile fatty acids: The effects of light and temperature. *Bioresource Technology*, **198**, 852-860.
Turon, V., Trably, E., Fouilland, E., Steyer, J.P. 2016. Potentialities of dark fermentation effluents as substrates for microalgae growth: A review. *Process Biochemistry*, **51**(11), 1843-1854.
U.S.F.D.A. 2016. Summary of Color Additives for Use in the United States in Foods, Drugs, Cosmetics, and Medical Devices. https://www.fda.gov/industry/color-additive-inventories/summary-color-additives-use-united-states-foods-drugs-cosmetics-and-medical-devices.
Unnithan, V.V., Unc, A., Smith, G.B. 2014. Mini-review: A priori considerations for bacteria–algae interactions in algal biofuel systems receiving municipal wastewaters. *Algal Research*, **4**, 35-40.
USDA. 2020. Soybeans: Yield by Year, US. https://www.nass.usda.gov/Charts_and_Maps/Field_Crops/soyyld.php.
Van Wagenen, J., De Francisci, D., Angelidaki, I. 2015. Comparison of mixotrophic to cyclic autotrophic/heterotrophic growth strategies to optimize productivity of Chlorella sorokiniana. *Journal of Applied Phycology*, **27**(5), 1775-1782.
Villarejo, A., Orus, M.I., Martinez, F. 1995. Coordination of photosynthetic and respiratory metabolism in Chlorella vulgaris UAM 101 in the light. *Physiologia Plantarum*, **94**(4), 680-686.
Voltolina, D., Gómez-Villa, H., Correa, G. 2005. Nitrogen removal and recycling by Scenedesmus obliquus in semicontinuous cultures using artificial wastewater and a simulated light and temperature cycle. *Bioresource Technology*, **96**(3), 359-362.
Wan, M., Wang, Z., Zhang, Z., Wang, J., Li, S., Yu, A., Li, Y. 2016. A novel paradigm for the high-efficient production of phycocyanin from Galdieria sulphuraria. *Bioresource Technology*, **218**, 272-278.
Wang, H., Zhang, Z., Wan, M., Wang, R., Huang, J., Zhang, K., Guo, J., Bai, W., Li, Y. 2020. Comparative study on light attenuation models of Galdieria sulphuraria for efficient production of phycocyanin. *Journal of Applied Phycology*, **32**(1), 165-174.
Wang, J., Yang, H., Wang, F. 2014. Mixotrophic cultivation of microalgae for biodiesel production: status and prospects. *Applied biochemistry and biotechnology*, **172**(7), 3307-3329.
WHO, J. 2007. Protein and amino acid requirements in human nutrition. *World health organization technical report series*(935), 1.
Wijffels, R.H., Barbosa, M.J. 2010. An outlook on microalgal biofuels. *Science*, **329**(5993), 796-799.
Wijffels, R.H., Kruse, O., Hellingwerf, K.J. 2013. Potential of industrial biotechnology with cyanobacteria and eukaryotic microalgae. *Current opinion in biotechnology*, **24**(3), 405-413.
Wilken, S., Schuurmans, J.M., Matthijs, H.C. 2014. Do mixotrophs grow as photoheterotrophs? Photophysiological acclimation of the chrysophyte Ochromonas danica after feeding. *New Phytologist*, **204**(4), 882-889.

Yang, C., Hua, Q., Shimizu, K. 2000. Energetics and carbon metabolism during growth of microalgal cells under photoautotrophic, mixotrophic and cyclic light-autotrophic/dark-heterotrophic conditions. *Biochemical Engineering Journal*, **6**(2), 87-102.

Zarrouk, C. 1966. Contribution a l'etude d'une Cyanophycee. Influence de Divers Facteurs Physiques et Chimiques sur la croissance et la photosynthese de Spirulina mixima. *Thesis. University of Paris, France.*

Zijffers, J.-W.F., Schippers, K.J., Zheng, K., Janssen, M., Tramper, J., Wijffels, R.H. 2010. Maximum Photosynthetic Yield of Green Microalgae in Photobioreactors. *Marine Biotechnology*, **12**(6), 708-718.

Summary

Microalgae can reach higher areal productivity than terrestrial plants, do not require arable land or fresh water, and can use fertilizers with almost 100% efficiency. Microalgae-derived products are therefore considered a promising sustainable source of food and other commodities. Microalgae can provide nutrients, such as vitamins, pigments and essential fatty- and amino acids, to support human health. Their high protein content (up to 72%) and well-balanced amino acid profile make microalgae a promising novel source of proteins.

Microalgae are commonly grown exploiting their photoautotrophic capacity (henceforth referred to as autotrophic), in which cells harvest light energy, use carbon dioxide (CO_2) as a carbon source, and release oxygen (O_2) as a byproduct. CO_2 and aeration are provided to prevent carbon limitation and oxygen accumulation. When not efficiently utilized, CO_2 supply represents a major contributor to production costs while aeration requires substantial energy. Autotrophic cultures are maintained at low biomass concentration in order to allow adequate light penetration into the culture. Diluted cultures increase harvesting costs and the volume of liquid that needs to be handled. These limitations are amongst those currently restricting algae production to high value products, such as pigments (e.g. astaxanthin, phycocyanins) or Ω-3 fatty acids (e.g. EPA, DHA). In order to utilize microalgae as a source of protein in food and feed the production costs need to be reduced.

Mixotrophic cultivation of microalgae is a promising strategy to decrease the production costs. In this trophic mode, light and reduced organic carbons are simultaneously exploited within a single microalgal monoculture. In mixotrophic cultivation, the simultaneous presence of two energy sources allows for significant increases of biomass productivity. Moreover, higher biomass concentration can be reached reducing downstream processing cost. Mixotrophic cultivation has also potential to drastically reduce the need of gas-liquid exchange due to the internal O_2 and CO_2 recirculation between photosynthesis and respiration.

The principal aim of this thesis was to design a balanced mixotrophic strategy where autotrophic and heterotrophic metabolic contributions to the overall mixotrophic growth were equilibrated. Reaching this aim would allow algae production processes to be simplified and intensified leading to lower production costs.

In **Chapter 2**, *Chlorella sorokiniana* SAG 211-8K was used as model organism in designing the new mixotrophic cultivation method denominated "oxygen balanced" mixotrophy. In "oxygen balanced" mixotrophy the dissolved oxygen concentration is controlled by adjusting the substrate supply rate to the rate of photosynthesis. Using this approach with 24h/24h illumination, a closed photobioreactor was operated without any gas exchange. Under these conditions, mixotrophic stoichiometry could be described as the sum of heterotrophic and autotrophic stoichiometry and the overall biomass productivity was exactly the sum of the two metabolisms. The presence of two complementary growth modes within a microalgal monoculture led to doubled biomass productivity and concentration in comparison with an autotrophic reference. Furthermore, 94% of the substrate was converted into biomass. The photosystem II maximum quantum yield (F_v/F_m) and the average absorption cross section of the microalgal cells indicated that mixotrophic cultivation does not affect photosynthesis.

When sunlight is utilized, microalgae are exposed to day-night cycles and seasonal variations of the irradiance on a microalgal cultivation system. For this reason, in **Chapter 3** "oxygen balanced" mixotrophy in *C. sorokiniana* was explored under day-night cycles. The reactor was operated at a fixed dilution rate (i.e. chemostat), only diluted during daytime and not during the night (cyclostat). During daytime the reactor was under "oxygen balanced" mixotrophy and operated without any gas-liquid exchange. Under mixotrophic conditions the biomass productivity and concentration doubled compared to an autotrophic reference culture. Over 24h, 88% of the substrate was converted into biomass. Mixotrophic and autotrophic cultures had

similar nighttime specific oxygen consumption rate and biomass losses. Over 24 h, mixotrophy required 60 times less gaseous substrates compared to autotrophy.

Contamination caused by bacteria and fungi is a notable challenge when microalgae are cultivated in a medium containing a source of organic carbon. In **chapter 4** cultivation of the acidophilic microalgae *Galdieria sulphuraria* ACUF 64 was successfully used as a solution to prevent undesired contamination by heterotrophic microorganisms. In order to successfully cultivate light sensitive *G. sulphuraria* the specific light supply rate needed to be optimized. This was done using a series of repeated batch experiments where the specific light supply rate continuously decreased during the batch phase because of the increasing biomass concentration. Under optimal light regime, biomass productivity in autotrophic mode was 1.8 to 7.7-fold higher than previously reported. Autotrophy was compared to 'oxygen balanced' mixotrophy, where aeration was not needed and 91% of the substrate carbon was converted into biomass. In mixotrophy, biomass productivity was 1.8 times higher than in autotrophy and linear growth was maintained at high biomass concentration (9.7 $g_x \cdot L^{-1}$).

In repeated batch, after each dilution *G. sulphuraria* experienced a sudden change in the specific light supply rate that provoked photo-inhibition. This caused a reduction on biomass productivity in the days following the dilution. Moreover, the culture acclimatized to the new light regime by lowering its pigment content. In **Chapter 5,** *G. sulphuraria* was cultivated in chemostat at a high biomass concentration. This strategy succeeded in obtaining constant and high biomass production along with high C-phycocyanin (*C-PC*) content. 10% w/w *C-PC* content combined with high areal biomass productivity in mixotrophic culture lead to the highest *C-PC* areal productivity reported under 24h/24h illumination in *Galdieria,* and even higher than with autotrophic culturing of *Spirulina*. Autotrophy was compared to 'oxygen balanced' mixotrophy and no differences were found in *C-PC* and protein contents (w/w) between the two cultures. In mixotrophy the biomass productivity and concentration were

doubled compared to the autotrophic counterpart. In mixotrophy 89% of the substrate carbon was converted into biomass. The *C-PC* extracted from *G. sulphuraria* showed superior acid- and thermal stability compared to *C-PC* extracted in *Spirulina*. *G. sulphuraria* had protein content of over 60% w/w and compared favorably with the FAO dietary requirements for adults regarding amino acid composition. Moreover *G. sulphuraria* contains a high proportion of sulphurated amino acids compared with *Chlorella*, *Spirulina* and soybean protein. Due to its attractive amino acid profile and high protein content, *G. sulphuraria* is a good candidate for food and feed applications to overcome sulphurated amino acid deficiencies.

In **chapter 6**, the insights of this thesis were combined in a techno-economic model. Projections were made on biomass production costs for a hypothetical 100-hectare facility located in southern Spain. Our projections indicated that mixotrophic cultivation of *Chlorella sorokiniana* would decrease microalgal production cost from 4.9€·kg^{-1} in autotrophy to 2.6 €·kg^{-1}. Such a reduction in price is mainly due to the doubling of biomass productivity under mixotrophy. For *Galdieria sulphuraria*, because of the expected low efficiency of CO_2 uptake and the doubling of biomass productivity, the biomass production costs would decrease from 11.8€·kg^{-1} in autotrophy to 4.0 €·kg^{-1} in mixotrophy. Microalgal protein yield per hectare is expected to be 30-60 times higher than for soy beans while it would require 25-50 times less water. If glucose is used as a substrate for mixotrophic cultivation, the land and water consumption of sugar production substantially increases the overall water and land usage. However, when we consider the land and the water needed for sugar beet production, mixotrophic cultivation still requires 4 times less land and 7 times less water than soy beans. Altogether, this thesis successfully designed and applied oxygen balanced mixotrophy with two industrially relevant microalgal strains proving its effectiveness in reducing microalgal production costs. We are on the right track to achieve an economically feasible protein production from microalgae for food and feed purposes.

Acknowledgements

Completing a PhD is an intense experience that goes far beyond the mere acquisition of technical skills and scientific knowledge. There have been many moments of joy and despair which I got to share with a countless numbers of people, whom to I'd like to express my gratitude here. You are so many, that I'm sure that I'll forget someone from this list, please forgive me but know that you have surely made an impact.

Firstly, I'd like to thank my promoter **René**. You initially offered a PhD position for me in 2011, which, even though I unfortunately had to decline, encouraged me to continue working with algae and gave me confidence about my capabilities. I'm even more thankful about the second chance you gave, which allowed me to start this PhD in 2016. It was one of the few PhDs in WUR not supported by a specific founding but financed directly by the department of BPE. All this trust that you put in me helped me to grow and to do my best. I enjoyed your friendly and informal attitude and I would be happy to continue collaborating in the future.

Marcel, my daily supervisor and the best 'algaeneer' that I ever met. You are a true algae visionary and your ideas are inspiring. Thank you for your patience and support with the innumerable complex calculations and the scientific writing needed to accomplish this thesis. You have taught a lot to me and, after almost 5 years of working together, I can finally consider myself a biologist with a good knowledge of process engineering.

Fred, you always managed to make the solving of technical challenges look way more easy than it was in reality. Without your help it would have been impossible to complete my MSc thesis and now the PhD. I'm sure that wherever I will go to work in future, I will miss you.

Marian, you have been not only a great supervisor but also a great mentor and almost an adoptive mother for me during my MSc project. Without you, my first impression of the Netherlands would have been much more traumatic. Thank you for welcoming me back on my retour in Wageningen, for the nice chats, dinners and amazing BBQs.

Maria, with your positive attitude and good vibes you have wiped away many of the cloudy Dutch days. I'll never forget our nice chat in San Diego on our philanthropic vision on microalgae and our common passion for sparkling drinks.

Hans, thank you for all the trust and freedom that you, as my first supervisor, gave me during my first year in the MAB 2.0 project. You showed me what it is to be a great project manager and you encouraged me to do a PhD.

Giuseppe O, grazie mille per aver portato un po' dell'allegria e dell'ottimismo di Napoli a BPE. Sei il mio ingegnere chimico preferito, senza il tuo aiuto i miei process schemes assomiglierebbero molto di piu' ai disegni di un bambino. Grazie per avermi fatto conoscere le alghe acidofile e messo in contatto con Prof. **Antonino Pollio**.

Antonino, senza il tuo supporto la mia tesi avrebbe un aspetto molto diverso. Sono felice di poter continuare a collaborare con te e ti prometto che presto pubblicheremo il nostro articolo sulle microalgae acidofile.

Wendy, **Snezana** and **Sebaastian**, without you no one in BPE would be able to do proper research. I have never seen a lab working so efficiently as in BPE. Thank you also for the nice atmosphere that you created during each coffee break.

I would like to also express my gratitude to all of the MSc and BSc students that have helped with the research done for this thesis. Among all, special thanks go to **Jon**, **Egbert** and **Hugo**, who did not only contribute in the lab work but also gave me a lot of useful comments and ideas.

All staff members are kindly thanked: **Sarah, Arjen, Dirk, Ruud, Michel, Miranda, Marina**. You always found time to help me and to have a chat during all the social events.

Pedro, you have been one of the last PhD students I've met in BPE, and we mainly had to have online meetings due to the pandemic. Despite that, your contributions to this thesis has been remarkable and I'm happy to leave the group knowing that you are continuing this research. Thanks for your help and I hope to collaborate with you again in future.

Many special thanks goes to our amazing Radix office 2.135: **Jorijn**, **Pieter**, **Narcis** and **Sabine**. It has been a privilege to share an office completely dedicated to algal research. The many discussions, conversations and sharing laboratory experiences have been really useful in solving most of the algae related challenges. **Pieter**, apart from the office, thank you for also sharing many amazing 'work trips' converted to holidays. We luckily managed to visit both American coasts, enjoying beaches, rollercoasters, BBQs and all that jazz. **Narcis**, you are an amazing person and a great scientist. Sorry for torturing you with too many questions about

your research! I have no doubt that you will successfully finish your PhD and have an amazing career. Thank you so much for also finding time to help me while doing your famous sampling!

Thanks to all the BPE's colleagues, BestPeopleEver and Beer/Dinners group members: **Abdulaziz**, **Agi**, **Anna**, **August**, **Barbara**, **Calvin**, **Camilo**, **Catalina**, **Christian**, **Chunzhe**, **Edgar**, **Enrico**, **Iris**, **Jin**, **Jorijn**, **Jort**, **Youri**, **Kylie**, **Marta**, **Narcis**, **Pauline**, **Pieter**, **Sebastian**, **Stephanie**, **Renske**, **Robin**, **Rocca** and **Wendy**. Borrels and Friday night dinners with you have been epical. You made my BPE experience amazing and funny. Partying and traveling with you made me feel at home. **Youri**, in the years spent together in Wageningen you have been always open to go for drinks, dinner or a party. You showed me how beautiful and chill a party in the Dutch countryside can be. You are a true Brabant: friendly, joyful and welcoming. Thanks for sharing your family joys with me. I wish you, **Sunne**, **Moos** and new born **Nena** all the best.

A special mention to my paranymphs: **Iris** and **Enrico**.

Iris, from the first time you joined BPE we had immediately a great connection. Your optimism and empathy helped me in getting past a hard time made of fear for the future and important life decisions. We had a lot of long chats and became good friends. I'm sure that wherever I'll go in future I can count on you. I wish you all the best with your entrepreneur adventure!

Enrico, mi ricordo il primo momento in cui ti ho incotrato un venedi di fine 2015 al bar dell' Orion. Dalla prima conversazione su goliardia e vita in San Diego ho subito capito che eri una persona speciale con cui creare un bel rapporto di amicizia. Semplicita', spontanita' e allegria sono rare da trovare in uno scienziato del tuo livello. Grazie per le mille discussioni su ogni possibile tematica della vita, e per la tua visione sempre ottimista che si contrappone al mio pessimismo cronico. Sono sicuro che in questi anni abbiamo creato le fondamenta per un'amicizia duratura.

Now that work-related friends and colleagues have been mentioned I can focus on all the other people who supported me during the last 5 years.

Prima di tutto **Giulia B**. Abbiamo cominciato la nostra avventura in Olanda quasi insieme ed entrabi abbiamo influenzato le nostre vite vicendevolmente. Io ti ho fatto conoscere 'I Greco' e tu mi hai aiutato a tornare in Olanda. Una volta arrivato mi hai accolto ed aiutato a ricominciare la mia vita a Wageningen. Senza di te tutto sarebbe stato piu' difficile. **Christos**,

I introduced Giulia to you, while you introduced whisky to me. Do you find it a fair trade? Thanks for your friendship and for sharing your love story and the joy of making a family.

Marco, se ben piu' giovane di me, tu sei stato uno dei miei punti di riferimento a Wageningen. La tua mente geniale ed la tua etica del lavoro sono un asitoto a cui posso solo puntare senza mai raggiungerli. Sei stato per me grande motivo di crescita e di incoraggiamento. Grazie per essere stato piu' di un coinquilino ideale, sei stato come un fratello, che ti vuole bene sempre, e nonostante combini qualche casino e' sempre pronto ad accoglieri e farti sentire bene. Grazie per le serate spenzierate passate a strimpellare cantando a squarciagola.

Grazie agli altri 2 italiani della Casa del popolo, **Niccolo** e **Riccardo**. Siete riusciti a trasformare la clausura forzata dovuta al covid, in una vita normale e tranquilla, quasi come se non stesse accadendo niente intorno a noi. BBQs, chitarra, partite a scacchi, cinema e musica live. Un microcosmo dal sapore di normalita'.

Grazie a tutti i membri del gruppo designed drinkers: **Camilla**, **Marco**, **Enrico O**, **Enrico (Roscio)**, **Giulia**, **Pietro (drokato)**, **Lavinia**, **Francesca**, **i Francio**, **Nicola (gufo)**, **Erika**, **Elisa**. Un grazie speciale a **Camilla** creatrice del gruppo. Grazie per aver messo insieme un gruppo cosi' variegato di Italiani a Wageningen e per avermi fatto conoscere tutte le persone che ti venivano a travore a Wag ;-) **Francesca** se pur ci siamo visti poco e per tempo, hai avuto un grande impatto nella mia vita. Grazie per avermi convinto ad uscire nonostante la stanchezza quel 10/7/19. **Elisa**, sei come una sorella maggiore per me. Il tuo modo di ridimensionare ogni tipo di problema mi ha aiutato molto a superare un momento difficile. Seppure siamo cresciuti in posti molto lontani, condividiamo le stesse passioni per il cibo, il mare e la campagna. Spero di riuscire a venire a trovarti il prima possibile nella tua bella Galicia.

Mariaelena, grazie per aver condiviso con me la tua gioia di vivere e di divertirsi. Le feste e le scampagnate con te sono tra i piu' bei ricordi dell'Olanda. Grazie per aver ascoltato pazientemente per ore le mie disavventure cercando di darmi sempre il consiglio per te piu' giusto.

Stefano, a quanto pare sono stato una delle prima persone che hai conosciuto al tuo arrivo a Wageningen nel 2011 e tu sei stato uno delle prime che mi ha contattato al mio rientro a Wageningen. Da subbito abbiamo cominciato subito a discutere di ficocianina e di come fare business con le microalghe. Spero che la nostra recente colloborazione sia proficua e duratura. Grazie per avermi aiutato ad appropiarmi della Casa del Popolo e per avermi mostrato cos'e' l'arte della diplomazia.

Carl, you are a great man and a brilliant scientist. You advise on life, career and science have been really important to me. Apart from that, you also taught me how to swim in a swimming pool. I'll keep training and one day my butterfly style will be better than yours ;)

Thank you to all of the members of the fantastic **PCC volleyball team**. Playing with you has been my main sport activity in Wageningen. I hope you can keep playing again soon.

Ora ci spostiamo in Italia e non solo, dove nonostante le migliai di Km che ci hanno separato diverse persone non hanno mai smesso di farmi sentire il loro supporto.

Sarita, sono anni che non ci vediamo ma nonostante cio' mi sei stata sempre vicina. La nostra connessione ha del paranormale e ti considero il Guru della mia vita, in ogni momento difficile ad ogni decisione importante appari al momento giusto e sei pronta a dare una spiegazione ai miei dubbi esistenziali. Grazie della tua amicizia e della pazienza mostratami nelle nostre infinite telefonate.

I membri del gruppo 'Mirto e' ancora vivo?': **Alberto**, **Salatino**, **Viera**, **Alfredo**, **Amodeo**, **Giovanni**, **Giuseppe**, **Luigi**, **Max**, **Annasara**, **Pierpaolo**. Siamo amici dai tempi delle elementari. Riuscire a mandere un rapporto cosi' intimo e duraturo e' uno dei tesori piu' grandi che si possano desiderare. Grazie per avermi regalato momenti di adolescenza ad ogni mio rientro a Mirto.

Giuseppe F, grazie per la tua amicizia per il tuo supporto e per avermi scelto come 'compare di nozze', puoi essere certo che un giorno di rendero' il piacere di essere il mio. Sei piu' fratello, piu' di un punto di riferimento, sei una delle fondamenta della mia vita.

I membri del gruppo Italiani Medi: **Federico**, **Gabriele**, **Filippo**, **Sergio**, **Lorenzo**, **Stefano**. Ci siamo conosciuti in viaggio, ed abbiamo continuato a viaggiare insieme quasi ogni anno. Spero continueremo a farlo per tanto e tanto tempo ancora. Grazie **Federico** per aver condiviso con me questo fantastico gruppo di amici.

I membri del **PODVS**. In particolare i probi viri **Neanderthal** e **Spugna**. Ci siamo conosciuti per gioco in una serata a Firenze e siete stati tra i pochi che mi sono venuti a trovare in Olanda e che ci tenevano a salutarmi ad ogni mio rientro a Firenze. Specialmente **Alessandro F** e' stato la persona che mi ha visitato di piu' in assoluto. Grazie per avermi regalato cosi' tanti momenti di spenzieratezza.

Farhad e **Alessandro C**, siete tra i miei pochissimi amici con cui sono rimasto in contatto dai tempi della casa dello studente. La nostra amicizia e' solida e nonostante le distanze siete nel

mio cuore. Speriamo che un giorno riusciremo ad organizzare in nostro tanto sognato viaggio in Iran sul tappeto volante.

Papa' e **Viviana**. Grazie per avermi accolto ad ogni mio rientro a Firenze e per avermi fatto sentire a casa. Grazie per la cura e l'amore che avete dedicato a **Rex** in tutti questi anni.

Samuele, tu tra tutti sei quello che ha sofferto di piu' della mia assenza. Grazie per aver resistito tutti questi anni e per avermi dato l'opportunita' di finire il mio dottorato.

Tutti i mebri della famiglia Beraldi: **la Nonna, Ida, Zio Antonio, Zia Barbara, Carla, Zia Daniela B, Zia Daniela V, Marius, Mirko , Pasqualino, Zia Pina, Zio Pino, Sara**. I vostri messaggi, foto, le conserve, l'olio ed i limoni sono stato il carburante che mi ha fatto resistere tutti questi anni lontano da casa. Non ci sono parole per descrivere quanto mi sento fortunato ad avervi come parenti.

Duncis in fundo, **Niina**. Mi hai conosciuto in uno dei momento piu' bui della mia vita. Sei entrata nella mia vita con una naturalezza disarmante. Sei stata paziente, mi hai dato il tempo di rimettere insieme i miei pezzi e mi hai dato la colla per poterlo fare. Mi sei stata a canto nella difficolta' mettendo davanti i miei interessi e le mie priorita' alle tue. Hai avuto il coraggio, dopo poco tempo che ci eravamo conosciuti, di lasciare la tua vita per seguirmi. A causa del lock down, abbiamo passato mesi insime in una stanza di 15 m^2 senza mai litigare o avere niente da ridire. Hai dedicato mesi ad incoraggirmi, a calmarmi, coccolarmi e ad aiutarmi a scrivere la tesi. Ora mi hai seguto fino a Firenze e stai spendendo la maggior parte tuo tempo a rendere la nostra cosa un luogo bello e accogliente. Se e' vero che 'dietro ad ogni uomo c'e' sempre una grande donna', se mai diventero' un grande uomo lo dovro' principalmente a te. Spero che continuerai a starmi a finco per il resto della mia vita.

In fine un pensiero a va a mia **Mamma**. Se fosse stata con noi sicuramente sarebbe stata orgoglisa di me. **Mamma** spero un giorno di rincontrati e mostrati la bella pergamena del dottorato.

About the author

Fabian Abiusi was born in Pinerolo, Italy, on the 15th of July, 1985. After high school he began to study biotechnology at the University of Florence. In 2008 Fabian graduated with a BSc thesis on pharmacogenomic determinants potentially predictive of chemotherapy effectiveness, which was carried out at the Department of Human Health. He continued with his MSc studies on industrial and environmental biotechnology and in 2010, carried out his MSc thesis at the Bioprocess Engineering Group of Wageningen University on the effects of dynamic changes in oxygen concentration on growth and biomass composition of *Nannochloropsis* sp. After obtaining a MSc degree in 2011, Fabian started to work as research fellow in Prof. Tredici's group at the University of Florence. Here he worked on two European projects: BIOFAT, a microalgae-to-biofuel demonstration project, and in GIAVAP, focusing on genetic engineering of microalgae for carotenoids and PUFA production.

In 2015 Fabian Abiusi moved back to the Netherlands, where he worked as research assistant on the C-KIC project MAB2.0 at the Bioprocess Engineering Group of Wageningen University. During this period he focused on waste water treatment by microalgae.

In July 2016, he started his PhD research in the same group working on mixotrophic cultivation of microalgae. The results of Fabian's PhD research are described in this thesis.

List of publications

Published

Nagy, B.J., Makó, M., Erdélyi, I., Ramirez, A., Moncada, J., Gursel, I.V., Ruiz-Martínez, A., Seco, A., Ferrer, J., **Abiusi, F**., Reith, H., Broek, L.A.M.v.d., Seira, J., Garcia-Bernet, D., Steyer, J.-P., Gyalai-Korpos, M. 2018. MAB2.0 project: Integrating algae production into wastewater treatment. The EuroBiotech Journal, 2(1), 10-23.

Abiusi, F., Wijffels, R.H., Janssen, M. 2020a. Doubling of Microalgae Productivity by Oxygen Balanced Mixotrophy. ACS Sustainable Chemistry & Engineering, 8(15), 6065-6074.

Abiusi, F., Wijffels, R.H., Janssen, M. 2020b. Oxygen Balanced Mixotrophy under Day–Night Cycles. ACS Sustainable Chemistry & Engineering, 8(31), 11682-11691.

Submitted

Abiusi, F., Trompetter, E., Hoenink, H., Wijffels, R.H., Janssen, M. 2021. Autotrophic and mixotrophic biomass production of the acidophilic *Galdieria sulphuraria* ACUF 64.

Abiusi[§], F., Moñino Fernández[§], P., Canziani, S., Janssen, M., Wijffels, R.H., Barbosa, M. 2021. Algae blues: Is Galdieria the new Spirulina? § Authors contributed equally

Zanolla, V., Biondi, N., Niccolai, A., **Abiusi, F.**, Rodolfi, L., Tredici, M.R. 2021. Protein, phycocyanin and polysaccharide production by *Arthrospira platensis* grown with LED light in annular photobioreactors

Overview of completed training activities

Disciple specific activities

Courses

Microalgae Process Design: from cells to photobioreactors (VLAG, Wageningen, The Netherlands, 2016)

Bioprocess Design (VLAG and BSDL, Delft, The Netherlands, 2017)

Advanced Course Microbial Physiology and Fermentation Technology (BDSL, Delft, The Netherlands, 2018)

Conferences

1st IWA Conference on Algal Technologies for Wastewater Treatment and Resource Recovery (Poster) (Delft, The Netherlands, 2017)

BioSC International Workshop N/P/C storage pools in algae and cyanobacteria and nutrient uptake from waste streams.(Poster) (Jülich, Germany) 2018

NBC-19: The Sound of Biotech (Oral presentation) (Ede, The Netherlands) 2019

Algae biomass summit (Oral presentation) (Orlando, USA) 2019

ALGAEUROPE (Oral presentation) (Paris, France) 2019

General courses

VLAG PhD week (VLAG, Baarlo, The Netherlands, 2016)

Project and time management (VLAG, Wageningen, The Netherlands, 2018)

Scientific writing (WGS, Wageningen, The Netherlands, 2018)

Basic statistics (Sense, Wageningen, The Netherlands, 2019)

Presenting with Impact (WGS, Wageningen, The Netherlands, 2019)

Start to teach (ESC, Wageningen, The Netherlands, 2019)

Writing Grant Proposals (WGS, Wageningen, The Netherlands, 2019)

Career Orientation (WGS, Wageningen, The Netherlands, 2019)

Optional activities

Preparation of research proposal (2016)

BPE group meetings (2016)

PhD trip to San Diego (San Diego, USA, 2018)

Cover design by Giuseppe Silvestri

Printed by Digiforce || ProefschriftMaken